Analysis of cell allocation in GFP chimeric blastocysts by confocal microscopy

By

Gillian E MacKay

Doctor of Philosophy

The University of Edinburgh

2003

Disclaimer:

I (Gillian Elizabeth MacKay) performed all of the experiments presented in this dissertation unless otherwise clearly stated in the text. No part of this work has been, or is being submitted for any other degree of qualification.

Date: 30/10/03

Acknowledgements:

I would like to thank my supervisor, Dr. John West for his support, help and encouragement throughout my PhD.

I would also like to thank my second supervisor Prof. Johnathan Bard.

I would also like to thank the past and present members of the West lab. Jean Flockhart and Margaret Keighren for teaching me all my lab techniques and Martin Collinson for his advice. I also thank Simon Chanas and Thaya Ramaesh. I must also thank Linda Sharp for all her help with the confocal microscope and Dr. Tom Pratt and Dr. Jenny Nichols for their help.

I am also grateful to my parents for their emotional and financial support especially when I have been writing up and my sister Caroline. I also thank Hazel for putting up with me and doing the dishes, Caff, Julie, Jamie, RB and Kirst.

Abstract:

This study combined confocal microscopy with the use of a tau-GFP (green fluorescent protein) transgenic mouse strain to study cell fate in two main types of chimeric blastocysts. In each case one component of the chimera was known to contribute poorly to the fetal lineage at later stages. The experiments were designed to test whether this was due to non-random allocation to different tissues at the blastocyst stage.

The initial part of this thesis involved the establishment of confocal microscopy techniques and the characterisation of two novel tau-GFP transgenic mouse strains. A method of culturing embryos on the confocal microscope was established for use in further studies. Two tau-GFP transgenic mouse lines, TgTP6.3 and TgTP6.4, were evaluated for their use in following chimera studies by assessing the timing of the onset of GFP expression during preimplantation development and the viability of heterozygote and homozygote mice.

The remaining studies involved the use of tau-GFP chimeric embryos. Mouse tetraploid↔diploid chimeras have previously been used as a model of confined placental mosaicism (CPM). Approximately 2% of human conceptuses investigated by chorionic villus sampling contain chromosomally abnormal cells that are confined to the placenta. This condition, known as human CPM, can lead to incorrect prenatal diagnosis. Animal models would be useful for investigating the mechanisms responsible for the exclusion of abnormal cells from the fetus. As

spontaneous chromosomal mosaicism is rare in mouse embryos, mouse aggregation chimeras have been used as a model. Previous results have shown that tetraploid cells are excluded from the epiblast derivatives, including the fetus, of mid gestation tetraploid↔diploid chimeras. Tetraploid cells have been shown to be preferentially allocated to the trophectoderm, in particular the mural trophectoderm, of mouse tetraploid↔diploid blastocysts. However, tetraploid cells are present within the inner cell mass region of the blastocyst. Therefore, the current study used tau-GFP tetraploid↔diploid aggregation chimeras to determine if tetraploid cells are present within the epiblast and lost later or are excluded from the epiblast region by preferential allocation to the hypoblast. Tetraploid↔diploid chimeras were produced using TgTP6.3 embryos. Analysis of these chimeras at E3.5 and E4.5 has confirmed that tetraploid cells are preferentially allocated to the mural trophectoderm. However, tetraploid cells were present within the region of the blastocyst that forms the epiblast. Analysis of expanded chimeric blastocysts at E5.5 and E7.5, produced by transferring them to delayed implantation females, also showed that tetraploid cells were present within the epiblast region. This suggests that tetraploid cells are initially present within the epiblast region but lost from the epiblast later by some mechanism of cell selection against tetraploid cells.

Embryos from some inbred strains, such as BALB/c, also tend to contribute poorly to chimeras, so producing 'unbalanced chimeras'. Therefore unbalanced BALB/c chimeras could be a possible model of CPM.

BALB/c↔GFP aggregation chimeras were analysed using the established time-lapse technique. This was to determine if BALB/c cells are underrepresented in mid-gestation BALB/c chimeras by preferential allocation of BALB/c cells to the mural trophectoderm. These results showed that BALB/c cells were not preferentially allocated to the mural trophectoderm and indicate that a general cell selection mechanism takes place.

CONTENTS

Figures:

Tables:

Abbreviations:

2n	Diploid
4n	Tetraploid
GPI	Glucose Phosphate Isomerase
hrs	hours
ICM	Inner Cell Mass
i.p.	intra peritoneal
l	Litre
m	Meter
M	Molar
mins	minutes
mTE	Mural Trophectoderm
N	Number
P	Probability
PBS	Phosphate Buffered Saline
p.c.	Post coitum
pTE	Polar Trophectoderm
s.c.	sub cutaneous
SE	Standard Error
secs	seconds

Chapter 1: Introduction

Human confined placental mosaicism (CPM) occurs when chromosomally abnormal cells are present in the extraembryonic membranes of the human conceptus, but are excluded from the fetus (Kalousek and Dill, 1983). Using chorionic villus sampling approximately 2% of conceptuses analysed have CPM. This can lead to incorrect prenatal diagnosis and it is important to understand the mechanisms leading to the exclusion of aneuploid or polyploid cells from the fetus.

The experimental work in this thesis describes the analysis of two mouse models of CPM, using tau tagged green fluorescent protein (tau-GFP) aggregation chimeras and confocal microscopy. Two transgenic tau-GFP mouse lines were evaluated for their use in this analysis and a method for confocal microscopy of living preimplantation mouse embryos were established.

This first chapter provides a review of polyploidy, polyteny and aneuploidy in mammals, specifically in preimplantation embryos. The exclusion of chromosomally abnormal cells from mammalian fetuses, illustrated in the occurrence of human CPM and several animal models of CPM, is discussed. The experiments in this thesis involve the use of chimeric preimplantation mouse embryos. Therefore, an overview of preimplantation embryo development, and preimplantation mouse aggregation chimeras is given.

1.1 Development of the Preimplantation Embryo

An overview of the aspects of mouse preimplantation development, which are relevant to the experimental chapters of this thesis follows.

Fertilisation of the mouse oocyte takes place in the ampulla of the oviduct, and is followed by the completion of meiosis and the formation of the second polar body. Approximately one day later the first cleavage division occurs to produce a 2-cell embryo. As the embryo develops to the blastocyst stage it is swept towards the uterus by the cilia in the oviduct (Theiler, 1989; Kaufman, 1992; Hogan *et al.*, 1994). Following cleavage to the 8-cell stage the mouse embryo undergoes compaction to form a morula (Pratt *et al.*, 1982; Peyrieras *et al.*, 1983; Sutherland and Calarcogillam, 1983; Winkel *et al.*, 1990). The morula divides to the 16-cell stage after which the blastocyst cavity is formed, by the secretion of fluid from the trophectoderm (TE) cells. The cell membranes of the TE cells contain a sodium pump (a Na^+/K^+-ATPase) facing the blastocyst cavity. The accumulation of sodium ions in the cavity draws in water osmotically. As a result the blastocyst cavity expands (Wiley, 1984). As the 128/256-cell blastocyst expands it hatches from the zona pellucida and implants in the uterine wall (Strickland *et al.*, 1976; Brenner *et al.*, 1989; Carson *et al.*, 1993).

The chimera experiments in this thesis involve the analysis of blastocyst stage preimplantation embryos. The early blastocyst contains three main lineages, the inner cell mass (ICM), the polar trophectoderm (pTE) and the

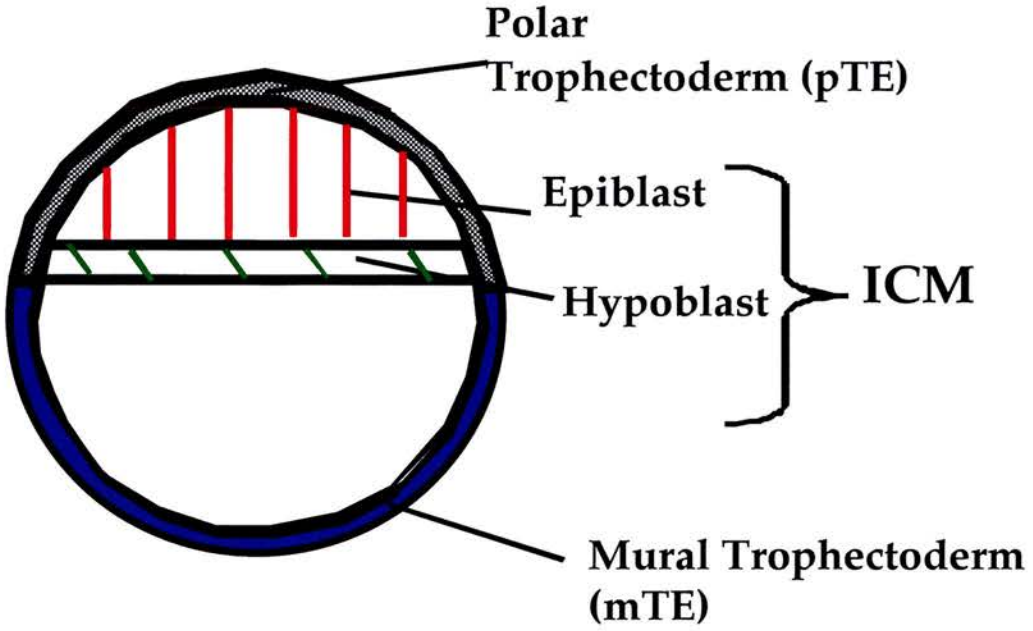

Fig 1.1: Schematic Diagram of a Mouse Blastocyst

mural trophectoderm (mTE) (Fig 1.1 & 1.2). The ICM then differentiates into the epiblast (primitive ectoderm) and hypoblast (primitive endoderm) at E4.5. The epiblast lineage forms the entire fetus. It also produces the chorionic mesoderm, allantois, amnion and the visceral yolk sac mesoderm of the postimplantation conceptus. The hypoblast lineage produces the visceral yolk sac endoderm and the parietal endoderm (Reichert's membrane). The pTE lineage produces the trophoblast giant cells, spongiotrophoblast, labyrinthine trophoblast and the chorionic ectoderm, which form part of the chorioallantoic placenta. Some pTE along with the mTE differentiate into trophoblast giant cells, which contribute to the parietal yolk sac.

Fig 1.2: Lineage diagram of mouse development

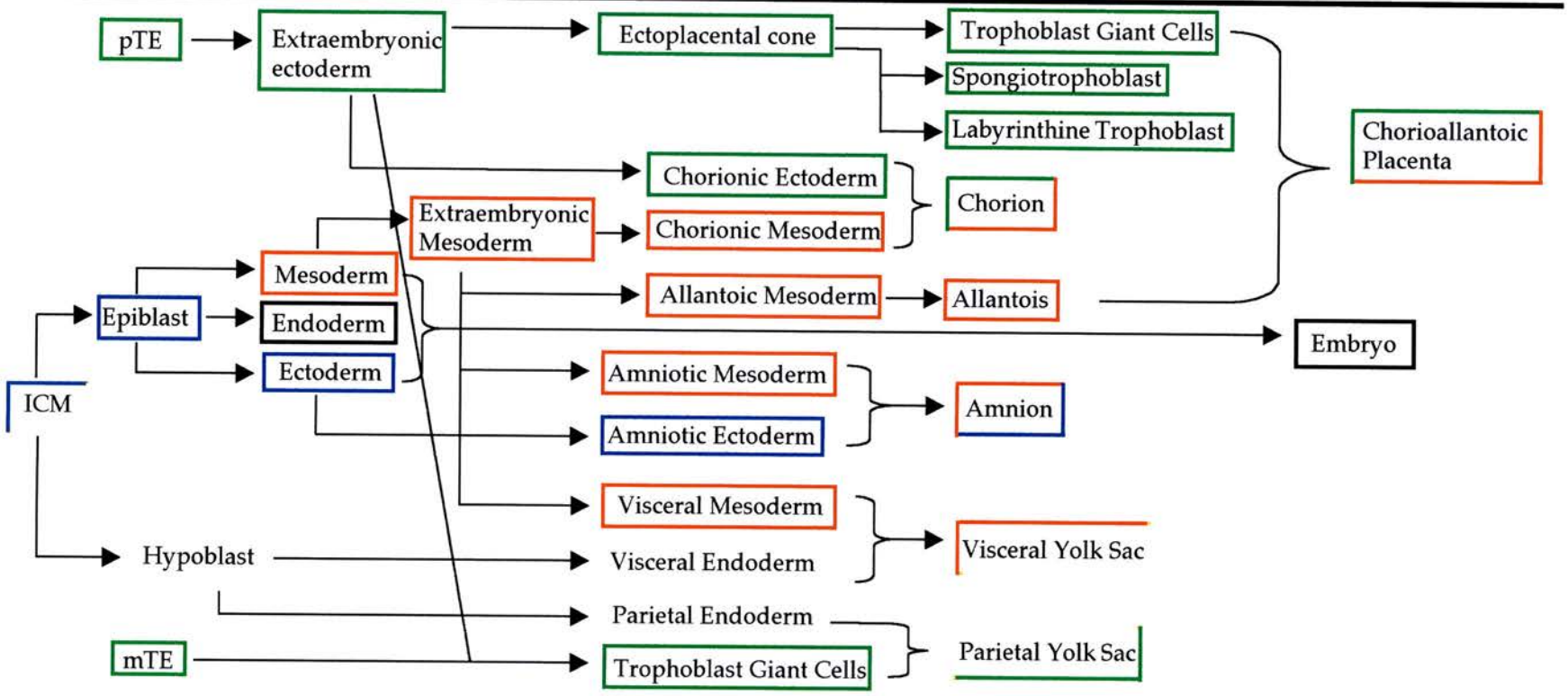

Figure 1.2: Mouse lineage diagram showing the fates of the different regions of the blastocyst, the Inner cell mass (ICM),polar trophectoderm (pTE) and mural trophectoderm (mTE).

1.1.1 The Onset of Zygotic Gene Expression

An important aspect of preimplantation development is the transformation from a differentiated oocyte to a totipotent 2-cell stage embryo. The oocyte contains a vast diversity of maternal mRNAs and biosynthetic apparatus for making proteins, which are necessary to control this oocyte to embryo transition (Bachvarova and DeLeon, 1980; Gardner, 1996). The translation of these stored maternal mRNAs is regulated during this stage, one mechanism being the polyadenylation of transcripts (Stutz *et al.*, 1998; Svoboda *et al.*, 2000).

For many genes the onset of zygotic gene expression occurs at the late 2-cell stage (Taylor and Piko, 1987; Telford *et al.*, 1990; Rothstein *et al.*, 1992; Ko *et al.*, 2000). However, there is evidence of some genes being activated at the 1-cell stage (Clegg and Piko, 1983; Ram and Schultz, 1993; Ko *et al.*, 2000). More recent understanding of this process has suggested that there is a global onset of gene expression during the 1 to 2-cell stage. The transcription of specific genes is repressed by changes in chromatin structure (Ma *et al.*, 2001).

A substantial amount of maternal mRNA transcripts are degraded at the 2-cell stage (Bachvarova and DeLeon, 1980; Piko and Clegg, 1982; Ko *et al.*, 2000). During this period, the mRNAs coding for actin and histones decline by as much as tenfold (Giebelhaus *et al.*, 1983; Giebelhaus *et al.*, 1985). Following this, there is another substantial reduction in maternal transcripts between the 8-cell and the blastocyst stage, which coincides with a large

increase in embryonic mRNA (Bachvarova and DeLeon, 1980; Steuerwald *et al.*, 1999). Therefore, some maternal transcripts remain to late preimplantation stages and possibly have a role in blastocyst formation. Renard *et al.*, (1994) confirmed this by demonstrating a maternal factor that was required for the formation of the blastocyst.

1.1.2 The Cleavage Rate of Preimplantation Embryos

The timing of the initial cleavage divisions depends on the genetic background of the embryo (McLaren and Bowman, 1973; Niwa *et al.*, 1980). Following the 4-cell stage the timing of the cell cycle doesn't vary significantly and is approx 10hrs (Pedersen, 1986). However, if the initiation of cleavage is later this can significantly delay embryo development (McLaren and Bowman, 1973).

One gene, which controls the rate of cleavage, has been identified as the pre-implantation embryo development (*Ped*) gene (Warner *et al.*, 1998). The *Ped* gene encodes the Qa-2 antigen, which is a class 1b major histocompatibility complex (MHC) protein. There are two alleles of the *Ped* gene, fast (which is dominant) and slow. Mouse strains, homozygous for the fast allele tend to have larger litter sizes and increased pup weights at birth and weaning. Other genes must be involved in the control of cleavage rate as certain strains of embryo, for example some BALB/c substrains, including the substrain used in this thesis develop slowly despite having a *Ped*-fast genotype (Flaherty *et al.*, 1985).

1.1.3 The Establishment of the Inner Cell Mass and Trophectoderm

There are several factors involved in determining the fate of a blastomere to become either TE or ICM.

At the 8-cell stage there is a structural and functional reorganization of the individual blastomeres. Each blastomere becomes polarized, with apical (outward facing) and basolateral (inward facing) domains (Randle, 1982; Johnson and Ziomek, 1983; Fleming and Pickering, 1985; Maro *et al.*, 1985). Following the next division the fate of the two daughter cells is dependant on the orientation of the cleavage plane (Fig 1.3). If the cleavage plane is oriented approximately perpendicular to the axis of polarity a differentiative division occurs. One cell inherits the apical domain and remains polar, and the other cell lacks an apical domain and is apolar. A conservative division, when the cleavage plane runs parallel to the axis of polarity, produces two polar cells (Johnson and Ziomek, 1981a). There is an equal probability of a conservative or a differentiative division occurring at this stage (Pedersen, 1986). Therefore, at the 16-cell morula stage two types of cells exist, outer (polar) cells and inner (apolar) cells. These two types of cell have similar properties to the differentiated cells of the blastocyst, as TE cells are polar and ICM cells are apolar (Fleming *et al.*, 1984).

Although two morphologically distinct populations of cells exist at the morula stage, previous experiments have shown that they are totipotent (Handyside, 1978; Rossant and Vijh, 1980; Ziomek *et al.*, 1982). By the 32-cell stage when the definitive blastocyst is formed the outer cells are a clonally

Fig1.3: Differentiative and Conservative Division

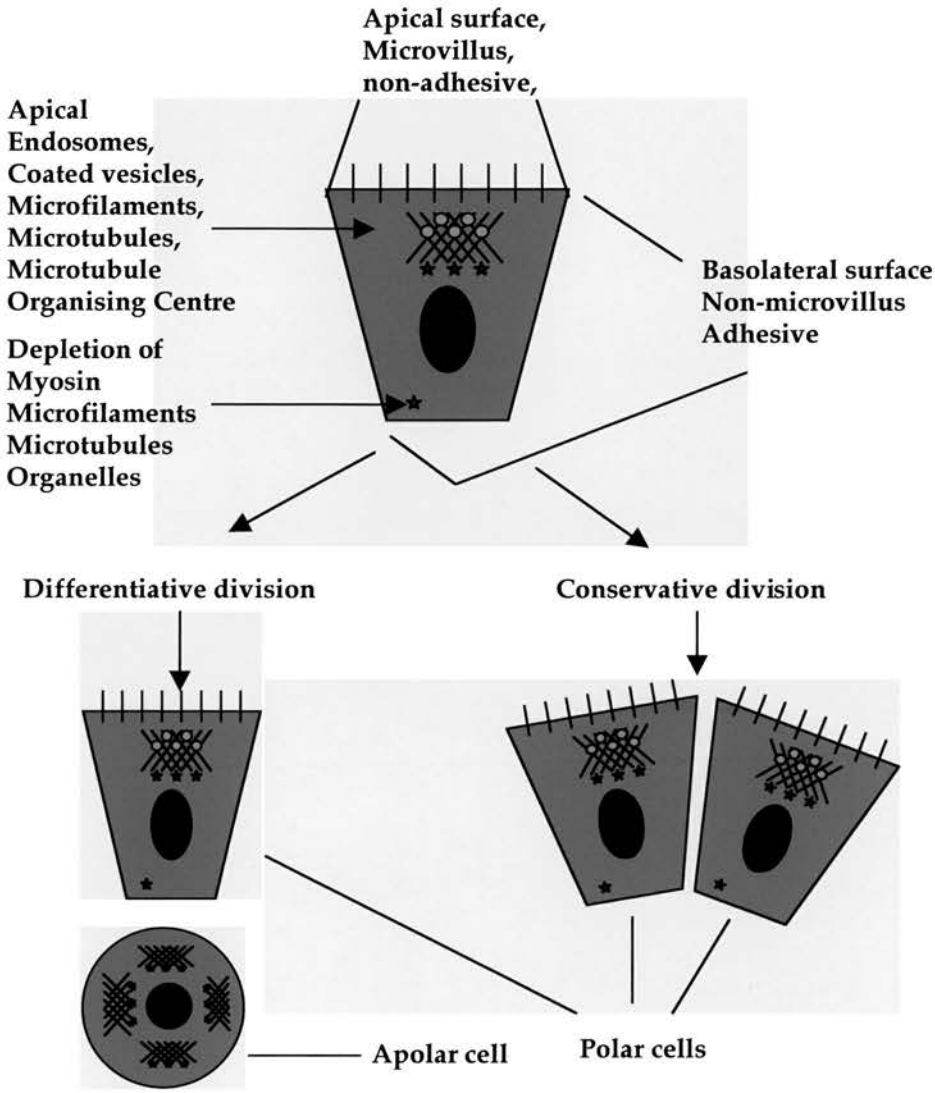

Fig 1.3: Division of the blastomeres of a morula. A differentiative division produces a polar and an apolar cell, whereas a conservative division produces two polar cells.

distinct population from the inner cells (Pedersen, 1986).

Early studies indicated that cells that happen to be on the inside of the 16-cell morula produced ICM cells and cells on the outside of the morula form TE cells (Tarkowski and Wroblewska, 1967; Hillman *et al.*, 1972; Graham and Deussen, 1978; Sutherland *et al.*, 1990). This work lead to the "inside outside" hypothesis. However, it was subsequently shown that polar (outside) cells are capable of contributing to the ICM lineage up to the 32-cell stage. Studies have shown that the majority of ICM cells are descended from inner apolar blastomeres (approximately 75%). However, the remainder of the ICM cells are derived from outside, polar blastomeres (Fleming, 1987).

Although apolar (inner) cells are totipotent they are normally prevented from occupying an outer position, as polar cells are adhesive on their basolateral surface (Johnson and Ziomek, 1983). Therefore, they do not express their potential to polarise and as a result do not contribute to the TE lineage. The TE lineage is therefore derived entirely from polar (outer) cells of the morula.

At the 16-cell stage the ratio of polar to apolar cells differs among different embryos. The number of inner cells can range from 2-7 cells (Fleming, 1987). This is determined by the proportion of conservative to differentiative divisions in the 8-cell stage embryo (Johnson and Ziomek, 1981b; Pedersen, 1986). However, at the 32-cell stage the ratio of ICM to TE cells is similar among different embryos. Therefore, the outer, polar, cells contribute to the

ICM through differentiative divisions to compensate for the variation among inner and outer cell numbers. The number of polar cells that contribute to the inner population is possibly controlled by the relative size of the outside cell population at the 16-cell stage (Fleming, 1987).

The division of the blastomeres within the mouse embryo is asynchronous and frequently odd numbers of cells can be found. The first cell to divide to the 4-cell stage produces descendants, which tend to divide ahead of those cells produced by its slower partner, up to the blastocyst stage. It has been found that the advanced blastomeres contribute disproportionately more descendants to the inner cells of the morula or the ICM of the blastocyst (Barlow and Sherman, 1972; Kelly *et al.*, 1978; Graham and Lehtonen, 1979; Piotrowska and Zernicka-Goetz, 2001).

More recently it has been claimed that the position of sperm penetration in the oocyte determines the first blastomere to divide from the 2-cell stage (Piotrowska and Zernicka-Goetz, 2001; Piotrowska and Zernicka-Goetz, 2002). In contrast to these findings Davies and Gardner, (2002) claim there is no relationship between the sperm entry point and the first blastomere to divide at the 2-cell stage.

It is possible that the initial blastomere to divide contributes more to the ICM as it gives rise to a greater proportion of smaller cells. These would be preferentially enclosed by later dividing cells. However, the analysis of parthenogenetic embryos has revealed that despite dividing asynchronously,

the first blastomere to divide does not necessarily contribute more cells to the ICM (Piotrowska and Zernicka-Goetz, 2002). Therefore, on its own, asynchronous cleavage divisions might not be responsible for determining blastomere fate.

Fate mapping experiments have also shown that, if left undisturbed, one of the cells at the 2-cell stage tends to produce mTE and hypoblast and the other tends to produce pTE and epiblast (Ciemerych *et al.*, 2000; Piotrowska and Zernicka-Goetz, 2002).

1.2 Mouse Aggregation Chimeras

The use of mouse chimeras is an established technique for the study of developmental biology and as a model for studying human pathologies. The experiments in this thesis use mouse aggregation chimeras as a model for human confined placental mosaicism.

A chimera is defined as an organism that consists of cells derived from more than one individual, usually of different genotype (Rossant and Spence, 1998). The first aggregation chimeras were produced in 1961 by Tarkowski (Tarkowski, 1961). The method used involved the mechanical removal of the zona pellucida following which the "naked" embryos were pushed together in a drop of culture medium. Currently acid tyrode solution is commonly used to remove the zona pellucida and exposure to phytohaemagglutinin (PHA) is widely used to facilitate adhesion of the embryos (Mintz *et al.*, 1973).

1.2.1 Markers Used to Identify Cells in Aggregation Chimeras

The experiments in this thesis analyse the allocation of cells in aggregation chimeras at the blastocyst stage. It is therefore crucial to be able to identify the origin of cells within a chimera. Several markers are available for the analysis of chimeric adult mice, postimplantation chimeric embryos and specifically preimplantation chimeras.

Coat and eye pigmentation is commonly used as a marker for adult chimeras, however another marker is required for investigating non-pigmented tissues or specifically preimplantation embryos. A cell marker used to distinguish one chimera component from another should ideally fulfil a number of criteria. The marker should be cell-localised, cell autonomous, stable and distributed ubiquitously among all the tissues and cell lineages of the mouse. It should be easy to detect, both grossly and in histological sections, and ideally could be used to analyse chimeras during several stages of development (McLaren, 1976). A cell marker should also not affect cell selection or cell mixing within a chimera and therefore be developmentally neutral (West, 1984).

Glucose phosphate isomerase-1 (GPI-1) was developed as a marker in chimeras. This technique makes use of allelic variants of this enzyme, which can be visualised by electrophoresis and histochemical staining for GPI-1 enzyme activity (Chapman *et al.*, 1971; West, 1999). GPI-1 is particularly useful as a quantitative marker, and is used in chapter 6 to analyse the percentage contribution of each type of embryo to E12.5 postimplantation

chimeras. However, this type of marker does not give spatial information, which is required for the following studies.

There have been several techniques developed to show spatial information in chimeric preimplantation blastocysts. A single blastomere or group of cells can be labelled by the injection of a fluorescent dye (Gardner and Cockroft, 1998; Piotrowska and Zernicka-Goetz, 2001). Alternatively an embryo can be labelled with a vital dye. An analysis of the use of vital dyes to label one half of a chimera is given in Chapter 3.

Transgenes are now largely used to identify the origin of different cells in chimeras, as they can be detected easily, are non-invasive and provide spatial information.

The E.coli β-galactosidase gene is a widely used marker for chimera analysis. Activity of the β-galactosidase gene can be detected by a histochemical stain for lac-Z expression on whole embryos or sectioned material. The ROSA26 transgenic mouse line (Friedrich and Soriano, 1991) expresses the β-galactosidase gene almost ubiquitously so provides a lineage marker for chimeras made by the aggregation of a ROSA-26 embryo with a non-transgenic embryo (Wong *et al.*, 1996; Zambrowicz *et al.*, 1997). Previous attempts by our group to use this marker for the analysis of chimeric blastocysts were unsuccessful possibly because the protein is not expressed sufficiently at this stage (Tang & West, unpublished). However, this marker has been used to analyse cell fate in aggregation chimeras to the blastocyst

stage (Neganova *et al.*, 1998). This technique requires the use of a chromogenic substrate, as a result blastocysts must be fixed for β-galactosidase staining and can only be analysed at one developmental stage.

It is possible to spatially analyse the contribution of cells in chimeric blastocysts using DNA-DNA in situ hybridisation, using probes to multicopy transgenic sequences. The β-globin TgN(Hbb-b1)83Clo transgene can be detected by DNA-in situ hybridisation following fixation and sectioning. This transgene has previously been used to detect polyploid nuclei for example by counting the number of hybridisation sites per nucleus (Lo, 1983; Lo, 1986; Keighren and West, 1993; Everett and West, 1996). This technique was used in the studies that preceded this thesis, to analyse the contribution of tetraploid cells in tetraploid↔diploid blastocysts (Everett and West, 1996). However, this technique is very laborious for analysing preimplantation embryos, as a large number of histological sections are required. Again embryos can only be imaged during one stage of development.

The transgenic marker chosen to identify cells in the chimeric blastocysts analysed in this study was green fluorescent protein (GFP). There are several properties of GFP that make it a potentially valuable cell marker for preimplantation chimeras. It can be easily detected using standard long wave UV, or blue light. There is no requirement for the introduction of a substrate, unlike β-galactosidase. There are no special conditions required and it avoids the need to chemically fix cells. Therefore, for the purpose of analysing chimeric blastocysts the majority of the criteria described above are fulfilled.

It was therefore decided to use GFP embryos to identify cells that comprise one half of the aggregation chimeras in this study. As a laser scanning confocal microscope had recently been purchased, it was possible to image whole mount, live blastocysts.

GFP expressing ES cells were established, and used to produce the first GFP expressing transgenic lines of mice (Hadjantonakis *et al.*, 1998b). These mice expressed GFP ubiquitously throughout development and adulthood. Subsequently several other GFP transgenic mice lines have been produced, including the ones used in this study (Hadjantonakis *et al.*, 1998a; Pratt *et al.*, 2000).

The two transgenic mouse lines evaluated in this study, were produced by Pratt *et al* (2000). Embryos from one of these transgenic lines were used to create aggregation chimeras. These transgenic mice ubiquitously express a tau-GFP fusion protein. As tau is a microtubule binding protein, cellular features can be visualised. The GFP is therefore attached to the microtubule component of the cytoskeleton, and is excluded from the interphase nucleus. Further characterisation of both transgenic mouse lines is discussed in Chapter 4.

The use of GFP as a cell marker has already made a contribution to developmental studies in mouse preimplantation chimeras. Zernicka-Goetz *et al.* (1997) injected single blastomeres at the 2-cell stage with mRNA encoding MmGFP. They then used confocal microscopy to follow the fate of

the GFP blastomeres to the blastocyst stage. Weber *et al.* (1999) injected ICM cells of the early blastocyst with MmGFP mRNA to determine the fate of these cells in postimplantation development. Confocal microscopy has also been combined with the use of GFP to analyse the fate of GFP expressing ES cells in postimplantation chimeras (Zernicka-Goetz *et al.*, 1997). Shimada *et al.* (1999) used ES cell lines expressing GFP to follow the fate of ES cells during blastocyst formation.

Other applications of GFP include a mechanism for non-invasively sexing preimplantation embryos by the production of a transgenic mouse line that have an X-linked GFP transgene (Hadjantonakis *et al.*, 1998a). The potential use of double stranded RNA to disturb specific genes during preimplantation development, and its general use in the mouse have also been assessed using GFP. Preimplantation embryos expressing MmGFP provide a rapid visual assay for the elimination of expression of the marker gene. Thus it was shown that injection of MmGFP dsRNA into the single cell zygote prevents the onset of the appearance of green fluorescence at 2-4 cell stages (Wianny and Zernicka-Goetz, 2000).

1.3 Chromosomal Abnormalities

Polyploid cells have three (triploid), four (tetraploid), five (pentaploid) or more complete chromosome sets. These are described as 3n, 4n or 5n where n denotes a full chromosome set and 2n describes a diploid nucleus.

Polyploidy is a relatively common occurrence in the plant kingdom. The spontaneous origin of polyploid individuals, by meiotic non-disjunction, has played an important role in the evolution of plants (Culotta, 1991). In contrast to this, naturally occurring polyploids in the animal kingdom are rare.

Polyploidy and binucleate diploidy (2x 2n) are normal features in some mammalian somatic cells. However, there is a large variation in the number of polyploid cells present in specific tissue types, even between species of the same order such as mice and guinea pigs (Brodsky and Uryvaeva, 1985). Some polyploid cells are obligate as they develop a polyploid DNA content regularly during the normal life cycle of the organism. Other polyploid cells develop in response to certain stimuli such as great functional stress or age. For example polyploid cells often occur in cancer, often with an intermediate DNA content present, for example 3n and 4.5n (Zimmet and Ravid, 2000). Aneuploidy is also a common feature of malignant tumours (Barlogie, 1984).

In mice and humans a proportion of the hepatocytes of the liver and cardiomyocytes in the heart, and all megakaryocytes are normally ploypoid (Brodsky and Uryvaeva, 1985; Epstein, 1986; Zimmet and Ravid, 2000). Bladder epithelium cells, fibroblasts and mesothelium have also been reported to be polyploid in mice and humans contain polyploid β-cells of the islets of Langerhans (Brodsky and Uryvaeva, 1985). The polyploid cells in these adult tissues arise during postnatal development, by polyploidizing mitosis (Brodsky and Uryvaeva, 1977). Polyloidy is also achieved in some of

these tissues by an intermediate binucleate diploid cell state, formed by acytokinesis, followed by the production of mononucleate polyploid cells during the next mitotic cycle (Zimmet and Ravid, 2000). The advantage of polyploidy is unknown but it may be to increase the synthetic capability of the cell, caused by an increase in gene copies (Klisch *et al.*, 2000). Another consequence of polyploidy is the enlargement of these cells accompanied by a change in the surface to volume ratio (Brodsky and Uryvaeva, 1977; Epstein, 1986).

During prenatal development polyploidy is normally found in the placental trophoblast, of a variety of mammals including humans, rats and ruminants and is also a normal occurrence in the human amnion (Gardner, 1982; Brodsky and Uryvaeva, 1985; Klisch *et al.*, 2000). In the mouse trophoblast polytene cells are found (Chapman *et al.*, 1972; Snow and Ansell, 1974). Polyteny is the repeated doubling of the number of chromatids in the diploid set of chromosomes, without a subsequent mitosis. This shortened mitotic cycle is frequently called endoreproduction, endoreplication or endoreduplication.

In the mouse blastocyst the cells of the mTE form primary trophoblast giant cells (TGCs), these stop dividing and accumulate huge quantities of DNA by repeated endoreduplications leading to polyteny (Snow and Ansell, 1974; Bower, 1987; Varmuza *et al.*, 1988; Barlow and Sherman, 1972; Chapman *et al.*, 1972). Following implantation some pTE cells spread around the embryo replacing the primary TGCs and become polytene.

The mouse placenta (Fig 1.4) is composed of a maternal tissue layer, the *decidua basalis*, and zygotic cells of both trophoblast and mesoderm origin. The onset of gastrulation in the mouse leads to the formation of the embryonic and the extraembryonic mesoderm from which the allantois and chorionic mesoderm are formed. The allantois fuses to the chorionic plate resulting in the chorioallantoic part of the placenta that occupies the labyrinthine zone. The labyrinthine zone contains embryonic trophoblast cell strands containing maternal blood and it is in this zone that maternal and embryonic circulation comes closest to each other and where gas and nutrient exchange takes place. The hormone and growth factor producing junctional zone, spongiotrophoblast zone and trophoblast giant cell zone isolate the embryo from the mother (Rinkenberger *et al.*, 1997).

Studies of the rat trophoblast have shown that polyploid cells exist in the junctional zone of the placenta in addition to the polytene TGCs. However, it is not known if these cells are polyploid in the mouse trophoblast (Brodsky and Uryvaeva, 1985).

Although polyploid cells are a normal feature in the development of the human placenta, polyploid or aneuploid cells are detrimental to the mammalian fetus. Approximately 2% of humans are born with a genetic defect, half of which are due to chromosome imbalance (Delhanty and Handyside, 1995).

Fig 1.4: Diagram of the Mouse Placenta

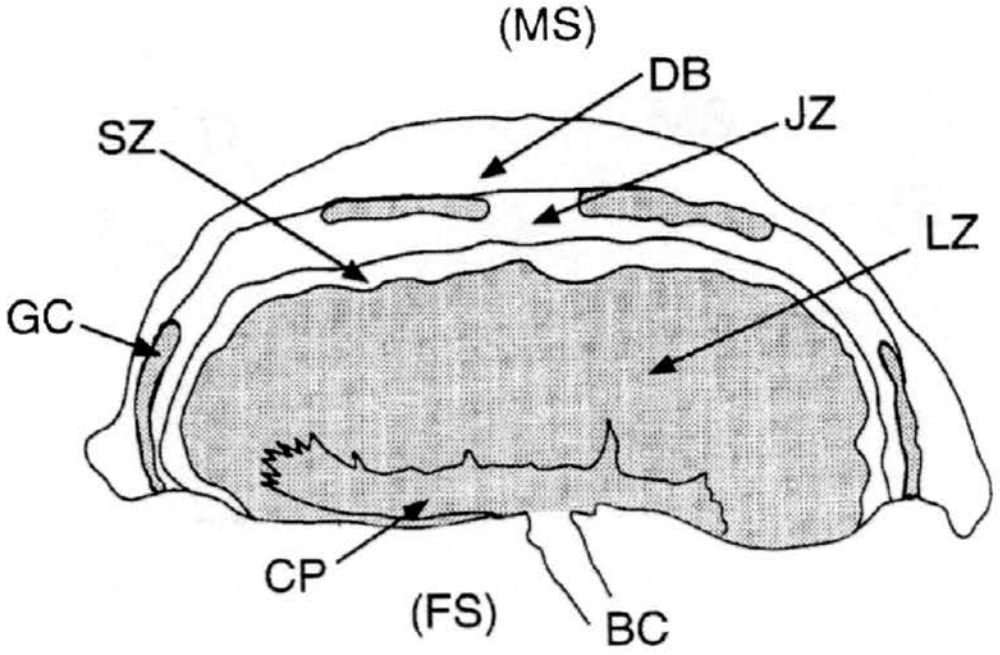

Fig 1.4: Schematic diagram of the mouse placenta at E15.5 from Sapin et al, 1997. BC, blood chord (umbilical cord); CP, chorionic plate; DB, *decidua basalis*; FS, fetal side; GC, giant cells; JZ, junctional zone; LZ, labyrinthine zone; MS, maternal side; SZ, spongiotrophoblastic zone.

Polyploidy, including tetraploidy in full or mosaic form is a very rare abnormality in live born human infants and very few are detected prenatally as the majority are spontaneously aborted (Kohn *et al.*, 1967; Kelley and Rary, 1974; Golbus *et al.*, 1976; Wilson *et al.*, 1988; Eiben *et al.*, 1990; Alonso *et al.*, 2002). Triploid/diploid mosaics often have congenital asymmetry due to an unbalance of the sex chromosomes (Gardner, 1982). The majority of trisomies do not survive and are responsible for approximately 75% of early pregnancy failures (Goldstein *et al.*, 1996).

In the mouse all trisomies have been experimentally produced. With the exception of trisomy 19, TS19, these do not survive beyond birth (Gropp, 1976; Epstein, 1985; Dyban and Baranov, 1987). Likewise experimentally produced mouse 4n embryos do not normally survive. Tarkowski *et al* (1977) found that 4n embryos failed to survive beyond 10 days in utero, whereas Henery *et al.* (1992) produced 4n embryos that survived up to 14 days in utero. Tetraploid liveborn mice have been produced, however they were eaten shortly after birth (Snow, 1975).

Thus polyploidy is a normal feature in certain types of extraembryonic and adult tissue during mammalian development. However, aneuploidy and polyploidy are not associated with normal fetal development. Despite this polyploid and aneuploid cells are frequently found in human preimplantation embryos.

1.4 Chromosomal Mosaicism in Preimplantation Embryos

Mixoploidy, mosaicism of diploid/polyploid or diploid/aneuploid cells, has been shown to occur in preimplantation embryos of several mammalian species, including humans and cattle (Delhanty *et al.*, 1997; Viuff *et al.*, 1999). These chromosomal abnormalities can arise before the 2-cell stage, during gametogenesis or fertilization, and be subsequently corrected in some cells following the 2-cell stage resulting in mosaicism. Alternatively chromosomal errors can arise in some cells during embryogenesis (Delhanty and Handyside, 1995). The high incidence of chromosomal errors in human embryos could be due to the lack of cell cycle check points during the early cleavage stages of the preimplantation human embryo (Harrison *et al.*, 2000).

Studies of chromosome abnormalities in bovine embryos using fluorescent in situ hybridization (FISH) have revealed that a high percentage of bovine blastocysts are mixoploid. It has been found that the most common chromosomal abnormalities in cattle embryos are diploid/triploid (2n/3n) and diploid/tetraploid (2n/4n) mosaics (Viuff *et al.*, 1999). Viuff discovered that 72% of in vitro produced (IVP) bovine blastocysts were mixoploid, however the majority of these mixoploid blastocysts (83%) contained low levels (less than 10%) of polyploid cells, with only a small proportion, 4%, containing more than 25% polyploid cells (Viuff *et al.*, 1999). This study also revealed a lower level of mixoploidy in bovine blastocysts developed in vivo, 25%, all of which contained less than 10% polyploid cells. However, this is still a relatively high frequency of mosaicism suggesting that mixoploidy is a common occurrence both in vivo and in vitro produced bovine embryos. It is

possible that the in vitro culture of either bovine oocytes or embryos is responsible for the increase in mixoploidy in bovine IVP embryos.

Several studies have shown that mixoploid bovine embryos are morphologically normal and develop at the same rate as diploid embryos (Kawarsky *et al.*, 1996; Viuff *et al.*, 1999; Viuff *et al.*, 2000). Further studies have also indicated that mixoploid embryos are capable of normal development, and the presence of polyloid cells does not appear to influence the establishment of pregnancy (Viuff *et al.*, 2000; Viuff *et al.*, 2001). A pregnancy rate of 64% from blastocysts with a mixoploidy level of 72% indicates that mixoploidy is of minor importance in the establishment of pregnancy (Viuff *et al.*, 2000).

In contrast polyploid bovine embryos develop at a slower rate, possibly as a result of an increase in the duration of the cell cycle due to an increase in the time taken to replicate the cells chromosomes (Kawarsky *et al.*, 1996). Polyploid bovine embryos arrest during the third cell cycle, this is prior to the major activation of the cattle embryonic genome (Viuff *et al.*, 2000). Therefore it is interesting that the presence of polyploid cells in mixoploid bovine embryos does not appear to affect the developmental rates of these embryos.

It has been demonstrated that chromosomal abnormalities occur in early preimplantation development in human embryos (Angell *et al.*, 1987; West *et al.*, 1987; West *et al.*, 1988). Subsequent studies using FISH on spare

preimplantation embryos derived by in vitro fertilization (IVF) have demonstrated that chromosome mosaicism is common in human embryos (Delhanty *et al.*, 1993; Delhanty *et al.*, 1997; Laverge *et al.*, 1997).

Mixoploidy has been observed in human morulae and blastocysts with earlier studies, using FISH with three probes, showing mixoploidy frequencies of approximately 30.8% of morulae and 29.3% of blastocysts (Benkhalifa *et al.*, 1993). As early FISH analysis revealed chromosomal mosaicism was common in human preimplantation embryos, FISH has been used with a variety of chromosome probes in the analysis of spare IVF embryos showing a high incidence of mosaicism (Delhanty *et al.*, 1993; Delhanty *et al.*, 1997; Laverge *et al.*, 1997). In one study analysing only normal developing embryos, approximately 30% were shown to be mosaic with a minor cell line showing aneuploidy or ploidy abnormalities (Harper *et al.*, 1995; Delhanty *et al.*, 1997). Subsequent more advanced studies using multicolour FISH of 11 chromosomes in 5 sequential hybridisations have confirmed a high incidence of postzygotic chromosomal mosaicism including both aneuploid and ploidy mosaicism (Harrison *et al.*, 2000). G-banding analysis of human IVF embryos has also revealed a high level of mosaicism, 23%, the majority being diploid/polyploid mosaics (Clouston *et al.*, 1997).

The frequency and types of mosaicism observed in in vitro produced human preimplantation embryos varies. The cause of this is possibly due to differences in certain culture conditions or hormonal stimulation protocols

(Munne *et al.*, 1997). Some couples also have an inherited predisposition towards producing chaotic mosaic embryos. It is also possible that the quality of preimplantation embryos available for use in these studies varied. The fact that IVF patients have difficulty achieving a viable pregnancy might also suggest a reason for the high levels of chromosome abnormalities observed. However, studies analysing IVF embryos from fertile women, requesting preimplantation genetic diagnosis (PGD), has revealed similar results. This indicates these chromosomal abnormalities are a common occurrence among fertile couples (Harper and Delhanty, 1996; Delhanty *et al.*, 1997).

Although the use of FISH has given some insight into the degree of mosaicism in human preimplantation embryos this technique is limited as it is not possible to look at all 23 pairs of chromosomes. A new technique based on whole genome amplification and comparative genomic hybridisation has made it possible to analyse the copy number of every chromosome in almost every cell of a cleavage stage embryo (Wells *et al.*, 1999; Wells and Delhanty, 2000). Using this method to analyse morphologically normal embryos, a high frequency (50%) of mosaic embryos was detected (Wells and Delhanty, 2000). Wells & Delhanty also showed that 25% were chromosomally normal. Therefore, it is interesting that the mosaic embryos could not be distinguished morphologically from the chromosomally normal embryos. It has been shown in previous studies that the second and third highest quality IVF embryos are equally likely to be chromosomally abnormal or normal (Delhanty *et al.*, 1997). This demonstrates that high rates of abnormalities are

tolerated during the early stages of human embryo development.

Although it would be predicted that a high proportion of these mixoploid embryos do not survive, it is possible that some do survive to produce chromosomally normal fetuses. There are several proposed mechanisms, which would exclude chromosomally abnormal cells from the fetus. It is possible that polyploid and aneuploid cells in both human and bovine mixoploid blastocysts are excluded from the fetus by preferential allocation to the trophectoderm.

However, a study examining the degree of mosaicism in the ICM of human blastocysts suggests a mechanism of selection against whole embryos containing abnormal cells as opposed to a selection eliminating abnormal cells from the ICM (Evsikov and Verlinsky, 1998). Using FISH analysis for chromosomes 13, 18 and 21 they found the mosaicism rate in the ICM was not significantly different from the overall blastocyst mosaicism rate of 10.5%. This mosaicism frequency is significantly lower than that of early cleavage stage embryos, which can be up to 50% of 4- to 8-cell embryos. Eviskov & Verlinsky (1998) conclude that a general selection mechanism against mixoploid embryos takes place at the morula-blastocyst transition. It has been suggested that this possibly takes place when the number of abnormal cells reaches a threshold level. However, it should be noted that the presence of abnormal cells in some human blastocysts suggests that in some cases these abnormalities are not detrimental to preimplantation development. Although Eviskov & Verlinsky suggest that a mechanism of

selection for a euploid ICM does not take place it is possible that this type of selection occurs following a general selection against whole mixoploid blastocysts. Thus perhaps there are a large number of mosaic embryos not capable of blastocyst formation due to gross chromosomal errors. Therefore, these embryos would be eliminated during cleavage stages. Following this initial selection there could be selection acting in the blastocyst itself to eliminate abnormal blastomeres.

Following implantation it is likely that there are several possible fates of a mixoploid blastocyst, which could be determined by the proportion of chromosomally abnormal cells and the type of chromosomal abnormality. Mixoploid conceptuses could therefore be spontaneously aborted, produce a low proportion of mosaic fetuses, or produce a chromosomally normal fetus. Confined placental mosaicism (CPM) demonstrates that chromosomally normal fetuses can be produced from a mixoploid conceptus (Lestou and Kalousek, 1998). The experiments in this thesis are designed to determine the mechanisms involved in the production of a diploid fetus from a mosaic preimplantation embryo.

1.5 Human Confined Placental Mosaicism

Confined placental mosaicism (CPM) is a human condition in which chromosomal abnormalities are found in the placenta but not in the embryo. This genetic inconsistency between the fetus and placenta was first described in 1983, and is now a medically recognised condition (Kalousek and Dill,

1983; Lestou and Kalousek, 1998). CPM usually involves trisomies but tetraploidy can also occur (Ledbetter *et al.*, 1992). CPM is identified in approximately 2% of human conceptuses analysed cytogenetically by chorionic villus sampling (CVS). This mosaicism could be incorrectly interpreted to represent the whole conceptus (Kalousek, 1994).

CVS can be carried out between 10 and 14 weeks gestation. It is advantageous as genetic defects can be diagnosed early on, it provides a rapid Karyotype analysis and it is a relatively safe technique. There is a 0.5 % risk of induced pregnancy loss from this method of tissue sampling for genetic diagnosis, which is higher than amniocentesis (Carroll *et al.*, 1999; Jenkins and Wapner, 1999; Eisenberg and Wapner, 2002). The procedure involves the removal of a sample of 10-20mg of chorionic villus. Two types of cells can then be enriched by two different methods. The direct method allows karyotype analysis of spontaneously dividing cytotrophoblasts, which is derived from the TE lineage of the human blastocyst (Hassold, 1980). The long term culture method analyses cells of the chorionic villous stroma, which are descended from the extraembryonic mesoderm (the epiblast lineage of the human blastocyst).

The discovery of CPM has highlighted the need for follow-up genetic diagnosis. Therefore, if a mosaicism is identified by CVS then amniocentesis or fetal blood sampling should follow to differentiate between generalised mosaicism, and CPM (Smith *et al.*, 1999).

There are three types of CPM, which are categorised according to the placental cell lineage, which contains the chromosomal abnormality. Chromosomally abnormal cells can be confined to the cytotrophobast, (Type I), the chorionic stroma (Type II) or both types of cell (Type III) (Kalousek and Vekemans, 1996). Type I CPM is more common than type II, and the occurrence of type III is the lowest. Mosaic types I and II mainly arise through somatic mitotic errors during early development. Non-mosaic type I CPM is usually meiotic in origin. Type III arises mainly by meiotic errors (Kalousek and Vekemans, 1996; Wolstenholme, 1996; Lestou and Kalousek, 1998). The mouse model for CPM analysed in this thesis relates to type I CPM, which is the most common type with the most severe consequences.

The outcome of pregnancies with CPM varies depending on the type of CPM and the specific chromosomal abnormalities involved (Fig 1.5). Severe complications have been documented for cases of type I CPM. Approximately 22% of pregnancies affected by type I CPM have resulted in spontaneous abortion, intrauterine growth retardation (IUGR), intrauterine death, or perinatal morbidity (Vaughan *et al.*, 1994; Lestou and Kalousek, 1998; Johnson *et al.*, 2000; Stipoljev *et al.*, 2001). In contrast, type II CPM mainly results in a normal pregnancy. IUGR and intrauterine death is common in type III CPM, specifically in cases of mosaicism of trisomy 16 (Benn, 1998). Another complication of CPM is uniparental disomy (UPD), where the fetus contains two chromosomes of only one parental origin. This can result in abnormal development if the chromosome involved contains imprinted genes. UPD mainly affects cases with type III CPM and sometimes

Fig 1.5: Trisomy Involvement for human types I, II and III Confined Placental Mosaicism

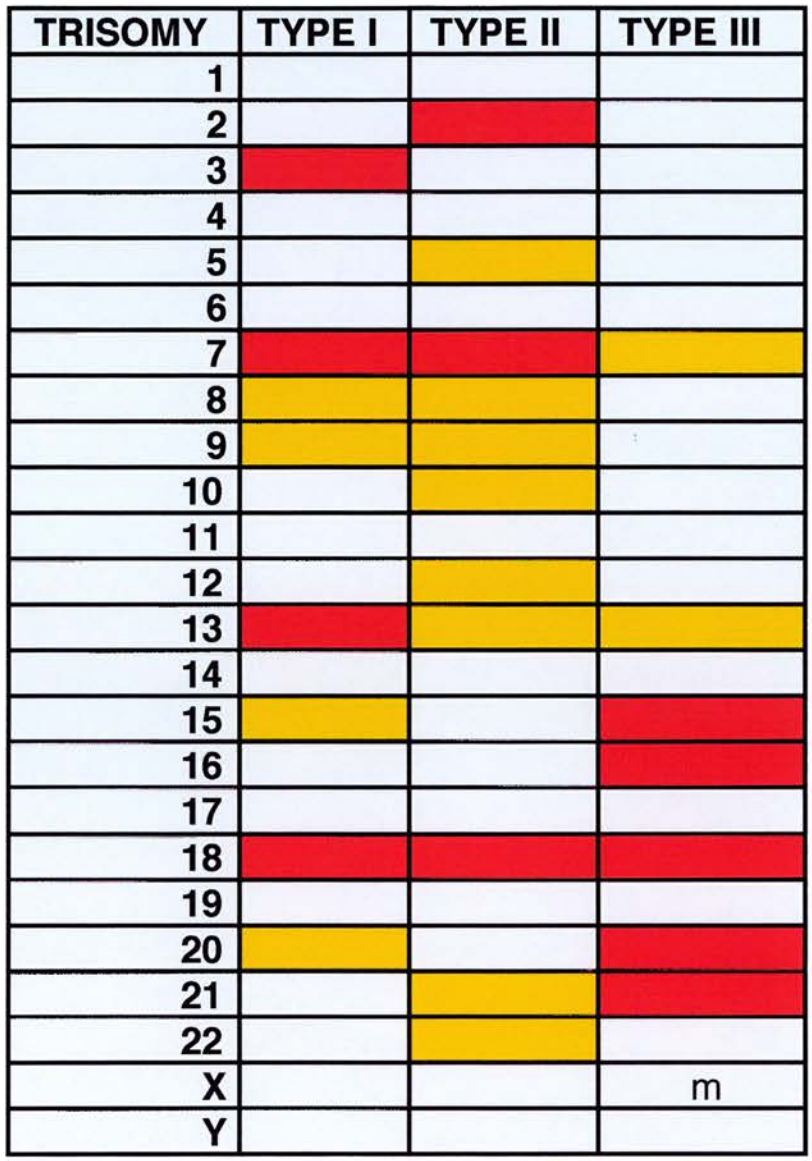

Fig 1.5: Illustration of the frequency of chromosome involvement of reported cases of trisomies for CPM. The colour of shading indicates the percentage of the total of analysed cases where red ≥ 10%, yellow ≥ 3% but < 10%. m indicates a commonly reported monosomy.

Figure adaptated from Lestou & Kalouek, 1998, results taken from two collaborative studies, Ledbetter et al, 1992 & Hahnemann Vejerslev, 1997.

type I CPM. This arises from zygotic "rescue" of a meiotic error, by non-disjunction during an early cleavage stage (Hahnemann and Vejerslev, 1997; Robinson, 2000). The mean maternal age of CPM cases involving trisomic meiotic errors is higher as spindle failure during meiosis is more likely to occur in older women (Robinson, 2000). Chromosome abnormalities in the intrauterine placenta may have an adverse affect on postnatal development therefore it could also be useful to detect CPM at birth by the cytogenetic analysis of the placenta (Lestou *et al.*, 2000).

Individual trisomies tend to be associated with specific types of CPM (Fig 1.5) (Lestou and Kalousek, 1998). This is interesting as it suggests that certain trisomies can be tolerated in the cytotrophoblast but not in the chorionic stroma and vice versa. Most studies have revealed similar trends of trisomy involvement relating to specific types of CPM. However, Wolstenholme, (1996) reviewed that trisomy 8 was only associated with type II CPM. In contrast to this a European collaborative found a similar frequency of trisomy 8 occuring in type I and type II cases (Hahnemann and Vejerslev, 1997).

Type I CPM has also been shown to occur in aneuploid gestations, where a diploid cell line is present in the placental cytotrophoblast. It is possible that the diploid cell line facilitates intrauterine survival. This has most commonly been described for viable trisomies 18 and 13 (Kalousek *et al.*, 1989). The most common chromosomal abnormalities involving the sex chromosomes in type I CPM are monosomies. Tetrasomy X is also relatively common. Trisomy X

however has not been found in conjunction with type I CPM (Kalousek, 1994; Noomen *et al.*, 2001).

The reasons for chromosomally abnormal cells being confined to the placental trophoblast in type I CPM are presently unclear. They may arise preferentially in the trophectoderm lineage after it has differentiated, this is not investigated in the models but is a possibility. Another possibility, which is investigated by the current models, is that two cell populations may arise during preimplantation development and become restricted to this lineage. As has been discussed earlier very few blastomeres contribute to the embryo proper. However, if there was no selection or random allocation against abnormal cells the distinct chromosomal patterns of CPM would not be seen. It could be that type I CPM arises by the preferential allocation of abnormal cells to the trophectoderm during development. Alternatively, there may be selection against the abnormal cells in the epiblast lineage.

1.5.1 Animal Models of Human Confined Placental Mosaicism

It would be useful to have an animal model of CPM to investigate the mechanisms leading to the unbalanced distribution of chromosomally abnormal cells within the human conceptus. Three different types of mouse aggregation chimeras have been analysed to determine if the cells of one embryo contribute preferentially to the extraembryonic membranes.

1.5.1.1 Aneuploid↔diploid Chimeras

Unlike human embryos, spontaneous aneuploidies and mosaicism are not a common occurrence in laboratory animals such as mice and rats (Epstein, 1986). Also, mouse chromosomes are not syntenic with human chromosomes, and the production of mouse trisomy↔diploid (TS↔2n) chimeras is technically demanding. As a result relatively few TS↔2n chimeras have been produced and analysed.

Mouse TS↔2n chimeras have been produced for TS 15, 16, 17 and 19 (Epstein and Travis, 1979; Magnuson *et al.*, 1982; Cox *et al.*, 1984; Epstein *et al.*, 1984; Fundele *et al.*, 1985). The analysis of these chimeras at late gestation revealed they were phenotypically normal, and the TS cells were not excluded from the fetal cells with a TS cell contribution to the majority of embryonic tissues. Therefore, this would suggest that these would not be suitable models of CPM. These chimeras were not specifically analysed as potential CPM models therefore the extraembryonic tissues were not studied in detail. A small series of TS3↔2n chimeras have been produced by our group, and the composition of embryonic and extraembryonic tissues were analysed. These chimeras did not show mosaicism confined to the extraembryonic tissues either (West, in preparation). Although mouse TS↔2n aggregation chimeras would be the mouse models of choice to study CPM, these do not display specific compartmentalisation of TS cells.

1.5.1.2 Tetraploid↔diploid Chimeras

Mouse tetraploid↔diploid (4n↔2n) chimeras and mosaics show a restricted tissue distribution, with an exclusion of 4n cells from the epiblast lineage in mid-gestation chimeras (Tarkowski *et al.*, 1977; James *et al.*, 1995). Therefore, 4n↔2n chimeras have been analysed as a mouse model of CPM.

Tarkowski et al, (1977) produced 4n/2n mosaic mouse embryos composed of two 2n blastomeres and one 4n blastomere. Analysis of these mosaics at mid-gestation showed that the 4n cells were excluded from the fetus, or contributed to less than 4% of dividing cells. Subsequently 4n cells have been used as "carrier" blastomeres to produce fetuses entirely derived from embryonic stem cells (Nagy *et al.*, 1990; Nagy and Rossant, 1993; Wang *et al.*, 1997; Tanaka *et al.*, 2001).

There has only been one report to date of a contribution of 4n cells to the adult tissues of chimeras, produced using standard chimera techniques (Lu and Markert, 1980). In this instance one chimera was retarded in growth with neurological abnormalities and the other chimera was slightly retarded in growth. Tarkowski *et al.*, (2001) found one 4n↔2n chimera from a series of 8 contained 4n cells in the heart and lungs. This chimera was produced by aggregating one 4-cell blastomere with either a two or three-cell 4n embryo. It is therefore likely that the reduced proportion of 2n blastomeres led to a 4n contribution to the epiblast derivatives. Goto *et al.*, (2002) also reported a contribution of 4n cells in live-born mice and in embryonic tissues of mid-gestation chimeras following aggregation of 4-cell stage diploid and

tetraploid embryos. It is possible that the difference in age between the 2n and 4n embryos led to a contribution of 4n cells in the epiblast derivatives, as the 2n embryo was produced a day later than the 4n embryo. Other chimeras with a contribution of 4n cells to the epiblast derivatives were also produced by Goto et al (2002), by aggregating a 2n, 8-cell stage, embryo with two 4n, 4-cell stage, embryos. Therefore, there was a reduced proportion of 2n cells to these chimeras. In addition to this the diploid cells carried a Robertsonian X–autosome translocation which might have had an effect on cell allocation.

Mouse 4n↔2n chimeras have been extensively studied as a potential mouse model of CPM in our lab. James et al, (1995) revealed that 4n cells rarely contribute to any tissues of the epiblast lineage but are frequently present in the hypoblast and trophectoderm lineages at 7.5 and 12.5 days of gestation. In comparison to normal diploid chimeras, tetraploid chimeras were smaller at E7.5. However, at E12.5 4n↔2n chimeras only differed from diploid chimeras by having a significantly larger placenta. One possible explanation for this difference in conceptus size is that prior to E7.5 4n cells are eliminated from the epiblast thus resulting in smaller fetuses however by E12.5 they might have caught up with normal diploid chimeras by size regulation mechanisms.

It is possible that selective cell death acts on a few chimeras that have extensive contributions of 4n cells in the epiblast derivatives. A few abnormal E7.5 embryos that had 4n cells in epiblast derived tissues were present but were not seen at E12.5. However, there were no massive

embryonic losses observed at either stages, therefore it is unlikely that selective embryonic death of 4n↔2n chimeras is the main mechanism for eliminating 4n cells from the epiblast of chimeras.

Analysis of 4n↔2n blastocysts, using DNA in situ hybridisation to a β-globin transgene, has shown that 4n cells contribute to all tissues of the blastocyst but make a significantly greater contribution to the trophectoderm, specifically the mural trophectoderm at E3.5 (Everett and West, 1996, 1998) As it is already known that 4n cells are largely eliminated from the epiblast by E7.5, a mechanism for this removal must be acting between E3.5 and E7.5. The contribution of 4n cells to 4n↔2n chimeras was reduced between E3.5 and E4.5 indicating that cell selection was taking place (Everett and West, 1998).

It is possible that the restricted distribution pattern of the tetraploid cells in 4n↔2n chimeras is a result of the blastocyst cavity forming at the tetraploid half of the chimaera. This could be due to over-expression of the genes encoding the Na/K-ATPase, which causes the formation of the blastocyst cavity in the tetraploid cells. However analysis of reconstructed 3-d images of blastocysts did not show strikingly different distribution patterns between 2n↔2n chimeras and 4n↔2n chimeras. In all 4n↔2n chimeras however, some 4n cells were located adjacent to the blastocyst cavity, thus further evidence is needed (Everett *et al.*, 2000).

Studies have shown that tetraploid cells are present in the ICM of 4n↔2n

chimeric blastocysts (Everett and West, 1996). However, due to technical difficulties, Everett and West were unable to differentiate between the epiblast and hypoblast in histological sections.

These studies of 4n↔2n chimeras as a mouse model of type I CPM have given insights into the possible mechanisms taking place to reduce abnormal cells from human fetuses. However, it is still not known if tetraploid cells in the ICM are preferentially allocated to the hypoblast or if cell selection against tetraploid cells is taking place within the epiblast. Therefore, the experiments in chapter 5 were designed to distinguish between these two possibilities.

The 4n embryos that were used to create the 4n↔2n chimeras, studied as models of CPM and in this thesis, were the same age but differed from the diploid embryos in cell size and cell number as well as ploidy. Therefore, these factors may have an effect on the restricted tissue distribution seen in 4n↔2n chimeras.

Previous evidence has indicated that the more advanced, smaller blastomere makes a significantly greater contribution to the ICM than the TE, during embryo development (see Chapter 1.1.3). However analysis of chimeras has revealed conflicting results.

By aggregating a single blastomere from a 2-cell stage embryo to two blastomeres from a 4-cell embryo it was shown that the progeny of the 2-cell

stage blastomere made a significantly greater contribution to outer rather than inner cells (Surani *et al.*, 1984). Therefore, this evidence indicates that in chimeras the smaller more advanced blastomeres have a significantly greater chance of contributing to the inner cells and forming the ICM. Spindle also investigated this by creating giant aggregation chimeras (Spindle, 1982). When an 8-cell embryo was aggregated to three 4-cell embryos the 8-cell embryo contributed more to the ICM than expected by chance. However, results from the reciprocal combination of one 4-cell embryo aggregated to three 8-cell embryos were inconclusive due to technical reasons. When two 4-cell embryos were aggregated to two 8-cell embryos the contribution of the 4-cell embryos to the ICM were not significantly different to the contribution of the 8-cell embryos. These aggregates involved unequal numbers of embryos, which could prejudice the outcome of the experiments.

In contrast, three separate analyses of 4-cell↔8-cell chimeras, failed to show a preference of the 8-cell embryo to contribute to the ICM (James *et al.*, 1995; Everett and West, 1996; Tang and West, 2000). It is possible that differences in cell stage do not affect the contribution of cells in chimeras. Alternatively it is possible that in these instances there was insufficient time for spatial reorganisation to occur.

Tang *et al.* (2000) however did show that, in a one cell embryo aggregated to a blastomere from a two-cell embryo, the smaller blastomere contributed more to the ICM. They also showed that 4n cells, which differed in ploidy but not in cell size or cell number from cells of the aggregated partner 2n

embryo, made a significantly greater contribution to the mTE than the ICM. Therefore, it was concluded that both ploidy and cell size are likely to affect the allocation of 4n cells in 4n↔2n chimeras.

It is possible that 4n cells divide at a slower rate than 2n cells. This could be a factor responsible for reducing the percentage of 4n cells in the epiblast derivatives at mid gestation. Polyploid bovine embryos develop at a slower rate than diploid embryos (Kawarsky *et al.*, 1996). However, studies on mouse embryos have given conflicting results. Koizumi and Fukuta, (1995) demonstrated that the cell cycle of 4n cells, produced by cytochalasin B treatment, were longer than 2n cells. However, Henery and Kaufman, (1991) showed there was no difference in doubling times of 4n embryos, produced by electrofusion, compared to 2n embryos.

1.5.1.3 Unbalanced Chimeras

Another possible mouse model of CPM is an unbalanced aggregation chimera combination. Initial analysis of the contribution of coat pigmentation in different series of mouse aggregation chimeras revealed that some inbred strains including BALB/c tended to show a poor contribution (Mullen and Whitten, 1971). In E12.5 BALB/c↔(C57BL x CBA)F_2 chimeras, aggregated at the 8-cell stage, the BALB/c component was underrepresented typically contributing less than 20% of the chimera (West and Flockhart, 1994). This was true of the fetus, placenta, yolk sac endoderm, yolk sac mesoderm and trophoblast overlying Reicherts membrane. This showed that the BALB/c

cells were underrepresented in the derivatives of three main lineages of the blastocyst: polar trophectoderm (pTE), epiblast and primitive endoderm (Fig 1.1). However, the mural trophectoderm (mTE) contributes little to the 12.5 day conceptus, therefore it is possible that the BALB/c cells are preferentially allocated to the mTE. In 20 out of 34 chimeras analysed, BALB/c cells were not present in the fetus but contributed to at least one of the extraembryonic tissues. This raises the possibility that BALB/c unbalanced chimeras could provide another mouse model that is relevant to CPM. It is, therefore, of interest to determine whether the BALB/c cells are preferentially allocated to the mTE or depleted from all lineages.

It has been shown that the lower contribution of BALB/c embryos to chimeras cannot be attributed to the death of chimeras with a significantly higher proportion of BALB/c cells (West *et al.*, 1995). This is because the proportion of pre or post-implantation losses is not significantly higher in BALB/c chimeras than in other series of chimeras. More recently it has been shown that acute selection during size regulation does not cause BALB/c cells to be depleted in BALB/c chimeras. Tang and West, (2001) showed that the BALB/c strain made a poor contribution to the tissues of mid gestation chimeras made from aggregates of two half embryos when size regulation was absent or minimal (Tang et al, 2000).

In a previous study, Dvorak *et al.* (1995), also showed a significantly lower contribution of BALB/c cells in the embryonic and extra-embryonic tissues of E7.5 C3H/HeN↔BALB/c chimeric conceptuses. An overall reduction of

BALB/c cells was not seen at the E3.5 blastocyst stage. However, they did not analyse late or expanded blastocysts or look specifically for preferential allocation of cells to the mTE within the chimera.

There is little cell mixing at the blastocyst stage (Garner and McLaren, 1974; Dvorak *et al.*, 1995; Gardner and Cockroft, 1998). However, it is possible that the blastocyst cavity forms within the BALB/c half of the chimera resulting in a high proportion of BALB/c cells confined to the mTE, as discussed for 4n↔2n chimeras in Chapter 5.

1.6 Aims of the Study

The aims of this study were to investigate the fate of 4n cells in 4n↔2n chimeras and to investigate the fate of BALB/c cells in chimeras. Experiments were designed to determine if 4n cells are present within the epiblast region of 4n↔2n chimeras and to determine if BALB/c cells are preferentially allocated to the mTE of aggregation chimeras.

The analysis of these mouse aggregation chimeras (in chapter 5 and 6 of this thesis), involve the use of confocal microscopy and tauGFP mouse embryos. Therefore, this thesis also includes an evaluation of this method of chimera analysis and further characterisation of the transgenic mice used. Chapter 3 describes the use of confocal microscopy, in particular the establishment of a new technique used to analyse GFP preimplantation embryos. The use of a possible live cell marker is also analysed. The experiments in chapter 4 were designed to determine if tauGFP embryos are suitable for use in mouse

aggregation chimeras. This was by establishing if the onset of zygotic expression occurred at a suitable stage and further characterising both transgenic mouse lines.

Chapter 2: Materials and Methods

Methods that only apply to one chapter are described in the appropriate chapter. Methods that are used more widely are described below.

2.1 Animals

2.1.1 Mouse Strains

Details of the mouse strains used in these experiments are described in Table 2.1.

Abbreviated Stock names	Detail	Genotype		
		albino	gfp	Gpi 1
AAF_1	(BALB/c × A/J)F_1 hybrid	c/c	-/-	a/a
BALB/c	BALB/c/Eumm	c/c	-/-	a/a
BF_1	(C57BL/Hsd × CBA/Ca)F_1 hybrid	C/C	-/-	b/b
CF_1	(CC × CALB)F_1 hybrid	c/c	-/-	c/c
GFB	BF_1 × TgTP6.3	C/C	+/-	b/b

Table 2.1 Details of mouse stocks

Female genotypes are shown first in any cross. Transgenic tauGFP mice (strain TgTP6.3 on a largely outbred MF1 background; Pratt et al (2000) were maintained by crossing to (C57BL/Hsd × CBA/Ca)F_1 hybrid ("BF_1") mice. The stock was made homozygous for *Gpi1*$^{b/b}$ and hemizygous for the GFP transgene. "CF_1" mice used as embryo recipients are F_1 hybrids of two homozygous c,

Gpi1^{c}*/c*, *Gpi1*^{c} strains, which were partially congenic on C57BL (strain "CC") and BALB/c (strain "CALB") genetic backgrounds respectively, (West, 1984). The (C57BL/Hsd × CBA/Ca)F_1 hybrid (BF_1) female mice were purchased from the Anne Walker animal facility, University of Edinburgh. These mice were also used as embryo recipients and were mated with vasectomised males at the Anne Walker animal facility, University of Edinburgh. All other animals were bred and maintained in the Medical Faculty Animal Area (MFAA), Universily of Edinburgh, with a light dark cycle of 14 hours light (05:00h-19:00h) and 10 hours dark (19:00h-05:00h).

2.1.2 Superovulation

Adult female mice were superovulated by intraperitoneal injections of 5 i.u. pregnant mare's serum gonadotrophin (PMSG) at midday, followed by 5i.u human chorionic gonadotrophin (hCG) 48hrs later. The females were mated individually to males, and checked for the presence of a vaginal plug the following morning; this is designated 0.5 days post coitum.

2.1.3 Production of Pseudopregnant Females

CF_1 females were selected in oestrus and mated to vasectomised CF_1 males. Those females with a vaginal plug the following morning were designated as 0.5 days of pseudopregnancy. Some pseudopregnant BF_1 females were purchased

from the Anne Walker animal facility, University of Edinburgh (see section 2.1.1).

2.1.4 Embryo Transfer to Produce E12.5 Chimeras

On 2.5 days of pseudopregnancy these females were anaesthetised with 0.25ml per 30g body weight of a 1:1 (v/v) mixture of a 50% aqueous dilution of Hypnorm (0.315 mg/ml fentanyl citrate and 10mg/ml fluanisone; Janssen Pharmacuticals) and a 50% aqueous dilution of Hypnovel (2mg/ml midazlam hydrochloride; Roche). Between 6 and 8 chimeric morula or blastocysts were transferred into a uterine horn. The resulting pregnancies were timed according to the pseudopregnant females, with the day of transfer being E2.5.

2.2 Embryos

2.2.1 Preimplantation Embryo Collection

Plugged females were sacrificed by cervical dislocation at 0.5 days for 1-cell embryos, 1.5 days for the collection of 2-cell embryos, 2.5 days for 8-cell embryos.

1-cell embryos were flushed from the oviducts in KSOMH handling medium and transferred to hyaluronidase (Sigma, 100 I.U. per ml PBS) to remove the cumulus cells (Appendix B). Embryos were subsequently washed in KSOMH handling medium and cultured in KSOM (Appendix B).

2-cell embryos were flushed from the oviducts and 8-cell embryos were flushed from the oviducts or uterus using M2 or KSOMH handling medium (Appendix A & B). Embryos were subsequently washed in handling medium and kept in either M16 or KSOM culture medium before use (Appendix A & B).

8-cell embryos that were heterozygous for the GFP transgene were identified using a Leica fluorescent dissecting microscope.

2.2.2 Chimera production

The zona pellucidae was removed from the embryos using acid Tyrode's solution, pH 2.5, at 37°C (Nicholson, 1975). Embryos were subsequently washed in M2 or KSOMH handling medium. Aggregation chimeras were produced by standard procedures involving aggregation of pairs of zona-free embryos (Tarkowski, 1961), in the presence of phytohaemaglutinin (Mintz *et al.*, 1973). Pairs of zona free embryos were pushed together in individual drops of medium containing phytohaemagglutinin (PHA, M-form, Gibco, cat. No. 10576-015) which was made up by adding one part PHA to 19 parts M2 or KSOMH (Pratt, 1987). Aggregates were then washed in M2 medium or KSOMH.

Chimeras were cultured in M16 or KSOM culture medium under mineral oil (SIGMA) or silicon oil (BDH) in an incubator (37°C, 5% CO_2 in air) prior to either culture on the confocal microscope, imaging without culture on the confocal

microscope or embryo transfer. Methods used to culture embryos in an incubation chamber on the confocal microscope are described fully in chapter 3.

2.3 Confocal Microscopy

Images were captured with a Leica TCS NT confocal system attached to a DMIRBE inverted microscope. GFP images were taken using the 488nm line of excitation. The emission signal was collected by passing through a 525/50 BandPass filter, which limits the collection of emission wavelengths to between 500 and 550. TRITC images were taken using the 568nm line of excitation. The emission signal was collected through a 600/30 BandPass filter, which collects emission wavelengths between 585 and 615nm. Brightfield images were acquired simultaneously, with the transmitted light photomultiplier detector. These images are non-confocal.

2.4 Statistical analysis

As chimera data is always presented as percentages and the resulting chimerism is often not normally distributed, this was analysed using non-parametric statistical tests. The Kruskal-Wallis test (a non-parametric, 1-way analysis of variance type of test) was used to compare percentage data among three or more groups. If this revealed significant differences among the groups, multiple pairwise tests were performed using the Mann-Whitney U-test (a non-parametric equivalent of the unpaired t-test) to identify the sources of the variation.

Parametric tests were used to compare physical parameters such as fetal and placental weight and crown rump length. The unpaired t-test was used to compare two groups.

Statistical tests were performed on an Apple Macintosh computer using the statistical package 'StatView 4.0' (Abacus Concepts Inc., Berkley, USA). A routine established on an Excel spreadsheet (Microsoft corporation) was used to calculate Chi-square values.

Chapter 3: Techniques used to image live preimplantation embryos using confocal microscopy

3.1 Introduction

This chapter is intended to provide an overview of the methods that were established to culture and image live preimplantation embryos on a confocal microscope.

Confocal microscopy is a useful tool for imaging live preimplantation embryos as it allows direct non-invasive serial optical sections from intact specimens. Single photon confocal microscopy was chosen for the following studies as conventional fluorescent microscopy generates out-of-focus blur. This is because the entire field of view of a specimen is illuminated in conventional fluorescence microscopy. Therefore, this excites fluorescence emmissions or reflections throughout the whole depth of the specimen. Much of the light collected by the objective lens to form the image comes from regions above and below the selected focal plane thus seriously degrading the image by reducing the sharpness and contrast.

In contrast to this, confocal microscopy virtually eliminates out-of-focus blur. Fig 3.1 shows a schematic diagram of the confocal principle. Light from the confocal laser is passed through a pin-hole to a dichroic mirror which splits the laser light into one, two or three separate wavelengths. The light is then passed through an objective lens, which focuses the wavelength to a specific point on a focal plane of the specimen. The beam is scanned in an x-y

Fig 3.1:
The Confocal Principle

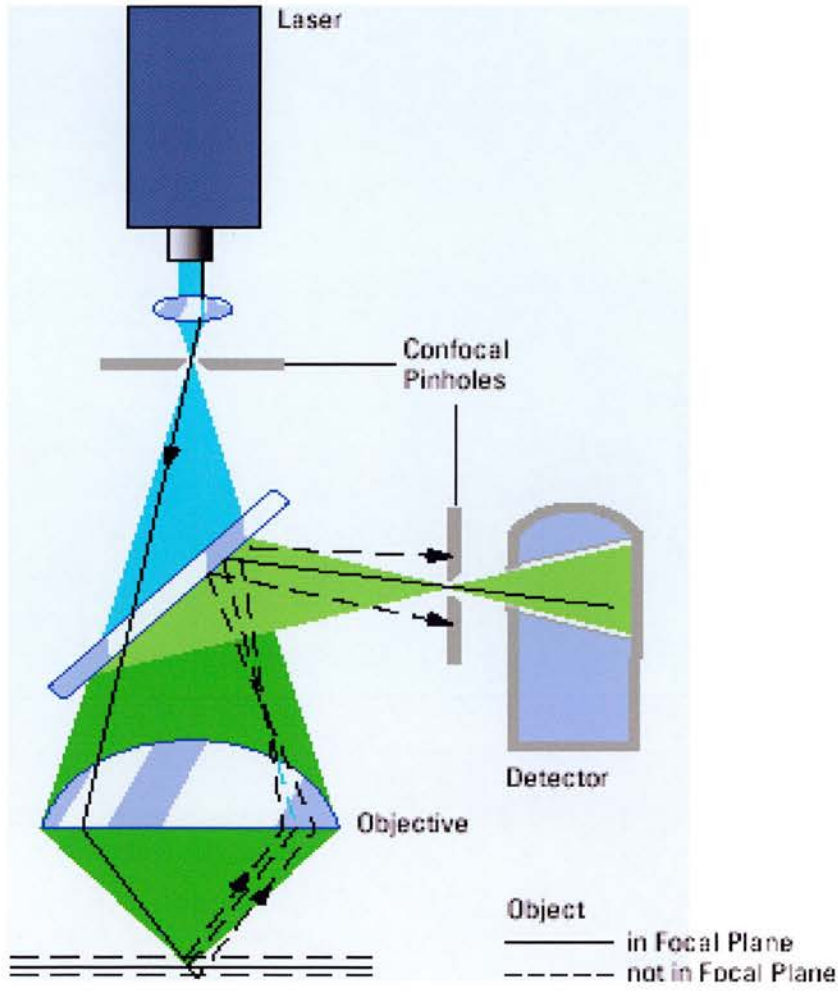

Fig. 3.1:
Schematic diagram of the confocal principle, showing the path of the laser light to the specimen and the resulting emission signal. (Figure from Leica Microsystem Web site http://www.leica-microsystems.com)

direction by a galvanometer. Emission from the fluorochromes is focused back through the lens towards a confocal aperture. For each optical lens there is an optimum confocal aperture size, which rejects as much out-of-focus light as possible without compromising the image. The light is then passed through the first of a series of filter blocks. The first of these is a short pass filter block which selects light below 580nm. This emission is further refined by passing through a bandpass filter which selects for wavelengths between 500-550nm (green fluorescent light). Light above a wavelength of 580nm passes through to the next short pass filter block, which selects for wavelengths under 660nm. This part of the emission is passed through a bandpass filter, which selects light of a wavelength between 585 and 615nm (red fluorescent light). The remaining light above 660nm is reflected by a mirror and passed through a long pass filter, which only collects emissions above 665nm (Cy5). Each selected range of wavelengths of light pass from the emission filters to a separate photomultiplier tube where the signal is converted by the software into a digital image.

A series of optical sections can be generated by moving the sample in the z-axis in a series of measured steps, while scanning in an x-y direction. A projected focus image can be built up by stacking these images together using the computer software. Providing enough sections are imaged throughout the sample, a 3D image can be generated and rotated using computer software.

For conventional fluorescent microscopy a maximum usable thickness of tissue section is approximately 10 microns whereas relatively thick objects such as mouse blastocysts can be imaged using confocal microscopy.

Several of the experiments described in later chapters require tauGFP preimplantation embryos to be analysed on the confocal microscope during constant time intervals over a period of 24hrs. A method for culturing preimplantation embryos on the heated stage of the inverted confocal microscope was established, to allow the same embryo to be analysed by time-lapse confocal microscopy during different stages of development. This is a useful technique as the embryos can be imaged in the same orientation over an extended period of culture. It is also beneficial, as it does not involve sudden changes in temperature and CO_2 levels, which could be caused by removing embryos from a culture incubator for imaging.

As tauGFP was being used as a marker in chimeric preimplantation embryos the possibility of using a fluorescent vital dye to label the other half of the chimera was also evaluated. This would especially benefit the analysis of images taken, as the transmitted light imaged is not acquired using confocal microscopy thus generating out-of-focus blur. Therefore, in-focus sections of the non-tauGFP part of the chimera could be generated. It would therefore be possible to produce surface rendered objects from a stack of optical sections using advanced computer software (e.g. Imaris software packages, Bitplane). This would be useful to analyse the compositions of mouse

blastocysts as it would be possible to calculate volumes from 3D surface rendered objects using this software.

Several vital dyes have been assessed for use as cell markers for pre-implantation embryos. To be a useful marker for GFP chimeras they must complement GFP and not interfere with pre-implantation development.

3.2 Materials and Methods

3.2.1 Confocal Microscopy

Images were captured on the confocal microscope as described in section 2.3. Details of the culture dishes and methods used for time-lapse microscopy are described in section 3.3.1 of this chapter.

3.2.2 Preimplantation Embryos

Details of the mouse strains used in this chapter can be found in Table 2.1. Embryos were collected, cultured and aggregated as described in section 2.2. Blastocysts were staged according to the size of the cavity. In early blastocysts the blastocyst cavity compromised <50% of the total area, the cavity was 50-75% of the total area in late blastocysts and greater than 75% for expanded blastocysts (see chapter 6, Fig 6.2).

3.2.2 Staining of Embryos with Vital Dyes

The SYTO red sampler kit containing 7 SYTO dyes, SYTO 17 and SYTO 59-64, which stain the nucleus red, was purchased from Molecular Probes, Netherlands (cat no s-11340). 5mM stock solutions were diluted in M2 handling medium. Individual embryos were transferred to drops of diluted dye and incubated for 2 hours (as directed by the Molecular Probes protocol), washed in M2 handling medium twice and transferred to M16 culture medium, using a manual pipette for transferring the embryos. Embryos were also incubated for less than a minute and washed in M2 culture medium, giving the same results.

Lysotracker red, which stains lysosomes was purchased from Molecular Probes, Netherlands (cat no l-7528). Lysotracker was diluted 1:1000 in PBS or M2. 8-cell embryos were incubated for less than a minute and washed in fresh M2 medium.

CM-Di-I was purchased from Molecular Probes, Netherlands (cat no c-7001). This was diluted 1mg in 200µl of ethanol then further diluted 1:10 in 0.3M glucose. Embryos were transferred to a drop of diluted dye and immediately removed and washed in M2 medium.

A PKH-26 dye kit was purchased from Sigma (cat no MINI-26) and diluted 1:500 in diluent C (supplied in the kit). Embryos were immediately washed in M2 medium.

3.3 Results

3.3.1 Time-Lapse Confocal Microscopy of Living Tau-GFP Embryos

Several methods of culturing embryos on the stage of the confocal microscope were tested before establishing the method used in later studies.

As embryos are cultured under mineral oil it was not possible to use an upright confocal microscope. This is because there is a possibility of getting oil on the objective lens and the quality of the image is reduced. The fluorescent confocal laser image is seriously degraded through plastic, so several types of culture dishes were evaluated to allow scanning from an inverted confocal microscope.

Imaging Coverwell perfusion chamber gaskets (Molecular Probes cat no c-24727) (Fig 3.2a) were sealed to tissue culture flasks (Iwaki, cat no. 3100 025) with a hole mechanically punched out of the base (Fig3.2b). Embryos were transferred to a pre-equilibrated drop of culture medium, which was on top of the gasket under mineral oil. The flasks were kept in an incubator, maintained at 5% CO_2 and 37°C, for 1 hour. Following this they were sealed by tightening the top and placed on the heated stage of the confocal microscope. Four time-lapse experiments were initially carried out overnight, however the chimeric embryos did not survive probably because the CO_2 level would not be maintained within the flask at a constant 5%.

Fig 3.2
Embryo Culture Dishes for Time-Lapse Microscopy

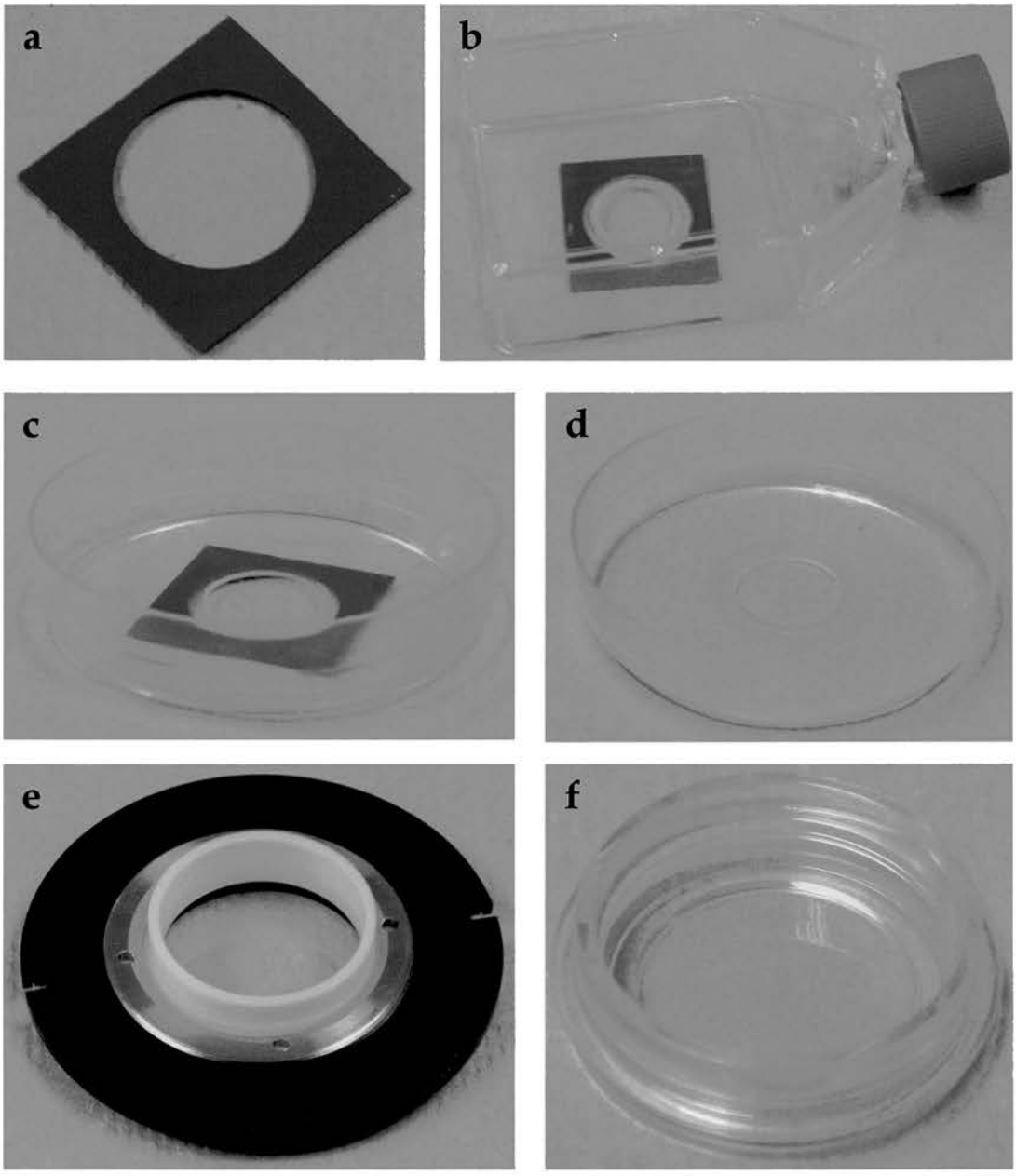

Fig 3.2
a: Coverwell imaging gasket which consists of a 1mm layer of optically clear plastic sealed to a hollow rubber square which attaches to glass or plastic. **b:** Sealed plastic culture flask with a hole punched out of the base and a gasket sealed across the hole. **c:** plastic culture dish with a hole punched out of the base and a gasket attached across the hole. **d:** plastic culture dish with a glass coverslip attached across the hole. **e:** Leica perfusion chamber, with a glass coverslip base, which fits directly onto the microscope stage. **f:** Sterile Willco glass coverslip bottomed microwell dish (35mm diameter, glass 22mm diameter, 9.9mm high).

For subsequent trials an incubation chamber (Leica ref no 11521587) was purchased creating a sealed environment on top of the stage of the confocal microscope (Fig 3.3 & 3.4). Various types of embryo dishes (discussed below) were placed on top of the heated stage (at 37°C) and a foam sleeve was placed around the lens for insulation. An infra-red gas monitor was purchased (Model 3600, Mine safety appliences, Pennsylvania) to maintain the CO_2 level at 5%.

2 successful time-lapses of experimental BALB/c↔(BF_1 x TgTP6.3) and control (BALB/c x A/J)↔(BF_1 x TgTP6.3) chimeras were carried out using an imaging gasket sealed to a plastic petri dish (Sterlin Ltd, cat no.123) with a hole in the base (Fig 3.2c). These time-lapse images were taken using the 10x objective (Fig 3.5a-c) and are included in the analysis in chapter 6. However, as there were problems with the gaskets not attaching to the plastic dish properly it was decided not to use them in case mineral oil leaked onto the microscope.

Three time-lapse studies were carried out using nail varnish to attach a glass coverslip (with a drop of culture medium under mineral oil) to a plastic petri dish with a hole cut in the bottom (Fig 3.2d). This method was not suitable as the nail varnish interfered with the GFP, making the fluorescent image appear grainy. Other methods of attaching a glass coverslip to a plastic petri dish were evaluated. Super glue (Henkel Home Improvement & Adhesive Products, Cheshire) and rubber glue (Weldtite, South Humberside) appeared to stop the growth of embryos, and both aquarium sealant (Building

Fig 3.3
Inverted Leica Confocal Microscope with Incubation Chamber

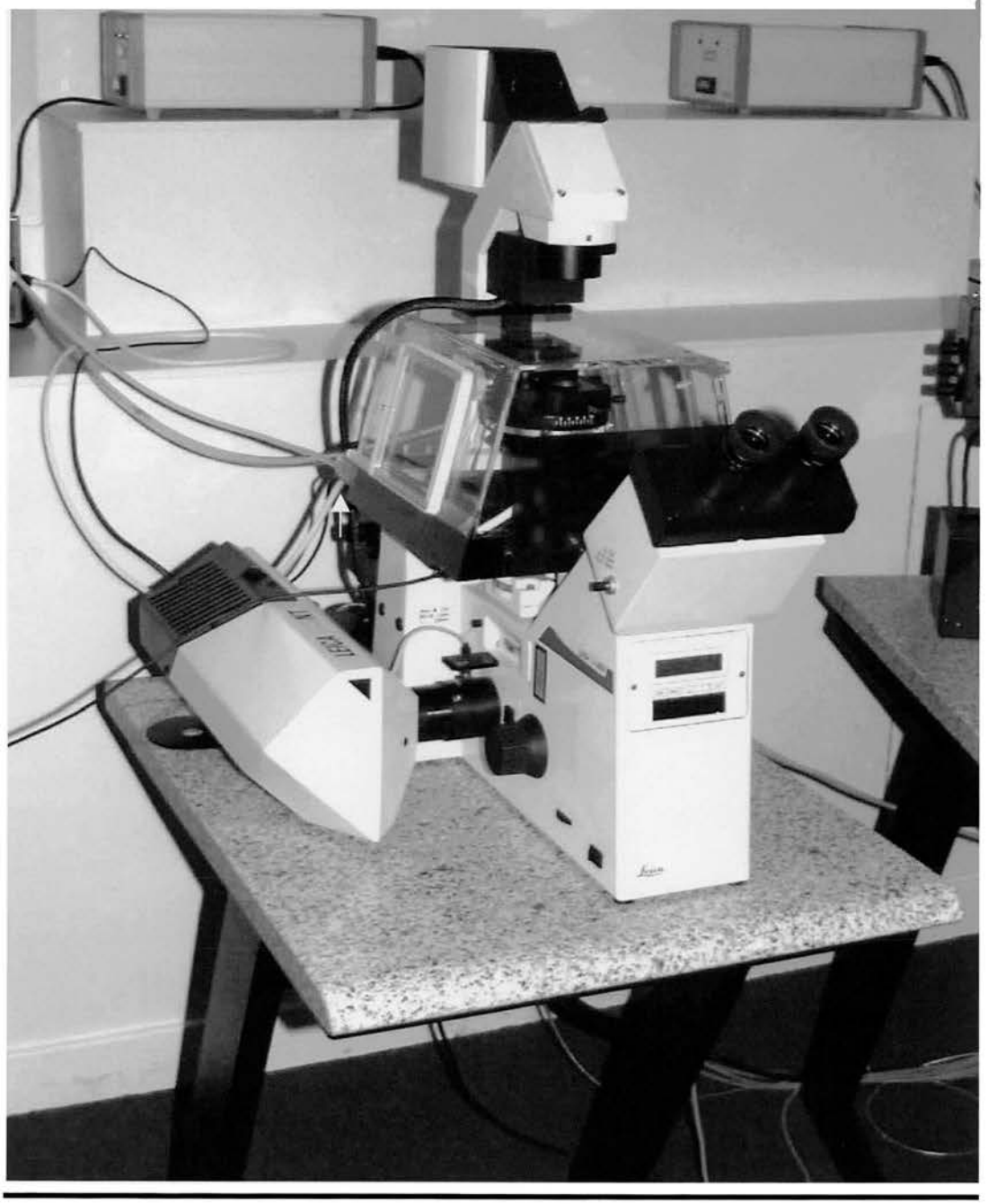

Fig 3.3
The Leica Incubation Chamber for time-lapse confocal microscopy. The plastic tube on the left hand side (arrow) is attached to an infra-red gas monitor (not in view), to sample the CO_2 level. CO_2 is pumped into the chamber from the plastic tube on the right hand side of the chamber when the level drops below 5%.

Fig 3.4
Leica Incubation Chamber

Fig 3.4

Incubation chamber for time-lapse confocal microscopy. An embryo dish is placed on top of the heated stage of the inverted confocal microscope. The heating block can be seen at the right hand side of the chamber (blue arrow). The CO_2 sampler (white arrow) is attached to the infrared gas monitor.

Fig 3.5:
Time-Lapse Confocal Microscopy

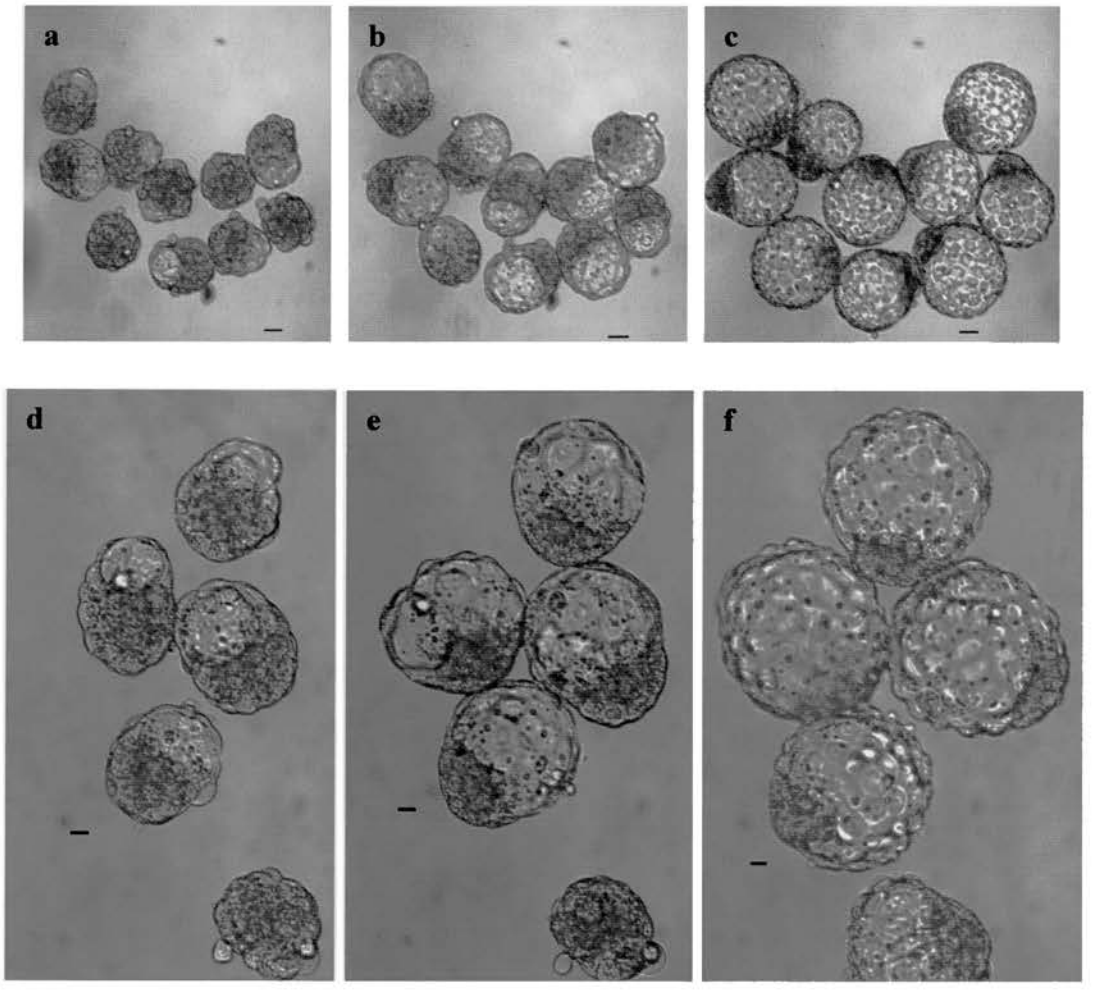

Fig 3.5: Time-lapse confocal microscopy of GFP chimeras cultured from the morula to the blastocyst stage. Overlay images of GFP and transmitted light optical sections. **a-c:** Images, taken using 10X lens, of chimeras cultured on a gasket sealed to a plastic dish. **d-f:** Images, taken using 20X lens, of chimeras cultured in a Willcowell glass bottomed dish.
Scale bar = 15 microns.

Chemical Research Ltd, Manchester) and Aquamount (BDH cat no 362262H) were dissolved by the mineral oil. A POC perfusion chamber (Perfusion, Open and Closed Cultivation Chamber, H. Saur, Rentlingen, Germany, supplied by Leica, D-72734) (Fig 3.2e) was used, which has a glass coverslip in the base. However either the gasket expanded in the chamber or oil on the gasket breached the seal, causing the oil to leak and as a result the drop of culture medium containing the chimeras dried out.

Glass-bottomed Willco microwell dishes (Intracel Ltd, HBSt.3522) (Fig3.2f), were purchased. Tests carried out in a normal incubator, maintained at 5% CO_2 and 37°C, confirmed that preimplantation embryos cultured from the 8-cell stage to the blastocyst stage grow at the same developmental rate as embryos cultured in plastic petri dishes. This confirmed that these glass-bottomed dishes do not affect the growth of embryos from the 8-cell stage to the blastocyst stage and are not affected by the mineral oil.

8-cell embryos were cultured without exposure to the confocal laser. Table 3.1 shows the stages of development achieved following culture of 8-cell embryos in a standard CO_2 incubator and in the incubation chamber without exposure to the laser. After 29hrs of culture the proportion that reached the late or expanded blastocyst stage in the incubation chamber (12/16; 75%) was not significantly different from those in the standard incubator (11/15; 73.3%; χ^2=0.11 ;P>0.999). These experiments show that a comparable rate of development can be achieved over a period of 24-29hrs culture in KSOM in both types of incubator.

Table 3.1: The Stages of Development achieved following Culture in a standard $C0_2$ Incubator, Compared to the Incubation Chamber on the Confocal Microscope without exposure to the laser

Type of incubator	Day and time	No. of embryos in drop	Stage achieved				
			8-cell	Morula	Early Blastocyst	late blastocyst	exp blastocyst
Standard incubator	Day 1. 10.00am	15	15				
	Day 2. 10.00am	15		5	3	5	2
	Day 2. 3.00pm	15		1	3	7	4
Incubation chamber on the confocal microscope	Day 1. 10.00am	16	16				
	Day 2. 10.00am	16		3	3	4	6
	Day 2. 3.00pm	16		2	2	5	7

Table 3.1: Stages of development achieved following 24hrs of culture in a standard CO_2 incubator or the incubation chamber on the confocal microscope without exposure to the confocal laser. $(BALB/c \times A/J)F_2$ embryos were flushed at the 8-cell stage, and cultured in KSOM for 24hrs in a Willco glass coverslip bottomed microwell dish.

Time-lapse confocal microscopy experiments of embryos cultured in these dishes within the incubation chamber, have been successful (Fig 3.5d-f). However, sporadic problems were encountered when trying to culture embryos on the confocal microscope using this technique. Table 3.2 shows the stages of development achieved following the culture of chimeric embryos for 24hrs using this system, compared to culture in a normal CO_2 incubator. Chimeric embryos were cultured from the compacted morula/ early blastocyst stage to the late/ expanded blastocyst stage over a period of 24hrs. 5 optical sections at a wavelength of 488nm were taken every 20mins using the laser scanning confocal microscope. Table 3.2a shows that 73.3% of 75 chimeric embryos reached the blastocyst stage and 60% reached the expanded blastocyst stage. However 12% did not survive to form a late blastocyst and 14.7% of the blastocysts had started to collapse and die. Some of the chimeras that were cultured in the incubation chamber were slightly delayed, at the late blastocyst stage, compared to the chimeras that were cultured in the normal incubator (Table 3.2b). All 16 of the chimeras cultured in the normal incubator formed expanded blastocysts. Four of 14 time-lapse experiments failed to produce any expanded blastocysts. This could be due to sporadic technical failure (discussed below). If these experiments are ignored, 77.6% of 58 blastocysts reached the expanded blastocyst stage. The proportion of expanded blastocysts produced after exposure to the 20x lens (excluding these four failed experiments) was not significant than the proportion of expanded blastocysts in the control experiment (45/58 versus 16/16; P=0.0582).

Table 3.2: Stages of Development achieved following Time-Lapse Confocal Microscopy or Culture in a normal CO_2 Incubator, from E2.5

a

DATE	objective lens used	No. of embryos in drop	Stage achieved after culture in incubation chamber for 24hrs			
			Abnormal	Abnormal blastocyst	late blastocyst	expanded blastocyst
12.06.00	20x	7		1		6
26.06.00	20x	5		2		3
10.07.00	20x	6				6
25.07.00	20x	5				5
08.08.00	20x	5			2	3
22.08.00	20x	5	1		4	
30.08.00	20x	3	2	1		
20.09.00	20x	5	4		1	
31.10.00	20x	4	1	1	2	
07.11.00	20x	6		3	1	2
14.11.00	20x	3				3
12.12.00	10x	5	1			4
30.01.01	10x	9				9
06.02.01	10x	7		3		4
total		**75**	**9**	**11**	**10**	**45**
% of total			**12.0**	**14.7**	**13.3**	**60.0**

b

DATE	No. of embryos in drop	Stage achieved after culture in incubator for 24hrs			
		Abnormal	collapsing blastocyst	late blastocyst	expanded blastocyst
10.07.00	5				5
25.07.00	3				3
08.08.00	2				2
22.08.00	3				3
20.09.00	3				3
Total	**16**	**0**	**0**	**0**	**16**
% of Total		**0**	**0**	**0**	**100**

Table 3.2: BALB/c or (BALB/c × A/J)F_2 Embryos were flushed and aggregated to (BF_1 × TgTP6.3) embryos at the 8-cell stage, cultured in M16 for 24hrs to the late morula, early blastocyst stage in a normal CO_2 incubator then transferred to a drop of M16 in a Willco glass coverslip bottomed microwell dish and cultured **a:** for a following 24hrs in the incubation chamber for time-lapse confocal microscopy. **b:** for a further 24hrs in a standard CO_2 incubator.
Embryos were classified as abnormal if they were dead or unrecognisable as any preimplantation stage. Blastocysts were classified as abnormal if they had collapsed or contained several degenerating blastomeres.

2-cell mouse embryos were also imaged using the same time-lapse microscopy technique. A single optical section was taken every 15 mins. Table 3.3 shows the stages of development achieved following time-lapse microscopy for 24hrs. A total of 47.9% out of 192 2-cell embryos survived at the 4-cell stage, 2.1% survived at the 3-cell stage and 0.5% reached the 6-cell stage. 7 embryos (3.6%) reached the 4-cell stage but did not survive for the full 24hrs of culture. Therefore, 50.5% of the embryos cleaved and survived, 23.9% failed to survive for 24hrs in the culture chamber and 14.1% remained at the 2-cell stage. Table 3.3 shows considerable variation among time-lapse experiments. Most time-lapse experiments either contained high numbers of embryos that cleaved and survived or high numbers of embryos that did not survive. Although direct controls in a normal incubator were not included for these time-lapse experiments the same batches of culture medium were used successfully on other preimplantation embryos being cultured for different experiments. Sporadic technical failure in the chamber probably accounts for most of the problems encountered (discussed below).

The system is dependent on the correct level of CO_2 and temperature being achieved and maintained. There was a consecutive run of unsuccessful time-lapse series (22.08.00 - 07.11.00) most likely due to a fall in environmental temperature. As a result of this, the heating block was added to the incubation chamber to try and maintain the temperature closer to 37°C.

It is generally known that the laser power can cause damage to live cells during confocal imaging (Squirrell *et al.*, 1999) (discussed in section 3.4 of this

Table 3.3: Stages Of Development Achieved Following Time-Lapse Confocal Microscopy From the 2-cell Stage

DATE	No. of embryos in drop	Stage achieved after culture in incubation chamber for 24hrs						
		Abnormal	Abnorm 2-cell	Abnorm 4-cell	2-cell	3-cell	4-cell	6-cell
27.11.00	14		5				9	
04.12.00	15		12			3		
16.02.01	15	3			4		8	
19.02.01	21	2			4		14	1
12.03.01	12						12	
25.04.01	10				9	1		
14.05.01	10				1		9	
21.01.02	15		2		8		5	
28.01.02	22		15	7				
04.02.02	28				1		27	
04.09.02	8						8	
Total	**170**	**5**	**34**	**7**	**27**	**4**	**92**	**1**
% of totals		**2.9**	**20.0**	**4.1**	**15.9**	**2.4**	**54.1**	**0.6**

Table 3.3: Stages of development achieved following 24hrs of culture in the incubation chamber for time-lapse confocal microscopy. (BF_1×TgTP6.3), (BF_1×TgTP6.4), (TgTP6.3 × BF_1) or (TgTP6.4 × BF_1), were flushed at the 2-cell stage and cultured in KSOM in a Willco glass coverslip bottomed microwell dish in the incubation chamber for time-lapse microscopy from 9am to 9am. Embryos were classified as abnormal if they were dead or unrecognisable as any preimplantation stage. Embryos starting to die at the 2 or 4-cell stage were classified as 2-cell abnormal or 4-cell abnormal.

chapter). As a result of this, the laser power that the chimeric blastocysts were exposed to during the time-lapse microscopy was attenuated to 10%. This did not affect the resolution of the green fluorescent images. An objective lens no greater than 20x was used for time-lapse microscopy. Following a time-lapse experiment some embryos were imaged at a higher resolution, using a 40x lens. These blastocysts usually collapsed shortly after imaging. This was probably due to exposure of a high intensity of laser power. Other blastocysts, which had only been imaged using a 20x lens were transferred to a normal CO_2 incubator. However, these embryos failed to survive culture for a further 24hrs whereas control embryos, which had not been cultured in the incubation chamber or exposed to the confocal scanning laser were still viable (expanded blastocyst stage). Twelve out of 16 (75%) expanded blastocysts, which were imaged using the 10x lens, survived for a further 24hrs in a normal CO_2 incubator.

On some occasions the chimeric blastocysts could not be analysed because they moved out of focus. To counteract this problem the confocal pinhole diameter was widened, which effectively increases the depth of field of the lens. An increase in pinhole diameter causes a consequent loss in image resolution, as more "out-of-focus" signal is collected. However, this did not have a marked effect on the images collected, and prevented the loss of focus previously encountered. Chimeras could not be analysed if they floated out of view, or if it was not possible to see the inner cell mass

In conclusion, a successful time-lapse experiment could be achieved providing the incubation chamber was maintained at approximately 5% CO_2 and 37°C. Although there are several factors that can go wrong using this technique, it has been possible to culture embryos from the 2-cell to the 4-cell stage or from the late morula to the expanded blastocyst stage over a period of 24hrs. This indicates that this technique could be a valuable tool for the analysis of preimplantation development.

3.3.2 Exogenous Cell Markers For Living Preimplantation Embryos

Pre-implantation embryos were stained with 7 different red SYTO nuclear dyes 17, 59-64 initially at concentrations of 5μM, 100nM and 10nM. 8-cell stage embryos stained with these dyes and imaged on the same day, did not show specific nuclear staining possibly due to penetration problems. There was no visible staining in embryos cultured at a concentration of 10nM. SYTO dyes 17 and 59 were detrimental to embryonic development at a concentration of 5μM. The other SYTO dyes exhibited poor staining with the exception of SYTO 64 at 100nM. Further analysis of GFP embryos stained with SYTO 64 at varying concentrations 100nM, 50nM, 25nM and 12.5nM revealed a diffuse staining throughout the embryo (Fig 3.6 a & b). However, these embryos failed to develop and started to die 24 hours after staining.

Di-I has been previously used for studies without impairing development (Dr. Jenifer Nichols, pers. com.). This dye was assessed as a cell marker for possible use with GFP. However, following aggregation of GFP embryos to Di-I (non-GFP) embryos it was found that Di-I fluoresces in the green

Fig 3.6:
Embryos Stained With Vital Dyes

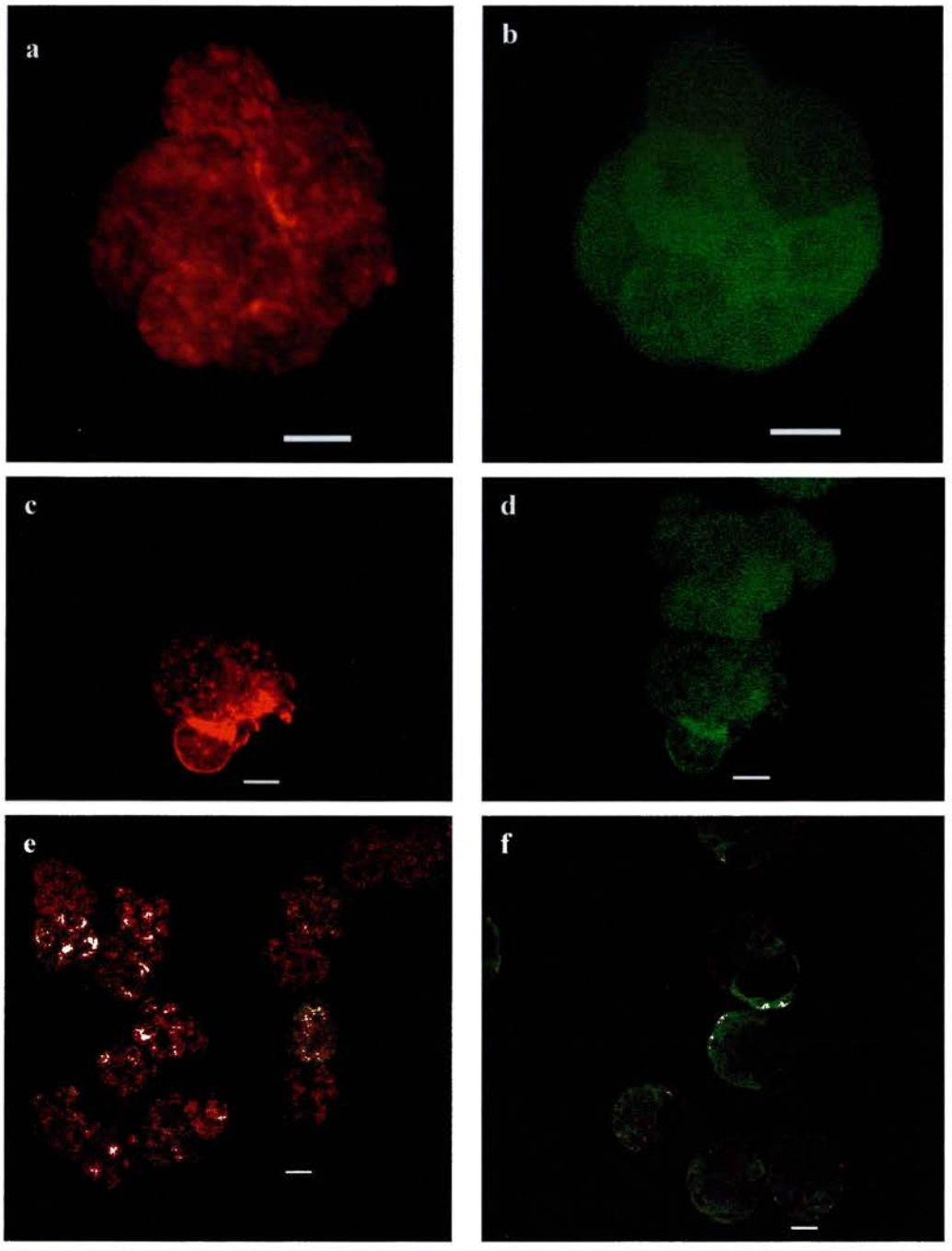

Fig 3.6: Comparison of vital dyes, **a:** 8-cell GFP embryo stained with SYTO 64 at 50nM, showing red fluorescence. **b:** GFP image of the same embryo showing green fluorescence. **c:** Red fluorescent image of a GFP embryo aggregated to a non-GFP embryo stained with Di-I. **d:** Green fluorescent image of the same chimera showing bleed through emission from Di-I in the lower embryo (not GFP). **e:** Image of a GFP↔lysotracker red (non-GFP) chimera showing overlay of green and red fluorescence, the lysotracker red dye has passed into the non-stained GFP embryo. **f:** the same chimeras 24 hrs later showing very little red fluorescence.
Scale bar=30microns

channel. Usually during confocal microscopy emissions from all selected wavelengths are collected simultaneously. When there is cross talk between two fluorochromes it is possible to scan sequentially. This involves exciting and collecting one fluorochrome at a time. However, this did not reduce the level of Di-I fluorescence in the green channel. Therefore Di-I is not suitable as a cell marker for GFP chimaeras as the curve of emission is so wide that bleed-through occurs in the green channel, which could not be separated by sequential scanning (Fig 3.6 c & d).

Embryos incubated in lysotracker red (Molecular Probes), which stains the lysosomes were aggregated to GFP embryos. This marker diffused rapidly into the GFP partner embryo (Fig 3.6 e) and was diluted out after 24 hours (Fig 3.6 f). Therefore, lysotracker red would not be a suitable marker for use in time-lapse studies of chimeras.

PKH-26, a membrane dye, was used to stain non-GFP embryos which were aggregated to GFP embryos. This dye was used in some initial 4n↔2n chimera experiments, which were not analysed (Fig 3.7). This cell dye showed a fragmented labelling of the cell membrane and is not diluted following 24 hours of development. However, it was thought that internalisation of the dye occurred as it appeared to be present within some GFP cells in the chimera (Fig 3.7c). This can be seen more clearly when looking at a 3D rotation image of the chimeric blastocyst. The green fluorescent image of the chimeric blastocyst also shows that there is some bleed-through emission of the PKH-26 dye in the green channel (Fig 3.7d). It

Fig 3.7
PKH-26↔GFP Chimeric Blastocysts

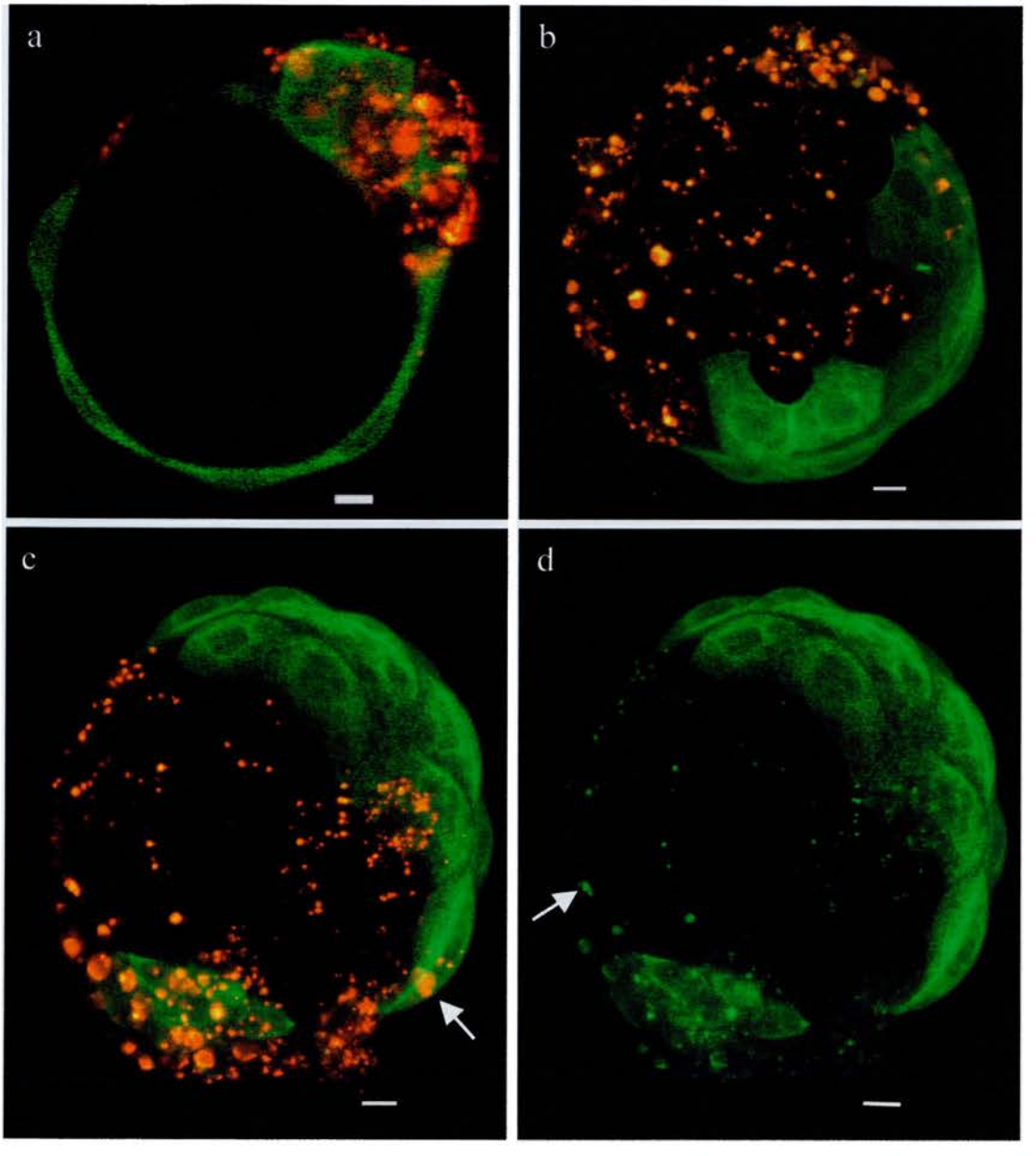

Fig 3.7: PKH-26 stained diploid embryos (8-cell stage) were aggregated to GFP tetraploid embryos (4-cell stage) and imaged at E4.5. **a:** Optical section of a chimeric blastocyst showing overlay of green and red fluorescence. **b:** Projected focus image of a chimeric blastocyst showing overlay of green and red fluorescence. **c:** Projected focus image of a chimeric blastocyst showing overlay of green and red fluorescence. There appears to be internalisation of the PKH-26 dye in some non-stained GFP cells (arrow). **d:** Projected focus image showing green fluorescence, demonstrating bleed through emission from the PKH-26 membrane dye (arrow).
Scale bar =10 microns

was therefore decided that this would not be a suitable embryo marker aiding the analysis of time-lapse chimeras. As it is a membrane dye it would have been necessary to check that it did not affect the allocation of stained cells within the chimera perhaps by altering cell surface properties.

3.4 Conclusion

The experiments carried out in this study indicate that the methods established to culture embryos for the use of time-lapse confocal microscopy is a powerful tool for the analysis of preimplantation stage mouse embryos. The time-lapse experiments carried out have indicated that a stable environment can be produced for the culture of preimplantation embryos for a period of approximately 24hrs. The exposure to high intensity wavelengths using a 20x lens was usually compatible with normal development over this period, as most reached the expanded blastocyst stage. However, the results indicate that imaging using the 20x lens, compared to the 10x lens, does affect the long-term viability of the embryos as they do not survive for a further 24hrs.

Squirrell *et al.*, (1999) previously showed that exposure to high intensity light from laser scanning confocal microscopy affected the development of 2-cell hamster embryos. 2-cell hamster embryos failed to develop over a period of 8hrs during confocal scanning, every 15 mins with a 40x objective lens. They found that the damage was caused directly by the exposure to these wavelengths as opposed to damage caused by the excitation of the fluorophore or the altering of the culture medium. However, these hamster

embryos were exposed to a higher intensity of laser power than the mouse embryos imaged using a 10x or 20x objective lens presented in this chapter.

It was shown that the viability of the embryos was affected solely due to exposure to the confocal laser as embryos grew at the same rate in the incubation chamber as a standard CO_2 incubator. The results from the two time-lapse experiments carried out using the 10x lens also showed that by reducing the intensity of the laser light, 75% of the embryos survive for a following 24hrs in a normal incubator.

It was decided that the vital dyes tested were not suitable to label the non-GFP part of a mouse chimera. Therefore, tauGFP alone was used as a marker to analyse mouse chimeras in the following studies. Fluorescent images were overlayed on transmitted light images and the area of GFP was calculated in optical sections where the ICM could be seen.

Chapter 4: Characterisation of TgTP6.3 and TgTP6.4 Transgenic Mice

4.1 Introduction

The chimera studies in the following chapters of this thesis involve the use of transgenic tau-GFP mouse embryos to analyse cell allocation in aggregation chimeras. The experiments in this chapter characterise the tau-GFP transgenic mice and assesses the use of tau-GFP as a marker in preimplantation stage aggregation chimeras.

Two transgenic mouse lines were produced by Pratt *et al.* (2000), TgTP6.3 and TgTP6.4. These express a tau-GFP fusion protein, under the control of a CAG promoter which is reported to drive ubiquitous expression of fusion constructs when randomly incorporated into the genome. tau is a microtubule associated protein therefore, cytoskeletal features can be visualised in these mice.

Previous characterisation of these transgenic mouse lines has revealed that TgTP6.3 and TgTP6.4 differ. TgTP6.3 mice exhibit strong stable expression throughout all tissues. However, TgTP6.4 mice show expression of tau-GFP in all tissues except parts of the brain (Pratt *et al.*, 2000; Sharp, 2001). Previous analysis of fetal weights has shown that TgTP6.3 heterozygotes weigh significantly less than their wild-type litter mates from E14.5 (M.A. Keighren & J.H. Flockhart, unpublished). This difference increased following weaning

at 21 days. Analysis of weight, between birth and 91 days, showed a significant difference between male TgTP6.4 heterozygotes and their wild-type litter mates. However, there was no significant difference between female TgTP6.4 heterozygotes and their wild-type litter mates at these ages.

Breeding evidence has demonstrated that neither of the tauGFP transgenes are X-linked. Homozygous and heterozygous GFP transgenic mice are not distinguishable by the intensity of GFP fluorescence or, as yet, by molecular tests. Previous (unpublished) test mating experiments have shown that out of 17 GFP-positive offspring of two TgTP6.3 heterozygotes, no homozygotes were present. (When crossed to non-transgenic mice, each of the 17 GFP-positive TgTP6.3 offspring produced some non-transgenic progeny). It is therefore likely that the TgTP6.3 homozygotes do not survive to reproductive maturity. The viability of TgTP6.4 homozygotes is analysed in this chapter.

The experiments in this chapter were designed to further characterise both transgenic mouse lines, in order to determine when the transgene was expressed, for further use in chimeric blastocysts. The viability of adults homozygous for TgTP6.4, and the viability of fetuses homozygous for each transgene, was also investigated.

4.2 Materials and Methods

4.2.1 Genotyping of GFP Mice

The presence of the GFP transgene in adult mice was determined from GFP fluorescence of ear clips using a Leica dissecting fluorescent microscope. The offspring of GFP test matings were genotyped at 1-2 weeks by GFP fluorescence of tail tips. E14.5 whole fetuses were examined under the Leica fluorescent microscope for GFP expression.

4.2.2 Collection of Embryos

Details of the mouse strains used in these experiments are described in chapter 2, Table 2.1.

Adult female mice were superovulated as described in chapter 2, section 2.1.2. Injections of pregnant mare's serum gonadotrophin (PMSG) and chorionic gonadotrophin (hCG) were administered at 12 noon. The time of mating was assumed to occur at 12 midnight (the middle of the dark period). The age of the embryo in hours post coitum (h.p.c) was assumed to be hours post hCG + 12 hrs.

2-cell embryos were collected as described in chapter 2 section 2.2.1. (CF_1×TgTP6.3), (CF_1×TgTP6.4), (TgTP6.3×(BALB/cxA/J)F_2) & (TgTP6.4×(BALB/c×A/J)F_2) embryos were collected in M2 medium at the 2-cell stage and cultured in M16 culture medium. 2-cell (BF_1×TgTP6.3),

(BF_1×TgTP6.4), (TgTP6.3×BF_1) & (TgTP6.4×BF_1) embryos were collected in KSOMH handling medium and cultured in KSOM culture medium.

4.2.3 Time-Lapse Microscopy

2-cell embryos were cultured on the inverted confocal microscope for 24 hours as described in chapter 3. Images were captured as described in chapter 2, section 2.3.

4.2.4 Analysis of Time-Lapse Images

The average pixel intensity was measured using Scion Image computer software (www.scioncorp.com). This was calculated from a region of interest, which was created by drawing round the outline of an embryo, at each time-point. Embryos which did not divide, or became fragmented were not included in the analysis. The graphs show the pixel intensity for each embryo at each time-point. Several time-lapse files were created over the 24hr period as the embryos were re-focused at certain time-points. An initial 1-2hr time-lapse was carried out during which the embryos tended to settle in the culture dish and therefore drift out of focus. The set-up was also re-examined prior to overnight scanning. This resulted in minor differences in the pixel intensities between each time-lapse file, which can be seen on the graphs. These were caused by slight fluctuations in the laser power between the completion of one scan and the start of another. However, this did not affect the general trend of the graphs.

4.2.5 E14.5 Fetal Dissections

E14.5 (TgTP6.3×TgTP6.3), (TgTP6.4×TgTP6.4) & control (TgTP6.3×BF_1) & (TgTP6.4×BF_1) whole conceptuses were dissected from the uterus and the placenta and fetus were isolated using forceps (Richardsons of Leicester).

4.2.6 Statistical Analysis

The following formula, used by Kelly and West, (1996) and based on that used by Lyon, (1970), was used to calculate the percentage of genetically abnormal embryos induced by the experimental heterozygote × heterozygote cross and corrects for the presence of sporadic abnormal embryos in the control heterozygote × wild-type or wild type × heterozygote cross:

$$\left[1 - \left(\frac{\text{Normal embryos in experimental cross}}{\text{Implantation sites in experimental cross}} \Big/ \frac{\text{Normal embryos in control cross}}{\text{Implantation sites in control cross}}\right)\right] \times 100$$

Statistical tests were performed as described in chapter 2, section 2.4.

4.3 Results

4.3.1 Onset of GFP Paternal Expression in TgTP6.3 and TgTP6.4 Preimplantation Embryos Using Time-Lapse Microscopy

Time-lapse confocal microscopy was used to determine when the onset of embryo encoded expression occurred in embryos from crosses between non-GFP females and GFP males. This mating produced approximately 50% transgenic embryos and 50% non-transgenic embryos. Therefore, both types of embryos were imaged during the time-lapse to compare the level of fluorescence.

The paternal onset of expression was assessed visually from the 1-cell stage (9hrs p.c) to early 2-cell stage (33 hrs p.c.) TgTP6.3 and TgTP6.4 embryos using time-lapse microscopy for 24hrs (Fig 4.1). These images showed that there was no detectable transgene expression, which would be expected in approximately 50% of the embryos, prior to the 2-cell stage and immediately after cleavage. These embryos could only be cultured in the incubation chamber on the confocal microscope for approximately 24hrs (as discussed in chapt 3). Therefore, the onset of expression was assessed, by imaging transgenic and non-transgenic embryos from the 2-cell stage.

Two separate time-lapse experiments were carried out to determine the time of onset of embryo-encoded expression of the tau-GFP transgene in wild-type × TgTP6.3 embryos.

Fig 4.1: Single Section Confocal Images of 1-cell & Early 2-cell embryos -/- × GFP/-

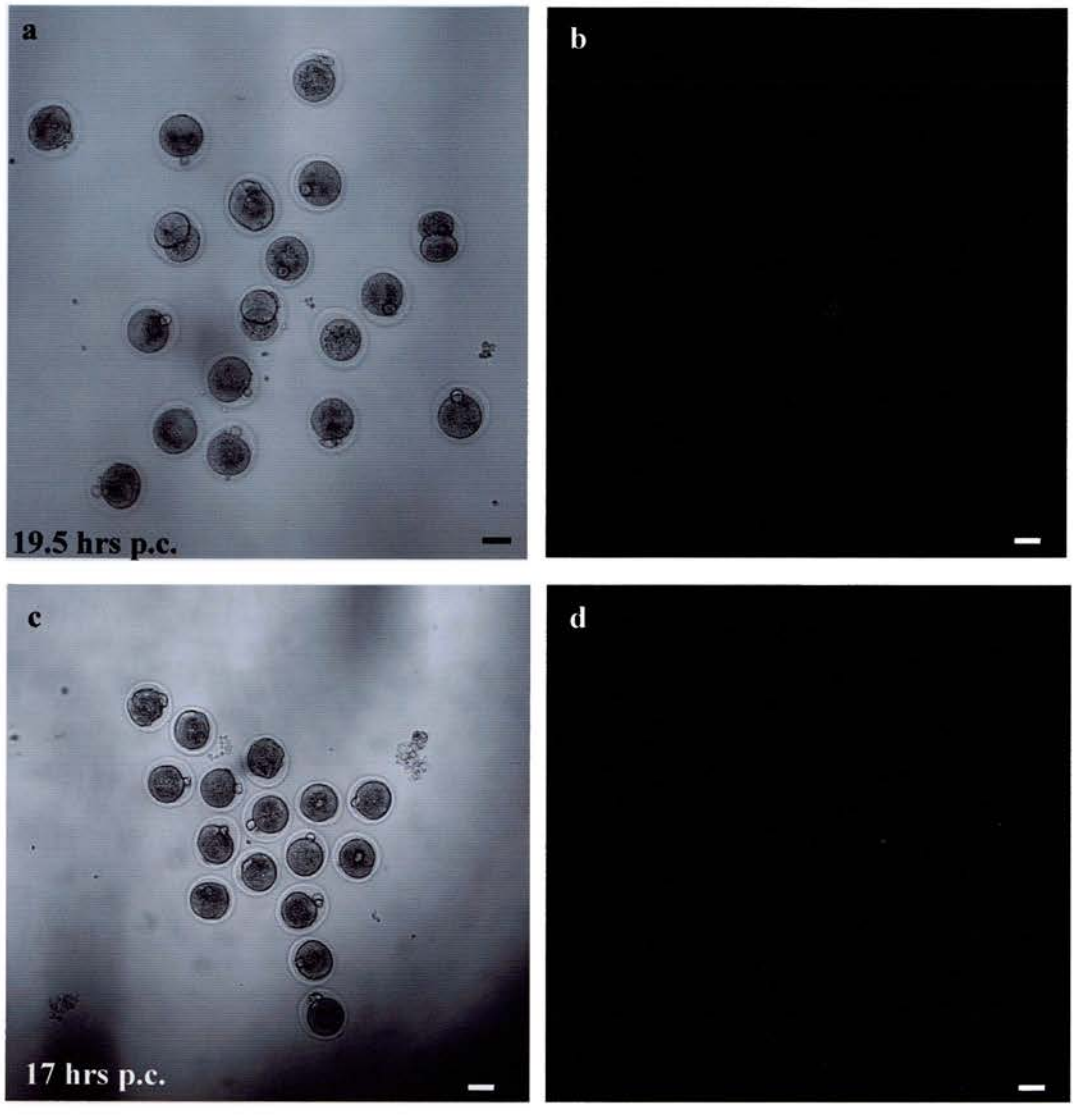

Fig 4.1: a & b: Transmitted light & GFP images of 1-2-cell BF_1×TgTP6.3 embryos, **c & d:** Transmitted light and GFP images of 1-cell BF_1×TgTP6.4 embryos. Half of the embryos should inherit the transgene but both GFP images show there is no GFP expression at this stage.

Scale bar=50microns.

An initial time-lapse experiment was carried out using 14, CF_1×TgTP6.3 embryos. These were cultured between the 2-cell and 4-cell stage. The average pixel intensity was measured at each time-point for each embryo. This was to demonstrate the level of fluorescence of each embryo, to give an indication of the expression of the transgene. Of the 14 embryos, 8 were shown to express the transgene, by an increase in fluorescence at approximately 42hrs p.c. (data not shown), although both groups of transgenic and non-transgenic embryos could be distinguished prior to the start of the time-lapse (34hrs p.c.).

This time-lapse experiment was repeated using BF_1×TgTP6.3 embryos. This was to determine if the timing of the onset of expression varied with genetic background, and also because CF_1 mice have an unstable form of glucose phosphate isomerase and so may have an abnormal energy metabolism. BF_1 mice were chosen as both TgTP6.3 and TgTP6.4 mouse lines used in this study were bred onto a BF_1 background (see chapter 2, section 2.1.1).

The average pixel intensity of 14 individual embryos, from the BF_1×TgTP6.3 cross, was measured at each time-point between 34.5 and 57.5 hours p.c. (Figure 4.2). The pixel intensity of 6 embryos was higher than the pixel intensity of the remaining 8 embryos by the end of the time-lapse. Therefore, this showed that 6 of the embryos were transgenic and 8 were non-transgenic. Figure 4.2 shows the transgenic embryos had a slightly higher pixel intensity from the start of the time-lapse but this difference was not statistically significant. This may be because there were not enough embryos

Fig 4.2: Onset of Expression in BF_1×TgTP6.3 Embryos

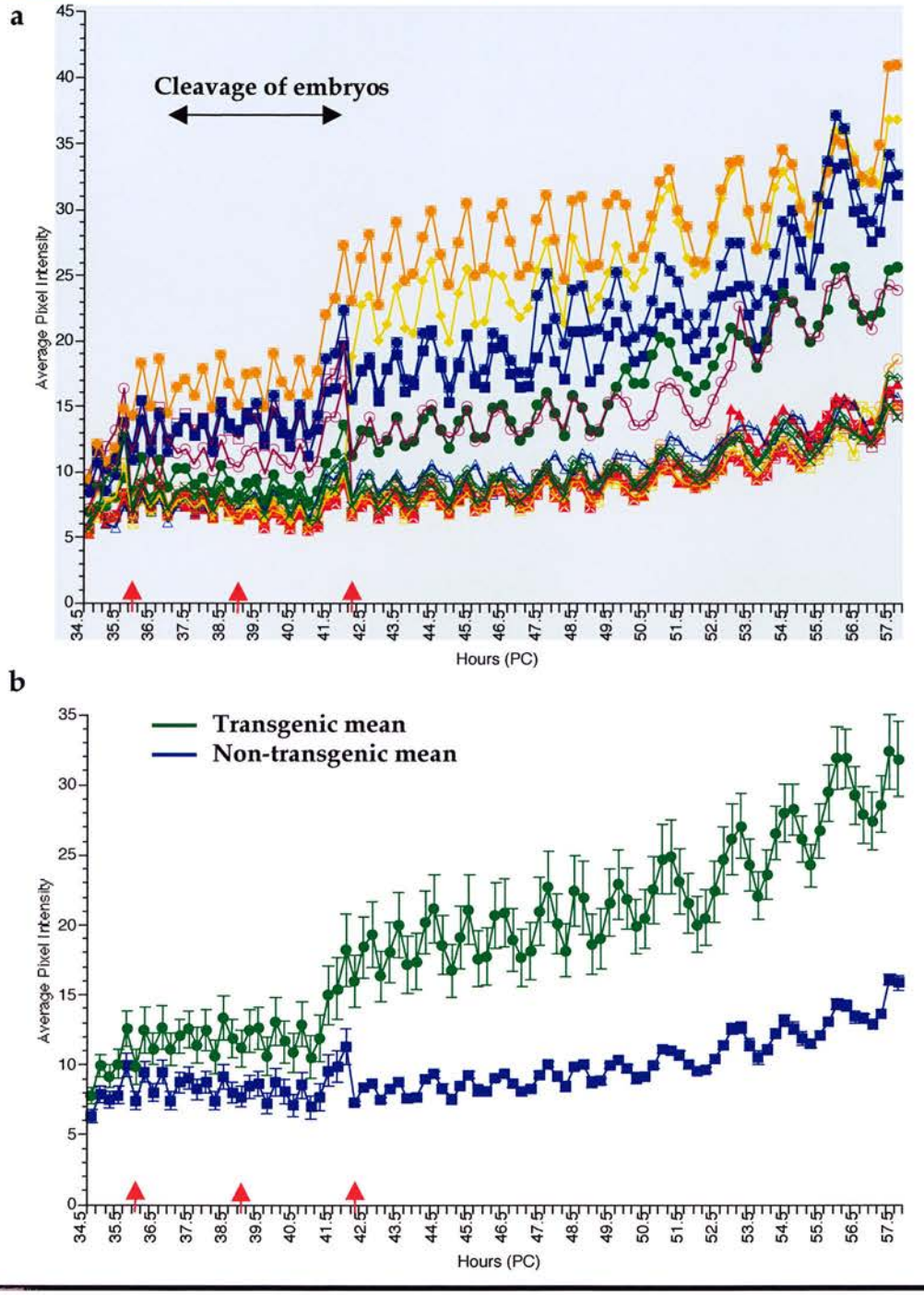

Fig 4.2: a: The individual average pixel intensity of 14 BF_1×TgTP6.3 embryos **b:** The mean values of 6 transgenic embryos & 8 non-transgenic embryos. Embryos were imaged for 23hrs between 34.5 & 57.5 hrs p.c. (2-cell to 4-cell stage). Red arrows indicate when the time-lapse was restarted causing differences in pixel intensity.

to detect a small difference. The pixel intensity of the transgenic embryos was significantly higher than the pixel intensity of the non-transgenic embryos by 36.25 hours p.c. ($p<0.05$ by unpaired t-test). However, this difference appeared to increase at 42hrs p.c. In conclusion, both time-lapse experiments indicated that the expression of the embryo-encoded TgTP6.3 tau-GFP transgene occurred near the start of the time-lapses and may have occurred just prior to the start, at 34.5h (2-cell stage).

The timing of the paternal onset of the tau-GFP transgene was also assessed in TgTP6.4 embryos. An initial time-lapse experiment (data not shown) of 11 $CF_1 \times$TgTP6.4, included 3 transgenic and 8 non-transgenic embryos. Again both transgenic and non-transgenic embryos were distinguishable from the start of the time-lapse (at 35hrs p.c.). This experiment was repeated using $BF_1 \times$TgTP6.4 embryos. 20 embryos were imaged which included 9 transgenic and 11 non-transgenic embryos, which were identified by the differences in pixel intensity at the end of the time-lapse (Fig 4.3 & 4.4). There was a significantly higher pixel intensity of the transgenic embryos compared to the non-transgenic embryos from the start of the time-lapse ($P<0.01$ by unpaired t-test). Therefore, the onset of expression occurred before the start of the time-lapse, at 34.5 hrs. This difference appeared to gradually increase following 36 hours p.c. The gradual increase in fluorescence, which reflects the accumulation of GFP protein, can be clearly visualised in the time-lapse images shown in Figure 4.3.

Fig 4.3: Time-lapse Images Showing the Paternal Onset of Expression in BF_1×TgTP6.4 Embryos

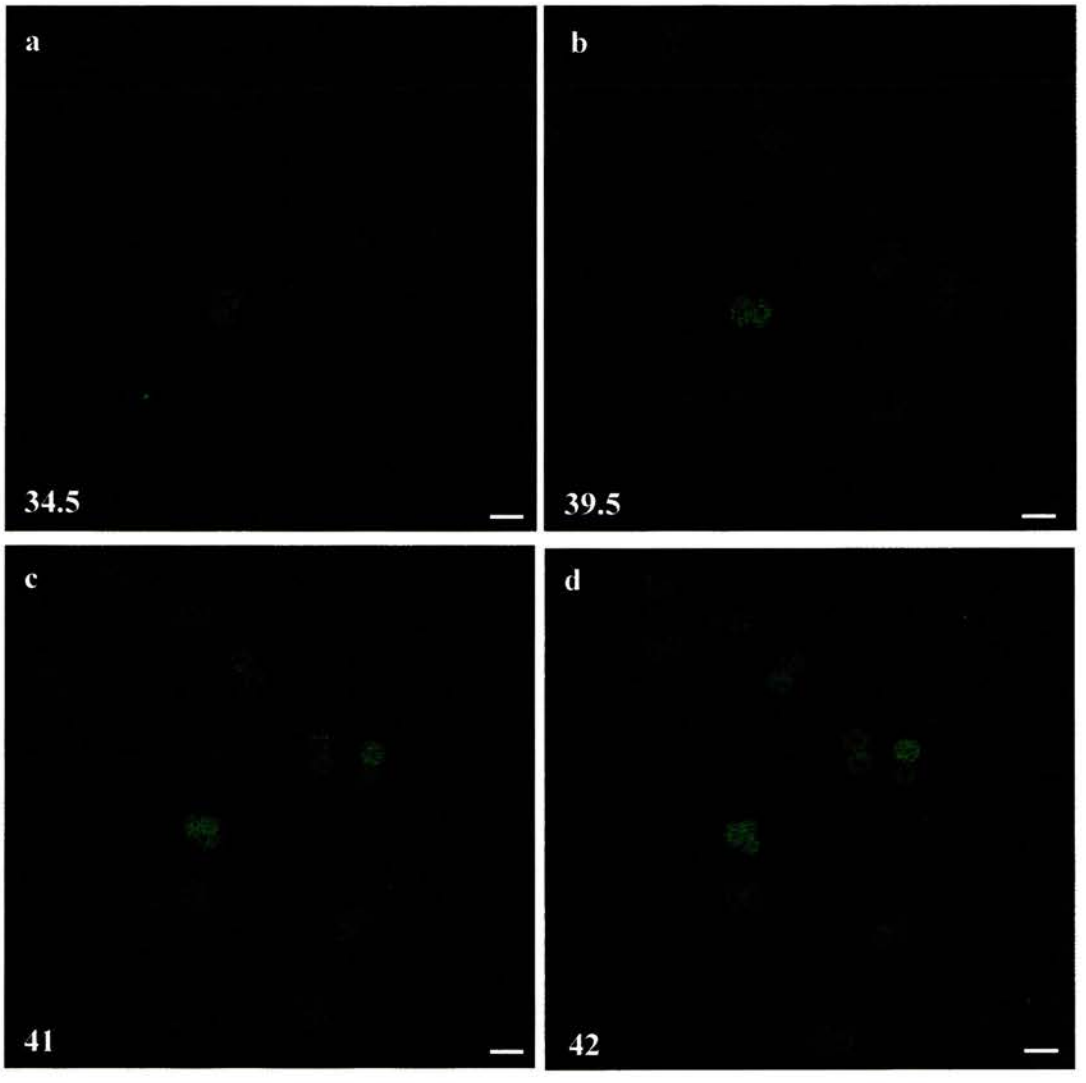

Fig 4.3:GFP images showing the accumulation of tau-GFP protein in BF_1×TgTP6.4 Embryos.Times shown in hrs p.c.

Scale bar=50microns.

Fig 4.4: Onset of Expression in BF_1×TgTP6.4 Embryos

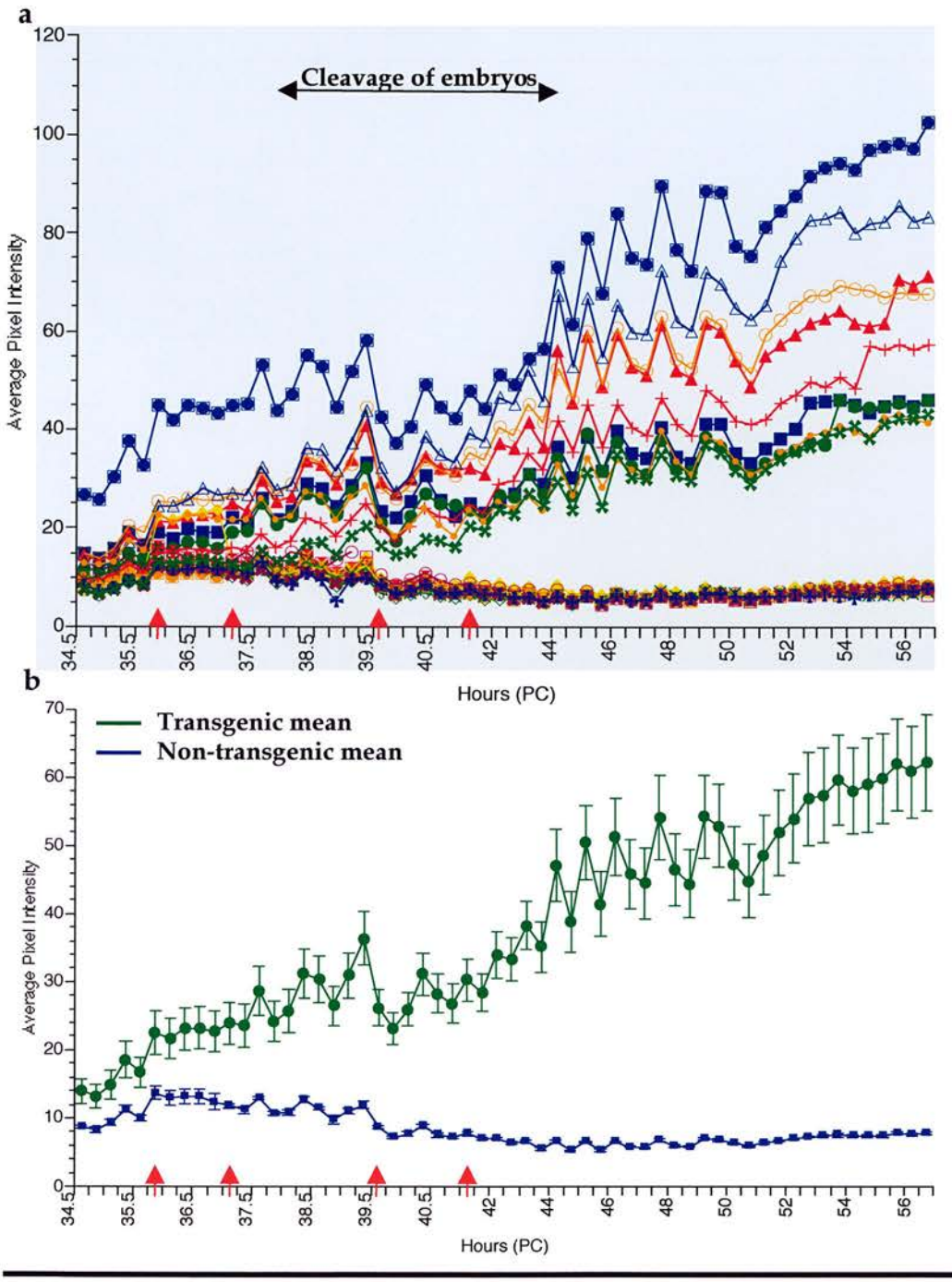

Fig 4.4: a: The individual average pixel intensity of 20 BF_1×TgTP6.4 embryos **b:** The mean values of 9 transgenic embryos & 11 non-transgenic embryos. Embryos were imaged for 22hrs between 34.5 & 56.5 hrs p.c 92-cell to 4-cell stage. Red arrows indicate when the time-lapse was restarted causing differences in pixel intensity.

Fig 4.5: Images Showing GFP Expression in BF_1×TgTP6.4 Embryos Cultured In-vivo

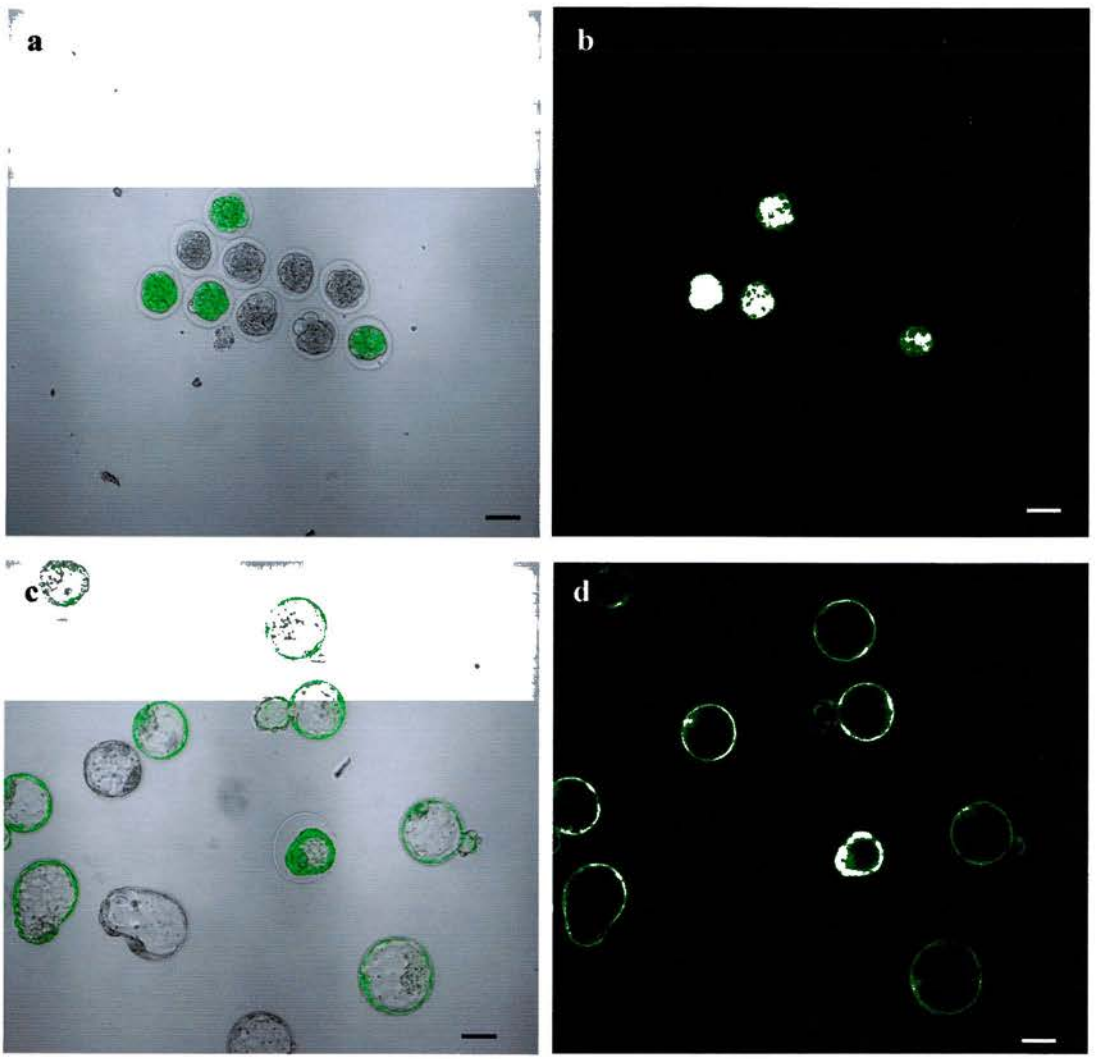

Fig 4.5:a: Overlay images of BF_1×TgTP6.4 morula, **b:** GFP images of the same embryos showing embryo encoded expression has been switched on at this stage. **c:** An overlay image and **d:** a GFP image of hatching blastocysts, transgenic and non-transgenic embryos can be clearly distinguished.

Scale bar=100 microns a & b, 50microns c & d.

Several females had been mated at the same time to provide embryos for the time-lapse studes. Remaining plugged females were flushed after this stage. Late E2.5 morula, and E4.5 blastocysts were imaged (Fig 4.5). These images clearly showed that TgTP6.4 embryos expressed GFP at both the morula and blastocyst stage. This is also the case for TgTP6.3 embryos, indicating that both transgenes are useful markers for experiments involving chimeric blastocysts.

4.3.2 Loss of GFP Maternal (oocyte-encoded) Expression in TgTP6.3 and TgTP6.4 Preimplantation Embryos

Embryos from crosses between TgTP6.3 females and non-GFP males were analysed from the 2-cell stage using the same techniques to determine the onset of embryo encoded expression (maternal allele) and the loss of oocyte encoded expression of the transgene.

A preliminary experiment of 10 TgTP6.3×(BALB/c×A/J)F_2 embryos was initially analysed (data not shown). Of these embryos 5 were shown to be transgenic, due to a higher level of fluorescence, and 5 were non-transgenic. Both the transgenic and non-transgenic embryos had a higher pixel intensity throughout the time-lapse, compared to the pixel intensity of the non-transgenic embryos analysed in both paternal onset time-lapse experiments (previous section). This indicated that the remaining maternal mRNA and/or protein was maintained in 4-cell TgTP6.3 embryos. From the start of this time-lapse there was a difference between the transgenic and non-

transgenic pixel intensities, which remained constant, indicating embryo encoded expression occurred before the start of the time-lapse (33 hrs p.c.).

Again this time-lapse was repeated using BF_1 male mice. Figure 4.6a shows the individual average pixel intensity of 20 TgTP6.3×BF_1 embryos. A group of transgenic embryos and a group of non-transgenic embryos could be distinguished from the start of the time-lapse, (at the 2-cell stage) due to the difference in the levels of fluorescence. This difference was significant, indicating embryo encoded expression had occurred before the start of the time-lapse at 34.8 hrs (Fig 4.7a)($p<0.01$ by unpaired t-test). However, after approximately 5 hours of imaging the embryos were failing to thrive, as can be seen by the drop in fluorescence levels. Therefore, it was decided to image a group of 7 embryos which had been flushed at the same time and cultured in an incubator. Analysis of the fluorescence levels of these embryos during the time-lapse showed that 2 embryos were transgenic and the remaining 5 were non-transgenic (Fig 4.6b). Again there was a significant difference between both groups of embryos from the start of the time-lapse at 40.3 hrs ($p<0.01$ by unpaired t-test). The difference between the pixel intensities remained constant throughout the time-lapse. This analysis also showed that the average pixel intensity values of the non-transgenic embryos from TgTP6.3 mothers were higher than the expected background levels throughout the time-lapse (see background levels of non-transgenic control embryos in Figs 4.8 & 4.9). This indicates that oocyte encoded tau-GFP remained in the 4-cell embryos.

Fig 4.6: Onset & Loss of Expression in TgTP6.3×BF_1 Embryos

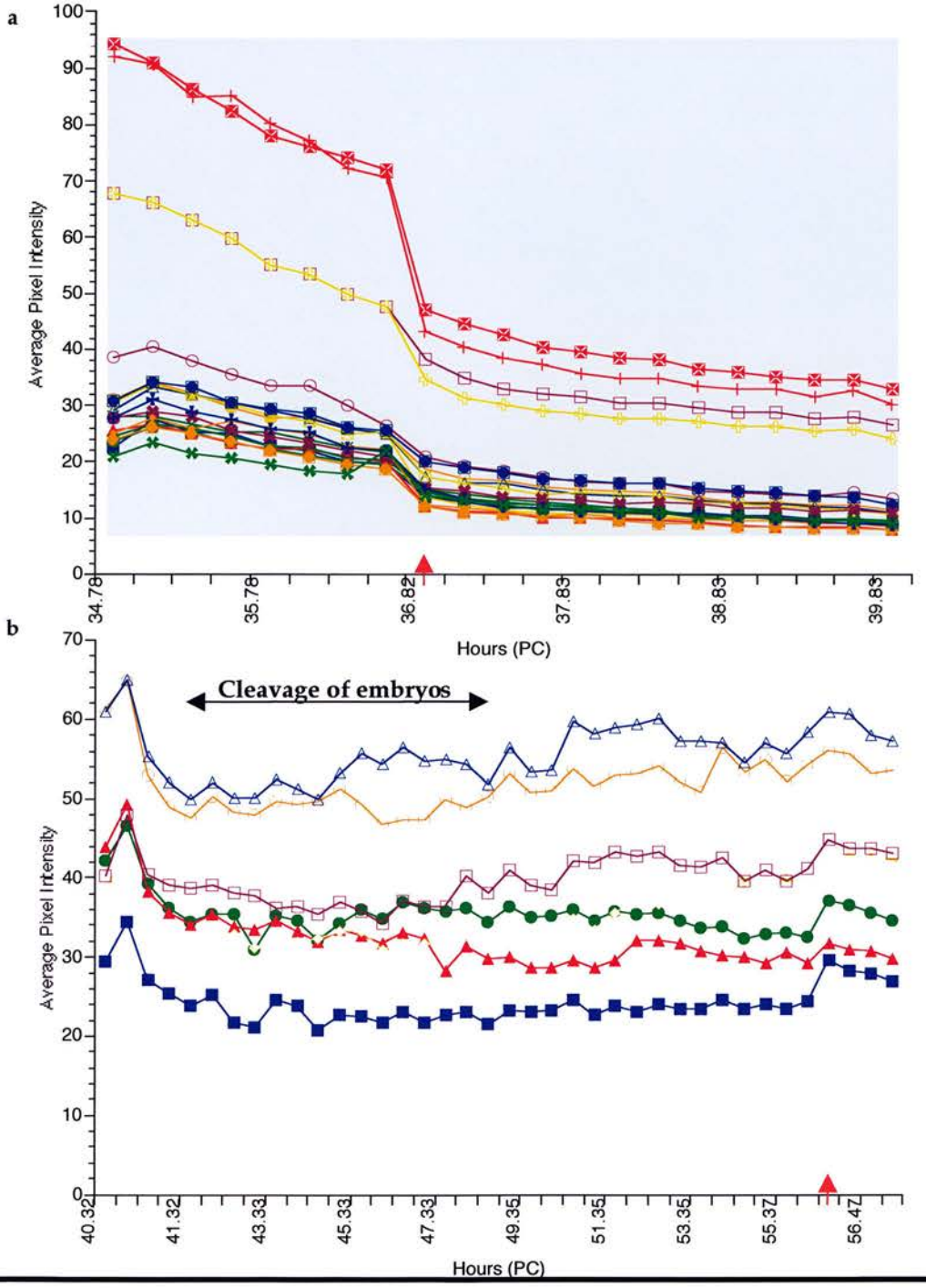

Fig 4.6: The average pixel intensity of two separate groups of TgTP6.3×BF_1 embryos which were flushed at the same time (2-cell stage). **a:** An initial group of 20 embryos were imaged but these did not survive. Therefore another group of 7 embryos, shown in **b,** were imaged. Embryos cleaved from the 2-cell to the 4-cell stage. Red arrows indicate when the time-lapse was restarted causing differences in pixel intensity.

Fig 4.7: Onset & Loss of Expression in TgTP6.3×BF_1 Embryos

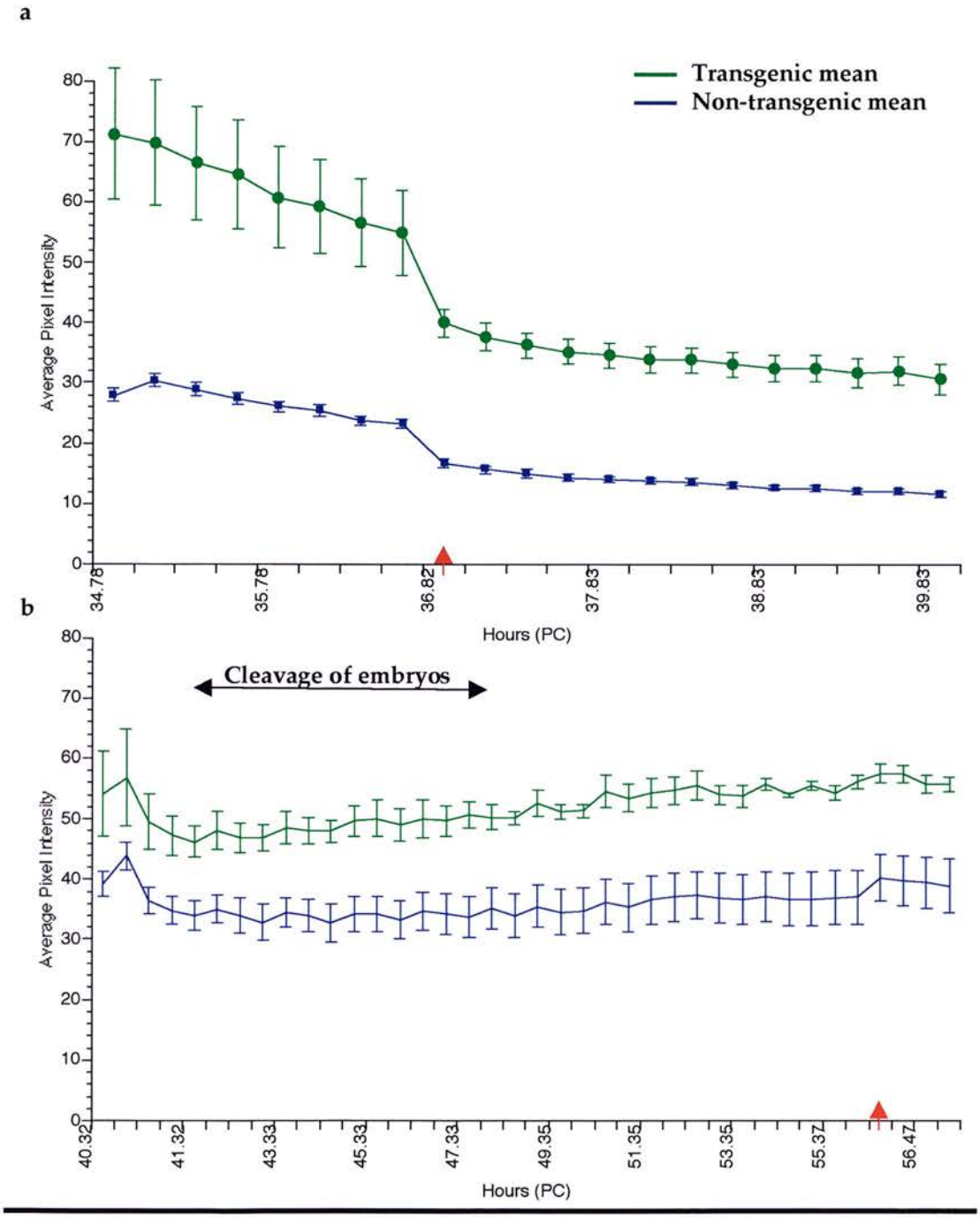

Fig 4.7: Mean values of average pixel intensity of **a:** 4 Transgenic embryos & 16 non-transgenic embryos imaged between 34.8 & 39.8 hrs p.c., and **b:** a separate group of 2 transgenic and 5 Non-transgenic embryos imaged between 40.3 & 56.7 hrs p.c. Red arrows indicate when the time-lapse was restarted causing differences in pixel intensity.

The TgTP6.3 time-lapse experiments were both similar to each other showing a difference between the fluorescence levels from the start of the time-lapse which remained constant. The time-lapse experiments designed to investigate the loss of maternal expression and the onset of embryo encoded expression in TgTP6.4 embryos differed from this.

The initial time-lapse experiment of 10 TgTP6.4×(BALB/c×A/J)F_2 revealed 5 embryos were transgenic and 5 were non-transgenic. The transgenic group of embryos had a higher fluorescence level than the non-transgenic embryos from the start of the time-lapse. Following 40 hours p.c. the fluorescence level of the transgenic embryos increased. The fluorescence level of the non-transgenic embryos was higher than background autofluorescence throughout the time-lapse. This showed that either maternal mRNA and/ or the tau-GFP fusion protein was still present in the cytoplasm.

This experiment was repeated using 17 TgTP6.4×BF_1 embryos and 2 (BALB/c×A/J)F_2 embryos added as a non-fluorescent control (Fig 4.8 & 4.9). A group of 13 embryos, judged to carry the transgene had a higher fluorescence level than a group of 4 embryos, which were non-transgenic. At the start of the time-lapse there was no significant difference between the levels of fluorescence of the transgenic and non-transgenic embryos although the mean was higher for the transgenic group. The group of transgenic embryos had a significantly higher level of fluorescence than the non-transgenic embryos from 38.08 hours p.c. ($p<0.01$ by unpaired t-test). The average pixel intensities of the transgenic group of embryos increased after

Fig 4.8: Time-lapse Images Showing the Maternal Onset and Loss of Oocyte-encoded Protein in TgTP6.4×BF_1 Embryos

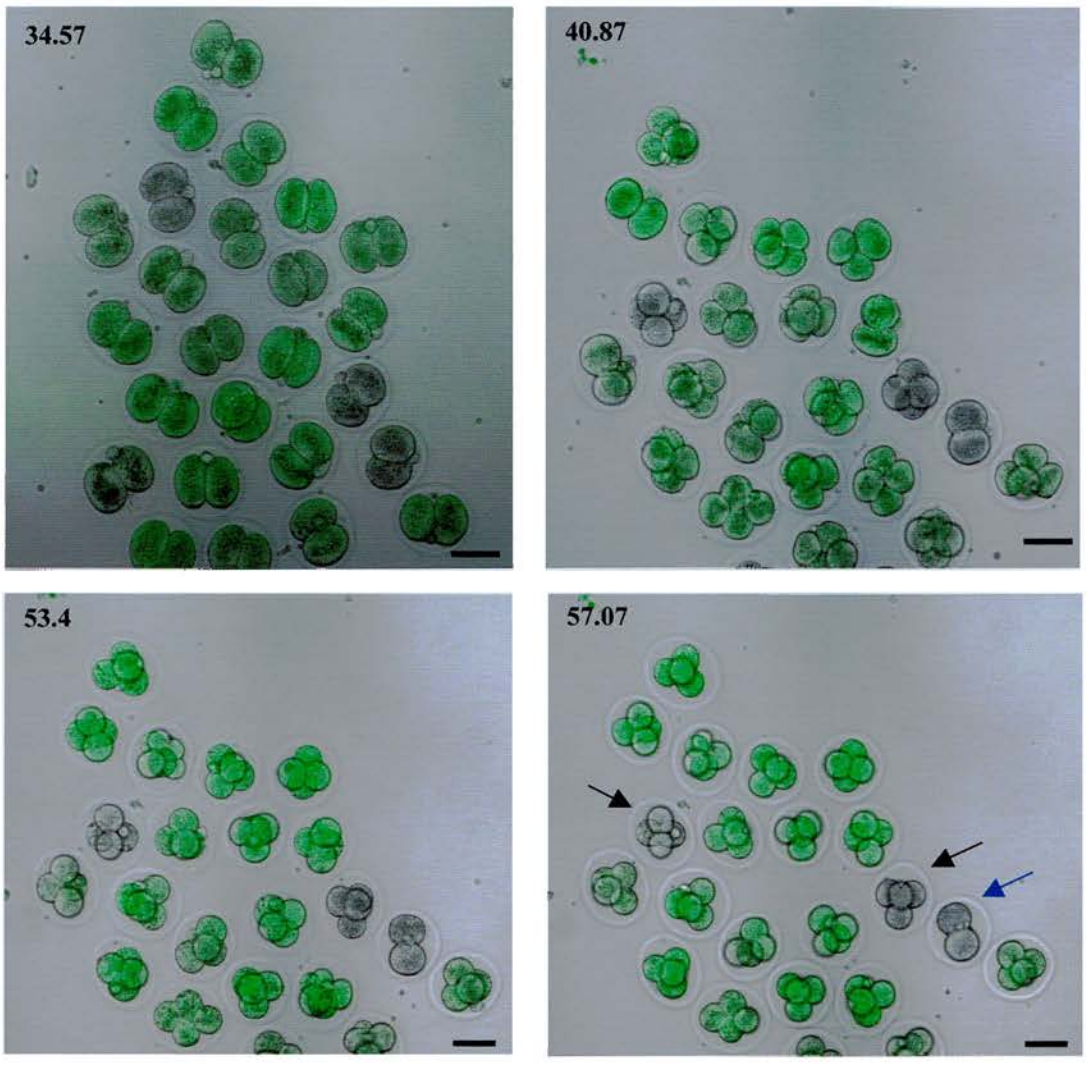

Fig 4.8:GFP images of the TgTP6.4×BF_1 time-lapse experiment. The black arrows indicate the control (BALB/c × A/J)F_2 embryos, the blue arrow indicates an embryo that did not cleave during the course of the time-lapse and did not fluoresce therefore was excluded from the study. Times shown are hrs p.c.

Scale bar=50microns.

Fig 4.9: Onset & Loss of Expression in TgTP6.4×BF$_1$ Embryos

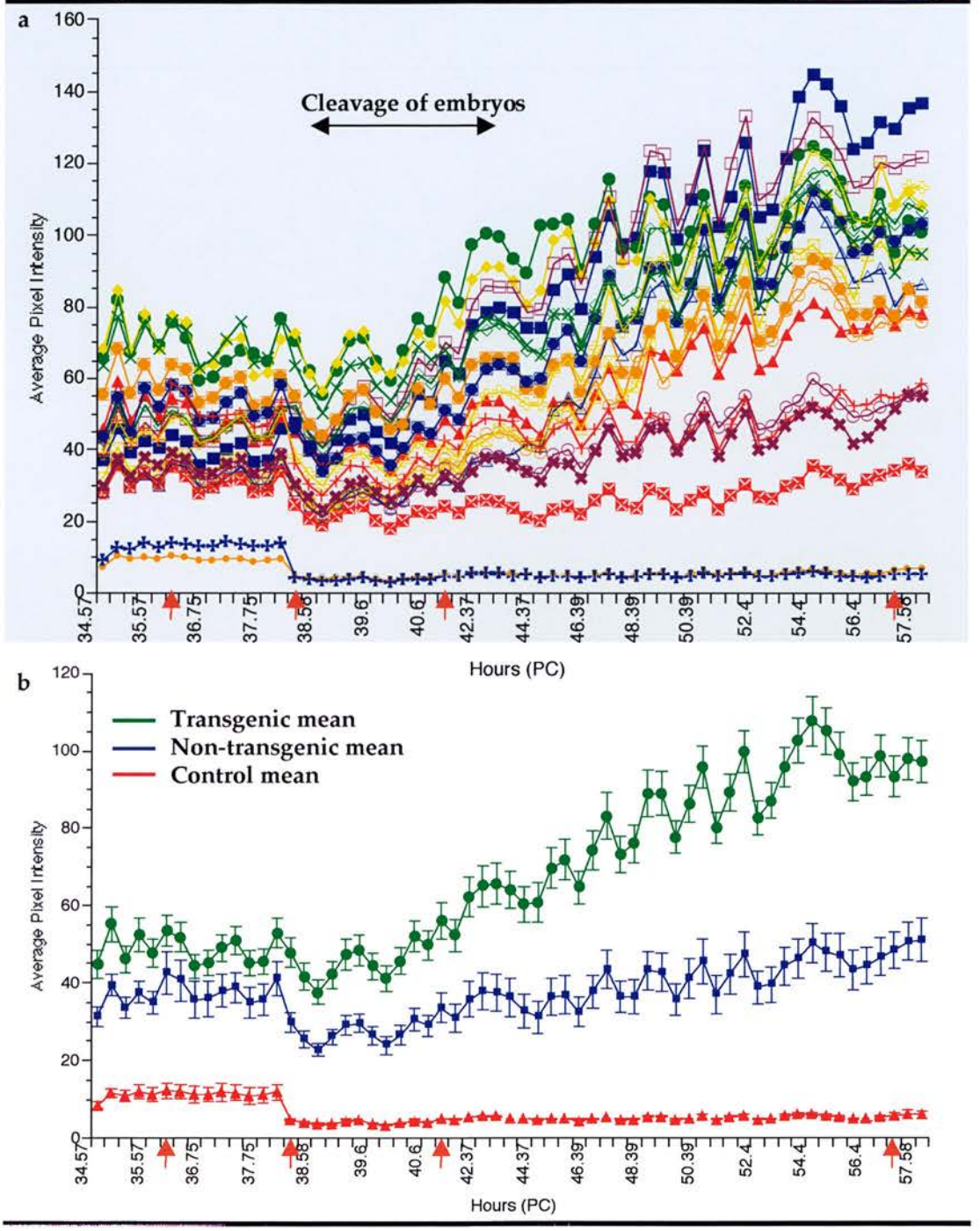

Fig 4.9: a: The average pixel intensity of 17 TgTP6.4×BF$_1$ embryos and 2 (BALB/c×A/J)F2 control embryos. **b:** The mean values of 13 transgenic embryos, 4 non-transgenic embryos and 2 control embryos. Embryos were imaged for 23hrs between 34.57 & 57.58 hrs PC. Red arrows indicate when the time-lapse was restarted

this stage, from a range of 40-60 at the start of the time-lapse, to a range of 90-110 at the end of the time-lapse. This increase in fluorescence must be due to an increase in embryo-encoded expression of the transgene. The 2 control embryos could easily be identified throughout the time-lapse as their fluorescence levels were low, within a range of 3-15, showing only background fluorescence. At the end of the time-lapse experiment the fluorescence of the non-transgenic group of embryos was significantly higher than the fluorescence levels of the control embryos ($p<0.01$ by unpaired t-test). This indicates that the tau-GFP fusion protein was still present in the cytoplasm at this stage, due to residual maternal mRNA or protein.

Both TgTP6.3× BF_1 and TgTP6.4× BF_1 embryos were flushed from plugged females and imaged at later stages to determine when the maternally expressed tau-GFP was degraded. A fall in the fluorescence intensity, to background levels, was shown in TgTP6.3× BF_1 embryos at the blastocyst stage. However, all the compacted morula retained their fluorescence indicating the degradation of maternal mRNA was stage rather than time dependant. This was also seen in TgTP6.4× BF_1 embryos. Figure 4.10 shows a residual fluorescence in non-transgenic morula. However, non-transgenic blastocysts had a much lower level of fluorescence, which was similar to the level of background fluorescence.

In conclusion, both embryonic alleles of TgTP6.3 and TgTP6.4 are expressed at the 2-cell stage. Oocyte-coded GFP persists to at least the morula stage in TgTP6.3 and TgTP6.4 embryos.

Fig 4.10: Images of TgTP6.4×BF_1 Embryos Cultured In-Vivo and Flushed on the Day of Imaging

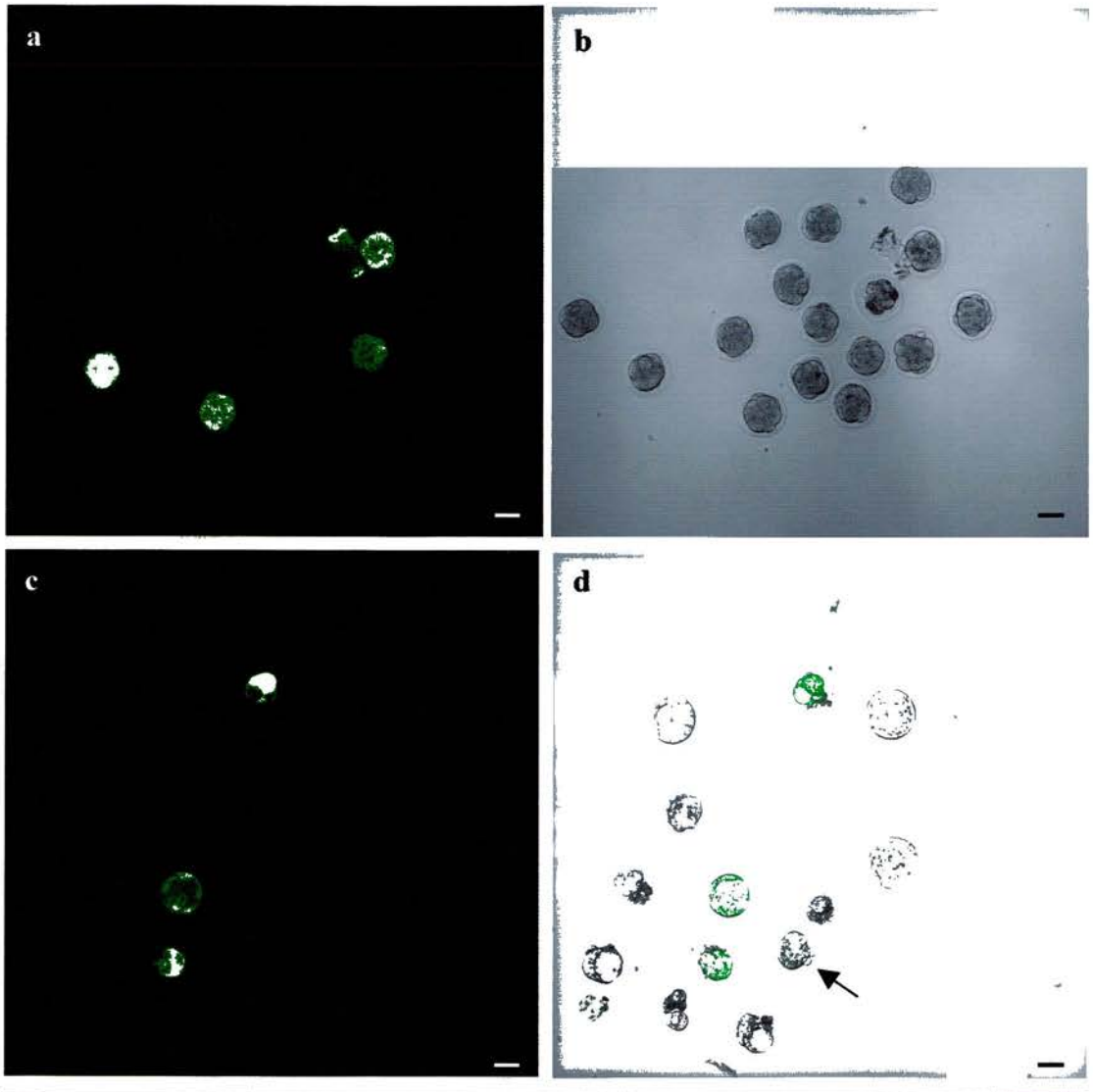

Fig 4.10:a: GFP image of TgTP6.4×BF_1 morulae. The transgenic embryos can be clearly visualised by their increased fluorescence. The non-transgenic embryos also have a higher fluorescence than normal background levels (blastocysts in image c). **b:**The transmitted image of the same embryos. **c:** A GFP image of blastocysts and morula, showing the fluorescence levels of the non-transgenic blastocysts is much lower than the non-transgenic morula. **d:** Overlay image of the same image, the arrow indicates a non-transgenic morula exhibiting a higher fluorescence level than the non-transgenic blastocysts.
Scale bar=50microns.

4.3.3. Test Mating of TgTP6.4 Mice to Determine if Adult Homozygotes are Viable

Previous (unpublished) work has shown that TgTP6.3 homozygotes fail to survive to adulthood but the viability of TgTP6.4 homozygotes had not been evaluated.

The offspring of TgTP6.4 heterozygote inter-crosses were test mated to determine if the homozygotes survived. However, after test mating possible homozygote mice, it was noted that the original crosses used to produce these mice gave a particularly low percentage of GFP positive mice. This suggested that some of the mice were not transgenic. As the original parents had been killed it was not possible to determine if this was the case. This study was repeated to ensure the TgTP6.4 mice being tested were the offspring of a heterozygote inter-cross. 28 of 50 (59.5%) offspring genotyped from the new first generation cross were GFP positive. The parents of the original crosses were tested twice to ensure that they were both GFP positive and therefore heterozygotes.

If all offspring of a heterozygote × heterozygote cross are viable, 1/3 of the GFP-positive offspring are expected to be homozygous. 19 GFP offspring were test mated, 17 of which produced offspring. 15 of these mice tested produced non-GFP offspring in their first litters indicating these mice were not homozygous for GFP. One female produced only GFP offspring (9/9) in her first litter. However, there were some non-GFP mice produced in a further two litters (7/8 and 9/12 GFP-positive) suggesting that it was not

homozygote for GFP. The high proportion of GFP offspring produced (25/29) could be explained if this female was a $GFP^{+/+}/GFP^{+/-}$ mosaic. This female could not be further tested as it was found dead 15 days after producing a third litter. The first litter from a test-mated male appeared to be entirely GFP-positive (10/10 analysed E13.5 fetuses) but 5/12 of a second litter were non-transgenic.

Therefore, none of the 17 mice that produced offspring were homozygous. The probability of this is $(2/3)^{17}=0.00102$. These test mating experiments have shown that it is likely that TgTP6.4 homozygote mice do not survive to reproduce unless the transgene is lost or inactivated in some cells to make them functional mosaics.

4.3.4. Analysis of Survival of Homozygous TgTP6.3 and TgTP6.4 Mice Between Birth and Weaning

It has been shown that homozygous mice of both mouse lines die before reaching reproductive maturity. Table 4.1 shows the % of GFP and non-GFP mice present after weaning offspring from heterozygote × heterozygote and wild-type × heterozygote crosses. The mice were typed for GFP after weaning. The proportion of GFP positive mice from the wild-type × TgTP6.3 heterozygote crosses was 54/117 (46.2%), which is not significantly different to the expected percentage of 50% ($\chi^2=0.6923$; $P>0.05$) suggesting that heterozygotes are viable. However, the proportion of GFP positive mice from the TgTP6.3 heterozygote × heterozygote cross was 68/125 (54.4%), which is significantly lower than the expected 75% if homozygotes survive (($\chi^2=28.29$;

Table 4.1: Analysis of TgTP6.3 and TgTP6.4 Mice Between Birth and Weaning

Cross	Total live-born mice	Total GFP +ve	Total GFP -ve	Live but not typed	Dead between birth & weaning	Dead after weaning	% of GFP+ve mice *	% of GFP-ve mice *	% of mice dead before weaning	% of mice dead after weaning†
BF1 x TgTP6.3	135	54	63	13	3	2	46.2	53.8	2.2	1.5
TgTP6.3 x TgTP6.3	153	68	57	9	18	1	54.4	45.6	11.8	0.7
BF1 x TgTP6.4	214	34	58	116	3	3	37.0	63.0	1.4	1.4
TgTP6.4 x TgTP6.4	247	108	86	19	29	5	55.7	44.3	11.7	2.0

Table 4.1: Analysis of the offspring of wild-type × heterozygote crosses and heterozygote × heterozygote crosses showing the % of GFP positive and negative mice produced and the % of deaths between birth and weaning. The mice were typed for GFP after weaning. 50% of the mice from a wild-type × heterozygote cross are expected to be GFP positive. If homozygotes survive 75%of the mice from a heterozygote × heterozygote cross are expected to be GFP positive.

* % of typed mice

† Number of mice that died naturally between weaning and collection of data

P<0.01). This value is also lower than the expcted 66.7% if all heterozygotes but no homozygotes survive ((χ^2=8.51; P<0.01). These results are therefore in agreement with the previous data, suggesting that TgTP6.3 homozygotes do not survive to this stage. The low percentage of GFP positive mice from the TgTP6.3 heterozygote × heterozygote cross could be explained if some heterozygote mice from this cross die prior to weaning.

Table 4.1 also shows the percentages of mice that died between birth and weaning. 11.8% of mice from TgTP6.3 heterozygote inter-crosses died between these stages. This was higher than the 2.2% that died from the wild-type × TgTP6.3 heterozygote crosses. The percentage of induced deaths on this genetic background was calculated from the total offspring and number of deaths between birth and weaning (see 4.2.5). 9.8% of the mice die for reasons attributable to the heterozygote × heterozygote cross, indicating a high proportion of mice that died were homozygotes. These results suggest that some TgTP6.3 homozygotes are born but do not survive to weaning. However, homozygotes from a heterozygote × heterozygote cross represent 25% of the offspring. Therefore, a significant number must die before birth or the recording of the birth, as the 9.8% of the mice that die do not represent all 25% of the homozygotes produced.

The TgTP6.4 control wild-type × heterozygote crosses produced a lower percentage of GFP mice than expected (Table 4.1) (χ^2=6.26; P<0.025). This could be caused by the sample size. Table 4.1 also shows that 108/194 (55.7%) of mice from the heterozygote × heterozygote crosses were GFP

positive. This is also significantly lower than the expected 75% or 66.7 (χ^2=38.66 and 10.63 respectively; P<0.01), suggesting that TgTP6.4 homozygotes die before weaning. The percentage of deaths between birth and weaning was also higher than the percentage of deaths from the control wild-type × heterozygote crosses, 11.7% compared to 1.4%. The percentage of induced deaths before weaning on this genetic background was calculated to be 8.3%. This data also shows that homozygote mice die between birth and weaning. The percentage of mice that died between birth and weaning does not account for the death of all 25% of homozygotes produced. Therefore, some homozygotes must die prior to birth or the recording of the birth.

4.3.5 Analysis of TgTP6.3 and TgTP6.4 E14.5 Conceptuses

It is possible that homozygotes of both crosses die immediately after birth and were not counted as they were born during the night. Alternatively TgTP6.3 and TgTP6.4 homozygote mice could die during pre-natal development.

To test the second possibility conceptuses from heterozygote × heterozygote and heterozygote × wild-type crosses were dissected and analysed at E14.5. It was necessary to use heterozygote females for the control cross to ensure the uterine environment was the same for both types of conceptuses. Table 4.2 shows the percentages of GFP positive and negative conceptuses, and the number of moles (reabsorbed conceptuses) produced. If homozygote mice die before E14.5 the percentage of GFP fetuses would be closer to 66.6% than

Table 4.2: Analysis of E14.5 TgTP6.3 and TgTP6.4 Conceptuses

Cross	GFP +ve	GFP -ve	Moles	Dead fetuses	Total fetuses	Total conceptuses	% of GFP +ve★	% of GFP -ve★	% of Moles	% of Dead fetuses
TgTP6.3 x BF1	105	76	14	6	181	201	58.0	42.0	7.0	3.0
TgTP6.3 x TgTP6.3	132	43	33	7	175	215	75.4	24.6	15.3	3.3
TgTP6.4 x BF1	85	96	9	2	181	192	47.0	53.0	4.7	1.0
TgTP6.4 x TgTP6.4	127	47	16	2	174	192	73.0	27.0	8.3	1.0

Table 4.2: Number of GFP positive and negative fetuses, moles and dead fetuses dissected at E14.5. TgTP6.3 and TgTP6.4 mice are heterozygotes. If all mice are viable 50% of the mice from a heterozygote × wild-type cross are expected to be GFP positive. 75%of the mice from a heterozygote × heterozygote cross are expected to be GFP positive.

★ % of typed mice

75%. If the homozygotes die between implantation and E14.5, a significantly higher proportion of moles would be expected from a heterozygote inter-cross compared to the control heterozygote × wild-type cross.

Table 4.2 shows that 105/181 (58%) of the offspring of the TgTP6.3 heterozygote × wild-type cross were GFP positive. This is significantly higher than the expected proportion of 50% of GFP fetuses produced from this cross (χ^2=4.65; P<0.05). The TgTP6.3 heterozygote × heterozygote cross produced 132/175 (75.4%) GFP positive fetuses which is not significantly different from 75% but is significantly different from 66.7% (χ^2=0.017 and 6.01 respectively; P>0.05 and P<0.025). This ratio of GFP positive fetuses would be expected if homozygote fetuses were present at E14.5. However, there was a high percentage of moles produced from this cross, 15.3%. This is higher than the 7% of moles produced by the control heterozygote × wild-type crosses. The percentage of induced deaths on this genetic background was calculated by comparing the number of moles and dead fetuses from the control and experimental cross. This value was 9.6%. Therefore, these results are inconclusive as the percentage of GFP positive mice indicate that TgTP6.3 homozygote fetuses are present at E14.5. However, in contrast to this the high percentage of moles and dead fetuses would suggest that a proportion of homozygote fetuses may have died prior to E14.5. As the 9.6% of deaths does not account for all the 25% of homozygote fetuses however, it is likely that most homozygotes are present at this stage.

Table 4.2 also shows that 127/174 (73%) GFP positive fetuses were produced from the TgTP6.4 heterozygote × heterozygote cross. This is not significantly different from 75% or 66.7%, (χ^2=0.376 and 3.10 respectively; P>0.05), although it is closer to 75%. This indicates that homozygote mice survive to E14.5. The proportion of moles from the heterozygote × heterozygote crosses was 8.3%, compared to 4.7% produced by the control heterozygote × wild-type cross. The calculated percentage of induced deaths was 3.9% on this genetic background but may not be significant. The TgTP6.4 data indicates that TgTP6.4 homozygotes survive to this stage.

Therefore, both results indicate that homozygous GFP mice are present at E14.5. Along with the previous data, this would suggest that some of the homozygotes of both transgenic mouse lines die during late postnatal development (after E14.5) or during the perinatal period. Following this, a proportion of homozygotes also die between birth and weaning.

4.3.6 Analysis of the Placental and Fetal Weight, and Crown Rump Length of E14.5 Conceptuses

Previous data has shown a significant difference in weight between green and non-green litter mates from wild-type × TgTP6.3 heterozygote crosses at E14.5 (M.A.Keighren and J.H. Flockhart unpublished). Therefore, the fetal weight, placental weight and crown rump length of the E14.5 conceptuses (above) were analysed.

Figure 4.11a shows the mean fetal weights of the offspring of the heterozygote × heterozygote cross and the heterozygote × wild-type cross of both transgenic mouse lines. (Male and female fetuses were not distinguished). These results show that green TgTP6.3 fetuses were significantly lighter than non-green fetuses produced from the same cross ($P<0.01$ by unpaired t-test). TgTP6.4 green fetuses were also lighter than non-green fetuses however this difference was only significant for the offspring of the heterozygote × wild-type cross ($P<0.05$ by unpaired t-test). Figure 4.11b shows there was no significant difference between the placental weights for any of the E14.5 comparisons. However, the difference between the mean crown rump lengths of the GFP and non-GFP fetuses of all four crosses was similar to the mean weight data (Fig 4.11c). This data shows that the GFP positive fetuses were smaller than their wild-type litter mates in all cases. However, this difference was not significant for the offspring of the TgTP6.4 heterozygote × heterozygote cross.

There was no significant difference between the weight and crown rump length of the non-green fetuses from a heterozygote × heterozygote and a heterozygote × wild-type cross for TgTP6.3. However, the green offspring from a heterozygote × heterozygote cross were significantly lighter than green offspring from a heterozygote × wild-type cross ($p<0.01$ by unpaired t-test). The crown rump length of the green offspring of the heterozygote × heterozygote crosses was also significantly less than the green offspring from a heterozygote × wild-type cross ($p<0.05$). Homozygote mice are likely to

Fig. 4.11: Mean Fetal and Placental Weight and Crown Rump Length of E14.5 Conceptuses

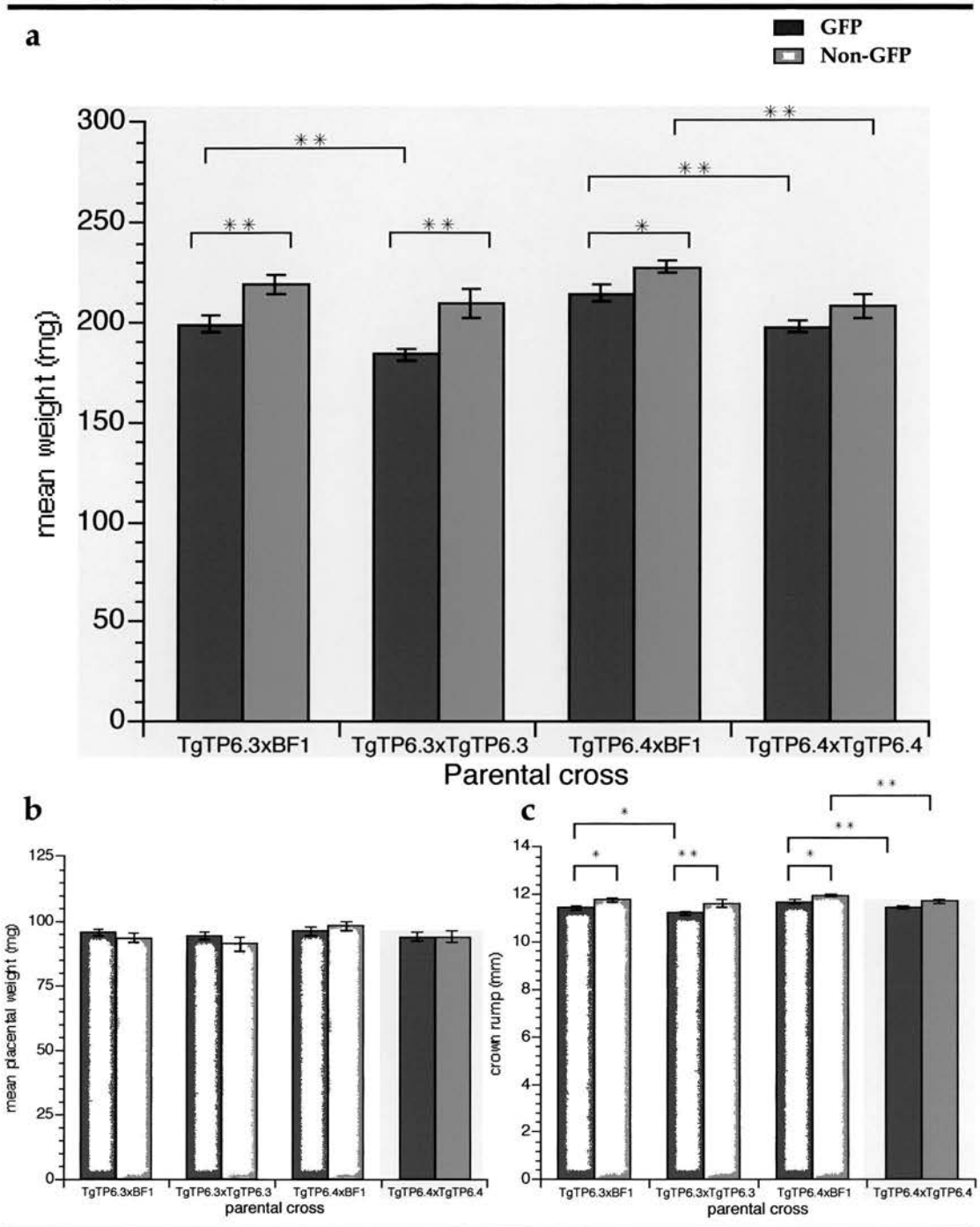

Fig.4.11:
Mean fetal and placental weights and crown rump length of E14.5 conceptuses from GFP heterozygte × heterozygote and heterozygote × wild-type crosses.
a: fetal weight **b:** placental weight **c:** crown rump length.

✳ ✳ $p<0.01$
✳ $p<0.05$

survive at this stage, therefore these results suggest that they are lighter in weight and smaller than TgTP6.3 heterozygotes.

Although the green offspring from the TgTP6.4 heterozygote × heterozygote cross were significantly lighter and the average crown rump length was significantly less than the green fetuses from a heterozygote × wild-type cross, the non-green fetuses from the heterozygote × heterozygote cross were also significantly lighter than the fetuses from the heterozygote × wild-type cross ($p<0.01$ by unpaired t-test). Therefore, no conclusions can be drawn from this.

The distribution of the weights of TgTP6.3 GFP and non-GFP fetuses from both crosses is shown in figure 4.12. A group of green mice weighing less than non-green mice can be seen in the offspring of the heterozygote × heterozygote fetuses (Fig 4.12b). However, the majority of green mice from the heterozygote × wild-type cross (Fig 4.12a) were within the same weight range as non-green fetuses, although overall they were significantly lighter.

The distributions of TgTP6.4 fetal weights show that most of the TgTP6.4 green offspring from both the control and experimental crosses were within the same weight range as the non-green fetuses (Fig 4.13). However, there is a number of green mice from heterozygote × heterozygote crosses that appear to be outwith the range of weights of the non-green fetuses.

Fig 4.12: Distribution of Weights of TgTP6.3 tau GFP and non tau GFP E14.5 Fetuses

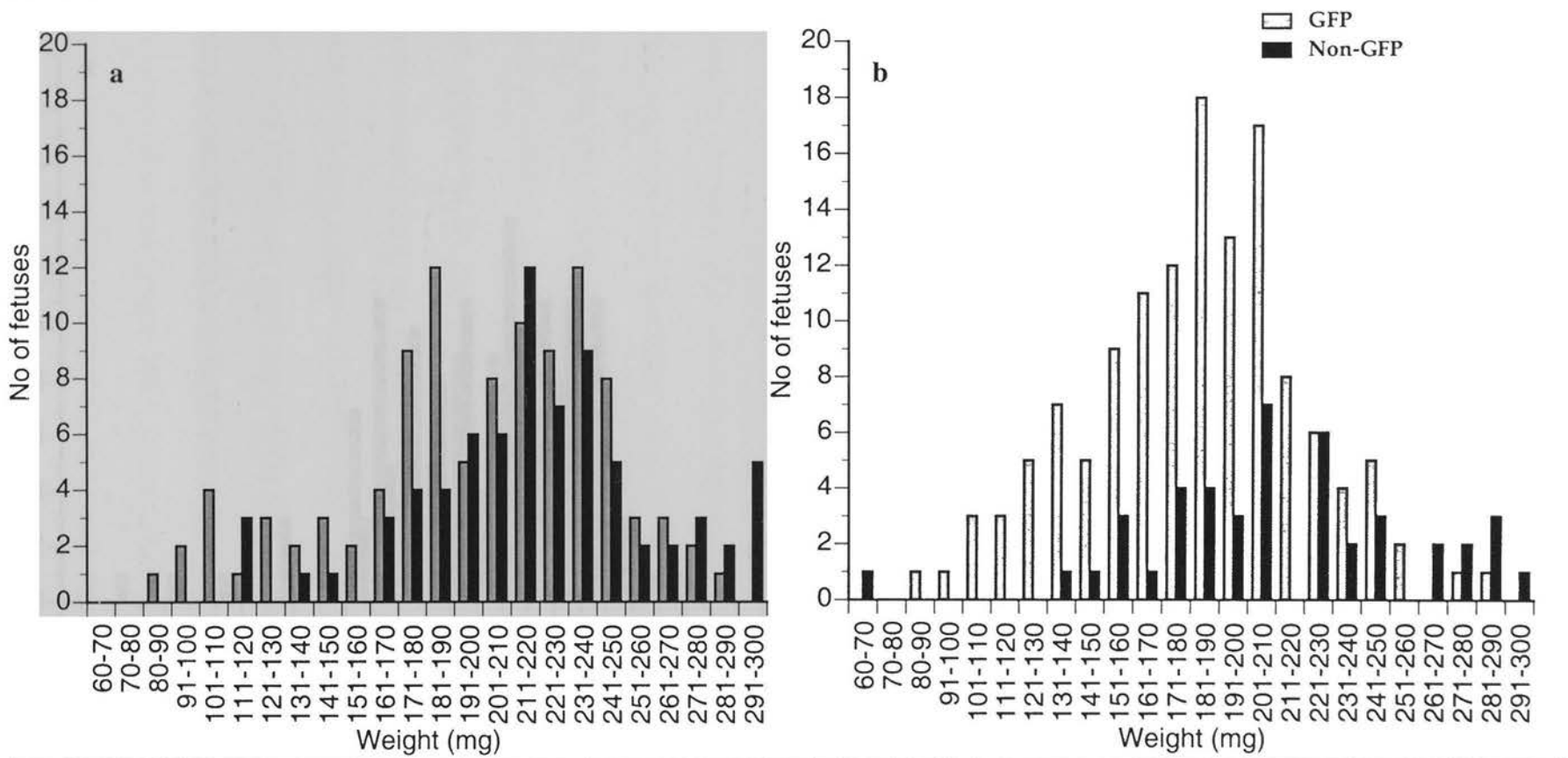

Fig 4.12: Histograms showing the distribution of weights of TgTP6.3 tau GFP and non tau GFP E14.5 fetuses from, a: control TgTP6.3 x BF_1 cross and b: TgTP6.3 x TgTP6.3 cross.

Fig 4.13: Distribution of Weights of TgTP6.4 tau GFP and non tau GFP E14.5 Fetuses

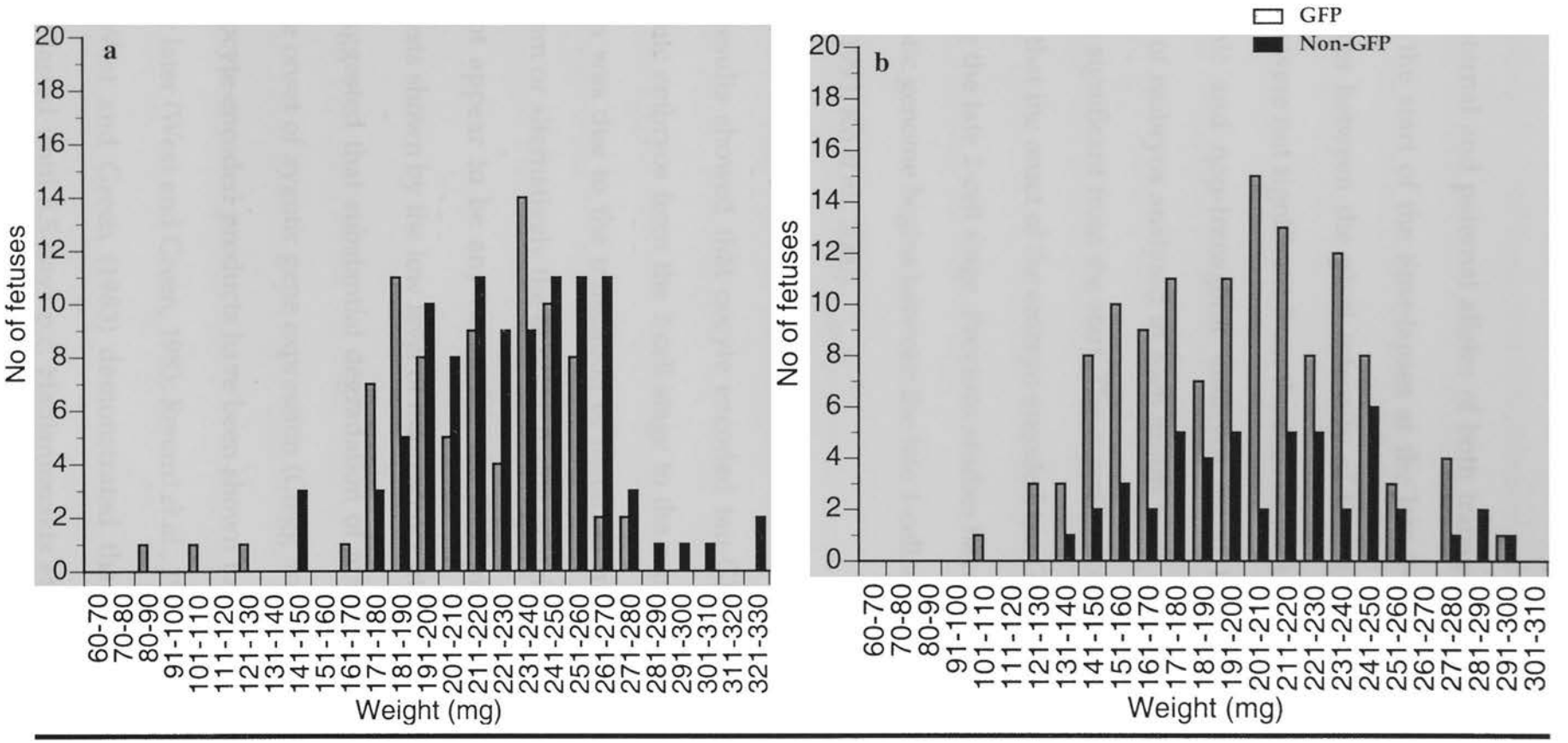

Fig 4.13: Histograms showing the distribution of weights of TgTP6.4 tau GFP and non tau GFP E14.5 fetuses from, a: control TgTP6.4 x BF_1 cross and b: TgTP6.4 x TgTP6.4 cross.

4.4 Conclusion

Both maternal and paternal alleles of both transgenic lines were activated prior to the start of the time-lapses at the late 2-cell stage. Although the differences between the pixel intensity of transgenic and non-transgenic embryos were not significant from the start of the time-lapses two groups of transgenic and non-transgenic embryos could be distinguished. If the number of embryos analysed in each group were expanded this difference could be significant from the start. The experiments in this chapter therefore showed that the onset of the embryo-encoded tau-GFP transgene occurred at or before the late 2-cell stage. Previous studies have shown the activation of the zygotic genome begins between the late 1-cell and 2-cell stage (Ram and Schultz, 1993; Ko *et al.*, 2000).

These results showed that oocyte encoded tau-GFP was present in non-transgenic embryos from the 2-cell stage to the morula stage. It is possible that this was due to the translation of maternal transcripts present in the cytoplasm or alternatively the tau-GFP fusion protein was very stable. There does not appear to be any remaining tau-GFP protein in non-transgenic blastocysts shown by the low level of fluorescence at this stage. Some studies have suggested that substantial degradation of maternal mRNA coincides with the onset of zygotic gene expression (Clegg and Piko, 1983). However, some oocyte-encoded products have been shown to persist to the blastocyst stage or later (West and Green, 1983; Renard *et al.*, 1994; Hadjantonakis *et al.*, 1998). West and Green (1983) demonstrated that oocyte-encoded GPI-1 enzyme lasted until 5.5 days p.c. Hadjantonakis et al (1998) demonstrated

maternal GFP expression was maintained in their GFP transgenic mice until after implantation. The controlled translation of maternal mRNAs is essential for meiotic maturation and early preimplantation development (Svoboda *et al.*, 2000). Renard et al (1994), showed that a maternal factor was essential for blastocyst formation, demonstrating that maternal mRNAs or oocyte encoded protein can have an effect on late preimplantation development. Stutz et al (1998) have suggested that the translation of maternal mRNAs is controlled by a masking mechanism which regulates the polyadenylation of transcripts. The results presented in this chapter demonstrate that the maternal mRNA or the maternally encoded tau-GFP protein is rapidly degraded following the morula stage.

Further characterisation of both transgenic mouse lines has demonstrated that TgTP6.3 and TgTP6.4 homozygotes die at late fetal and/or early postnatal stages. Heterozygotes are viable and fertile but are lighter in weight and smaller than wild-type littermates. An effect of the presence of a GFP transgene has not previously been reported in transgenic mice. This could therefore possibly be due to the fact that the GFP protein is fused to tau.

tau-GFP is expressed by the late 2-cell stage in both transgenic lines and by the 8-cell stage provides a bright fluorescence marker suitable for the analysis of preimplantation embryos. It was decided to use the TgTP6.3 mouse line for further studies. TgTP6.3 mice had been shown to exhibit ubiquitous expression throughout all tissues of the adult mouse, and were

also more abundant when the experiments were started. All GFP-positive embryos used for chimera experiments were heterozygous for TgTP6.3 which are viable as adults and fully fertile.

Chapter 5: Fate of 4n Cells in 4n↔2n Chimeric Blastocysts labelled with GFP

5.1 Introduction

This study involves the analysis of the allocation of 4n cells in chimeric blastocysts using tau-GFP and confocal microscopy.

Previous results have shown that 4n cells are largely excluded from the derivatives of the epiblast of 4n↔2n chimeras by E7.5, but consistently contribute to hypoblast and trophectoderm (TE) derivatives (James *et al.*, 1995) (as discussed in chapter 1, section 1.5.1.2). Therefore, 4n↔2n chimeras are a suitable mouse model of human confined placental mosaicism (CPM). An understanding of the cause of the restricted distribution of 4n cells within 4n↔2n chimeras could give an insight into how CPM arises.

Previous analysis of 4n↔2n chimeric blastocysts revealed that 4n cells were present in both the inner cell mass (ICM) and TE but were preferentially allocated to the mTE at E3.5 (Everett and West, 1996). The 4n and 2n cells do not intermingle exclusively until after the blastocyst stage (Garner and McLaren, 1974; Gardner and Cockroft, 1998). If the blastocyst cavity formed preferentially within the group of 4n cells this could cause 4n cells to contribute more to the mTE than pTE and more to the hypoblast than epiblast. Although previous analysis of reconstructed 3-dimensional (3-D) images of blastocysts did not show strikingly different distribution patterns between 2n↔2n chimeras and 4n↔2n chimeras some 4n cells were located

adjacent to the blastocyst cavity in all 4n↔2n chimeras analysed (Everett *et al.*, 2000).

Although 4n cells were largely excluded from the derivatives of the epiblast at E7.5, 4n cells were present within the ICM region prior to the differentiation of the epiblast and hypoblast (Everett and West, 1998). 4n cells could be reduced in the epiblast by preferential allocation of 4n ICM cells to the hypoblast at the blastocyst stage. Alternatively 4n cells could be present in the epiblast when it differentiates and some other form of cell selection acting between the blastocyst stage and E7.5, could be responsible for removing 4n cells from the derivatives of the epiblast (Fig 5.1). The experiments presented in this chapter were designed to determine if 4n cells are preferentially allocated to the hypoblast, using tauGFP as a marker in living chimeric blastocysts.

Two separate series of 4n↔2n (4nGFP↔2n, 4n↔2nGFP) and control 2nGFP↔2n chimeric blastocysts cultured in vitro were analysed at E3.5 and E4.5 to determine if 4n cells were preferentially allocated to the hypoblast. The E3.5 series were also analysed to determine the position of the blastocyst cavity relative to the distribution of 4n and 2n cells soon after cavity formation.

Cultured chimeric blastocysts were analysed at E3.5 and E4.5 but, because the epiblast and hypoblast could not be clearly distinguished, more advanced blastocysts were also analysed. These were produced by

Fig 5.1:
Alternative Fates of 4n↔2n Chimeras

Hypothesis 1:

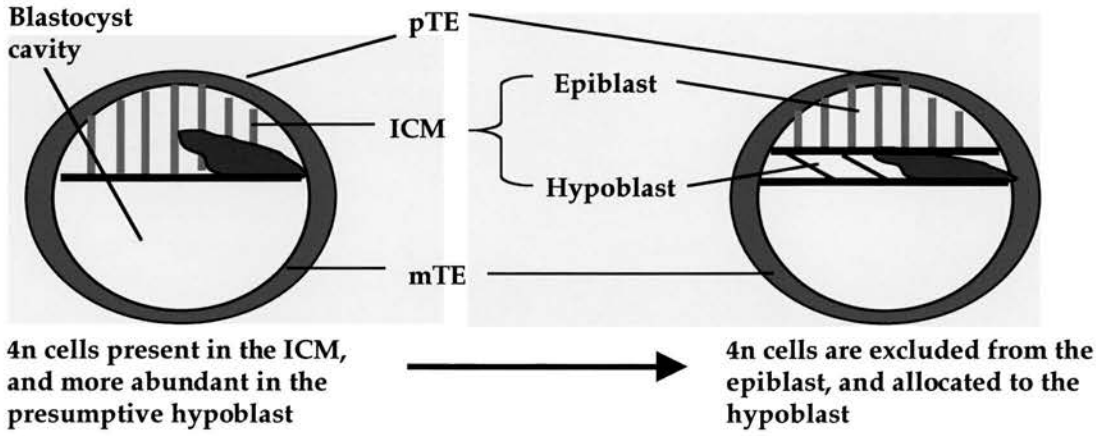

Hypothesis 2:

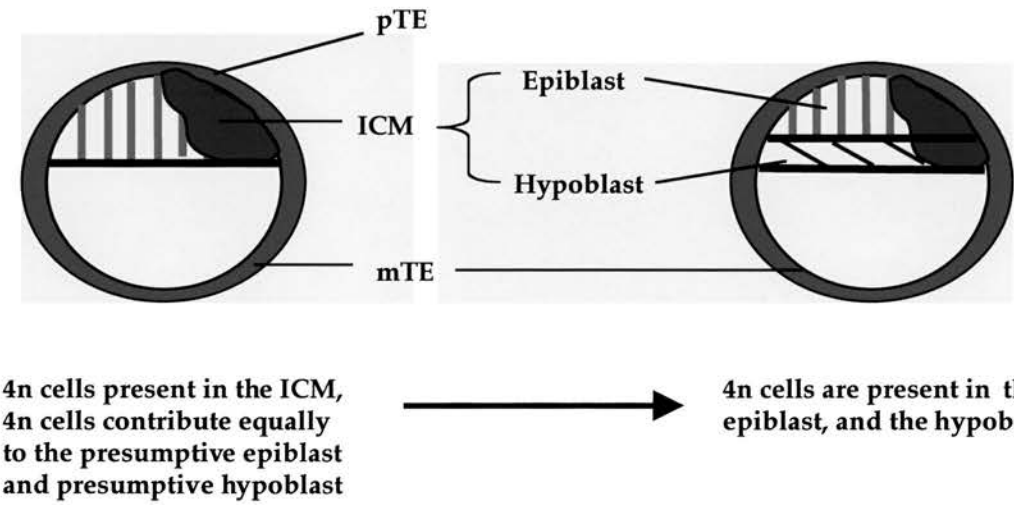

Fig 5.1: Two different hypotheses to explain the fates of 4n cells in the ICM of 4n↔2n chimeras. **a:** Hypothesis 1, 4n cells are excluded from the epiblast by preferential allocation of 4n cells to the hypoblast. **b:** 4n cells are present in the epiblast when it differentiates and are subsequently excluded from the epiblast derivatives by cell selection against 4n cells. 4n cells in the ICM are shown coloured green, 4n cells in the TE are not shown.

transferring E3.5 chimeras to pseudopregnant females injected with the anti-oestrogen tamoxifen to induce diapause. Two separate series of chimeras, 4nGFP↔2n and control 2nGFP↔2n, were analysed at E5.5 and E7.5 to test whether 4n cells were present within the epiblast and hypoblast regions.

5.2 Materials And Methods

5.2.1 Electrofusion of Embryos

A tetraploid embryo was produced, by fusing the cells of a 2-cell diploid embryo. The blastomeres were fused using an impulse generator and electrode chamber (BLS Ltd, Biological laboratory equipments, Budapest, model CF-150 impulse generator and GPT-250 electrode chamber), to produce a 1-cell tetraploid embryo.

2-cell embryos were flushed and collected in KSOMH handling medium (as described in chapter 2.2.1). The embryos were washed in a drop of 3M Mannitol then placed between the electrodes of the electrofusion chamber containing 200µl of electrofusion medium (0.3M mannitol, 0.1mM $MgSO_4$, 0.05mM $CaCl_2$ & 0.05mg/ml BSA). An A.C. pulse of 5 volts was applied for 5 seconds to align the embryos, followed by a D.C. pulse of 20 volts for 80 µseconds to degrade the cell membrane and therefore cause cell fusion (Fig.5.2). Embryos were subsequently washed in fresh KSOMH medium 4 times, using clean pipettes to avoid contamination of Mannitol, and transferred to pre-equilibrated KSOM culture medium under silicon oil (BDH) in a 37°C, 5% CO_2 in air incubator. Fused embryos were selected

Fig 5.2:
Electrofusion of 2-cell embryos

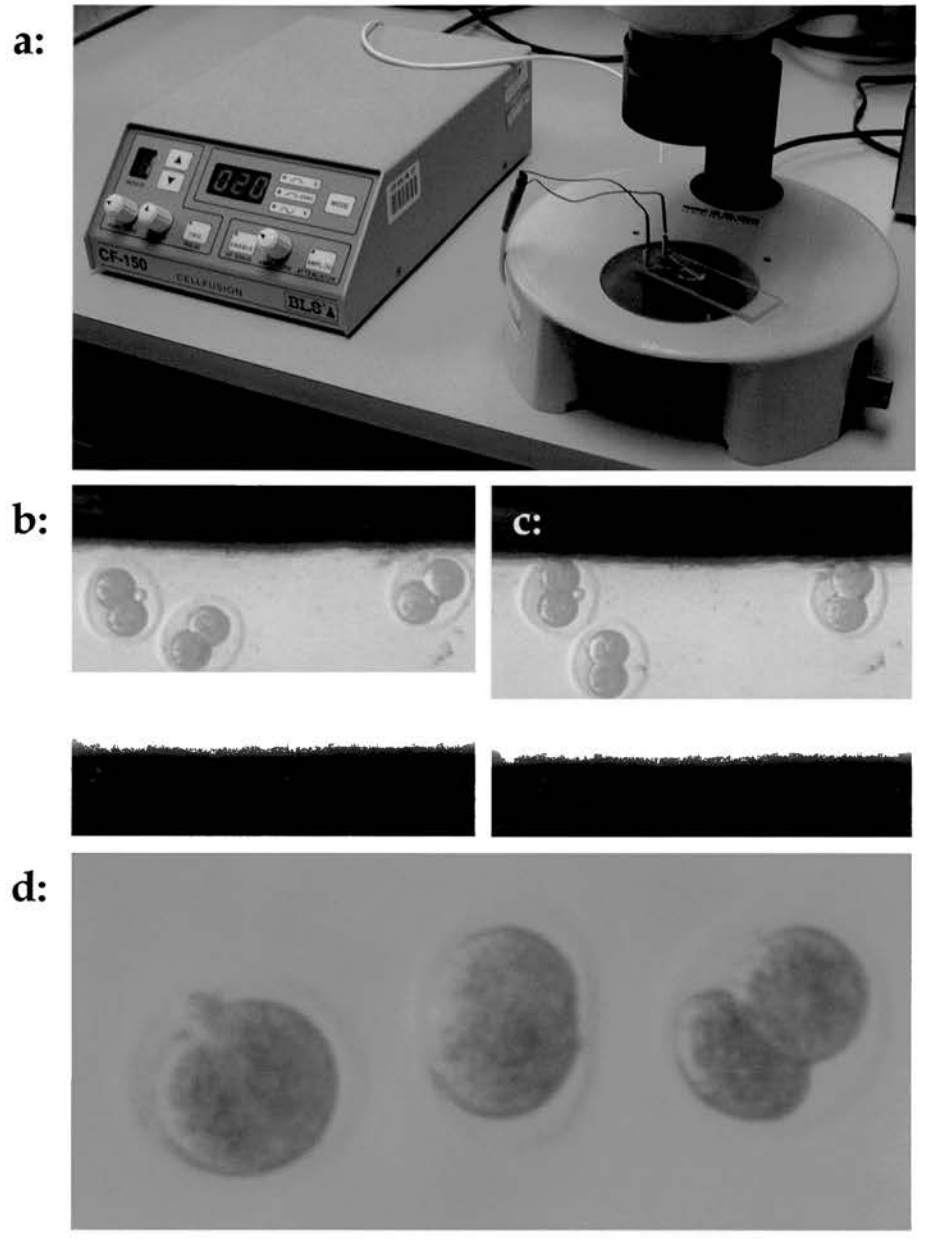

Fig 5.2: a: Elecrtofusion machine and chamber, **b:** 2-cell embryos before alignment with AC pulse, **c:** after AC and DC pulse, **d:** Fusion of blastomeres to produce a 1-cell 4n embryo, 20 minutes after electrofusion pulse. The 2-cell embryo on the right hand side has not fused.

fifteen to thirty minutes later and cultured overnight in KSOM medium to the 4-cell stage for aggregation.

5.2.2 Aggregation of Embryos

Details of the mouse strains used are described in Table 2.1. The methods of embryo collection and chimera production are described in chapter 2.2.1 & 2.2.2.

(BF_1×TgTP6.3) and (BALB/c×A/J)F_2 embryos were flushed at the 2-cell stage using KSOMH handling medium. Three groups of chimeras were produced for these experiments. For both experimental chimera series embryos of one genotype were electrofused and embryos of both genotypes were cultured overnight before aggregation. Therefore, 4-cell tetraploid (BF_1×TgTP6.3) embryos were aggregated to 8-cell diploid (BALB/c×A/J)F_2 embryos or 8-cell diploid (BF_1×TgTP6.3) embryos were aggregated to 4-cell tetraploid (BALB/c×A/J)F_2 embryos. The control series (BF_1×TgTP6.3) ↔(BALB/c×A/J)F_2 was made by aggregating 8-cell diploid embryos that had been collected at the 2-cell stage and cultured overnight. Chimeras were cultured in KSOM culture medium under silicon oil (BDH) in a 37°C, 5% CO_2 in air incubator before microscopy or surgical transfer to a pseudopregnant recipient.

5.2.3 Embryo Transfer to Produce Expanded Blastocysts

On 2.5 days of pseudopregnancy females were anaesthetised as described in chapter 2.1.4. Between 8 and 10 chimeras were transferred to each uterine horn. Following embryo transfer each female was injected i.p. with 10μg Tamoxifen (Sigma) and s.c. with 1mg Depoprovera (Genus Express), as described in Hunter and Evans, (1999). Blastocysts were staged according to the age of the embryo, rather than the stage of pseudopregnancy.

Alternatively following the transfer of 8 to 10 chimeras to recipient females, on 2.5 days of pseudopregnancy, females were ovariectomized and injected s.c with 2.5mg Depoprovera (Genus Express).

5.2.4 Confocal Microscopy

Chimeras that had been cultured in vitro or flushed from delayed implantation females were transferred to fresh drops of KSOM culture medium under silicon oil (BDH) in a glass bottomed Willco microwell dish (Intracel Ltd, HBSt 3522). These were kept in a 37°C, 5% CO_2 in air incubator for at least 3 hours prior to imaging, to ensure the blastocyst cavity re-expanded if it had collapsed after pipetting. The blastocysts were imaged on the heated stage of the inverted confocal microscope. Images were aquired as described in chapter 2.4.

5.2.5 Analysis of Chimeric Embryos

The % contribution of GFP to chimeric embryos was analysed in selected overlay confocal images of GFP on bright field, using Image Pro Plus software (Media Cybernetics, MD, USA). The epiblast and hypoblast cannot be distinguished in E3.5 blastocysts that have been cultured in vitro. However, Weber *et al.* (1999), Ciemerych *et al.* (2000), and Piotrowska *et al.* (2001) have shown that the position of cells within the ICM determines the fate of these cells. Therefore, the cells adjacent to the blastocyst cavity will usually develop into hypoblast cells and the cells adjacent to the pTE will normally develop into epiblast cells. The presumptive epiblast and presumptive hypoblast regions were determined by drawing a line halfway across the ICM (Fig 5.3). The % area of green and non-green in the epiblast and hypoblast were measured for both these regions. The % length of green and non green in the pTE and mTE were measured around the circumference (Fig 5.3).

The 4n↔2n chimeras were analysed by measuring the % GFP-postive and negative areas in the ICM, presumptive epiblast and presumptive hypoblast and the % GFP-postive and negative lengths in the TE, mTE and pTE. Therefore, these results give information about the percentage contribution of 4n cells to the different regions of the blastocyst but not the percentage of cell numbers. As the 4n embryos used in this study were produced by the fusion of a 2-cell embryo it can be assumed that a 4n blastomere is twice the volume of a 2n blastomere. However, the area of a 4n cell seen in an optical section within a chimera is not twice the area of a diploid cell. If both

Fig 5.3: Analysis of % GFP Contribution

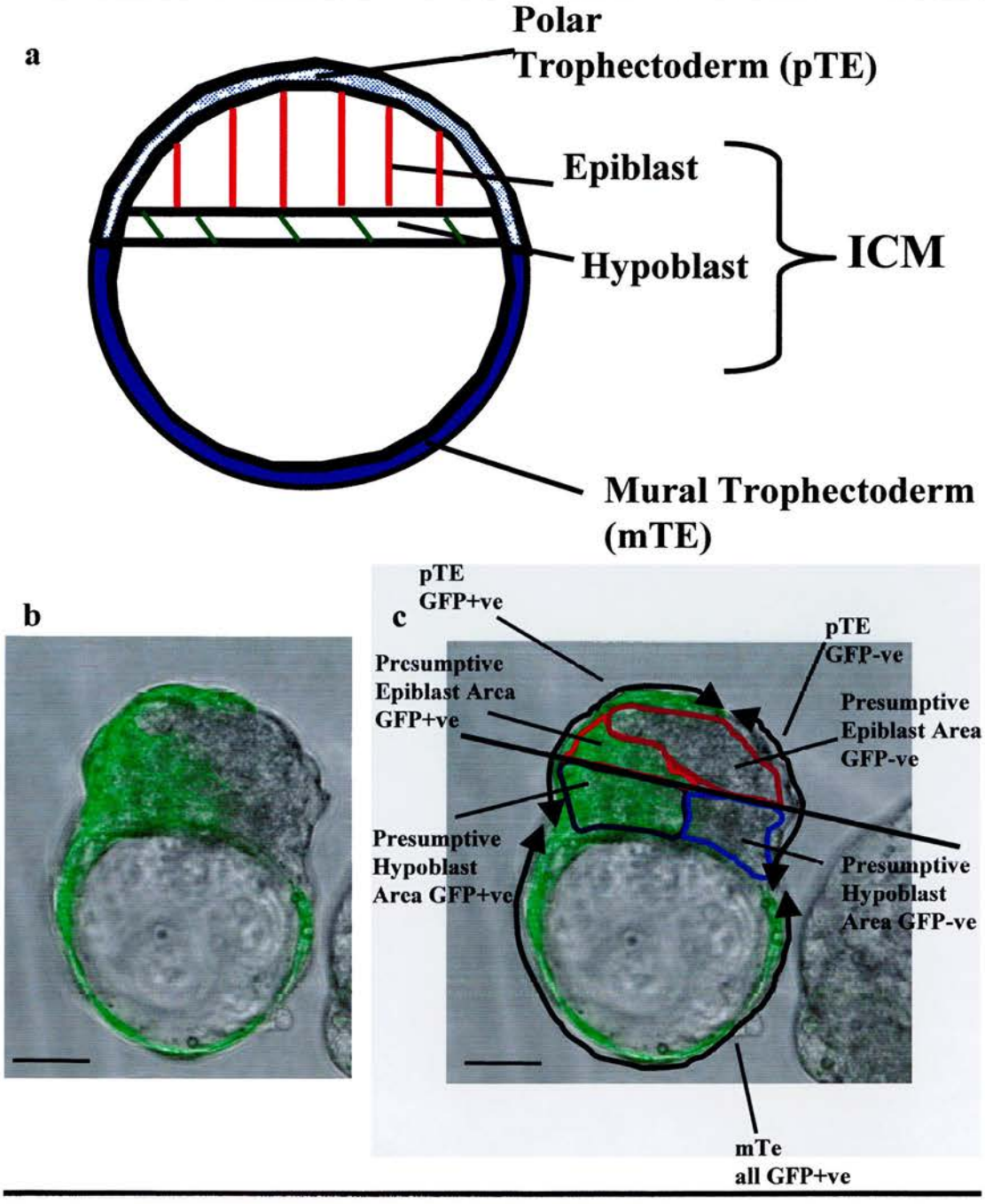

Fig 5.3: a: Schematic diagram of the different regions of the blastocyst, **b:** E3.5 GFP chimeric blastocysts that was cultured in vitro **c:** E3.5 & E4.5 GFP chimeric blastocysts that were cultured in vitro were analysed by drawing a line across the ICM to separate it into two regions , the presumptive epiblast and the presumptive hypoblast. The area of % GFP was measured in these regions. The % length of GFP in the pTE and mTE was also measured. Scale bar=50microns.

blastomeres are thought of as spheres, when the volume of one sphere is 2× the volume of another sphere, the radius (r) would be 1.26× the radius of the smaller sphere (as volume is equal to $^4/_3(\pi r^3)$) (Table 5.1). Therefore, the length of a 4n cell is expected to be 1.26× the length of a 2n cell. As surface area=$4\pi r^2$, the surface area of the larger sphere would be 1.59× the surface area of the smaller sphere. These calculations are approximate because they assume that blastomeres are spherical (Epstein, 1986).

Table 5.1: Calculation of the Ratio of length and areas of 4n/2n cells

	radius r	diameter 2r	surface area $4\pi r^2$	Area through a cell πr^2	volume $(4/3)\pi r^3$
Value 1	1	2	12.566	3.14	4.189
Value 2	1.260	2.520	19.948	4.984	8.378
Ratio 2/1	1.260	1.260	1.587	1.587	2.001

5.3 Results

5.3.1 In vitro analysis of E3.5 4n↔2n chimeras

Three groups of chimeras were produced and cultured in vitro. These were imaged using the confocal microscope at E3.5: control 2nGFP↔2n, and experimental 4nGFP↔2n and 4n↔2nGFP chimeras. The epiblast and hypoblast could not be distinguished therefore GFP and non-GFP contributions were analysed as described in section 5.2.5 of this chapter.

5.3.1.1 Control E3.5 2n↔2n chimeras

21 control 2nGFP↔2n chimeric blastocysts were cultured in vitro and imaged at E3.5. Individual overlay images of these chimeric blastocysts are

shown in Figure 5.4. Table 5.2 shows the measured individual, and mean percentage GFP contribution to the separate regions of these chimeric blastocysts.

The histogram in Figure 5.5a shows the mean percentage GFP contribution to the individual regions of the blastocyst. There was a significantly higher mean contribution of GFP cells in the TE than the ICM, in the mTE than the pTE and in the presumptive hypoblast than the presumptive epiblast ($p<0.05$ by Mann-Whitney U test) (Fig 5.5a). The small but significant difference in composition of the different tissues of the blastocyst could reflect genetic differences between the GFP and non-GFP embryos, sample variation or experimental variation attributable to methods used to estimate %GFP composition. However, both the 4nGFP↔2n and the reciprocal chimera combination, 4n↔2nGFP were analysed at E3.5 to ensure the same trends were observed in both experimental chimera combinations.

Fig 5.4: Confocal Images of Control E3.5 2nGFP↔2n Chimeras

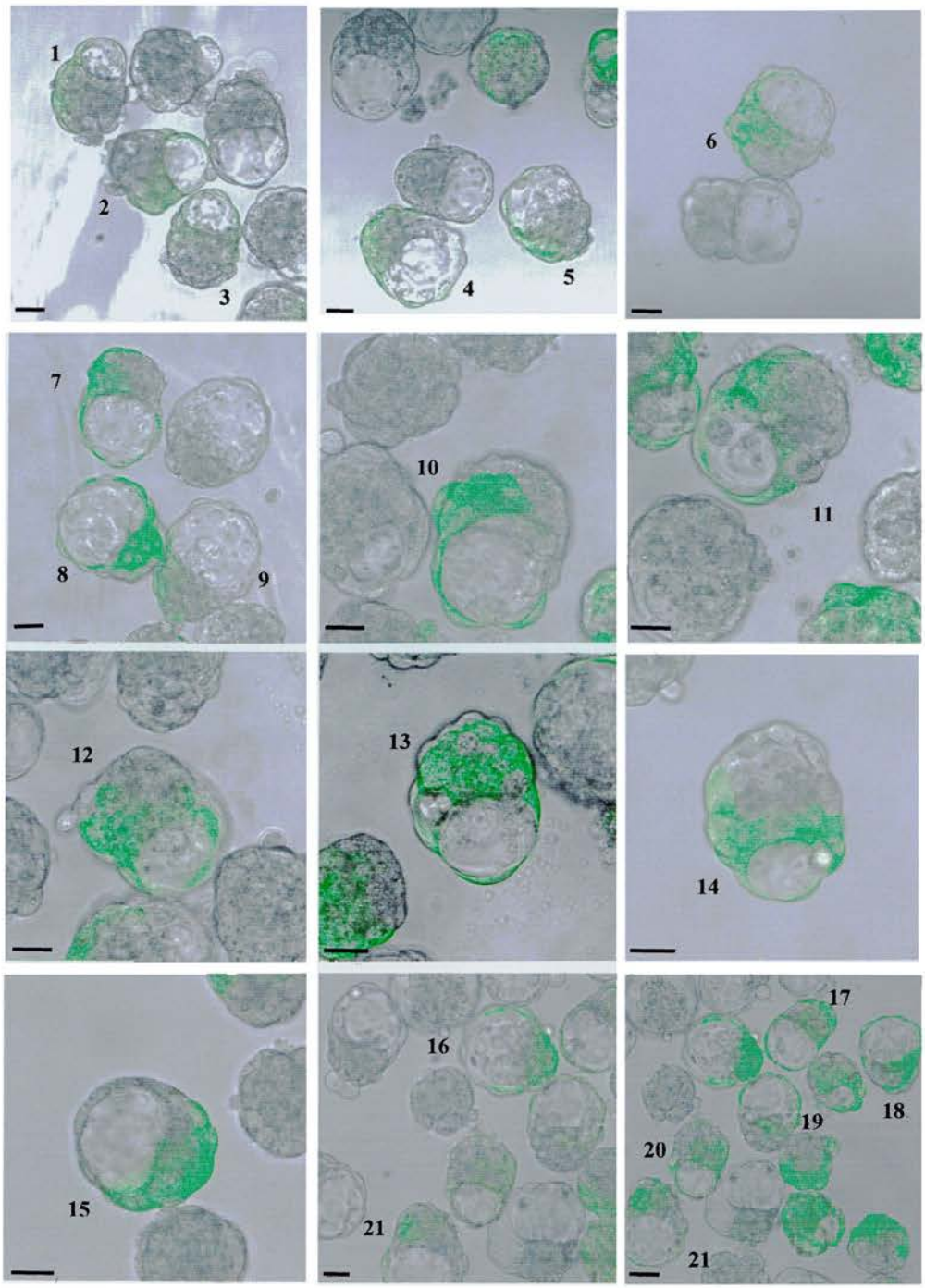

Fig 5.4: Overlay images of 21 E3.5 control 2nGFP↔2n chimeric embryos.
Scale bar=50microns.

Table 5.2:
% Contribution of GFP cells in E3.5 2nGFP↔2n Chimeras

Blastocyst	Total TE	Total ICM	mTE	pTE	Presumptive Epiblast	Presumptive Hypoblast
1	42	28	21	53	27	30
2	43	40	48	39	35	46
3	56	26	80	42	11	49
4	62	45	48	83	51	37
5	59	29	61	57	32	26
6	49	48	48	50	39	60
7	79	40	95	60	33	48
8	61	88	67	50	79	95
9	32	50	15	59	49	51
10	54	55	84	26	50	58
11	66	35	100	39	31	39
12	47	51	72	27	32	70
13	71	77	100	53	86	69
14	60	41	100	44	13	74
15	48	71	10	88	81	59
16	62	93	48	86	100	90
17	83	51	100	65	49	52
18	82	52	83	81	48	56
19	56	34	92	10	17	53
20	53	36	69	43	29	46
21	54	50	61	43	49	52
Mean % Length	**58.06**		**66.67**	**52.42**		
Mean % Area		**49.46**			**44.82**	**55.13**
SE	2.86	4.07	6.20	4.46	5.26	3.76
N	21	21	21	21	21	21
SD	13.13	18.64	28.40	20.44	24.12	17.24

Table 5.2:
Individual and mean % length of GFP cells in the TE, mTE & pTE and the % area of GFP cells in the ICM, including the presumptive epiblast and hypoblast, of E3.5 2nGFP↔2n chimeras.

SE= Standard Error, N= Number, SD= Standard Deviation.

Fig 5.5:
% Contribution of GFP or 4n cells in E3.5 Chimeras

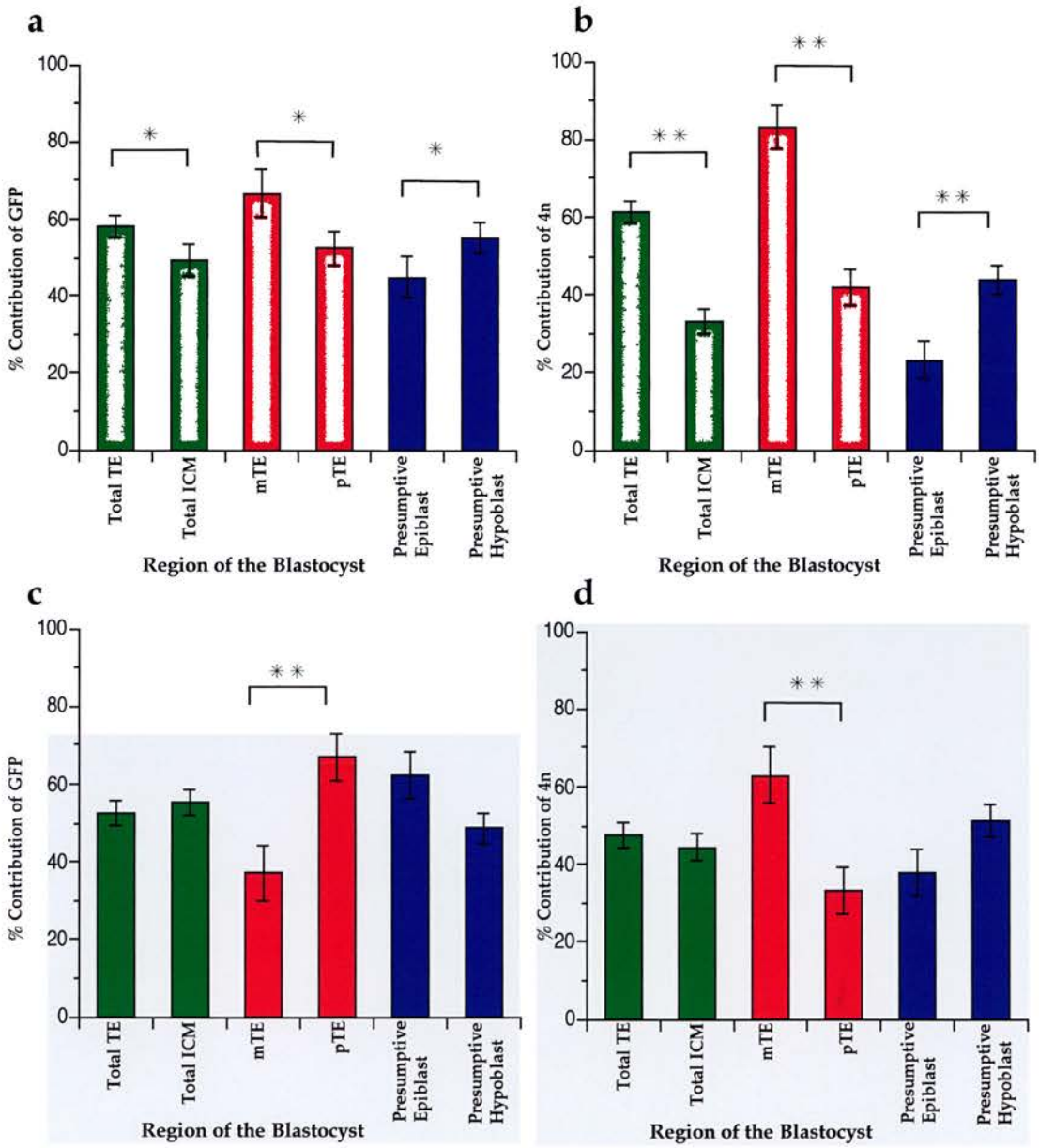

Fig 5.5: The mean % length in the TE and % area in the ICM, including the presumptive epiblast and hypoblast, of **a:** GFP cells in 2nGFP↔2n control chimeras, **b:** 4n cells in 4nGFP↔2n chimeras, **c:** GFP cells in 4n↔2nGFP chimeras, **d:** 4n cells in 4n↔2nGFP.
* P<0.05, * * P<0.01 (Mann-Whitney U-tests)

Mann-Whitney U-test probabilities for comparisons of %GFP in comparable tissues between control and experimental chimeras (a-c).

E3.5	TE	ICM	mTE	pTE	Epiblast	Hypoblast
2nGFP<->2n v 4nGFP<->2n (avb)	P=0.4592	P=0.0015	P=0.0177	P=0.1101	P=0.0051	P=0.0264
2nGFP<->2n v 4n<->2nGFP (avc)	P=0.3311	P=0.0936	P=0.0051	P=0.0475	P=0.0246	P=0.1698

5.3.1.2 E3.5 4nGFP↔2n Chimeras

Overlay images of E3.5 4nGFP↔2n chimeras are shown in Fig 5.6. The individual percentage GFP contribution were measured and means calculated (Table 5.3).

Figure 5.5b and Mann-Whitney U-tests show that at E3.5 the contribution of 4n tissue (GFP) was greater in the TE than ICM ($P<0.01$), greater in the mTE than the pTE ($p<0.01$) and greater in the presumptive hypoblast than the presumptive epiblast ($p<0.01$). Individual tissue differences between the 4nGFP↔2n and control 2nGFP↔2n chimeras are shown in the footnote to Fig 5.5 but it is more helpful to compare the differences between relevant pairs of tissues. The three pairwise differences are greater in the 4nGFP↔2n chimeras than in the control chimeras (Fig 5.5a compared to 5.5b, Table 5.4) and are significantly greater for the first two comparisons (TE v ICM and mTE v pTE). This suggests that tetraploid cells are not randomly distributed among different tissues of the blastocyst.

Table 5.4: Comparison between 4nGFP↔2n and control chimeras, for differences in % GFP for three pairs of tisssues

E3.5	TE-ICM	mTE-pTE	Hypoblast-Epiblast
2nGFP<->2n (n=21) Fig 5.5a	8.60 ± 4.61	14.25 ± 9.0	10.31 ± 4.48
4nGFP<->2n (n=23) Fig 5.5b	28.17 ± 3.04	40.88 ± 8.12	20.65 ± 5.25
2nGFP<->2n v 4nGFP<->2n (avb)	**P=0.022**	**P=0.016**	P=0.142

The mean percentages of 4n cell numbers were estimated from the means of the % GFP contribution (see section 5.2.5 of this chapter), and are shown in Table 5.3. The histograms show that the same trends were observed for cell

Fig 5.6: Confocal Images of E3.5 4nGFP↔2n Chimeras

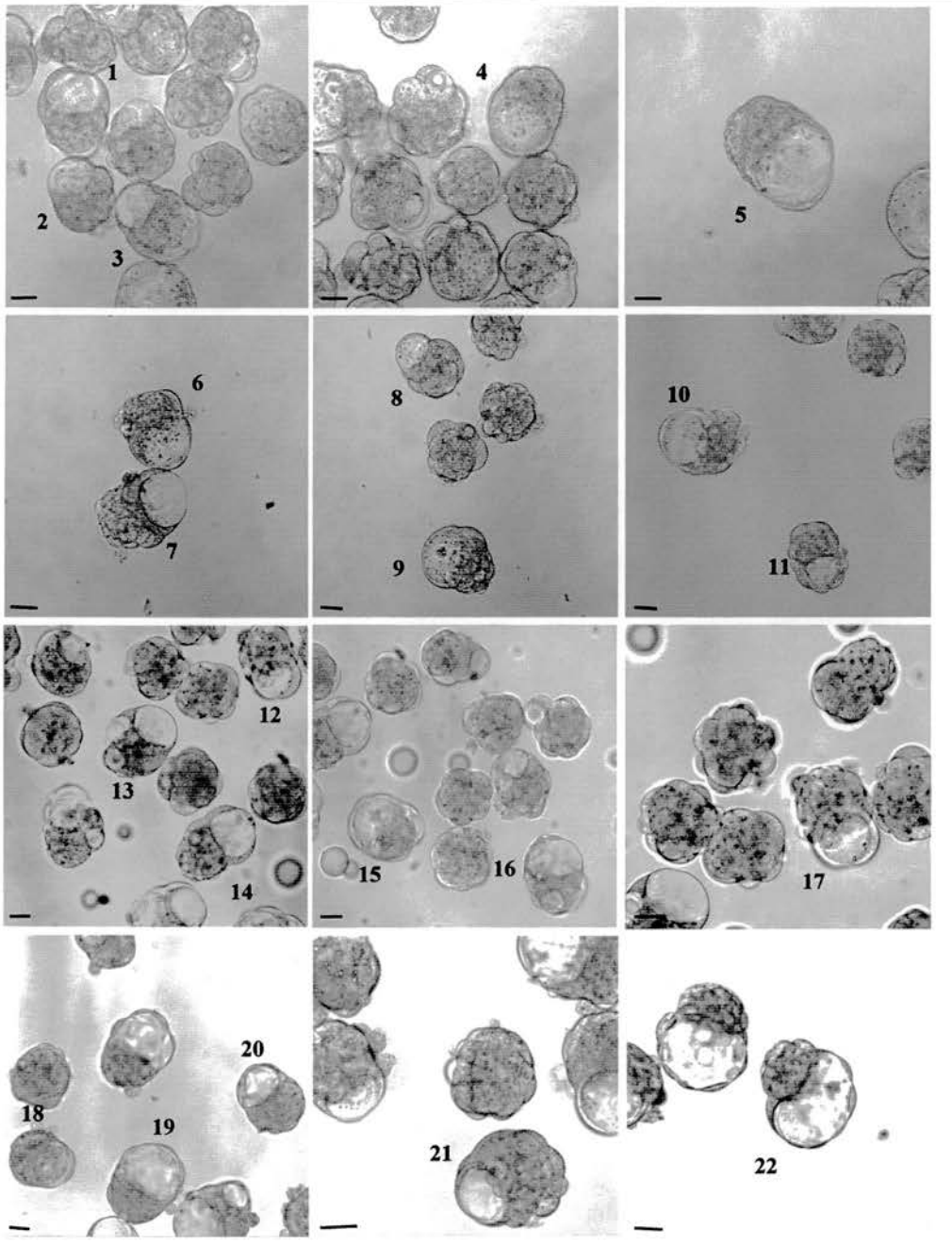

Fig 5.6: Overlay images of 22 E3.5 4nGFP↔2n chimeras.
Scale bar=50microns.

Table 5.3:
% Contribution of 4n cells in E3.5 4nGFP↔2n Chimeras

Blastocyst	Total TE	Total ICM	mTE	pTE	Presumptive Epiblast	Presumptive Hypoblast
1	61	18	100	20	1	39
2	72	41	100	56	41	41
3	60	36	100	38	10	54
4	79	29	100	59	20	39
5	67	30	86	45	22	43
6	68	36	100	33	33	40
7	45	23	67	28	0	46
8	65	31	86	55	8	56
9	63	11	100	16	0	18
10	53	25	76	32	6	43
11	76	46	100	57	37	58
12	48	32	65	36	34	30
13	60	25	100	38	0	55
14	60	35	100	22	6	72
15	52	30	85	21	3	64
16	48	42	18	77	46	37
17	48	35	59	39	29	43
18	44	8	77	20	0	15
19	96	87	100	92	85	90
20	38	46	0	68	51	42
21	75	35	100	62	44	26
22	61	13	91	0	0	22
23	72	48	100	58	57	37
Mean % Length	**61.30**		**83.01**	**42.13**		
Mean % Area		**33.14**			**23.13**	**43.79**
SE	2.84	3.35	5.62	4.60	4.89	3.61
N	23	23	23	23	23	23
SD	13.62	16.08	26.95	22.06	23.46	17.31
Corrected Value for % Cell Number	**55.7**	**23.77**	**79.5**	**36.62**	**15.91**	**32.88**

Table 5.3:
Individual and mean % length of 4n cells in the TE, mTE & pTE, and the % area of 4n cells in the ICM, including the presumptive epiblast and hypoblast, of E3.5 4nGFP↔2n chimeras. The corrected values for the % number of 4n cells is shown. These were calculated as described in section 5.2.5. If there was an equal contribution of 4n cells to all the regions of the blastocyst a proportion of 33.3% in each tissue would be expected.
SE= Standard Error, N= Number, SD=Standard Deviation.

number (Fig 5.7a) as were observed for percentage area and length contribution (Fig 5.5b). If 4n cells divided at the same rate as 2n cells, and both types of cell contributed equally to all regions of the blastocyst, the number of 2n cells would be expected to be twice the number of 4n cells. Therefore, the percentage 4n cell number would be expected to be 33.3% in each region of the blastocyst. However, this is not the case, more 4n cells are present in the TE, specifically the mTE, and there are more 4n cells in the hypoblast compared to the epiblast. This implies that the distribution of 4n cells (Fig 5.7a) is similar to the measured GFP tissue area or length (Fig 5.5b), discussed above.

5.3.1.3 E3.5 4n↔2nGFP Chimeras

Figure 5.8 shows the individual overlay images of 22 E3.5 4n↔2nGFP analysed chimeras. The individual and mean percentages of GFP (2n) contribution are shown in Table 5.5a and the mean percentages of non-GFP (4n) contribution are shown in Table 5.5b.

The histograms showing the mean % GFP (2n) contribution (Fig 5.5c) and mean % 4n contribution (Fig 5.5d) shows a slightly lower percentage of GFP contribution (higher % 4n) in the TE than the ICM. This difference is not significant. There was however, a significantly lower % GFP (higher % 4n) in the mTE than the pTE ($P<0.01$ by Mann-Whitney U-test) and in the mTE than the ICM ($P<0.05$ by Mann-Whitney U-test). When compared to the control chimeras in Fig 5.5a the 4n↔2nGFP chimeras in Fig 5.5c showed a trend towards less GFP (more 4n) in the TE than ICM. Comparison with control

Fig 5.7:
% of estimated 4n cell number in E3.5 & E4.5 Chimeras

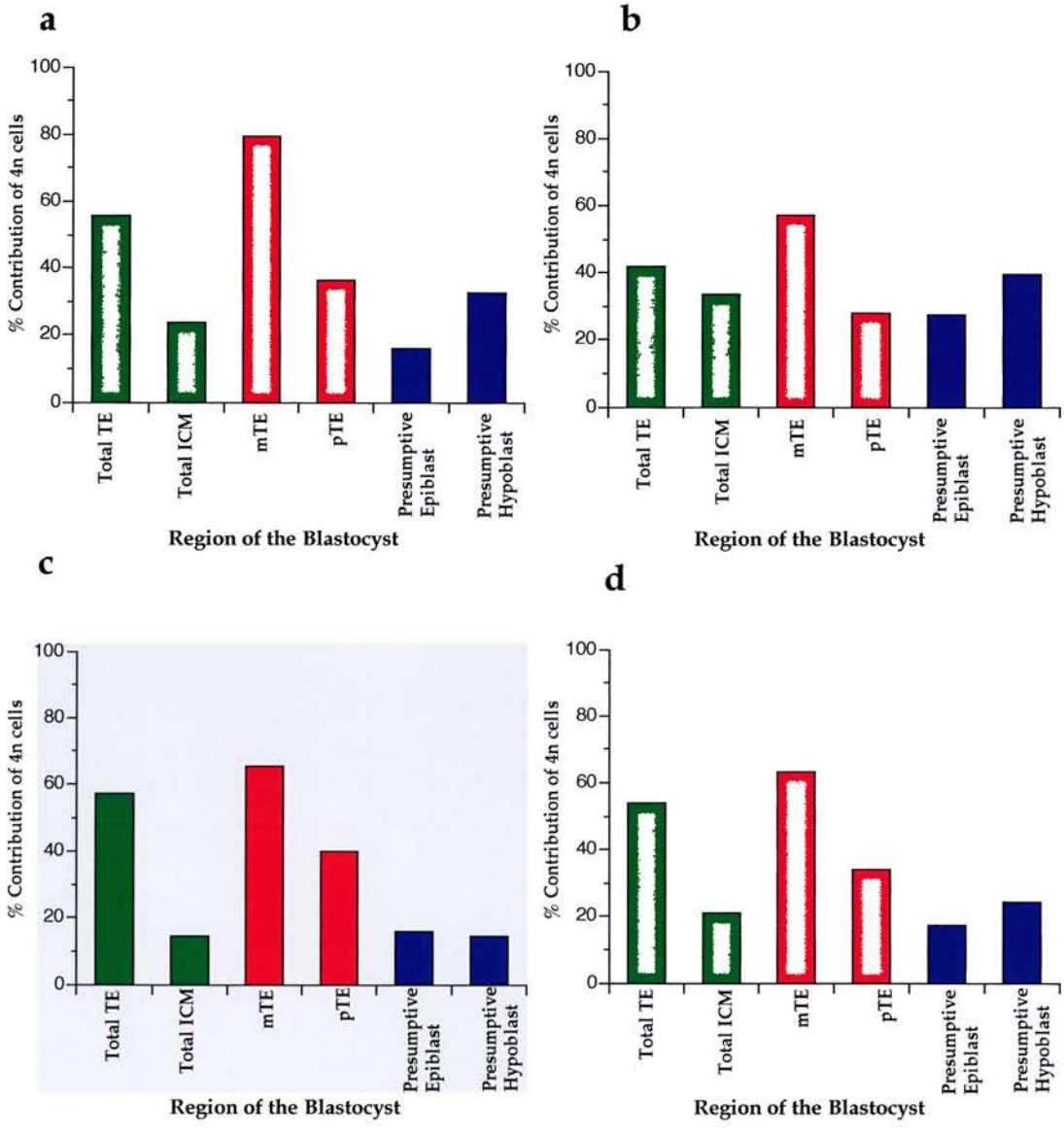

Fig 5.7:
The mean % estimated 4n cell number in the ICM, the presumptive epiblast, hypoblast, TE, mTE & pTE in **a:** E3.5 4nGFP↔2n chimeras, **b:** E3.5 4n↔2nGFP chimeras, **c:** E4.5 4nGFP↔2n chimeras, **d:** E4.5 4n↔2nGFP.

Fig 5.8: Confocal Images of E3.5 4n↔2nGFP Chimeras

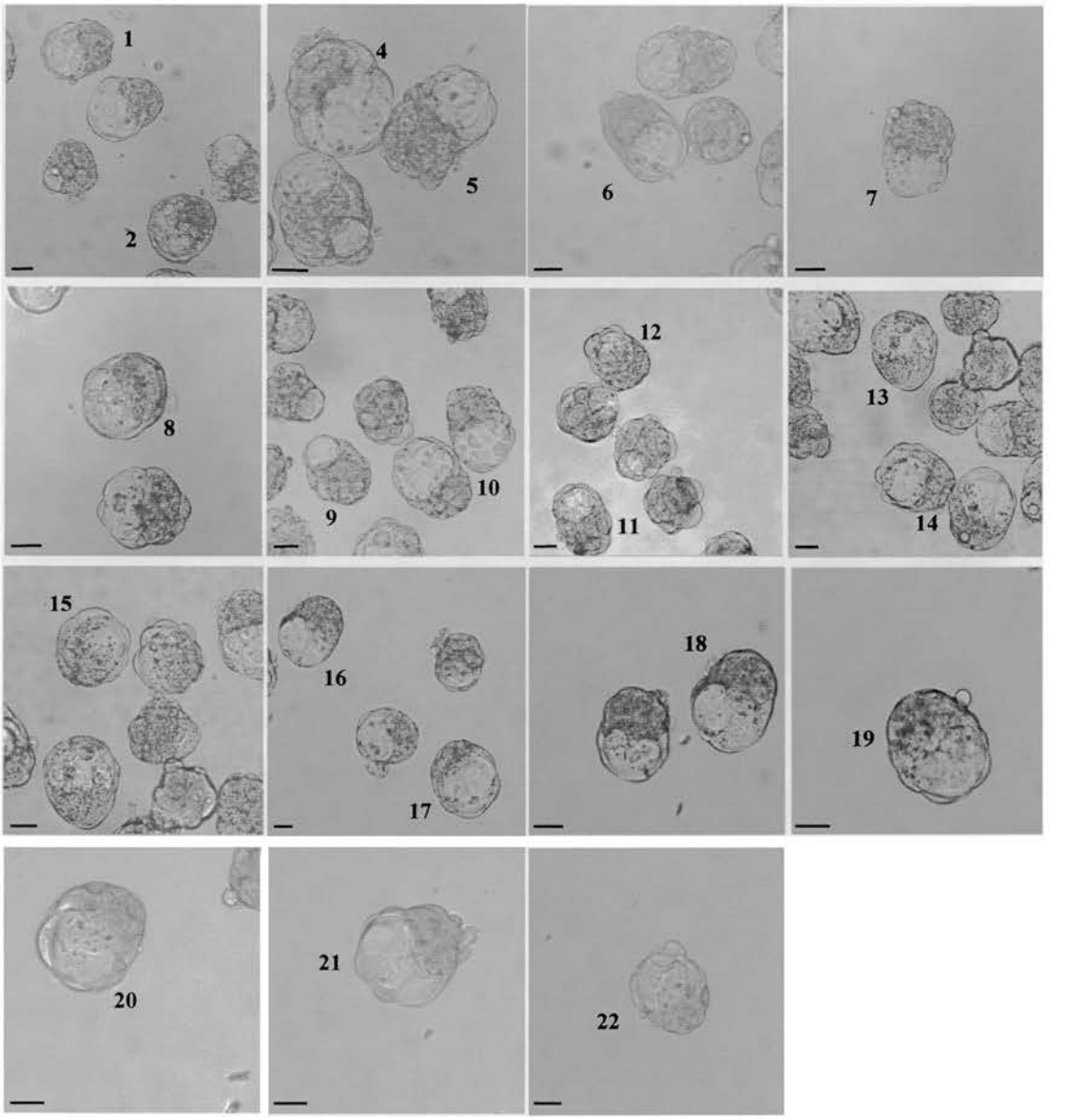

Fig 5.8: Overlay images of 4n↔2nGFP chimeric embryos.
Scale bar=50microns.

Table 5.5:
% Contribution of GFP and 4n cells in E3.5 4n↔2nGFP Chimeras

(a) % GFP

Blastocyst	Total TE	Total ICM	mTE	pTE	Epiblast	Hypoblast
1	70	43	94	42	32	51
2	33	32	34	30	45	22
3	14	47	6	21	0	79
4	79	36	100	53	32	41
5	56	55	18	85	65	42
6	61	52	37	89	88	22
7	51	65	0	100	94	38
8	47	47	77	14	32	58
9	60	56	0	83	75	39
10	61	48	50	71	49	46
11	33	42	16	45	60	19
12	41	57	0	62	76	40
13	66	59	39	100	49	65
14	72	53	92	53	38	67
15	61	61	34	100	64	59
16	41	63	25	60	84	48
17	52	65	28	100	94	44
18	43	74	19	72	98	50
19	61	35	83	36	34	36
20	43	80	0	90	96	65
21	64	50	64	65	64	43
22	44	100	0	100	100	100
Mean % Length	**52.49**		**37.11**	**66.90**		
Mean % Area		**55.51**			**62.31**	**48.80**
SE	3.24	3.34	7.20	5.87	5.89	4.03
N	22	22	22	22	22	22
SD	15.18	15.68	33.78	27.53	27.61	18.91

(b) % 4n

Mean % Length	**47.51**		**62.89**	**33.10**		
Mean % Area		**44.49**			**37.69**	**51.20**
SE	3.24	3.34	7.20	5.87	5.89	4.03
Corrected Value for % Cell Number	**41.80**	**33.51**	**57.36**	**28.20**	**27.56**	**39.75**

Table 5.5:
Showing **a:** the individual and mean % length of GFP cells in the TE, mTE & pTE, and the % area of GFP cells in the ICM, including the presumptive epiblast and hypoblast, of E3.5 4n↔2nGFP chimeras and **b:** the mean % length of 4n cells in the TE, mTE & pTE and the % area of 4n cells in the ICM, epiblast & hypoblast. The corrected values for the % number of 4n cells is shown. If there was an equal contribution of 4n cells to all the regions of the blastocyst a proportion of 33.3% in each tissue would be expected.
SE= Standard Error, N= Number, SD=Standard Deviation.

chimeras for pairwise differences by Mann-Whitney U-tests showed significantly less GFP (more 4n) in the mTE than pTE and also significantly less GFP (more 4n) in the hypoblast than epiblast (Table 5.6).

Table 5.6: Comparison between 4n↔2nGFP and control chimeras for differences in % GFP for three pairs of tisssues

E3.5	TE-ICM	mTE-pTE	Hypoblast-Epiblast
2nGFP<->2n (n=21) Fig 5.5a	8.6 ± 4.61	14.25 ± 9.0	10.31 ± 4.48
4n<->2nGFP (n=22) Fig 5.5c	- 3.02 ± 5.01	- 29.8 ± 11.2	- 13.51 ± 7.32
2nGFP<->2n v 4n<->2nGFP (avc)	P=0.0985	**P=0.01**	**P=0.007**

The mean percentages of 4n cell numbers were calculated (Table 5.5). This data shows the same trends as the % 4n contribution measured by area and length (Fig 5.7b compared to Fig 5.5d). The percentage of 4n cells in the TE, mTE and hypoblast is higher than the expected 33%.

5.3.1.4 Comparison between E3.5 Chimera Groups

The proportion of blastocysts that contained chimeric ICM's, epiblasts or hypoblasts did not vary significantly among the three groups (P>0.05 by Fisher's Exact test). However, the analysis of percentage cell contribution and the calculated values of percentage cell numbers show, at E3.5, 4n cells were preferentially allocated to the mTE rather than the pTE of 4n↔2n chimeras. One series, 4nGFP↔2n, had significantly more 4n in the TE than the ICM and although the other series also had a higher percentage in the TE this was not significant. Tetraploid cells were present in the presumptive epiblast region but there appeared to be a higher contribution of 4n cells to the presumptive hypoblast.

5.3.2 In Vitro Analysis of E4.5 4n↔2n Chimeras

A separate series of the same chimera combinations, 2nGFP↔2n, 4nGFP↔2n and 4n↔2nGFP were aggregated, cultured in vitro and imaged at E4.5. Again the epiblast and hypoblast regions could not be identified so the blastocysts were analysed as before (see section 5.2.5 of this chapter).

5.3.2.1 Control E4.5 2nGFP↔2n Chimeras

Overlay images of control 2nGFP↔2n E4.5 blastocysts are shown in figure 5.9. The individual and mean percentage GFP contributions are shown in Table 5.7, and histograms of the mean percentage GFP contribution are shown in Figure 5.10a. These results show that there was a higher mean percentage of GFP in the ICM than the TE, in the pTE than the mTE and in the presumptive epiblast than the presumptive hypoblast. These differences were not significant. The mean percentage of GFP was higher in the presumptive epiblast than the other tissues of the blastocyst. This was probably attributable to the small sample size, as 5 out of 8 blastocysts had a % GFP in the presumptive epiblast higher than 85% (Table 5.7).

The contribution from the GFP-positive embryo differed in the E3.5 and E4.5 control chimeras. This difference was significant for the mTE. It is probable that random allocation of cells occurs in 2nGFP↔2n chimeras because significant changes in composition between these ages in this group seem unlikely, between E3.5 and E4.5.

Fig 5.9: Confocal Images of Control E4.5 2nGFP↔2n Chimeras

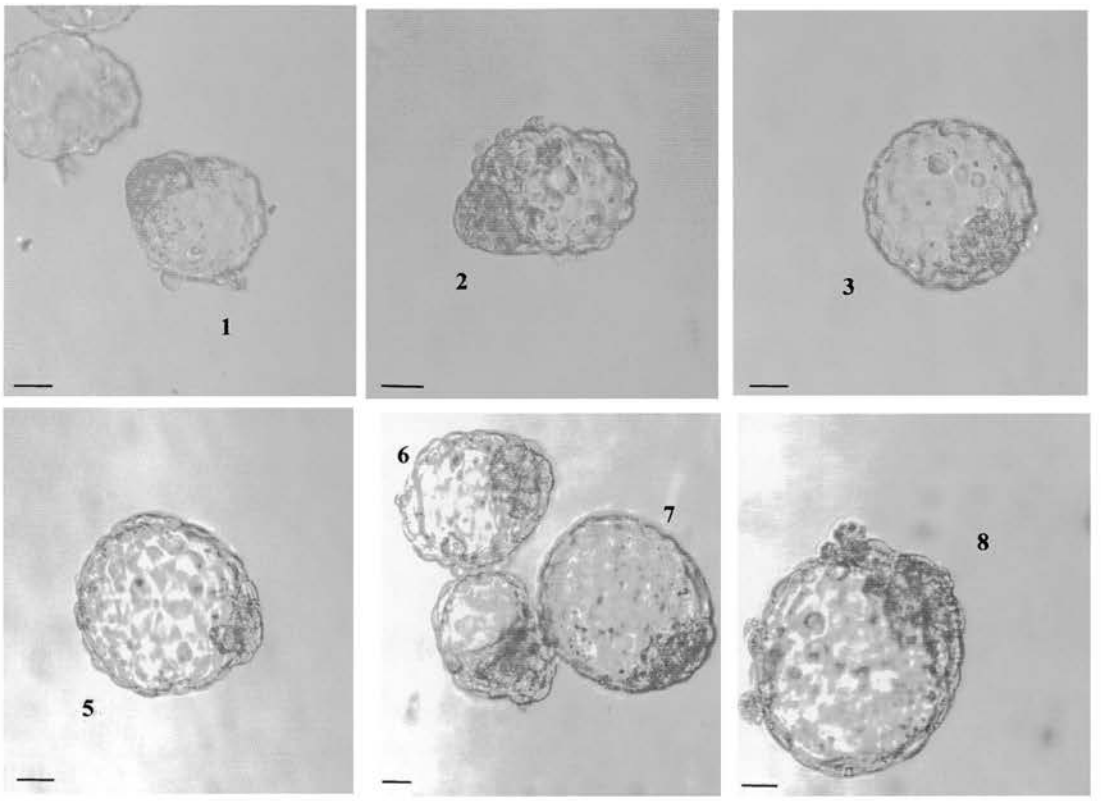

Fig 5.9: Overlay images of 7 out of 8 control E4.5 2nGFP↔2n chimeras.
Scale bar=50microns.

Table 5.7: % Contribution of GFP cells in E4.5 Chimeras

(a) Control 2nGFP↔2n

Blastocyst	Total TE	Total ICM	mTE	pTE	Presumptive Epiblast	Presumptive Hypoblast
1	26	96	11	63	92	100
2	55	52	52	63	88	19
3	38	97	41	26	100	95
4	40	11	43	28	25	0
5	47	56	51	29	50	60
6	44	74	23	90	98	50
7	66	65	60	88	99	33
8	61	0	76	23	0	0
Mean % Length	**47.16**		**44.57**	**51.10**		
Mean % Area		**56.44**			**68.99**	**44.65**
SE	4.62	12.62	7.26	9.96	13.79	13.76
N	8	8	8	8	8	8
SD	13.07	35.69	20.52	28.16	39.00	38.92

(b) 4nGFP↔2n

Blastocyst	Total TE	Total ICM	mTE	pTE	Presumptive Epiblast	Presumptive Hypoblast
1	50	19	52	46	18	20
2	49	0	60	26	0	0
3	71	0	100	20	0	0
4	70	12	70	70	16	9
5	53	13	66	12	3	19
6	63	53	84	26	86	53
7	69	84	58	100	80	90
8	47	23	39	81	42	11
9	88	14	100	56	4	17
10	90	17	100	66	10	20
11	39	0	46	0	0	0
Mean % Length	**62.57**		**70.46**	**45.74**		
Mean % Area		**21.40**			**23.45**	**21.74**
SE	5.04	7.70	6.73	9.50	9.62	8.18
SD	16.78	25.55	22.33	31.50	31.91	27.14
N	11	11	11	11	11	11
Corrected Value for % Cell Number	**57.02**	**14.62**	**65.43**	**40.08**	**16.15**	**14.87**

(c) 4n↔2nGFP (% GFP)

Blastocyst	Total TE	Total ICM	mTE	pTE	Presumptive Epiblast	Presumptive Hypoblast
1	55	75	55	56	78	73
2	56	59	39	86	55	63
3	25	60	13	63	67	50
4	51	79	52	51	80	79
5	55	83	43	90	97	67
6	24	43	13	51	64	34
7	33	74	24	44	60	92
8	22	86	13	43	100	73
Mean % Length	**40.20**		**31.37**	**60.40**		
Mean % Area		**69.98**			**74.97**	**66.14**
SE	5.42	5.12	6.29	6.35	5.96	6.31
SD	15.33	14.48	17.80	17.96	16.86	17.86
N	8	8	8	8	8	8

(d) 4n↔2nGFP (% 4n)

Mean % Length	**59.80**		**68.63**	**39.60**		
Mean % Area		**30.02**			**25.03**	**33.86**
SE	5.42	5.12	6.29	6.35	5.96	6.31
SD	15.33	14.48	17.80	17.96	16.86	17.86
N	8	8	8	8	8	8
Corrected Values for % Cell Number	**54.14**	**21.25**	**63.45**	**34.23**	**17.35**	**24.36**

Table 5.7: Showing the individual and mean % length of GFP cells in the TE and the mean % area of GFP cells in the ICM, including the presumptive epiblast and presumptive hypoblast, of E4.5 **a** 2nGFP↔2n, **b** 4nGFP↔2n chimeras, **c** 4n↔2nGFP chimeras and **d** the % 4n contribution in 4n↔2nGFP chimeras. SE= Standard Error, N= Number, SD=Standard Deviation.

Fig 5.10:
% Contribution of GFP or 4n cells in E4.5 Chimeras

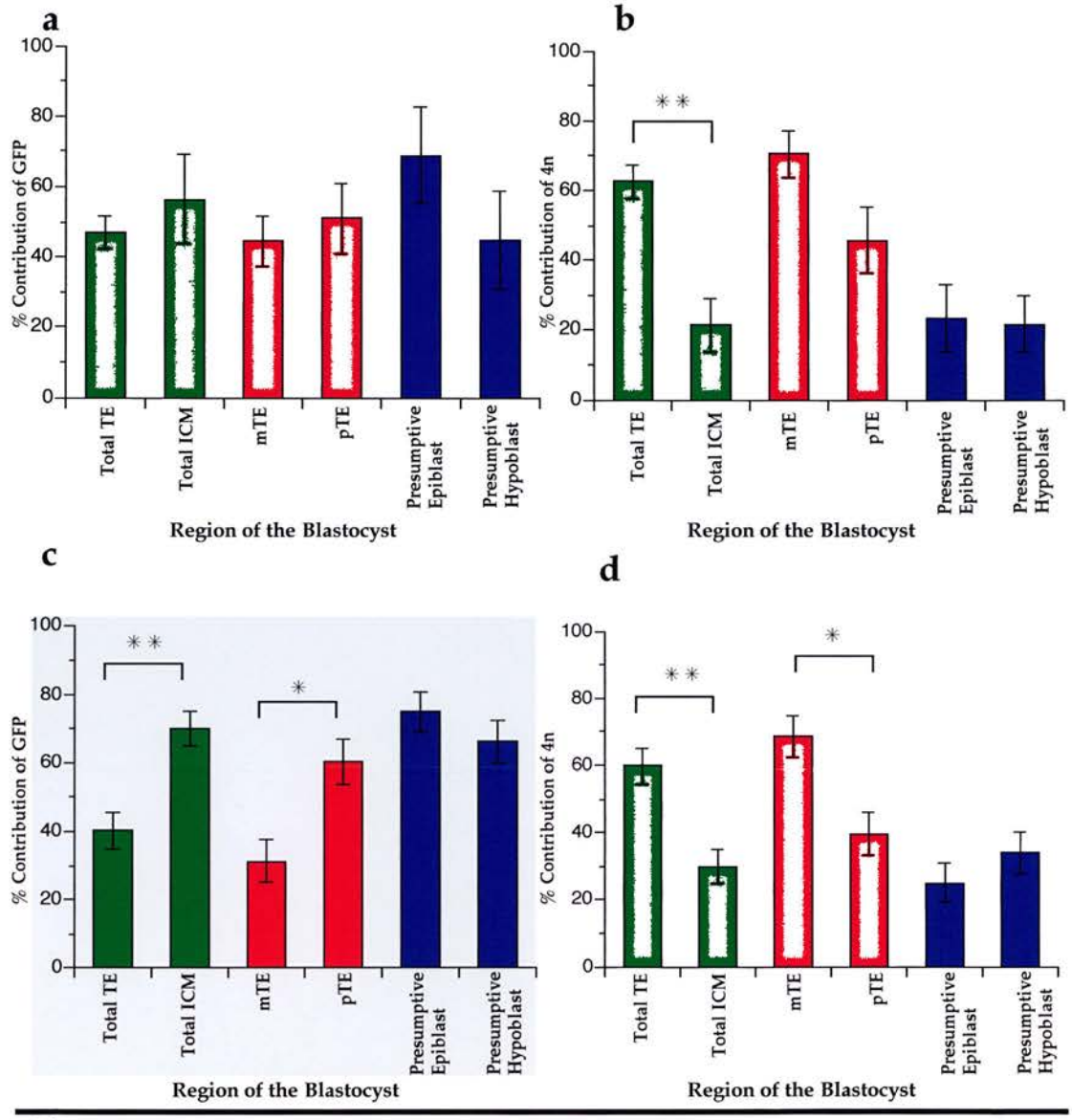

Fig 5.10:
The mean % contribution in the TE and the ICM, including the presumptive epiblast and hypoblast, of **a:** GFP contribution in 2nGFP↔2n control chimeras, **b:** 4ncontribution in 4nGFP↔2n chimeras, **c:** GFPcontribution in 4n↔2nGFP chimeras, **d:** 4n contribution in 4n↔2nGFP.

*P<0.05, ** P<0.01.

Mann-Whitney U-test probabilities for comparisons of %GFP in comparable tissues between control and experimental chimeras (a-c).

E4.5	TE	ICM	mTE	pTE	Epiblast	Hypoblast
2nGFP<->2n v 4nGFP<->2n (avb)	P=0.0430	P=0.0746	P=0.0314	P=0.5624	P=0.0144	P=0.1962
2nGFP<->2n v 4n<->2nGFP (avc)	P=0.3431	P=0.4306	P=0.2915	P=0.4929	P=0.8747	P=0.1883

5.3.2.2 E4.5 4n↔2n Chimeras

Eleven E4.5 4nGFP↔2n chimeras and 8 4n↔2nGFP chimeras were imaged (Fig 5.11 & 5.12). Table 5.7 shows the individual and mean percentage GFP contributions in both experimental chimera groups and the mean percentage 4n contribution in 4n↔2nGFP chimeras.

Figure 5.10b shows there was a higher mean % GFP (4n cell) contribution to the TE than the ICM and the mTE than the pTE. This difference was significant for the TE versus the ICM comparison ($p<0.01$ by Mann-Whitney U test). There was no significant difference between the presumptive epiblast and hypoblast of 4nGFP↔2n chimeras.

The mean percentage of GFP contribution was significantly less (more 4n) in the TE than the ICM ($p<0.01$ by Mann-Whitney U test) and significantly less in the mTE compared to the pTE ($p<0.05$ by Mann-Whitney U test) of 4n↔2nGFP chimeras (Fig 5.10c & d). There was no significant difference between the % GFP contribution in the presumptive epiblast and presumptive hypoblast of 4n↔2nGFP chimeras.

The proportion of blastocysts that contained chimeric ICM's, epiblasts or hypoblasts did not vary significantly among the three groups ($P>0.05$ by Fisher's Exact test).

Statistical analysis comparing both experimental groups of E4.5 chimeras with the control group is shown in the footnote to Fig 5.10. Pairwise

Fig 5.11: Confocal Images of E4.5 4nGFP↔2n Chimeras

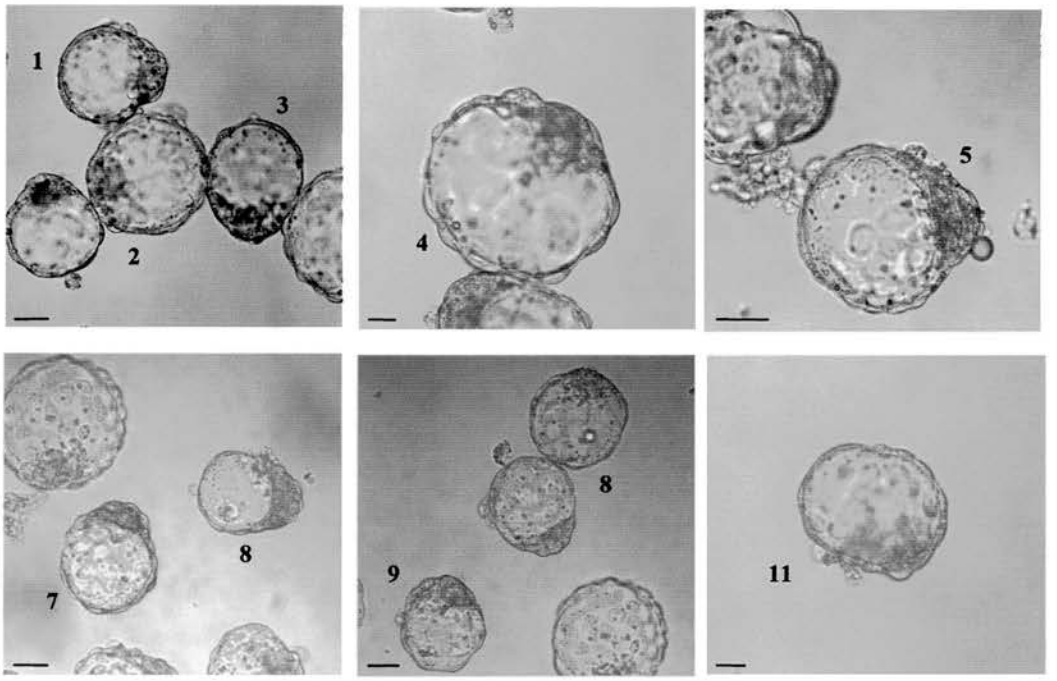

Fig 5.11: Overlay confocal images of 10 E4.5 4nGFP↔2n Chimeras.
Scale bar=50microns.

Fig 5.12: Confocal Images of E4.5 4n↔2nGFP Chimeras

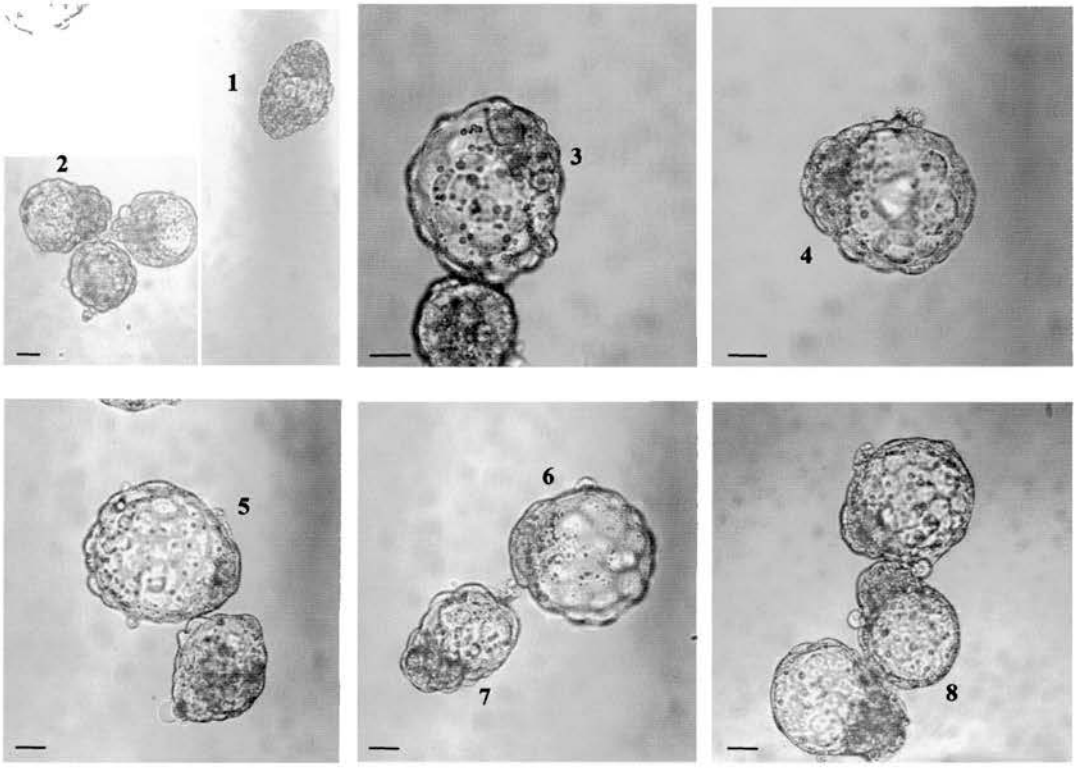

Fig 5.12: Overlay images of E4.5 4n↔2nGFP chimeras.
Scale bar=50 microns.

differences were also compared (Table 5.8). There was a greater pairwise difference between the TE and ICM, and between the mTE and pTE but a smaller difference between the presumptive epiblast and hypoblast of experimental chimeras than control chimeras. The pairwise difference between the TE and ICM was significant between the control and the 4nGFP↔2n groups. The pairwise difference between the mTE and pTE was not significant between these groups probably because of the small sample size in this series. There was also no significant difference in the pairwise difference between the hypoblast and epiblast between the control and the 4nGFP↔2n groups. The GFP (2n) cells in the 4n↔2nGFP group followed the same trends as the GFP cells in the control group and the pairwise differences were not significant.

Table 5.8: Comparison between 4n↔2nGFP and Control Chimeras for differences in % GFP for three pairs of tisssues

E4.5	TE-ICM	mTE-pTE	Hypoblast-Epiblast
2nGFP<->2n (n=8) Fig 5.11a	- 9.28 ± 15.45	- 6.53 ± 14.33	- 24.34 ± 11.54
4nGFP<->2n (n=11) Fig 5.11b	41.17 ± 8.48	24.72 ± 11.94	- 1.72 ± 4.95
4n<->2nGFP (n=8) Fig 5.11c	- 29.78 ± 6.31	- 29.03 ± 7.17	- 8.83 ± 7.69
2nGFP<->2n v 4nGFP<->2n (avb)	**P=0.0082**	P=0.0989	P=0.0970
2nGFP<->2n v 4n<->2nGFP (avc)	P=0.2480	P=0.248	P=0.5995

The relative % 4n cell number was estimated (see section 5.2.5 of this chapter) for both combinations of E4.5 chimeras (Table 5.7). These results show that there is an unequal contribution of 4n cells to each region of the blastocyst as both types of experimental chimera groups have more 4n cells in the TE and particularly the mTE.

The analysis of % GFP (4n) and % 4n cell number in 4nGFP↔2n chimeras (Figures 5.10b and 5.7c) and % 4n contribution and % 4n cell number in 4n↔2nGFP chimeras at E4.5 (Figures 5.10d and 5.7d) show the same trends of a higher contribution of 4n cells to the TE in particular the mTE. There was no preferential allocation of 4n cells to the presumptive hypoblast compared to the presumptive epiblast in 4nGFP↔2n and 4n↔2nGFP chimeras.

5.3.3 Analysis of Expanded E5.5 & E7.5 2nGFP↔2n and 4nGFP↔2n Blastocysts

The epiblast and hypoblast was not differentiated in the chimeric blastocysts that had been cultured in vitro. Expanded blastocysts were therefore produced by transferring them to pseudopregnant females which had been injected with tamoxifen (see section 5.2.3). This prevented the blastocysts from implanting and allowed them to grow in an in vivo environment. The epiblast and hypoblast can be more easily distinguished in the enlarged blastocysts that are in a state of diapause.

Before starting these experiments two methods of inducing diapause were compared. Ten embryos were each transferred into four pseudopregnant females which had been injected with tamoxifen. Nine embryos were recovered. This was compared to a recovery of nine embryos from the transfer of ten embryos each into three pseudopregnant females that had been ovariectomised. Therefore, this technique is probably as effective as using ovariectomy to produce expanded blastocysts but is preferable to use, as it is less invasive.

As the previous results had revealed that both 4n↔2n chimera combinations followed the same trends, only 4nGFP↔2n and control 2nGFP↔2n chimeras were produced. These chimera combinations were analysed at E5.5 & E7.5.

5.3.3.1 E5.5 Chimeras:

Overlay images of E5.5 4nGFP↔2n chimeras are shown in figure 5.13. The individual and mean percentages of GFP contribution to control and 4nGFP↔2n blastocysts are shown in Table 5.9.

The results from the E5.5 series of control chimeras revealed no significant difference between the percentage contribution of GFP cells to any of the regions of the blastocysts (Fig 5.14a). The 4nGFP↔2n chimeras had a significantly higher percentage contribution of 4n cells in the TE than the ICM and no significant difference between the mTE than the pTE or between the epiblast and the hypoblast (Fig 14b).

There was no significant difference in the number of blastocysts with chimeric epiblasts between the control and experimental groups (5/7 versus 3/7; Fisher's Exact P-value >0.05). There was also no significant difference in the proportion of 4nGFP↔2n chimeras that had a 4n contribution to the epiblast versus the hypoblast (3/7 versus 4/7; Fisher's Exact P-value >0.05).

Fig 5.13: Confocal Images of E5.5 4nGFP↔2n Chimeras

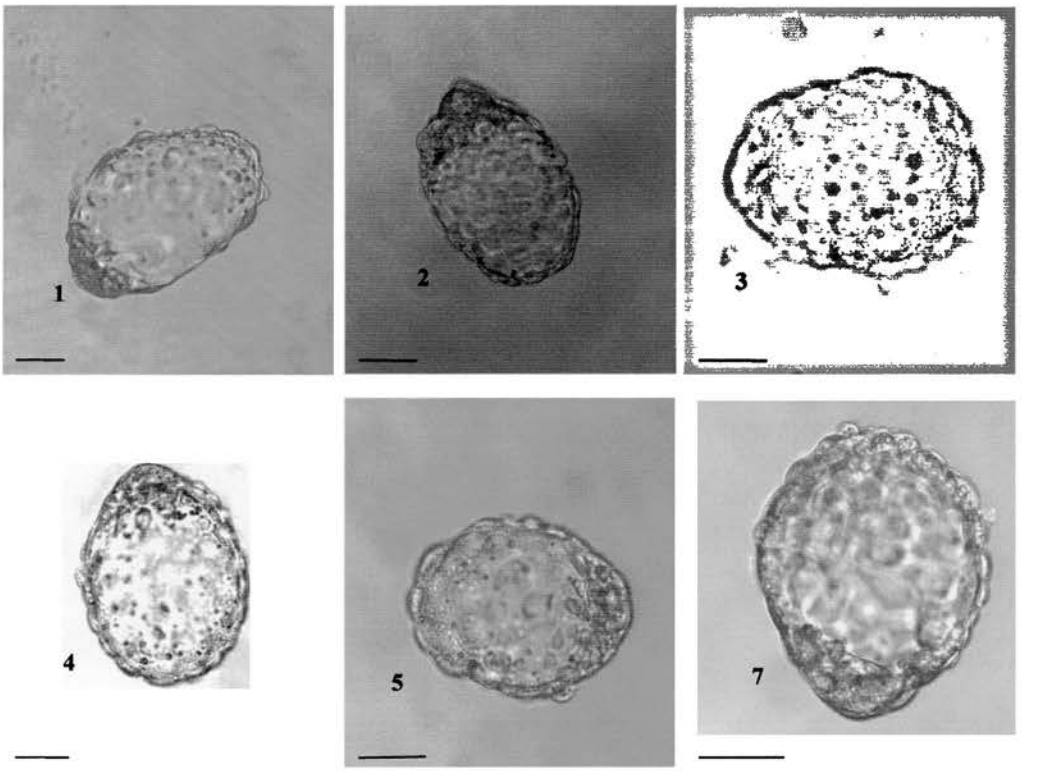

Fig 5.13: Overlay images of expanded E5.5 4nGFP↔2n chimeras. Most of the GFP, 4n cells are allocated to the TE, however chimeras 1 and 7 clearly show 4n cells present within both the epiblast and hypoblast regions.

Scale bar=50 microns.

Table 5.9:
% Contribution of GFP cells in E5.5 2nGFP↔2n Chimeras & E5.5 4nGFP↔2n Chimeras Cultured in Delayed Implantation Pseudopregnant Females

a: 2nGFP↔2n

Blastocyst	Total TE	Total ICM	mTE	pTE	Epiblast	Hypoblast
1	14	52	0	50	56	50
2	54	65	42	90	100	50
3	21	0	29	0	0	0
4	84	43	78	100	50	40
5	33	65	15	68	67	64
6	38	53	44	19	72	44
7	23	26	29	0	0	38
Mean % Length	**38.05**		**33.90**	**46.77**		
Mean % Area		**43.53**			**49.17**	**40.71**
SE	9.11	8.86	9.41	15.65	14.05	7.52
SD	24.11	23.43	24.88	41.41	37.17	19.89
N	7	7	7	7	7	7

b: 4nGFP↔2n

Blastocyst	Total TE	Total ICM	mTE	pTE	Epiblast	Hypoblast
1	70	61	58	100	86	36
2	31	15	10	66	27	2
3	29	0	37	0	0	0
4	52	5	33	97	0	10
5	58	0	81	0	0	0
6	49	0	64	0	0	0
7	64	40	51	91	37	45
Mean % Length	**50.19**		**47.74**	**50.59**		
Mean % Area		**17.27**			**21.40**	**13.32**
SE	5.94	9.10	8.81	18.35	12.23	7.25
N	7	7	7	7	7	7
SD	15.72	24.08	23.32	48.56	32.35	19.18
Corrected Value for % Cell Number	**44.44**	**11.61**	**42.03**	**44.83**	**14.62**	**8.81**

Table 5.9:
Showing the individual and mean % length of GFP cells in the TE, mTE & pTE and the % area of GFP cells in the ICM, including the epiblast and hypoblast, of E5.5 chimeras cultured in delayed implantation females. **a:** 2nGFP↔2n chimeras, and **b:** the % length & area of GFP (4n cells) in 4nGFP↔2n chimeras and the corrected values for % cell number. If there was an equal contribution of 4n cells to all the regions of the blastocyst a proportion of 33.3% in each tissue would be expected.

SE= Standard Error, N= Number, SD=Standard Deviation.

Fig 5.14:
% Contribution of GFP or 4n cells in E5.5 & E7.5 Chimeras Cultured in Delayed Implantation Females

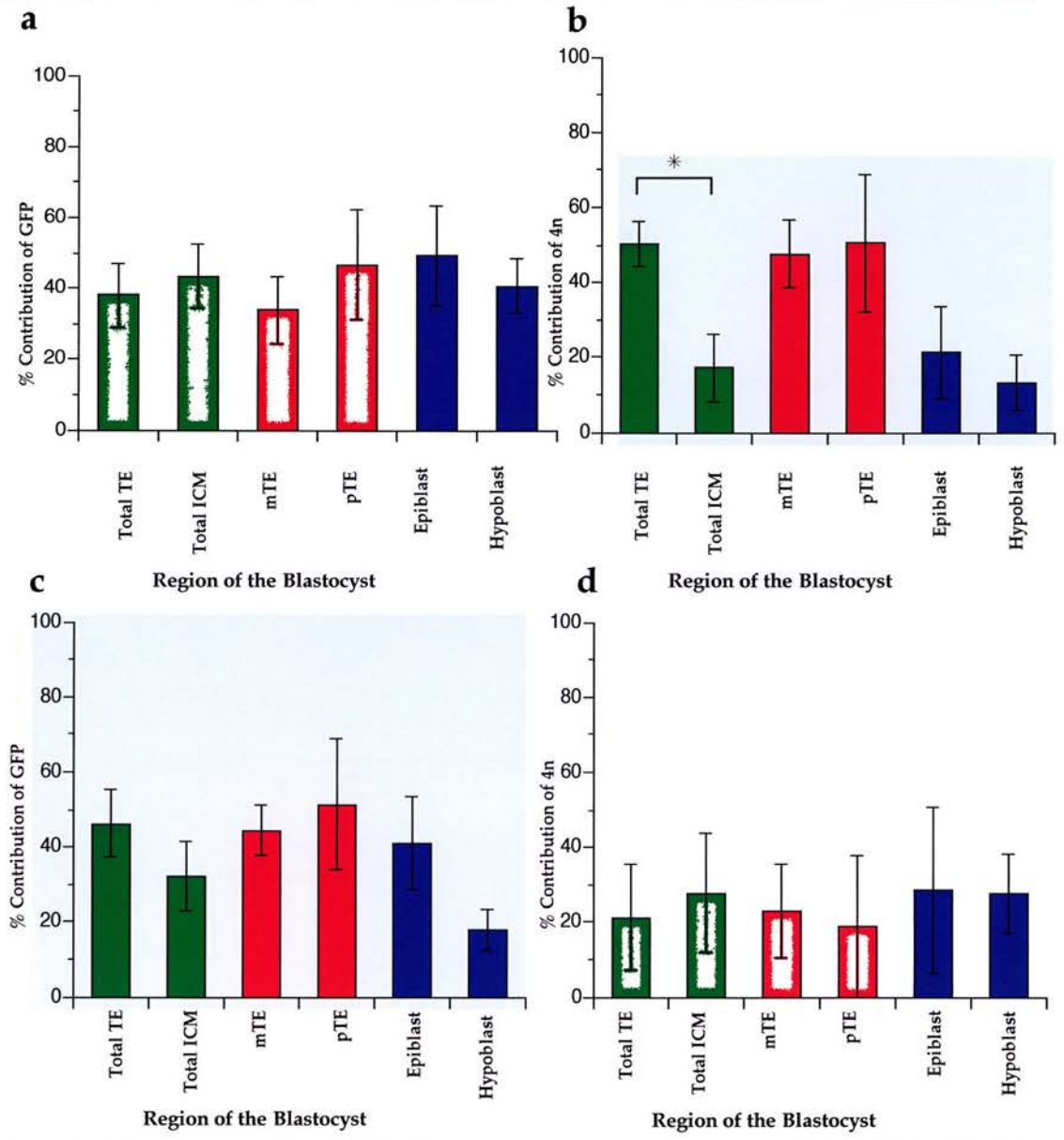

Fig 5.14:
The mean % length in the TE, mTE & pTE and % area in the ICM, including the epiblast and hypoblast, of **a:** GFP cells in 7 E5.5 2nGFP↔2n control chimeras, **b:** 4n cells in 7 E5.5 4nGFP↔2n chimeras, **c:** GFP cells in 5 2nGFP↔2n control chimeras, **d:** 4n cells in 4 E7.5 4nGFP↔2n . All chimeras were transferred, at E3.5, into pseudopregnant females in delayed implantation.
* $P<0.05$

Therefore, although there was a lower 4n contribution to the ICM, 4n cells were present in the epiblast and were not significantly more abundant in the hypoblast than the epiblast.

5.3.3.2 E7.5 Chimeras:

E7.5 control 2nGFP↔2n and 4nGFP↔2n blastocysts were imaged (Fig 5.15). The individual and mean percentages are shown in table 5.10. The E7.5 control data showed no significant difference between the percentage contribution of GFP cells to any of the regions of the blastocyst (Fig 5.14c). However, there appeared to be a lower contribution of GFP in the hypoblast and mTE compared to the epiblast and pTE. This is possibly due to the small sample size, as only 5 chimeras were analysed.

The percentage 4n contribution to all the lineages of the 4nGFP↔2n blastocysts varied widely among the 4 chimeras. Blastocyst 1 had a high overall percentage contribution of 4n cells. The other three chimeras had low proportions of 4n cells, with blastocyst 2 having only 2n cells in the TE and another having only 2n cells in the ICM. Blastocysts 2 and 3 had a higher percentage of 4n cell contribution to the hypoblast than the epiblast.

There was no significant difference in the numbers of chimeric epiblasts and hypoblasts within and between control and 4nGFP↔2n blastocysts ($P>0.05$ by Fisher's Exact test). This suggests that 4n cells are frequently present in the epiblast of E7.5 chimeras.

Fig 5.15: Confocal Images of E7.5 Chimeras

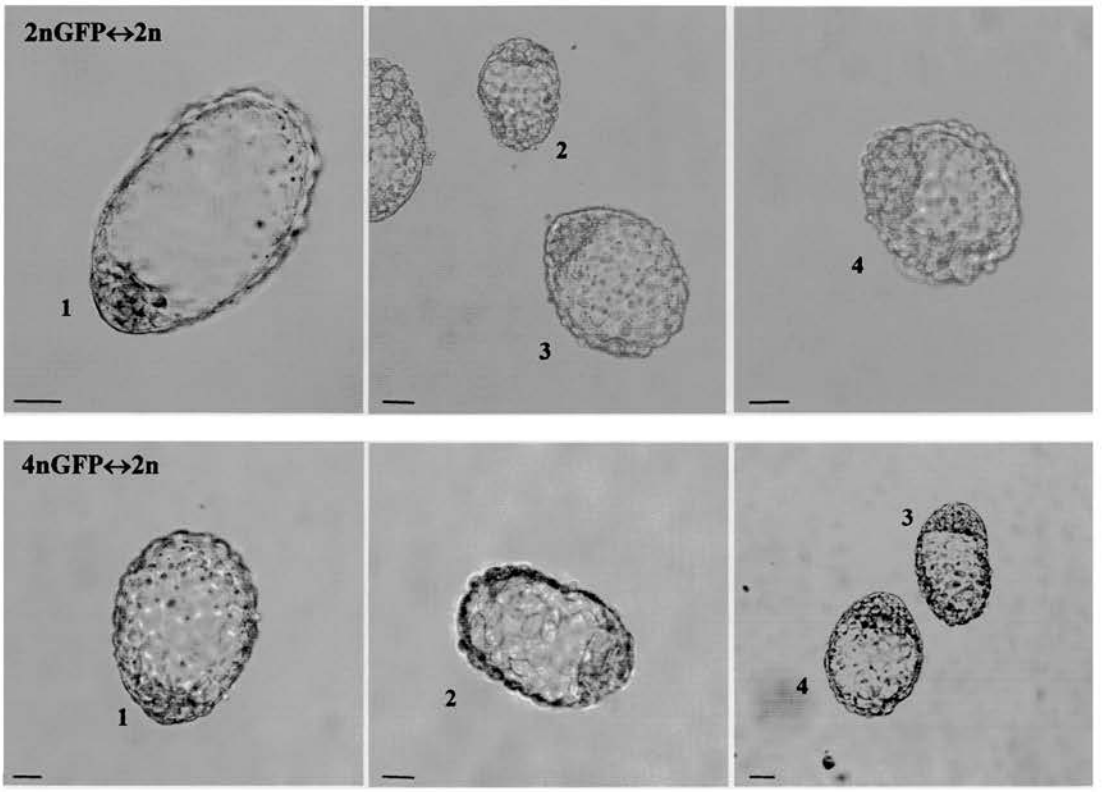

Fig 5.15: Overlay images of expanded E7.5 control 2nGFP↔2n and 4nGFP↔2n chimeric blastocysts. Both 4nGFP↔2n blastocysts 1 & 2 contain 4n cells within the epiblast region.
Scale bar=50 microns.

Table 5.10:
% Contribution of GFP cells in E7.5 2nGFP↔2n & 4nGFP↔2n Chimeras Cultured in Delayed Implantation Pseudopregnant Females

a: 2nGFP↔2n

Blastocyst	Total TE	Total ICM	mTE	pTE	Epiblast	Hypoblast
1	76	57	69	100	78	31
2	52	9	46	68	15	0
3	25	16	33	0	14	19
4	30	30	31	26	37	13
5	48	49	43	63	60	27
Mean % Length	**46.32**		**44.42**	**51.34**		
Mean % Area		**32.15**			**40.99**	**18.03**
SE	9.06	9.19	6.69	17.43	12.62	5.54
N	5	5	5	5	5	5
SD	20.27	20.55	14.96	38.98	28.23	12.38

b: 4nGFP↔2n

Blastocyst	Total TE	Total ICM	mTE	pTE	Epiblast	Hypoblast
1	63	72	58	75	95	39
2	0	29	0	0	15	48
3	10	10	14	0	4	23
4	13	0	19	0	0	0
Mean % Length	**21.21**		**22.94**	**18.82**		
Mean % Area		**27.82**			**28.53**	**27.58**
SE	14.04	16.01	12.49	18.82	22.28	10.57
N	4	4	4	4	4	4
SD	28.07	32.01	24.98	37.63	44.56	21.15
Corrected Value for % Cell Number	**17.60**	**19.51**	**19.11**	**15.54**	**20.07**	**19.32**

Table 5.10:
Showing the individual and mean % length of GFP cells in the TE, mTE & pTE and the % area of GFP cells in the ICM, including the presumptive epiblast and hypoblast, of E7.5 chimeras cultured in delayed implantation females. **a:** 2nGFP↔2n chimeras, and **b:** the mean % area & length of GFP (4n cells) in 4nGFP↔2n chimeras and the corrected values for % cell number. If there was an equal contribution of 4n cells to all the regions of the blastocyst a proportion of 33.3% in each tissue would be expected.

SE= Standard Error, N= Number, SD=Standard Deviation.

5.3.4 Comparison of % GFP Contribution at different ages

Fig 5.16 shows the percentage contribtion of GFP cells in the same regions of control 2nGFP↔2n and 4nGFP↔2n blastocysts between E3.5 and E7.5.

There was a reduction in the % GFP (4n) contribution in the TE, particularly the mTE between E3.5 and E7.5 of 4nGFP↔2n blastocysts which was not the case in control chimeras. Most of the reduction occurred at E5.5 and E7.5 when fewer chimeras were analysed. There was a significantly higher proportion of 4n cells in the ICM and the hypoblast at E3.5 than at E4.5 in 4nGFP↔2n blastocysts ($P<0.01$ for hypoblast, $P<0.05$ for ICM by Mann-Whitney U-test). This was also seen in the 4n↔2nGFP chimera group ($P<0.05$ for hypoblast, $P<0.01$ for ICM). Comparison of pairwise differences between the hypoblast and epiblast showed there was a significantly greater difference at E3.5 than E4.5 in the 4nGFP↔2n group (see footnote to Fig 5.16). This might suggest that the percentage of 4n cells are reduced in the hypoblast between E3.5 and E4.5. There is no significant difference in the % contribution to the hypoblast between E4.5 and E7.5.

There is a lower % GFP contribution in the presumptive epiblast and epiblast of the 4nGFP↔2n group than the control group at all stages. However, the % GFP in the 4nGFP↔2n group does not increase or decrease significantly between E3.5 and E7.5.

Fig 5.16: % GFP Contribution to individual regions of Control and 4nGFP↔2n blastocysts

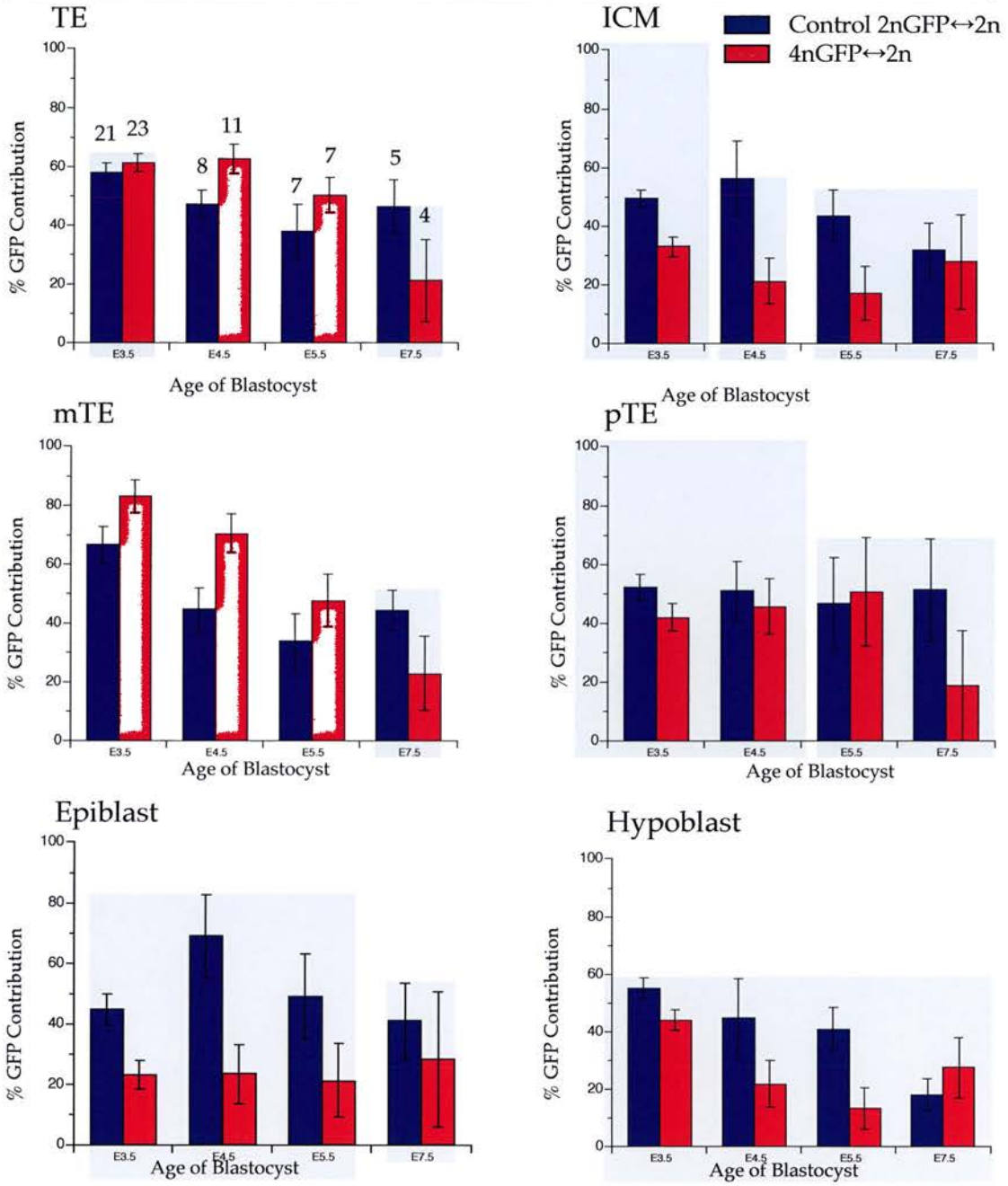

Fig 5.16: Mean % GFP contribution to control and 4nGFP↔2n chimeras in individual regions of the blastocyt at different ages. The numbers of blastocyst in each group at each age are shown. Mann-Whitney U-tests for comparisonof %GFP between different ages.

E3.5 v E4.5	TE	ICM	mTE	pTE	Epiblast	Hypoblast
2nGFP<->2n v 2nGFP<->2n	P=0.079	P=0.2046	P=0.0452	P=0.9223	P=0.0876	P=0.4206
4nGFP<->2n v 4nGFP<->2n	P=0.8684	P=0.0194	P=0.0619	P=0.8252	P=0.711	P=0.0029
E3.5 v E4.5	TE-ICM		mTE-pTE		Hypoblast-Epiblast	
2nGFP<->2n v 2nGFP<->2n	P=0.1719		P=0.2046		P=0.0112	
4nGFP<->2n v 4nGFP<->2n	P=0.1014		P=0.2615		P=0.0175	

5.3.5 Blastocyst Formation in E3.5 Chimeras

The E3.5 data showed a higher proportion of 4n cells in the presumptive hypoblast compared to the presumptive epiblast (5.3.1). However, at E4.5 there was no significant difference between the two lineages. It is possible that there is a higher tendency for the blastocyst cavity to form within the 4n half of the chimera, thus resulting in a higher proportion of 4n cells within the mTE and hypoblast (adjacent to the cavity) compared to the pTE and epiblast.

The percentage GFP in the pTE plus epiblast was subtracted from that in the mTE plus hypoblast and compared between chimera groups by Mann-Whitney U-tests (Table 5.11). This difference was significantly greater in the 4nGFP↔2n chimeras than the 2nGFP↔2n controls (P=0.0264) indicating a higher GFP (4n) contribution to the mTE plus hypoblast. The difference was significantly lower in the 4n↔2nGFP chimeras than the controls (P=0.0081) indicating a lower GFP (high 4n) contribution to the mTE plus hypoblast.

This shows that there were significantly more GFP (4n) cells surrounding the blastocyst cavity of 4nGFP↔2n blastocysts than GFP cells in 2nGFP↔2n control blastocysts. There were significantly fewer GFP (2n) cells surrounding the blastocyst cavity of 4n↔2nGFP blastocysts than GFP cells in 2nGFP↔2n control blastocysts. This would therefore imply that the blastocyst cavity does form preferentially within the 4n half of 4n↔2n chimeras.

Table 5.11: Analysis of % GFP Contribution surrounding the Blastocyst cavity E3.5 Chimeras

(a) Control 2nGFP↔2n

Blastocyst	mTE + H	pTE+E	(mTE+ H)-(pTE+E)
1	51	80	-29
2	94	75	19
3	130	53	77
4	85	134	-50
5	86	89	-3
6	108	89	19
7	142	94	49
8	161	129	33
9	66	108	-43
10	142	76	66
11	139	71	68
12	142	58	83
13	169	139	29
14	174	57	118
15	69	170	-101
16	137	186	-48
17	152	114	38
18	139	129	10
19	146	27	118
20	115	72	43
21	113	92	21
mean	**121.80**	**97.24**	**24.56**
SE	**7.68**	**8.64**	**12.28**
N	**21**	**21**	**21**
SD	**35.21**	**39.62**	**56.28**

(b) 4nGFP↔2n

Blastocyst	mTE + H	pTE+E	(mTE+ H)-(pTE+E)
1	139	21	118
2	141	98	43
3	154	48	106
4	139	79	60
5	128	67	62
6	140	66	73
7	113	28	84
8	142	62	79
9	118	16	102
10	118	37	81
11	158	94	64
12	95	70	24
13	155	38	117
14	172	27	145
15	149	23	126
16	55	123	-68
17	102	67	35
18	92	20	72
19	190	177	13
20	42	118	-77
21	126	107	20
22	113	0	113
23	137	115	22
mean	**126.80**	**65.27**	**61.53**
SE	**7.16**	**9.12**	**11.70**
N	**23**	**23**	**23**
SD	**34.32**	**43.75**	**56.10**

(c) 4n↔2nGFP

Blastocyst	mTE + H	pTE+E	(mTE+ H)-(pTE+E)
1	145	74	71
2	56	75	-19
3	85	21	64
4	141	85	56
5	60	150	-90
6	60	178	-118
7	38	194	-156
8	135	46	88
9	39	158	-119
10	97	120	-24
11	35	105	-70
12	40	138	-98
13	104	149	-45
14	159	91	68
15	93	164	-71
16	72	144	-72
17	72	194	-122
18	69	170	-100
19	119	70	49
20	65	186	-121
21	106	129	-23
22	100	200	-100
mean	**85.91**	**129.21**	**-43.00**
SE	**7.90**	**11.02**	**-3.00**
N	**22**	**22**	**22**
SD	**37.07**	**51.67**	**79.93**

Table 5.11: The % GFP contribution in the mTE & presumptive hypoblast (the region in which the blastocyst cavity is formed) compared to the pTE & presumptive epiblast and the difference between the (mTE & presumptive hypoblast) and the (pTE & presumptive epiblast).
H= presumptive hypoblast , E= presumptive epiblast.
SE= Standard Error, N= Number, SD=Standard Deviation.

5.4 Conclusion

The experiments in this study were designed to determine the mechanisms responsible for the exclusion of 4n cells from the epiblast derivatives of mid-gestation chimeras. These results indicate that 4n cells are present within the presumptive epiblast region and the differentiated epiblast region of 4n↔2n chimeric blastocysts.

The analysis of E3.5 and E4.5 4n↔2n chimeras showed that 4n cells are preferentially allocated to the TE (particularly the mTE) compared to the ICM. Previous analysis of chimeric blastocysts at E3.5 is in agreement with these data which showed a significantly greater contribution of 4n cells to the TE than the ICM. This was due entirely to a difference between the mTE and ICM (Everett and West, 1996).

The results presented in this chapter also suggest that 4n cells were preferentially allocated to the hypoblast at E3.5 but not at E4.5. This indicates that some form of cell selection decreases the percentage of 4n cells in the presumptive hypoblast between E3.5 and E4.5. Analysis of the E3.5 series suggested that the blastocyst cavity preferentially forms within the 4n part of a 4n↔2n chimera. This explains the non-random distribution of 4n cells within 4n↔2n chimeras that can be seen in both E3.5 and E4.5 chimera series analysed in this study, and in 4n↔2n blastocysts previously analysed (Everett and West, 1996). It could also provide an explanation for the initial prefential allocation of 4n cells to the hypoblast.

Previous analysis of E4.5 4n↔2n chimeric blastocysts showed a reduction in 4n cells in both the ICM and TE at E4.5 compared to E3.5 (Everett and West, 1996, 1998). Everett and West's results differ from the results presented in this chapter which do not show a decrease in the % 4n contribution between E3.5 and E4.5 in the TE. This difference could be caused by the different techniques used to analyse both types of 4n↔2n blastocyst. Alternatively it could be because the blastocysts analysed in this study were imaged at a slightly earlier stage than the blastocysts analysed by Everett and West, (1996, 1998).

The analysis of E5.5 and E7.5 diapause 4n↔2n blastocysts indicates that 4n cells are initially present within the differentiated epiblast region of late blastocysts. Absence from the lineage at later stages must therefore imply subsequent loss of 4n cells from this region by some form of cell selection.

There have been reported cases of 4n cells surviving in the epiblast derivatives of 4n↔2n adult chimeras (see section 1.5.1.2 of Chapter1) (Lu and Markert, 1980; Tarkowski *et al.*, 2001; Goto *et al.*, 2002). However, these chimeras had a higher ratio of 4n cells to 2n cells at aggregation. 4n cells have been shown to be largely excluded from E7.5 and E12.5 4n↔2n chimeras produced using the same techniques as described in this chapter (James *et al.*, 1995).

Although only 4 E7.5 4n↔2n diapause chimeras were analysed the results differ from the normally implanted E7.5 postimplantation chimeras

previously analysed by James *et al.* (1995). Only 2 out of 12 4n↔2n postimplantation chimeras contained 4n cells in the epiblast derivatives both of which were abnormal. The diapause E7.5 blastocyst data differs from this as, although the proportion of 4n cells in the epiblast were low in 2 of the chimeric blastocysts, 3 out 4 contained 4n cells in the epiblast. This could be caused by differences in the age of the chimeras. The 4n↔2n chimeras studied by James, *et al.* (1995) were staged according to the age of the pseudopregnant female and were therefore a day older than the expanded blastocysts analysed in this chapter. Alternatively it could be because cell proliferation (and possibly apoptosis) is suppressed in these diapause blastocysts. It is therefore possible that following implantation and the growth and differentiation of the epiblast further cell selection takes place, eliminating 4n cells from the epiblast between the late blatocyst stage and E7.5. One abnormal E7.5 postimplantation chimera studied by James *et al.* (1995) had a high overall proportion of 4n cells, which was similar to the diapause E7.5 blastocyst with a high contribution of 4n cells in all the regions of the blastocyst.

In conclusion the experiments in this study suggest there are several mechanisms taking place within 4n↔2n chimeras resulting in the restricted distribution of 4n cells within the blastocyst and the loss of 4n cells from the epiblast derivatives. The model shown in Fig 5.17 illustrates the mechanisms that may be involved. It is likely that initially the cavity tends to form more often within the 4n part of the chimera resulting in a higher proportion of 4n cells in the mTE and hypoblast compared to the pTE and epiblast. Following

Fig 5.17:
Proposed Model Resulting in the Exclusion of 4n Cells from the Epiblast of 4n↔2n Chimeras

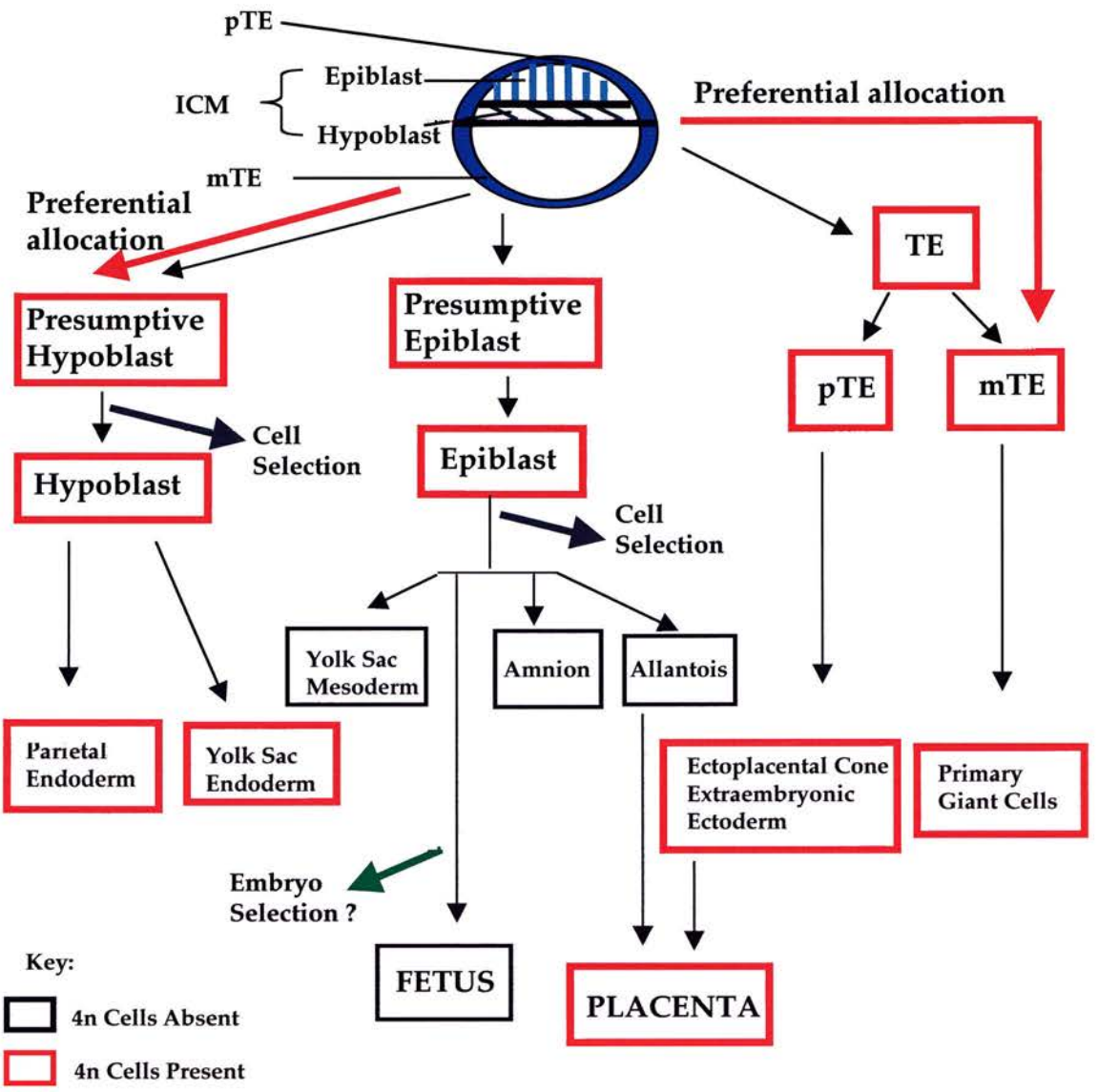

Fig 5.17:

Proposed model explaining the gradual loss of 4n cells from the epiblast derivatives of mid gestation 4n↔2n chimeras. Three mechanisms appear to be taking place, initially preferential allocation of 4n cells to the mTE, and the hypoblast within the ICM as a result of the cavity preferentially forming within the 4n part of the chimera. Subsequently 4n cells are reduced from the presumptive hypoblast region by cell selection, following which cell selection takes place in the epiblast derivatives to eliminate 4n cells. Finally it is likely that any fetuses containing 4n cells are eliminated through embryo selection.

this there is possibly a significant reduction in the percentage of 4n cells in the hypoblast. 4n cells are therefore, greatly reduced in the ICM region compared to the TE. However, the analysis of enlarged blastocysts in diapause indicates when the epiblast and hypoblast are formed 4n cells are present in the epiblast and are not exclusively allocated to the hypoblast within the ICM. Following the late blastocyst stage it is likely that 4n cells are reduced from the epiblast derivatives by cell selection against 4n cells. As James *et al.* (1995) showed that both E7.5 chimeras with 4n cells in the epiblast were abnormal, it is possible that a limited amount of selection against embryos with a significant number of 4n cells occurs, as a final mechanism to exclude 4n cells from the epiblast lineage. This proposed model may be relevant to the origin of some cases of CPM.

Chapter 6: Using Confocal Microscopy to Determine the Fate of BALB/c Cells in tau-GFP Aggregation Chimeras

6.1 Introduction

As discussed in chapter 1, section 1.5.1.2, BALB/c strain cells make a poor contribution to BALB/c mouse aggregation chimeras (Mullen and Whitten, 1971; West and Flockhart, 1994; Dvorak *et al.*, 1995; Tang and West, 2001). Previous analysis showed that BALB/c cells were under-represented in epiblast, hypoblast and pTE derivatives of E12.5 BALB/c↔(C57BL x CBA)F_2 chimeras, aggregated at the 8-cell stage (West and Flockhart, 1994). Of these chimeras, 20 out of 34 did not have a BALB/c contribution to the fetus but did have BALB/c cells in at least one extraembryonic tissue suggesting BALB/c chimeras could provide another mouse model of confined placental mosaicism. Consequently it is relevant to investigate how the depletion of BALB/c cells occurs. As the mural trophectoderm (mTE) contributes little to the 12.5 day conceptus, it is possible that, like 4n cells in 4n↔2n chimeras, BALB/c cells become preferentially allocated to the mTE. Alternatively some form of generalised cell selection against BALB/c cells could be responsible for the lower contribution of BALB/c embryos to these chimeras. The experiments presented in this chapter were designed to test the first possibility using confocal microscopy of BALB/c↔(BF_1 x TgTP6.3) chimeras and a control series of (BALB/c x A/J)F_2↔(BF_1 xTgTP6.3) chimeras.

As a new chimera combination was being used it was necessary to analyse the composition of two chimera series at E12.5 to determine that (BALB/c x A/J)F_2↔(BF_1 x TgTP6.3) chimeras are a balanced strain combination and BALB/c↔(BF_1 x TgTP6.3) chimeras are unbalanced with a low contribution of BALB/c cells.

To follow the fate of BALB/c cells within a chimeric blastocyst, BALB/c embryos were aggregated to (BF_1 x TgTP6.3) embryos at the 8-cell stage and cultured on the confocal microscope for time-lapse microscopy using the method described in chapter 3. It is possible to follow the fate of the tau-GFP expressing cells in a tau-GFP chimera during a period of preimplantation development and therefore, determine if the BALB/c (non tau-GFP) cells are preferentially allocated to the mTE. For time-lapse microscopy studies BALB/c↔(BF_1 x TgTP6.3) and (BALB/c x A/J)F_2↔(BF_1 x TgTP6.3) chimeras were produced by aggregating the embryos at the 8-cell stage. These chimera combinations were also aggregated at the 2-cell stage and individually imaged at the late blastocyst stage, to determine if aggregating at an earlier stage had an effect on the allocation of BALB/c cells within the chimeric blastocyst.

6.2 Materials and Methods

6.2.1 Aggregation of Chimeras

Details of the mouse strains used in these experiments are described in Table 2.1.

(BALB/c x A/J)F_2 embryos were aggregated to (BF_1 x TgTP6.3) embryos to produce control chimeras and BALB/c embryos were aggregated to (BF_1 x TgTP6.3) embryos to produce experimental chimeras. These embryos were aggregated at the 8-cell stage and 2-cell stage respectively in two separate series of experiments. 8-cell stage embryos were flushed using M2 handling medium and aggregation chimeras were cultured in M16 handling medium. The experiments with 2-cell stage aggregates were done after the 8-cell aggregates and by this time KSOM had replaced M16 as our standard culture medium. 2-cell stage embryos were flushed using KSOMH handling medium and cultured in KSOM culture medium following aggregation.

(BF_1 x TgTP6.3) 8-cell embryos that were hemizygous for the GFP transgene were identified using a Leica fluorescent dissecting microscope prior to aggregation. GFP positive 2-cell stage (BF_1 x TgTP6.3) embryos could not be identified at this stage therefore were identified after aggregation.

6.2.2 E12.5 Chimeric Embryo Dissection

E12.5 embryos were dissected for GPI1 electrophoresis. The decapitated fetus and placenta of E12.5 conceptuses were each homogenised and stored individually in 100µl of 50% glycerol in water in a 1.5 ml eppendorf microfuge tube in a freezer. The amnion, yolk sac mesoderm and yolk sac endoderm were dissected and stored individually in 10µl of 50% glycerol in water in a well of a 96 well plate in a freezer. The mesoderm and endoderm layers of the visceral yolk sac were separated by incubating the yolk sac in a trypsin/pancreatin solution (0.5g trypsin and 2.5g pancreatin in 100ml phosphate buffered saline) for approximately 3 hours at 4°C, followed by a wash in M2 medium for 30 minutes (Levak-Svajger *et al.*, 1969). The yolk sac endoderm was then removed from the yolk sac mesoderm using dissecting forceps (Richardsons of Leicester).

6.2.3 GPI Electrophoresis

The proportions of the two cell populations in the chimeric tissues were estimated from the proportions of GPI1-A and GPI1-B allozymes.

The sample tissues from the E12.5 conceptus were mechanically disrupted after being thawed and were then frozen and thawed a further two times to lyse the samples.

Cellulose acetate plates (Helena Laboratories, Titan III, cat. No. 3023) were soaked in GPI buffer (3g of Tris and 14.4g of glycine dissolved in 1 litre of distilled water, pH 8.1) for 30 minutes. The plates were then dried with a paper towel and put on an aligning base (Helena Laboratories, cat. No. 4086). Diluted samples were loaded into the sample well plates (Helena Laboratories, super Z, cat. No. 4085) then transferred to the acetate plates by a sample applicator (Helena Laboratories, super Z, cat. No. 4084).

Samples were run on an electrophoresis chamber (Helena Laboratories, cat. No. 1283), filled with 50 ml of GPI buffer in each of the buffer reservoirs, with a power supply (Bioblock Scientific, E455) at 200volts for an hour. The plates were then stained for GPI activity for 3-10 minutes on a 37°C hotplate in the dark. The reaction was stopped by immersing the plates in water. The plates were fixed in 5% acetic acid for 5 mins and rinsed in distilled water for at least 10 minutes. The plates were dried for 24 hours and scanned using a Helena Process-24 gel scanner to quantify the proportions of each GPI allozyme (Fig 6.1).

6.2.4 Confocal Microscopy

Prior to time-lapse or individual imaging on the confocal micoscope chimeras were cultured in a conventional CO_2 incubator. The 9 BALB/c↔(BF_1 x TgTP6.3) chimeras imaged with the x10 lens were cultured on the confocal microscope within the incubation chamber in M16 culture medium on a gasket attached to a plastic petri dish with a hole cut out the bottom as described in chapter 3 (Fig 3.2c). The remaining chimeras imaged

Fig 6.1: GPI Electrophoresis

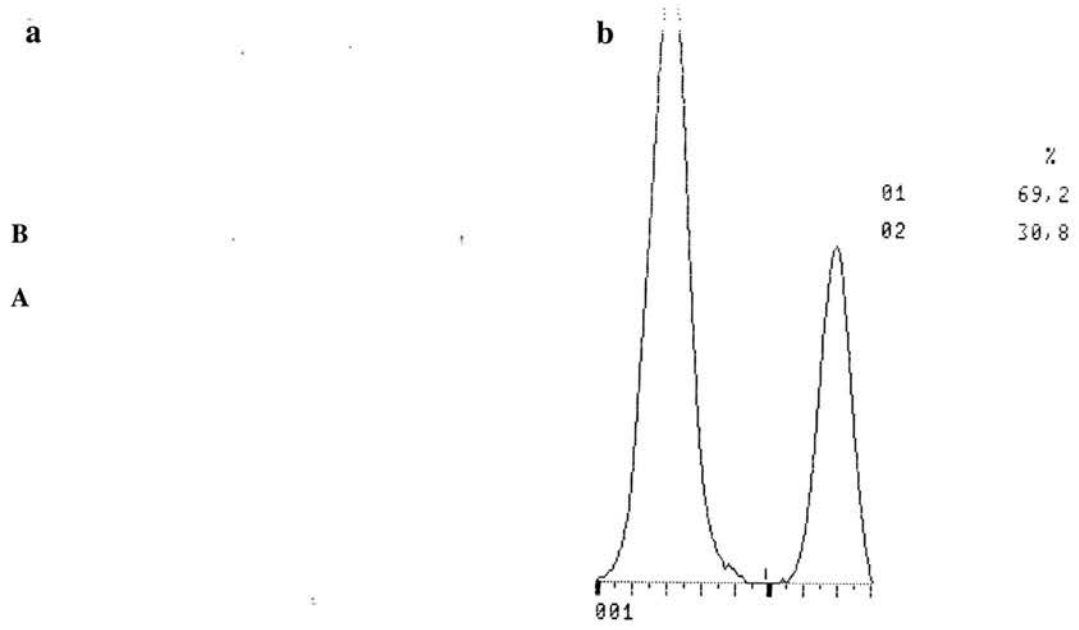

Figure 6.1: GPI Electrophoresis.
a: Example of an acetate plate after running homogenised tissue samples and staining for GPI activity. The different intensities of the A and B bands can be seen. **b:** An example of a printout from the Helena Process-24 gel scanner showing a GPI1-B proportion of 69.2% and a GPI1-A proportion of 30.8%.

using time-lapse confocal microscopy were cultured on the confocal microscope in M16 culture medium in Willcowell glass-bottomed dishes as described in chapter 3. Chimeras that were aggregated at the 2-cell stage were cultured in KSOM culture medium for 4 days in a conventional CO_2 incubator (the culture medium was changed after 2 days). Chimeras were imaged when the embryos were at the late/ expanded blastocyst stage (E5.5). Images were captured as described in chapter 2, section 2.3.

6.2.5 Analysis of Chimeric Embryos

Overlays of GFP and transmitted light images were produced using Adobe Photoshop. Time-lapse movies were produced using Adobe Premier.

Early, late & expanded blastocysts were defined by the size of the blastocyst cavity in proportion to the rest of the blastocyst. In early blastocysts the blastocyst cavity compromised <50% of the total area, the cavity was 50-75% of the total area in late blastocysts and greater than 75% for expanded blastocysts (Fig 6.2). Abnormal blastocysts or blastocysts with two cavities were excluded from the analysis.

The % contribution of GFP to chimeric embryos was analysed in selected images using Image pro plus (Media Cybernetics, MD, USA). The area of green and non-green were calculated for the ICM without dividing it into presumptive epiblast and hypoblast regions. The % green and non green in

Fig 6.2: Staging of Chimeric Blastocysts for Analysis of GFP Contribution

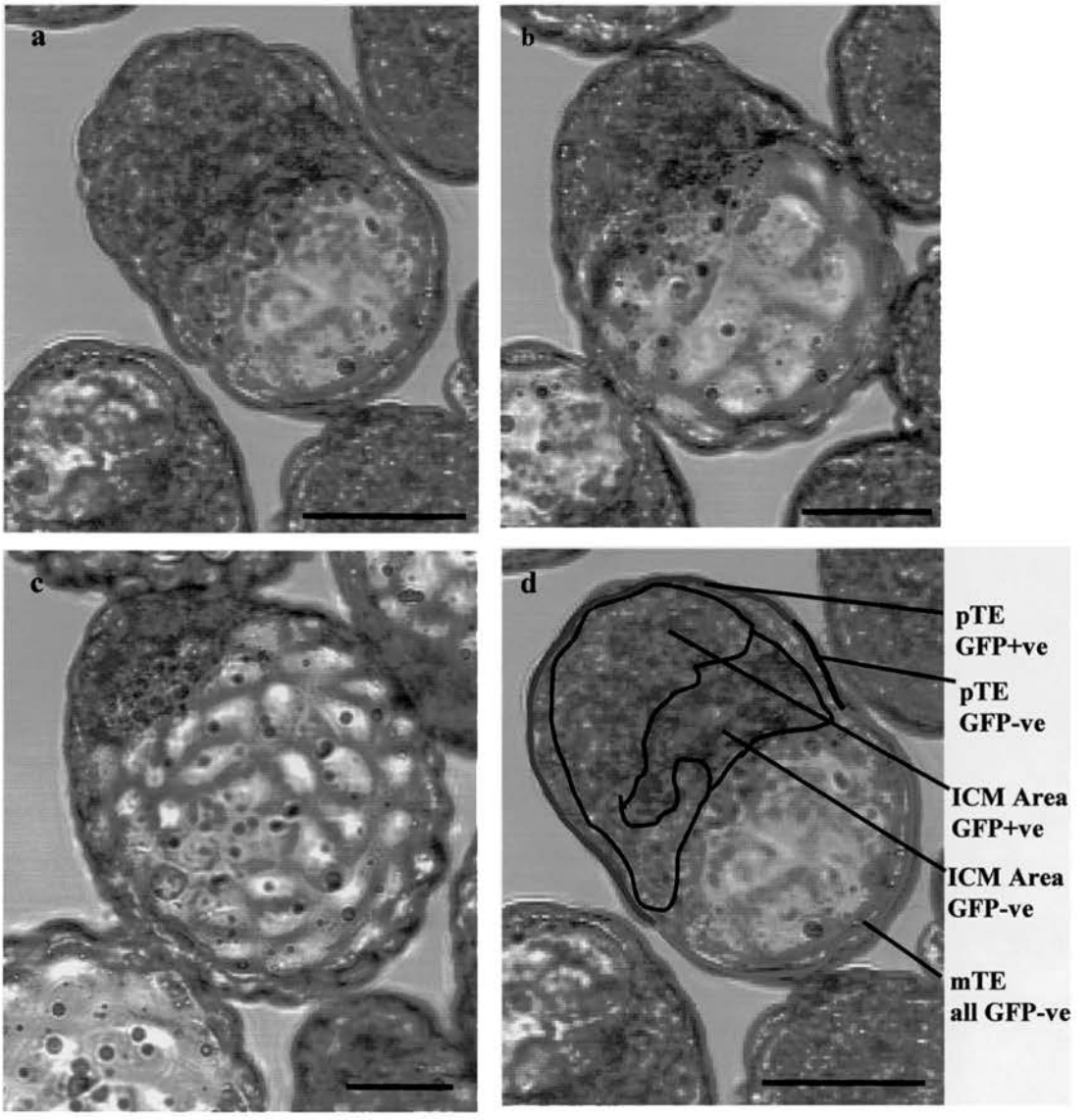

Fig 6.2: Blastocyst stages, **a;** Early, **b;** Late and **c;** Expanded. **d;** the GFP chimeric blastocysts were analysed by measuring the % area GFP in the ICM, and length of GFP in the pTE and mTE.

the pTE and mTE were measured as % lengths using the Image pro plus measurements software (Fig 6.2).

6.3 Results

6.3.1 GPI1 Control Experiment

Previous work has shown that if GPI1 electrophoresis plates are overstained, the contribution of the minor band is often overestimated (West and Green, 1983). To determine the accuracy of the staining technique, samples of known proportions of GPI1-A and GPI1-B were tested. A series of mixtures were prepared for homogenates of mouse kidneys from a GPI1-A strain and a GPI1-B strain. These were mixed in known quantities, ranging from 0 to 100% GPI1-A and coded prior to electrophoresis. Samples were separated using cellulose acetate electrophoresis and scanned to compare the percentage of GPI1-A and B detected on the gel plate, with the known percentages of GPI1 in the mixture. Fig 6.3 shows a plot of the expected percentage of GPI1-A against the percentage of GPI1-A detected. Fig 6.3 shows that the conditions used can estimate the %GPI1-A with sufficient accuracy for the present purpose.

6.3.2 GPI1 Analysis of E12.5 Chimeras

Two series of E12.5 GFP chimeras were produced and analysed by quantitative GPI1 electrophoresis to determine whether (BF_1xTgTP6.3)

Figure 6.3 Assessment of staining linearity

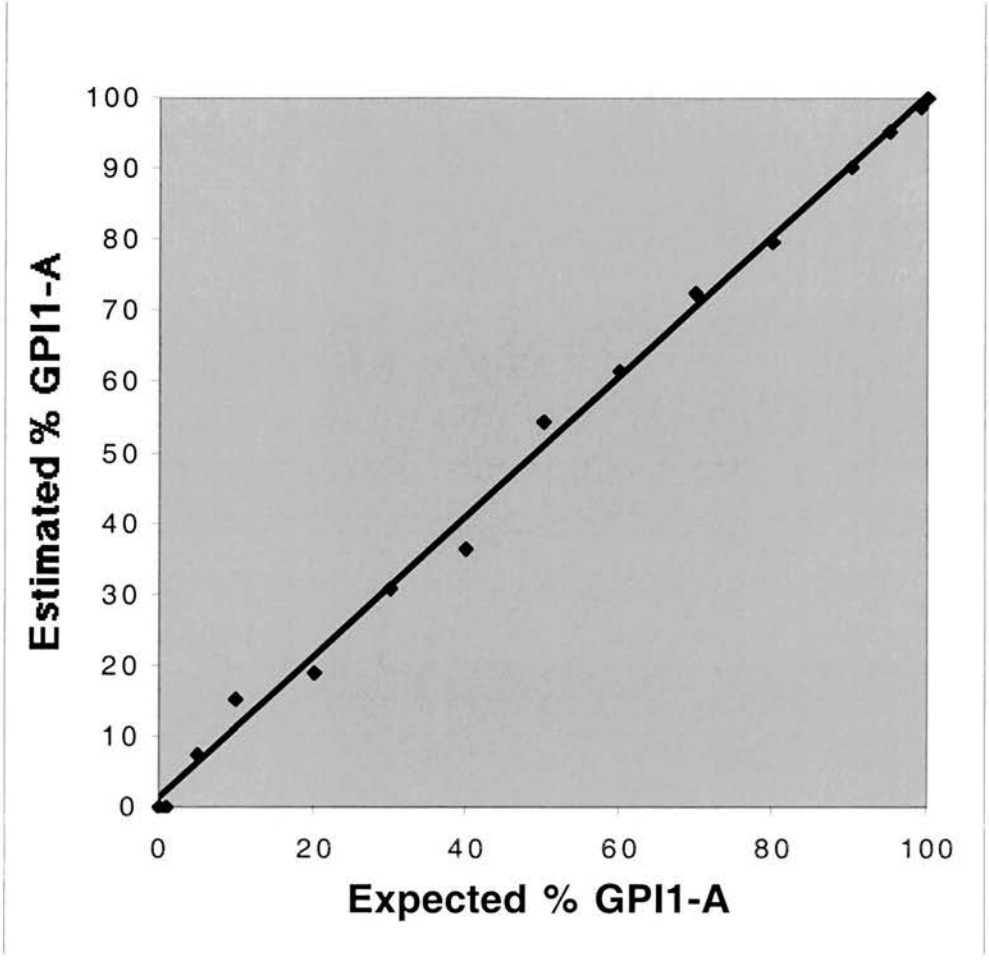

Fig 6.3:
Relationship between the expected percentage of GPI1-A and the detected percentage of GPI1-A in the mixtures of GPI1-A and GPI1-B homogenised kidneys.

embryos were capable of contributing normally to (BALB/c x A/J)F_2↔(BF_1xTgTP6.3) mouse chimeras and to test whether the BALB/c↔(BF_1xTgTP6.3) combination was unbalanced. BALB/c and (BALB/c x A/J)F_2 mice are homozygous for *Gpi1*^{a} and BF_1,(C57BL x CBA)F_1, mice and TgTP6.3 mice are homozygous for *Gpi1*^{b}.

The percentages of GPI1-A in the fetus, amnion, yolk sac mesoderm, yolk sac endoderm and placenta of 24 (BALB/c x A/J)F_2↔(BF_1xTgTP6.3) chimeras are shown in Table 6.1. 4 of these were non chimeric. With the exception of the yolk sac endoderm the mean %GPI1-A for each tissue sample was close to 50%, indicating that this is a balanced strain combination.

The percentages of GPI1-A in the five tissue types tested of BALB/c↔(BF_1xTgTP6.3) E12.5 chimeras are shown in Table 6.2. Out of the 29 chimeras analysed 8 were non-chimeric. The mean %GPI1-A for all the five tissue types are lower in this series of chimeras than in the (BALB/c x A/J)F_2 ↔(BF_1xTgTP6.3) chimeras. These differences are significant for the fetus and yolk sac mesoderm ($P<0.05$ by Mann-Whitney U test). This is shown in Figure 6.4, which compares the mean %GPI1-A between both series of chimeras analysed. These results indicate that BALB/c↔(BF_1xTgTP6.3) is an unbalanced strain combination so the distribution of BALB/c cells was investigated at the blastocyst stage (below).

Table 6.1: GPI1 analysis of E12.5 (BALB/c x AJ)F_2↔(BF1xTgTP6.3) chimeras

Chimera ref	% GPI-1 A				
	Fetus	Amnion	Yolk sac Mes	Yolk sac End	Placenta
non-chimeric					
GMA 12	0.0	0.0	0.0	0.0	0.0
GMA 21	0.0	0.0	0.0	0.0	0.0
GMA 1	100.0	no sample	100.0	no sample	100.0
GMA 15	100.0	100.0	100.0	100.0	100.0
chimeric	Fetus	Amnion	Yolk sac Mes	Yolk sac End	Placenta
GMA 7 *	0.0	14.7	5.5	0.0	0.0
GMA 19	15.6	5.9	0.0	0.0	0.0
GMA 16	20.5	19.0	19.4	5.8	0.0
GMA 6	24.6	8.3	22.1	22.5	8.9
GMA 5	24.7	25.5	14.2	27.5	70.9
GMA 18	25.0	24.0	34.0	53.4	80.8
GMA 24	32.9	8.9	0.0	28.4	76.0
GMA 13	42.7	8.6	38.0	21.6	30.3
GMA 17	43.6	56.0	62.9	17.3	91.7
GMA 2	44.5	41.3	41.0	46.5	42.5
GMA 20	62.4	50.5	74.6	66.0	100.0
GMA 4	62.8	50.8	48.5	14.6	97.5
GMA 22	63.5	100.0	65.4	40.2	100.0
GMA 9	63.9	63.6	68.7	14.4	0.0
GMA 11	65.0	66.4	75.9	86.4	66.9
GMA 10	67.7	27.6	40.1	31.3	92.4
GMA 8	75.5	75.4	100.0	80.4	100.0
GMA 14 *	100.0	100.0	100.0	44.2	100.0
GMA 23 *	100.0	100.0	100.0	47.5	100.0
GMA 3 *	100.0	100.0	100.0	70.0	100.0
Mean	**51.75**	**47.33**	**50.52**	**35.90**	**62.90**
SE	**6.53**	**7.63**	**7.71**	**5.74**	**9.17**
N	20	20	20	20	20
SD	29.20	34.14	34.47	25.67	41.01

Table 6.1: % of GPI1-A in the fetus, amnion, yolk sac mesoderm (Yolk sac Mes), yolk sac endoderm (Yolk sac End) and placenta in a series of E12.5 (BALB/c x A/J)F_2↔(BF1xTgTP6.3) chimeras.
* Chimerism was confined to extraembryonic tissues in 4 of the 20 chimeric conceptuses.
Mes = mesoderm, End = endoderm.

Table 6.2:

GPI1 analysis of E12.5 BALB/c↔(BF1xTgTP6.3) chimeras

Chimera ref	% GPI-1 A				
	Fetus	Amnion	Yolk sac Mes	Yolk sac End	Placenta
non-chimeric					
GMB 8	0.0	0.0	0.0	0.0	0.0
GMB 9	0.0		0.0	0.0	0.0
GMB 14	0.0	0.0	0.0	0.0	0.0
GMB 17	0.0	0.0	0.0	0.0	0.0
GMB 18	0.0	0.0	0.0	0.0	0.0
GMB 20	0.0	0.0	0.0	0.0	0.0
GMB 29	0.0	0.0	0.0	0.0	0.0
GMB 21	100.0	100.0	no sample	no sample	100.0
chimeric	Fetus	Amnion	Yolk sac Mes	Yolk sac End	Placenta
GMB 16 *	66.3	54.7	70.6	23.2	77.3
GMB 3 +	0.0	0.0	0.0	10.4	0.0
GMB 11 +	0.0	0.0	0.0	14.7	0.0
GMB 4 +	0.0	0.0	0.0	15.7	0.0
GMB 12 +	0.0	0.0	0.0	24.4	0.0
GMB 25	14.1	12.6	12.4	21.6	0.0
GMB 22	20.1	11.8	no sample	12.4	34.3
GMB 5	21.0	no sample	8.5	5.6	33.8
GMB 19	24.8	27.2	33.2	58.1	34.1
GMB 28	25.1	30.5	31.2	21.7	62.4
GMB 24	26.1	25.3	32.9	25.4	73.5
GMB 15	29.9	14.9	32.6	62.2	47.0
GMB 27	30.0	20.8	27.2	34.5	100.0
GMB 6	31.7	8.0	17.1	4.4	0.0
GMB 1	33.0	16.1	21.0	37.7	38.6
GMB 13	33.5	22.7	35.5	42.5	0.0
GMB 23	41.4	49.1	48.4	16.3	77.4
GMB 10	53.3	31.0	32.5	0.0	100.0
GMB 26	55.9	66.1	62.6	45.6	82.1
GMB 2 +	100.0	100.0	86.6	15.9	0.0
GMB 7 +	100.0	100.0	100.0	49.1	100.0
Mean	**32.00**	**28.22**	**30.62**	**25.91**	**39.16**
SE	**6.32**	**6.99**	**6.44**	**4.04**	**8.67**
N	20	19	19	20	20

Table 6.2:
% of GPI1-A in the fetus, amnion, yolk sac mesoderm (Yolk sac Mes), yolk sac endoderm (Yolk sac End), and placenta in a series of E12.5 BALB/c↔(BF1xTgTP6.3) chimeras.

* not included as it was dead

+Chimerism was confined to the extraembryonic tissue in 6 of the 20 chimeras

Mes = mesoderm, End = endoderm.

Fig. 6.4:
Mean % GPI1-A in (BALB/cxA/J)↔(BF$_1$xTgTP6.3) and BALB/c ↔(BF$_1$ x TgTP6.3) chimeras

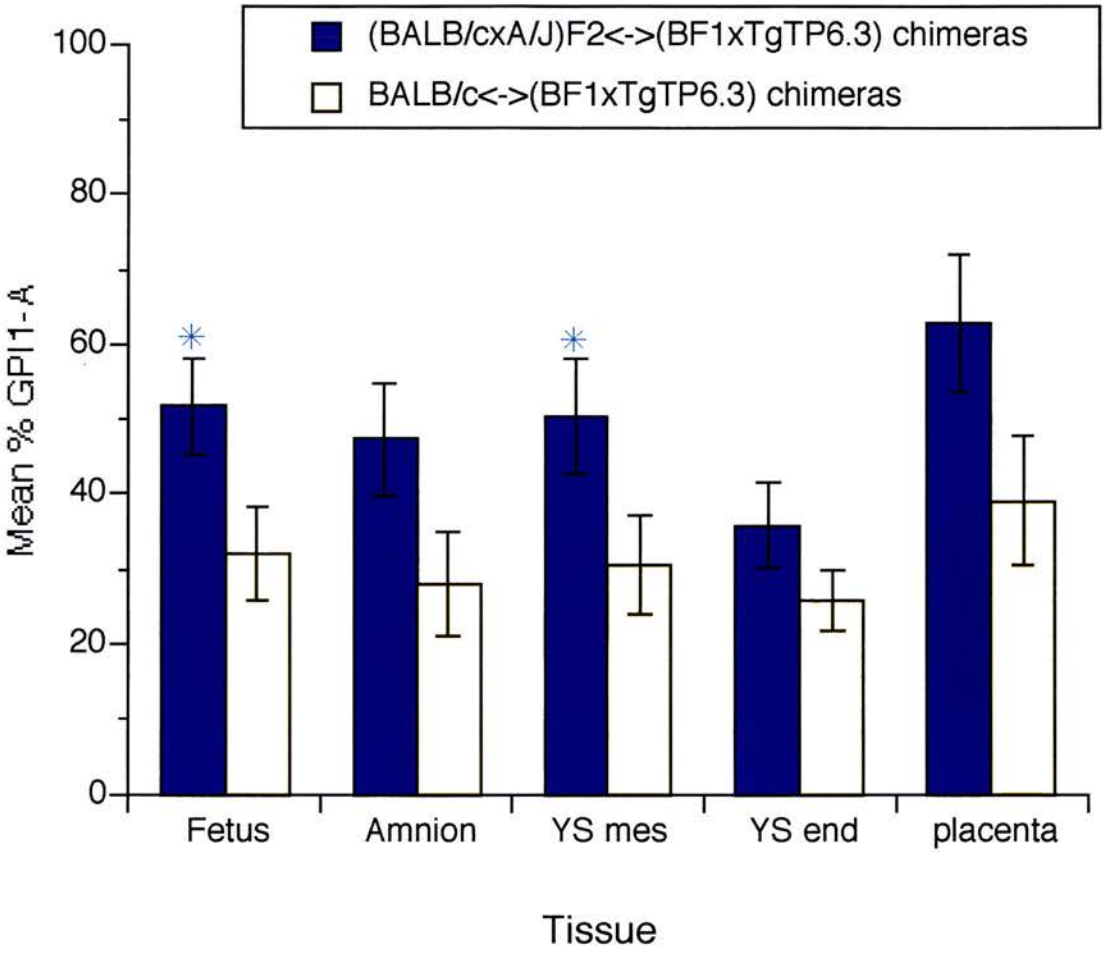

Fig. 6.4: Mean % (±SE) of GPI1-A in the fetus, amnion, YS mesoderm, YS endoderm and placenta of (BALB/c x A/J)↔(BF$_1$ x TgTP6.3) and BALB/c↔(BF$_1$xTgTP6.3) chimeras
✳ P<0.05 (Mann-Whitney U test)
YS = Visceral yolk sac

The proportion of chimeric conceptuses whose chimerism was confined to the extraembryonic tissues was not significantly greater in the unbalanced series (14/20 versus 16/20; χ^2= 0.13, P>0.05).

6.3.3 Time-Lapse Analysis of Tau-GFP Chimeras

Preimplantation chimeric embryos were imaged from the morula to the blastocyst stage to determine if BALB/c cells are preferentially allocated to the mTE during blastocyst development. As all chimeras do not develop at the same rate and this occurs over a period of approximately 24 hours, it was decided to use time-lapse confocal microscopy to image the embryos during constant time intervals. This allowed analysis of blastocysts at similar stages of development.

The % contribution of GFP embryos to (BALB/c x A/J)F_2↔(BF_1xTgTP6.3) and BALB/c↔(BF_1xTgTP6.3) chimeras was calculated to determine if BALB/c cells are preferentially allocated to the mTE. The analysis estimated the % area of GFP positive cells so a high contribution of BALB/c cells in the mTE would be seen as a low contribution of GFP cells in the mTE.

An initial time-lapse study using the 10x lens of the confocal microscope was carried out on 10 control (BALB/c x A/J)F_2↔(BF_1xTgTP6.3) chimeras and 9 BALB/c↔(BF_1xTgTP6.3) chimeric embryos aggregated at the 8-cell stage (Fig 6.5, 6.6 & 6.7a & b). The % contribution of the GFP embryos to the ICM, pTE and mTE of chimeric blastocysts was estimated from a single optical section

Fig 6.5: x10 Time-lapse Images of Control (BALB/c ×A/J)F_2↔(BF_1×TgTP6.3) Chimeras

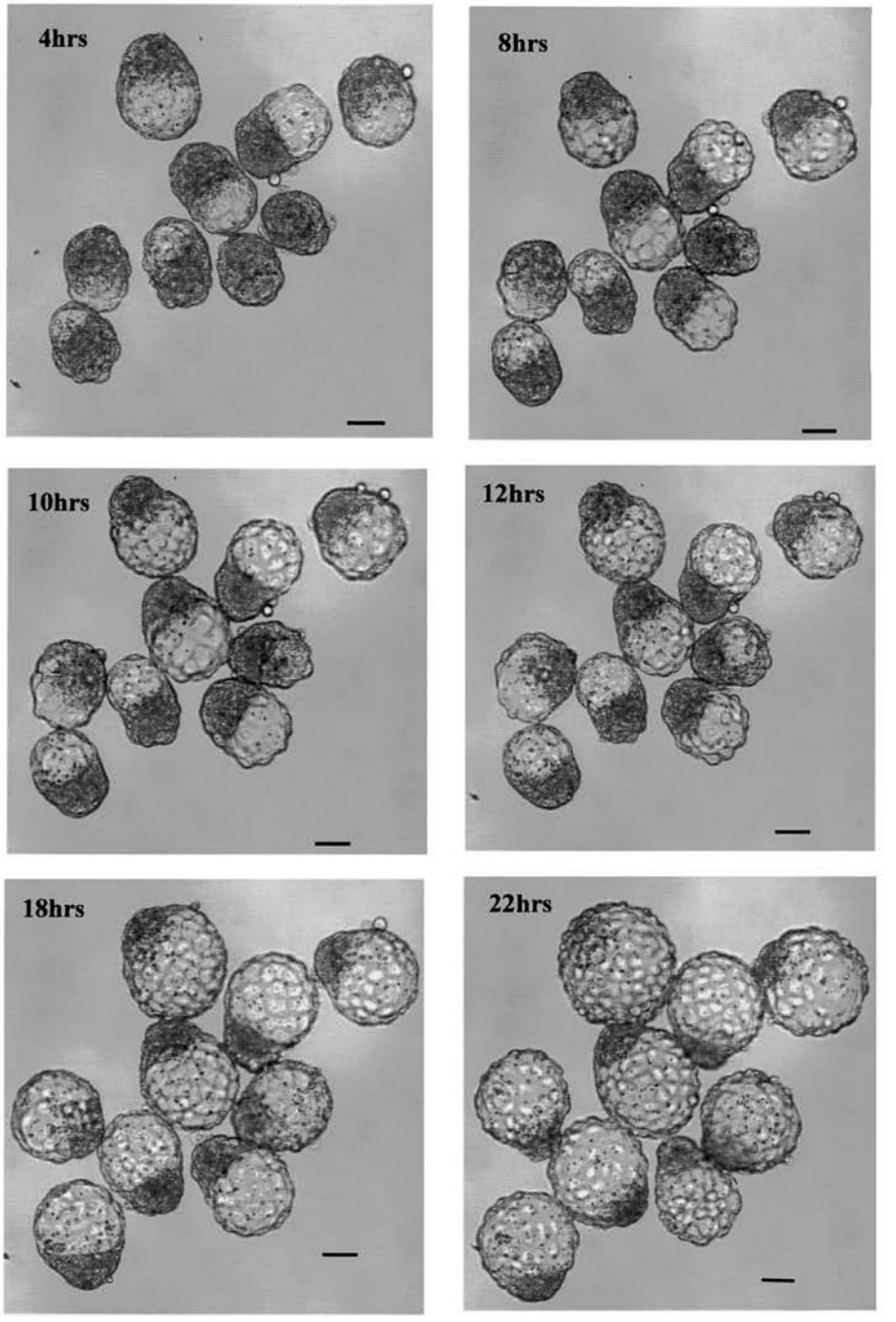

Fig 6.5: Single section overlay images of control (BALB/c×A/J)F_2↔(BF_1×TgTP6.3) chimeras imaged using the x10 lens of the confocal microscope. Embryos were aggregated at the 8-cell stage, and cultured for 24hrs in a normal incubator prior to the start of the time-lapse. Not all embryos are in focus as only the mid section for the whole group is shown (the ICMs of three blastocysts are not in focus in the last image). The images show a high proportion of GFP in the ICM region of the blastocysts which remains the case at the expanded blastocyst stage. The time elapsed from the start of the time-lapse is shown. Scale bar=50μ

Fig 6.6:
Time-lapse Microscopy of BALB/c↔(BF_1×TgTP6.3) Chimeras using the x10 Lens

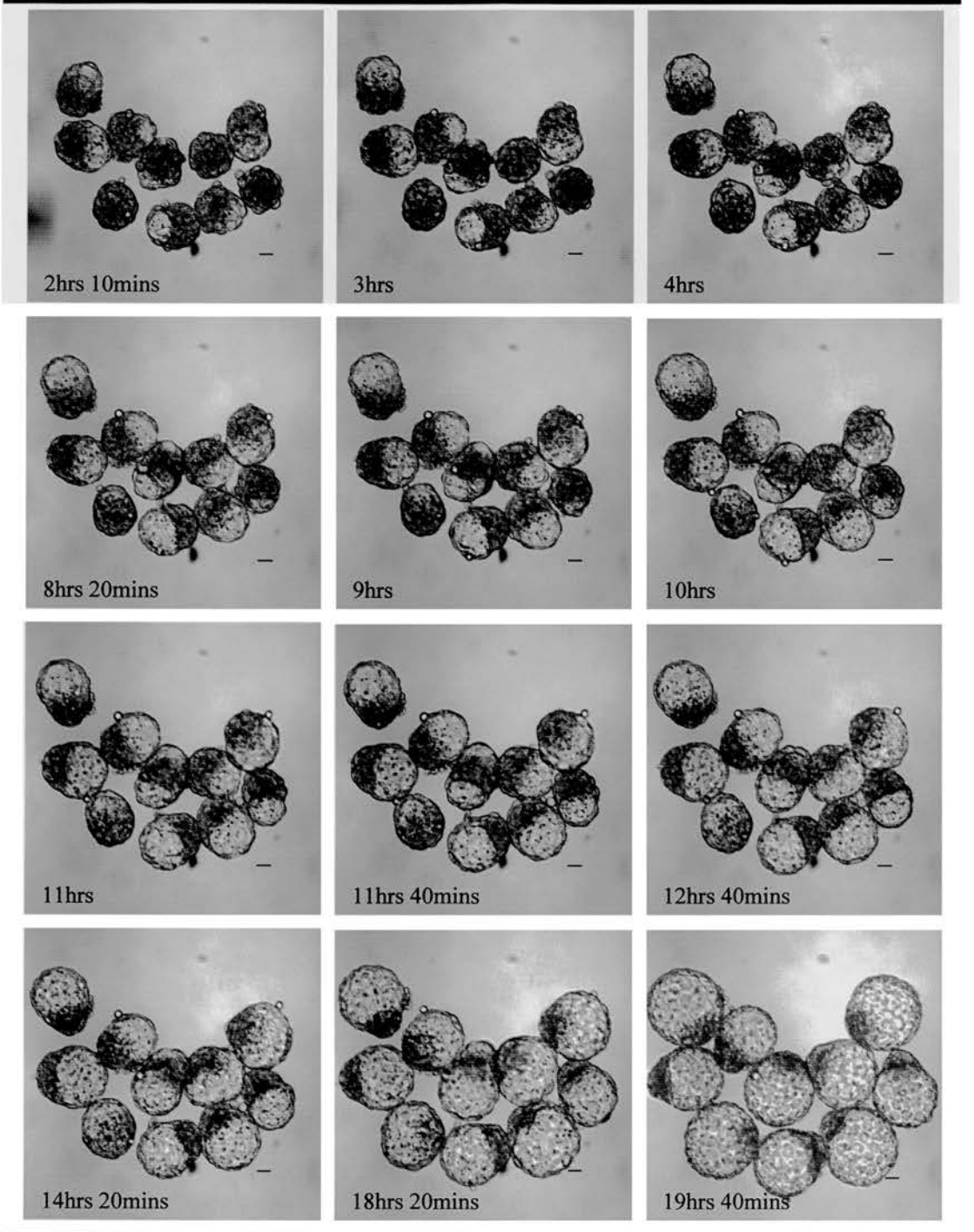

Fig 6.6: Single section overlay images of BALB/c↔(BF_1xTgTP6.3) chimeras imaged using the x10 lens of the confocal microscope. The time elapsed from the start of the time-lapse is shown. Not all embryos are in focus as only one optical section is shown for the whole group. These images show that the BALB/c (non GFP) cells are not consistently preferentially allocated to the mural trophectoderm. Scale bar =50μ

Fig. 6.7: Mean % contribution of GFP to control (BALB/c xA/J)F_2↔(BF_1xTgTP6.3) chimeras and to experimental BALB/c ↔(BF_1xTgTP6.3) chimeras

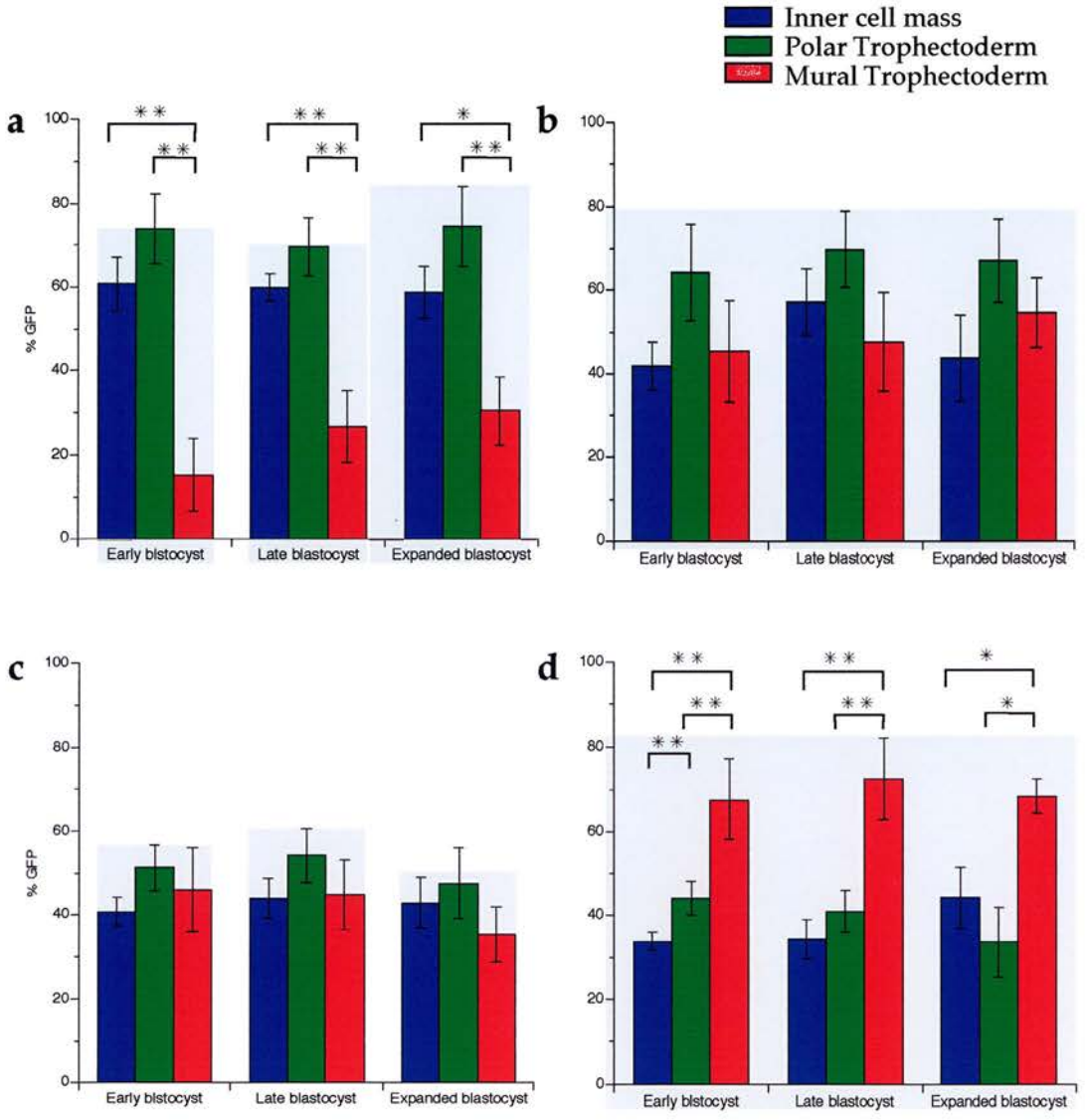

Fig.6.7:
% contribution of GFP embryos to the ICM, pTE and mTE at the early, late and expanded blastocyst stage, of **a:** 10 control (BALB/c x A/J)F_2↔(BF_1 x TgTP6.3) chimeras imaged using the 10x lens, **b:** 9 experimental BALB/c↔(BF_1 x TgTP6.3) chimeras imaged using the 10x lens, **c:** 13 control (BALB/c x A/J)F2↔(BF_1 x TgTP6.3) chimeras imaged using the 20 x lens, **d:** 11 experimental BALB/c↔(BF_1 x TgTP6.3) chimeras imaged using the 20x lens
$*P< 0.05$, $**P< 0.01$

(the mid section of the blastocyst where the ICM can be clearly seen) at 3 developmental stages, the early, late and expanded blastocyst (Fig 6.2).

Figure 6.7a shows the mean % contribution of GFP positive cells in 10 control (BALB/c x A/J)F_2↔(BF_1xTgTP6.3) blastocysts. The histogram shows there was a significantly lower overall contribution of GFP cells to the mTE in this chimera combination at all 3 developmental time points (pTE v mTE $P<0.01$ at all 3 stages, ICM v mTE at the early & late stage $P<0.01$, ICM v mTE at the expanded stage $P<0.05$ by Mann-Whitney U-test). This shows there is a high contribution of (BALB/c x A/J)F_1 cells in the mTE. There was no significant difference in composition of the ICM and pTE (ICM v pTE $P>0.05$ by Mann-Whitney U-test). Fig 6.5 also shows that there is a high proportion of non GFP cells within the mTE region of the majority of the chimeras at the early, late and expanded blastocyst stages.

Fig 6.7b shows there was no significant difference in the contribution of GFP cells between the 3 regions of the blastocyst in the experimental series of BALB/c↔(BF_1xTgTP6.3) chimeras at all 3 developmental time points ($P>0.05$ by Kruskal Wallis test). Therefore, despite the control data indicating that the GFP cells do not contribute well to the mTE there is an equal contribution of GFP cells and BALB/c cells to the mTE of the experimental series. Fig 6.7b and the images shown in Fig 6.6 suggests that there is no preferential allocation of the BALB/c cells to the mTE of the 9 blastocysts analysed (i.e the % GFP contribution is not low in the mTE). Also comparison of Figs 6.7a and 6.7b raises the possibility that BALB/c cells are less likely to be allocated

to mTE than (BALB/c x A/J)F_2 cells. This is the opposite of the hypothesis being tested.

Further time-lapse studies of a second control series of (BALB/cxA/J)F_2↔(BF_1xTgTP6.3) chimeras and a second experimental series of BALB/c↔(BF_1xTgTP6.3) chimeras aggregated at the 8-cell stage were carried out at a higher magnification using a x20 objective (Fig 6.7 c,d, 6.8 & 6.9). This was because it was easier to analyse the images captured using the x20 lens. As discussed in chapter 3, it may be optimal for embryo growth to image the embryos with a x10 lens. However, over a 24 hr time-lapse the blastocysts imaged using the x20 lens expanded to the late blastocyst stage, so were suitable for analysis. The % contribution of the GFP embryos to the ICM, pTE and mTE of chimeric blastocysts was calculated from an average of three optical sections at 3 developmental time points, the early, late and expanded blastocyst.

Fig 6.7c shows the average contributions of GFP positive cells in 13 control (BALB/c x A/J)F_2↔(BF_1xTgTP6.3) blastocysts. The results from this second series, the chimeras shown in Fig 6.8, showed that there was no significant difference between the average percentage contribution of GFP cells in the mTE, pTE and ICM at all 3 developmental stages ($P>0.05$ by Kruskal Wallis test). Fig 6.7d and 6.9 shows the average percentage contribution of GFP cells to the mTE of the experimental series of BALB/c↔(BF_1xTgTP6.3) chimeras was significantly higher than the contribution to the pTE and ICM (ICM v mTE at early & late stage $P<0.01$, $P<0.05$ at expanded stage, pTE v mTE at

Fig 6.8: x20 Time-lapse Images of Control (BALB/c×A/J)↔(BF$_1$×TgTP6.3) Chimeras

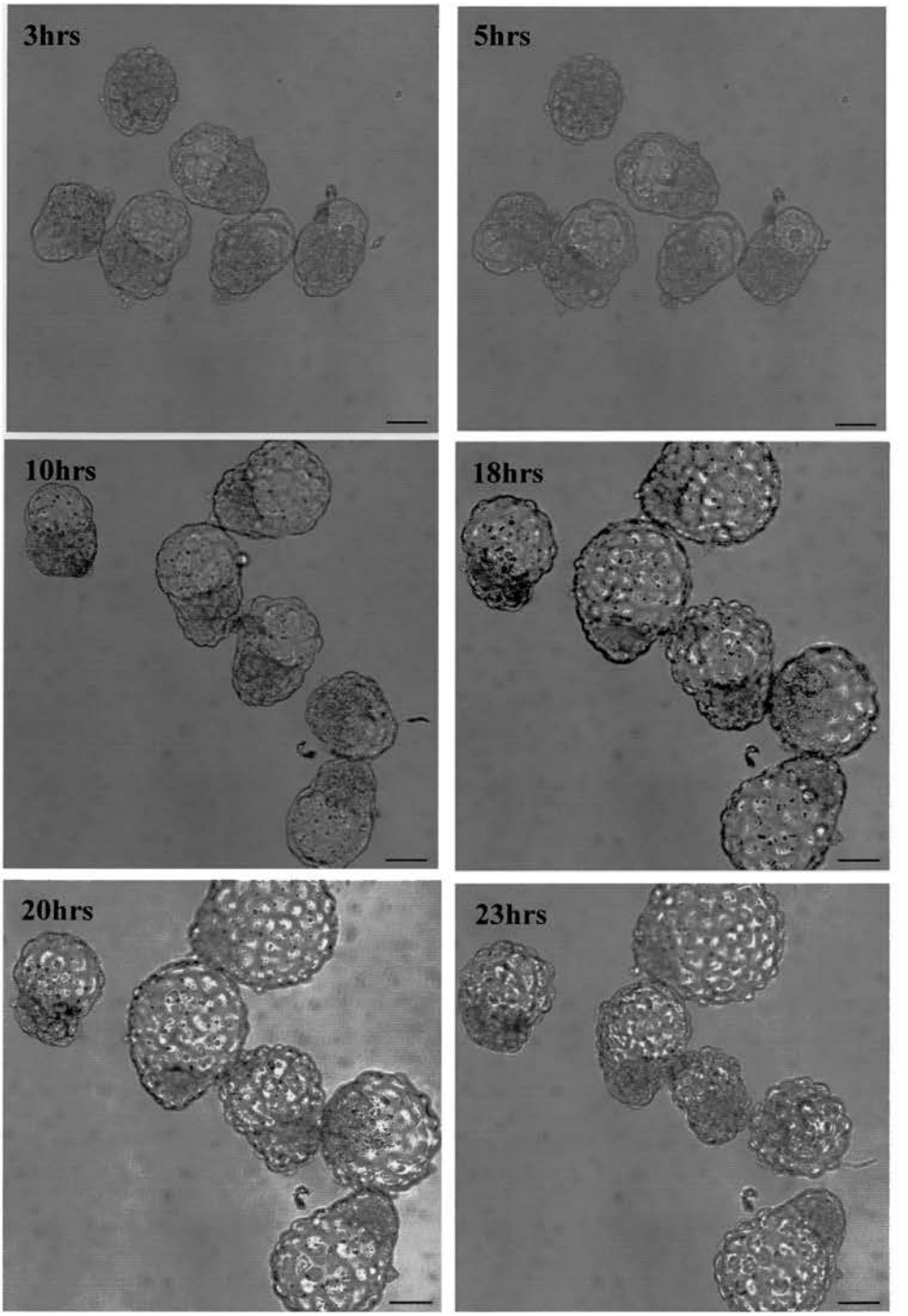

Fig 6.8: Single section overlay images of control (BALB/c×A/J)↔(BF$_1$×TgTP6.3) chimeras imaged using the x20 lens of the confocal microscope. Not all embryos are in focus as only the mid section for the whole group is shown. The time elapsed from the start of the time-lapse is shown. Scale bar=50μ

Fig 6.9: x20 Time-lapse Images of BALB/c↔(BF$_1$×TgTP6.3) Chimeras

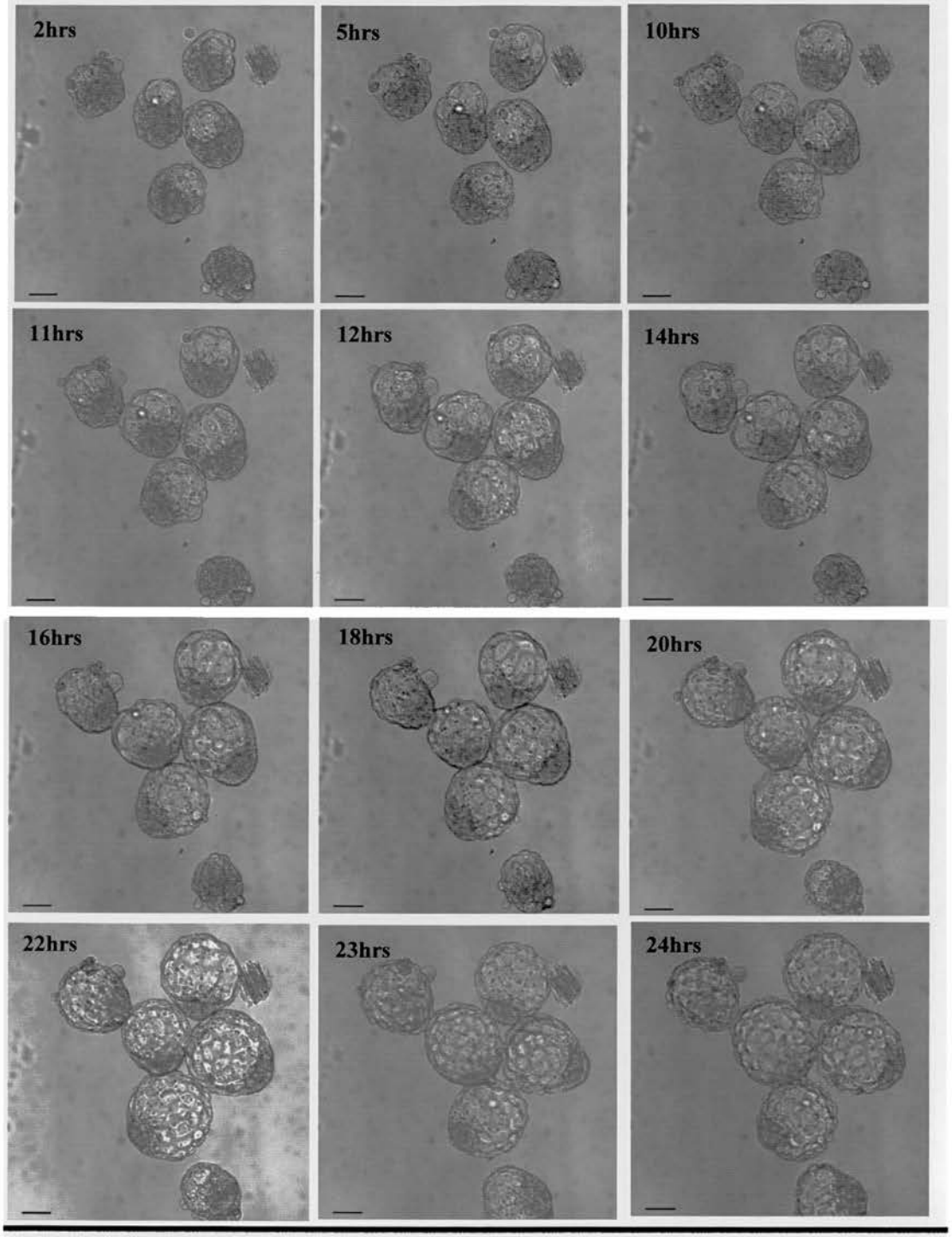

Fig 6.9: Single section overlay images of BALB/c↔(BF$_1$×TgTP6.3) chimeras imaged using the x20 lens of the confocal microscope. Not all embryos are in focus as only the mid section is shown for each group. The images show that there is a high %GFP contribution to the mTE of the chimeric blastocysts. Scale bar=50μ

early stage $P<0.05$, at late & expanded stage $P<0.01$ by Mann-Whitney U-test). This shows that there is a lower contribution of BALB/c cells to the mTE in this series of blastocysts. There is also a significantly higher % of GFP cells in the pTE compared to the ICM at the early blastocyst stage in this series of BALB/c↔(BF_1xTgTP6.3) chimeras ($P<0.05$ by Mann-Whitney U-test). Again, there was no evidence to support the hypothesis that BALB/c cells (non-GFP cells) were preferentially allocated to the mTE.

The percentage of GFP in the ICM, pTE and mTE was compared between the different control and experimental groups (Table 6.3). This data shows that there was no consistant significant differences between any tissues, at all blastocyst stages, between any two experiments. The differences between the pTE and ICM, the mTE and ICM, and the mTE and pTE were also compared among the same combination of control and experimental groups (Table 6.3). The difference between the pTE and ICM (pTE-ICM) did not differ significantly between groups. There were some significant differences between the composition of the mTE and either the pTE or ICM at some stages of blastocyst development. However, there were as many significant differences found when comparing both control groups or both experimental groups, as there were when comparing experimental and control chimeras.

Although the results from the two series of time-lapse experiments produced different results, neither provided any support for the hypothesis that BALB/c cells are preferentially allocated to the mTE of BALB/c↔(BF_1xTgTP6.3) chimeric blastocysts. In fact for each set of

Table 6.3: Statistical Analysis

x10 control v x20 control (avc)	ICM	pTE	mTE		pTE-ICM	mTE-ICM	mTE-pTE
Early	P=0.013	P=0.035	P=0.015		N.S	P=0.006	P=0.016
Late	P=0.022	N.S	N.S		N.S	P=0.047	N.S
Expanded	N.S	P=0.045	N.S		N.S	N.S	N.S
x10 Experimental v x20 Experimental (bvd)							
Early	N.S	N.S	N.S		N.S	N.S	N.S
Late	P=0.0135	P=0.02	N.S		N.S	P=0.017	P=0.03
Expanded	N.S	P=0.03	N.S		N.S	N.S	P=0.028
x10 control v x10 Experimental (avb)							
Early	P=0.041	N.S	P=0.025		N.S	P=0.014	N.S
Late	N.S	N.S	N.S		N.S	P=0.041	N.S
Expanded	N.S	P=0.043	N.S		N.S	N.S	N.S
x20 control v x20 Experimental (cvd)							
Early	N.S	N.S	N.S		N.S	N.S	N.S
Late	N.S	N.S	P=0.038		N.S	P=0.026	N.S
Expanded	N.S	N.S	P=0.002		N.S	P=0.025	P=0.012

Table 6.3: The % GFP contribution to the ICM, pTE and mTE was compared between contol and experimental groups for each tissue. The difference between the pTE & ICM, mTE & ICM and mTE & pTE was also compared between control and experimental groups. Letters in the brackets refer to the graphs in Fig 6.5.
N.S = not significant.

comparisons, BALB/c cells tended to make a poorer contribution to the mTE than the (BALB/c x A/J)F_2 cells did in the control chimeras.

Fig 6.7 also shows that the % of GFP cells in each region of the blastocyst does not differ significantly during the development of the blastocyst, in all four chimera series ($P>0.05$ by Kruskal Wallis test). This shows that BALB/c cells are not significantly depleted in the ICM, pTE and mTE during the development of BALB/c↔(BF_1xTgTP6.3) chimeric blastocysts from the early to expanded blastocyst stage.

6.3.4 Confocal Microscopy of BALB/c↔(BF_1xTgTP6.3) Chimeras Aggregated at the 2-Cell Stage

It is possible that by aggregating these embryos at the 8-cell stage there is little time to affect the randomness of cell allocation. Therefore a further series of both control and experimental chimeras were aggregated at the 2-cell stage and single optical sections, imaged at the late blastocyst stage using confocal microscopy, were analysed (Fig 6.10).

Fig 6.11a shows the percentage contribution of GFP embryos to 8 control (BALB/c x A/J)F_2↔(BF_1xTgTP6.3) blastocysts. There is no significant difference between the percentage contribution of GFP cells to the three regions of the blastocyst ($P>0.05$ by Kruskal Wallis test). Fig 6.11b shows the percentage contribution of GFP embryos to 8 experimental BALB/c↔(BF_1xTgTP6.3) chimera series. There is no significant difference between the average percentage contribution of GFP cells to the mTE

Fig6.10: BALB/c↔(BF_1×TgTP6.3) & (BALB/c×A/J)F_2↔(BF_1xTgTP6.3) Chimeras, Aggregated at the 2-cell Stage

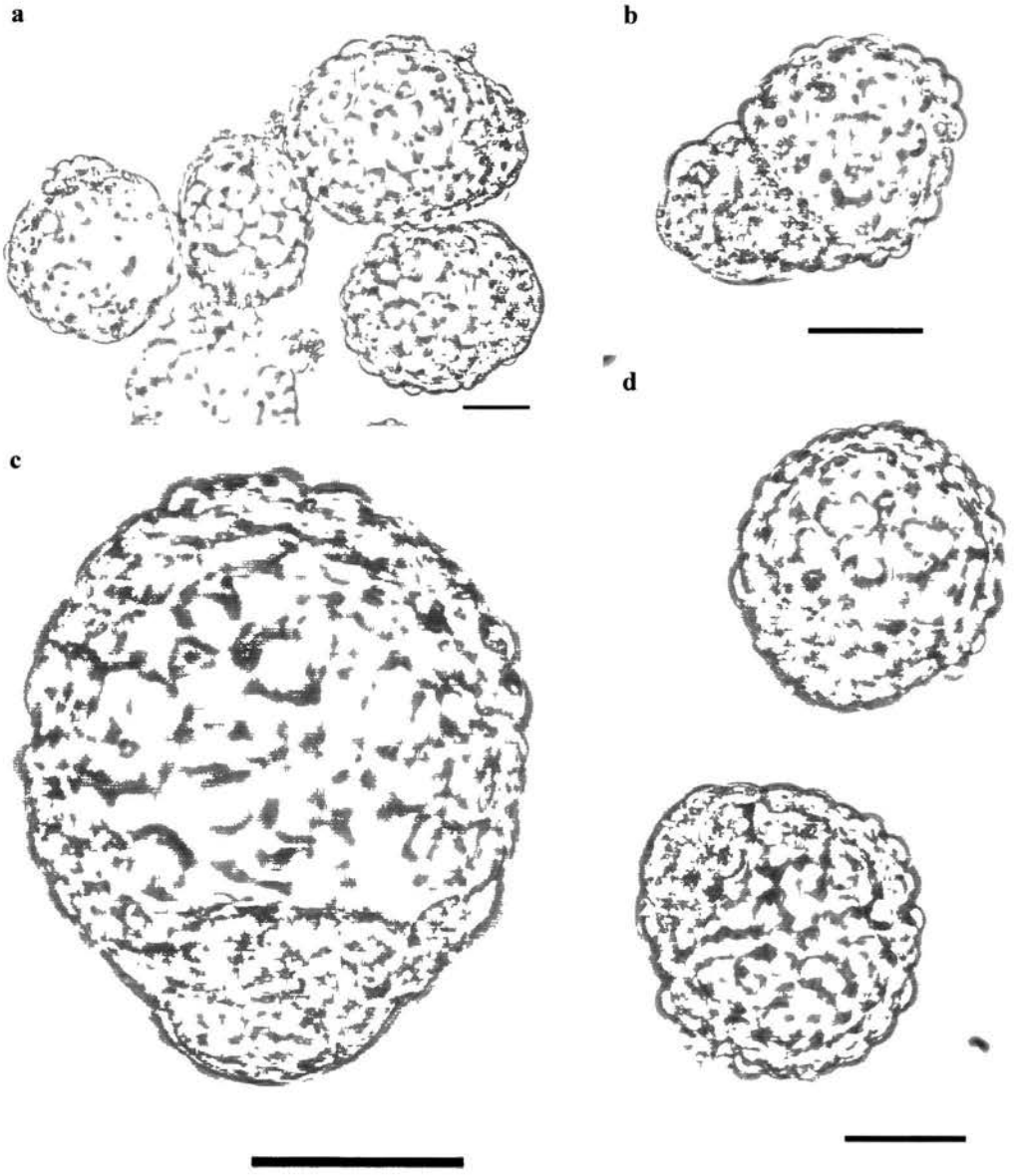

Fig 6.10: Overlay images of chimeras aggreagated at the 2-cell stage, cultured for 4 days and imaged at the late blastocyst stage. **a&b;** BALB/c↔(BF_1 × TgTP6.3) chimeras, **c&d;** (BALB/c×A/J)F_2↔(BF_1×TgTP6.3) chimeras.
Scale bar=50μ

Fig. 6.11: Mean % contribution of GFP to (BALB/c x A/J) F_2 ↔(BF_1 x TgTP6.3) chimeras and to BALB/c↔(BF_1 x TgTP6.3) chimeras aggregated at the 2-cell stage

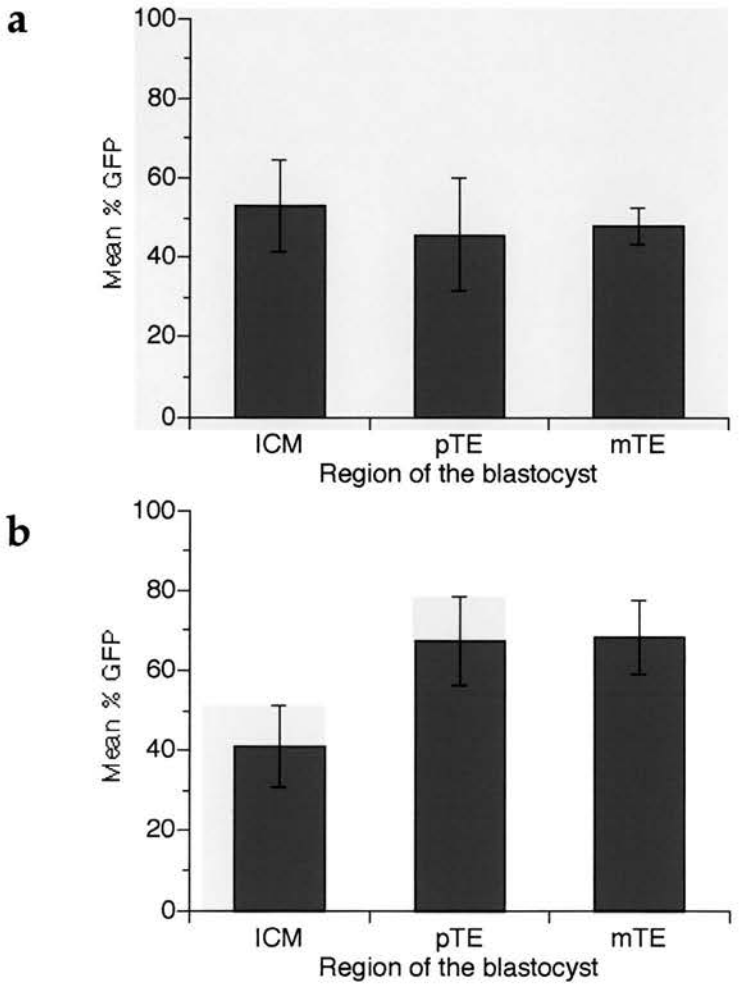

Fig. 6.11:
% contribution of GFP embryos to the ICM, pTE and mTE of chimeras produced by aggregating two 2-cell stage embryos.
a: 8 (BALB/c x A/J)F_2↔(BF_1 x TgTP6.3) chimeras imaged at the expanded blastocyst stage, **b:** 8 BALB/c ↔(BF_1 x TgTP6.3) chimeras imaged at the expanded blastocyst stage.

compared to the contribution to the ICM and pTE ($P>0.05$ by Kruskal Wallis test). There is no tendency for BALB/c cells to colonise the trophectoderm rather than the ICM. If anything there was a higher proportion of BALB/c cells (lower % GFP) in the ICM than the trophectoderm. Therefore, like the other results presented in this chapter, this shows that the BALB/c cells are not preferentially allocated to the mTE even when the embryos are aggregated at an earlier stage.

6.4 Conclusion

Preliminary studies of E12.5 chimeras showed that BALB/c strain embryos contributed poorly to BALB/c↔(BF_1xTgTP6.3) chimeras but the control series of (BALB/cxA/J)F_2↔(BF_1xTgTP6.3) chimeras was more balanced in composition. Three series of experimental BALB/c↔(BF_1xTgTP6.3) chimeras (Two 8-cell↔8-cell and one 2-cell↔2-cell) showed BALB/c cells were consistently allocated to the mTE but were not preferentially allocated to the mTE. This implies that some other mechanism is responsible for the depletion of BALB/c cells in the epiblast, hypoblast and pTE derivatives of BALB/c↔(BF_1xTgTP6.3) chimeras. This is likely to be some form of generalised cell selection against BALB/c cells.

BALB/c↔(BF_1xTgTP6.3) chimeras were aggregated at the 2-cell stage, as it was possible that late stage aggregation prevented BALB/c cells from being preferentially allocated to the mTE. As discussed in chapter 1, (section 1.1.3) previous studies have shown that the advanced blastomeres in an embryo

tend to contribute disproportionately more descendants to the inner cells of the morula or the ICM of the blastocyst (Kelly *et al.*, 1978; Graham and Lehtonen, 1979; Piotrowska *et al.*, 2001). However, previous analysis of aggregation chimeras to determine if the more advanced embryo contributes more readily to the ICM has revealed conflicting results (chapter 1, section 1.5.1.2). As noted earlier, BALB/c strain embryos tend to develop relatively slowly. Nevertheless, the data presented in this chapter showed that early aggregation of BALB/c↔(BF_1xTgTP6.3) chimeras did not affect the allocation of BALB/c cells to the different regions of the blastocyst.

Another study has examined the composition of groups of whole BALB/c↔(BF_1xTGB) and control (BALB/cxA/J)F_2↔(BF_1xTGB) chimeras at E4.5 and E6.5 by GPI electrophoresis (Tang, 1999). This revealed that there is no significant genotypic imbalance in BALB/c↔ (BF_1xTGB) chimeras at these embryonic stages. Dvorak *et al* (1995) also showed that BALB/c cells are not reduced at the blastocyst stage. The results described in this chapter are in agreement with this showing that BALB/c cells are not depleted in BALB/c↔(BF_1xTgTP6.3) chimeras by the expanded blastocyst stage. As the mechanism of preferential allocation of BALB/c cells to the mTE can now be excluded, this indicates that BALB/c cells are reduced in BALB/c chimeras after E6.5. Preferential death of BALB/c cells in the blastocyst is unlikely. However, this could be confirmed by analysing apoptosis in BALB/c chimeric embryos.

The most likely mechanism responsible for the depletion of BALB/c cells in aggregation chimeras would appear to be due to a difference between the developmental rates of the aggregated embryos. The pre-implantation embryo development (*Ped*) gene has already been identified as having a role in the rate of development of preimplantation embryos (Warner *et al.*, 1998). Although the BALB/c embryos analysed in this chapter have a fast allele of the *Ped* gene, previous data has indicated that BALB/c embryos have a slow rate of development (West, unpublished data). Therefore, different growth rates could result in fewer BALB/c cells present within BALB/c chimeras. Varying developmental rates of different strain embryos have been previously detected. Differences between the time of cleavage starting has been found in certain strain embryos (McLaren and Bowman, 1973; Niwa *et al.*, 1980). McLaren et al, have shown that the cleavage rates are the same, however the difference in the initiation of cleavage is sufficient to significantly delay the embryo development. Although both embryos were aggregated at either the 8-cell stage or the 2-cell stage it is possible that the BALB/c cells do not cleave as quickly as the other cells. This lag in development could be sufficient to reduce the numbers of BALB/c cells contributing to the chimera. This mechanism has been suggested for another unbalanced strain combination (Mystkowska *et al.*, 1979). However, evidence against this would be the fact that there is not a gradual decline in the proportion of BALB/c cells during blastocyst development but appears to be a decrease following implantation. (Tang, 1999), found no difference at E6.5 however, Dvorak et al, 1995 showed a difference at E7.5 and Tang

(unpublished) at E8.5. Further studies to test this hypothesis could include investigations of cell proliferation in these chimeras.

The results presented in this chapter show 4 individual BALB/c chimeras in the E12.5 series are only chimeric in the yolk sac endoderm and do not contain BALB/c cells in any of the other tissues. This is in agreement with previous data, which has shown chimerism is sometimes confined to either the placenta or yolk sac endoderm. However, unlike the 4n↔2n model the unbalanced BALB/c chimera does not consistently show confined chimerism.

It seems likely that the poor contribution of BALB/c cells to the epiblast and other lineages is a result of generalised cell selection rather than non random allocation of BALB/c cells to different developmental lineages. If so this indicates that CPM may occasionally result from generalised selection which happens to exclude one cell population from the fetus but not from extraembryonic tissues.

Chapter 7: Discussion

7.1 Confocal Microscopy to Image Mouse Chimeras

Two different methods of analysing mouse aggregation chimeras by confocal microscopy were used in this study, time-lapse microscopy and single time point microscopy of chimeras. This study has shown that both techniques are useful and have their advantages and disadvantages.

The time-lapse confocal microscopy technique provided an effective method for imaging preimplantation embryos over a period of approximately 24hrs. This was a particularly useful approach for investigating the timing of GFP expression and further experiments could be performed to better define when embryo encoded GFP is first detectable. It also provided the most effective way of analysing several chimeric blastocysts at equivalent developmental stages. However, the culture system on the confocal microscope was more prone to failure than culture in a normal CO_2 incubator.

As discussed previously in chapter 3 exposure to high intensity laser power affects the viability of mouse embryos (Squirrell *et al.*, 1999). This technique was compatible with normal development using a 10x and 20x lens however it would probably not be suitable to image embryos with a higher objective lens, for example a 40x lens. It may also be more advantageous to image embryos at fewer time points to reduce the exposure to the confocal laser.

Another disadvantage of the time-lapse technique is that fewer optical sections are acquired at each time point, therefore not all embryos in a group will be in the best plane of focus for analysis. If more optical sections are required for image analysis, for example for 3D reconstructions and volume analysis it would probably be more suitable to image embryos at a single time point and culture them in a standard incubator.

As discussed previously it would have been useful for the analysis of the chimeras to label the partner embryo in the chimera. Of the exogenous markers analysed PKH-26 could be a suitable marker. However, this was not available for the BALB/c experiments which were carried out prior to the 4n↔2n experiments. PKH-26 was not used for the 4n↔2n study as it could have affected the allocation of cells in a chimera, as it is a membrane dye. It was also decided to analyse all the chimeras in a consistent manner. If red fluorescent protein (RFP) (produced by Living Colors, Clontech Inc, Palo Alto, USA) transgenic mice had been available for this study they could have been used in conjunction with the tau-GFP embryos (Nakamura *et al.*, 2002; Lu *et al.*, 2003). As time-lapse microscopy was not used for the analysis of the 4n↔2n chimeras or the BALB/c chimeras aggregated at the 2-cell stage it may have been useful to have fixed them and stained them with a nuclear marker for example propidium iodide. However, after attempts to fix blastocysts the cavity collapsed. Therefore, it was decided not to use this technique as it was necessary to distinguish the different areas of the blastocyst for analysis.

7.2 Studies of 4n↔2n Chimeras

This study investigated 4n↔2n chimeras specifically as a mouse model of CPM. This demonstrated that there are several mechanisms responsible for the exclusion of 4n cells from the epiblast derivatives. The results in chapter 5 demonstrate it is likely that the blastocyst cavity forms within the 4n half of the chimera, resulting in a larger proportion of 4n cells being allocated to the trophectoderm. This could be due to an increase in the activity of the sodium pump in the 4n cells.

Tang et al. (2000) previously demonstrated that larger 2n blastomeres make a greater contribution to the TE of 2n↔2n chimeras. This is probably due to mechanical reasons, as smaller cells are likely to be positioned in the centre of the chimeric morula. Larger cells would be pushed to the outside region, which forms the TE. Therefore, the size of the 4n cells analysed in this study could also be responsible for the preferential allocation to the TE, as the 4n cells analysed in this study are larger than the 2n cells. However, Tang et al. (2000) also demonstrated that 4n cells which did not differ in cell size from the cells of the partner 2n cells, also made a significantly greater contribution to the mTE. Thus cell size is probably not solely responsible for the preferential allocation of cells to the TE.

It is possible that similar mechanisms are involved in the removal of 4n cells from the epiblast, and the reduction of BALB/c cells from all lineages of the blastocyst. As noted earlier, BALB/c strain embryos tend to develop relatively slowly, and it is possible that this is also true of 4n cells. Therefore,

slower proliferation rates of one type of cell in a chimeric embryo could significantly reduce these cells within the chimera. The proliferation rates of 4n embryos could be analysed following cavitation, along with nuclear morphology to assess apoptosis. Apoptosis could also play a role in the removal of cells from a specific lineage.

It is therefore possible that some of these mechanisms resulting in the depletion or loss of cells within specific regions of mouse chimeras could also be responsible for the exclusion of chromosomally abnormal cells from human epiblast lineage derivatives resulting in CPM.

There are also other uses of 4n chimeras that are relevant to developmental biology. Studies have made use of the fact that 4n cells do not tend to contribute to the derivatives of the epiblast at mid-gestation, but do contribute to the hypoblast and trophectoderm lineages. Therefore, the aggregation or injection of 4n cells with 2n cells or blastocysts has been used to investigate if mutants, with severe defects in the developing embryo at gastrulation, have primary defects in these extraembryonic lineages rather than the epiblast (Rossant and Spence, 1998). Using this technique researchers have shown that signalling events within the derivatives of the trophectoderm and hypoblast are responsible for the development of the embryo.

Mash-2, a mammalian member of the *achaete-scute* family, encodes a transcription factor. This gene is strongly expressed in the ectoplacental cone, the chorion and their derivatives in the placenta. The mutants of Mash-2 die

at 10 days p.c and fail to form a placenta (Guillemot *et al.*, 1994). By aggregating wild-type 4n embryos to *Mash-2* mutant embryos Guillemot *et al* (1994) produced viable and developmentally normal adult mice. This shows that *Mash-2* is essential for the development of the mammalian trophoblast lineage but does not have a role in the development of the embryo itself.

The mutants of HNF4, a transcription factor, and SMAD4, a signal transduction molecule, do not reach gastrulation and therefore fail to form mesoderm structures. However, they can be "rescued" by a wild-type 4n placenta and yolk sac endoderm (Duncan *et al.*, 1997; Sirard *et al.*, 1998). This shows that these genes are acting in a non-cell autonomous manner as they have a direct effect on the fetus itself. Alternatively, the injection of wild type ES cells into mutant 4n blastocysts for the type I activin receptor ACTR1B or the signalling molecule SMAD2 fails to produce embryos (Gu *et al.*, 1998; Waldrip *et al.*, 1998). More recently the retinoblastoma (*Rb*) tumour supressor gene has been demonstrated as having a key function in the placenta that is responsible for embryonic development and viability (Wu *et al.*, 2003). By aggregating wild-type 4n cells with mutant 2n cells Wu et al, (2003), demonstrated that a wild-type placenta could carry a mutant fetus to term.

Although it is not known if this is the case, it has sometimes been previously assumed that 4n cells are excluded from the epiblast of 4n↔ES cell aggregation chimeras (Fig 1, (Rossant and Spence, 1998)). The findings of this study, that 4n cells are present in the epiblast of 4n↔2n chimeras, indicate that 4n cells could also be present in the epiblast of 4n↔ES cell aggregation

chimeras. The same techniques used in the 4n↔2n chimera study could be used to analyse 4n↔ES cell chimeras to determine if this is the case.

7.3 Future Experiments

The BALB/c study showed that BALB/c cells were not preferentially allocated to the mTE. Other unpublished work (P.C. Tang) indicate that BALB/c cells are significantly depleted by E8.5 (see section 6.4). Therefore, BALB/c cells could be depleted from mid-gestation chimeras by a slower rate of proliferation compared to the cells from the partner embryo. Alternatively there could be specific cell death of BALB/c cells. BrdU or TUNEL staining could be used to investigate these possibilities. The same techniques could also be applied to investigate the mechanisms of cell selection against 4n cells remaining in the epiblast of 4n↔2n chimeras.

Appendix A:

M16 Embryo Culture Media

Stock solutions for handling and culture medium:

Stock A (10x) (100ml)	1M NaCl 0.05M KCl 1.2M KH_2PO_4 0.012M $MgSO_4$ 0.23M Na Lactate (60% solution) 5.5mM Glucose 60mg (10^5 units/mg) penicillin 50mg (750 units/mg)streptomycin
Stock B (10x) (100ml)	0.25M $NaHCO_3$ 0.01g phenol red
Stock C (100x) (100ml)	0.33M Sodium pyruvate
Stock D (100x) (100ml)	0.17M $CaCl_2.2H_2O$
Stock E (10x) (10ml)	0.25M HEPES (Ultrapure Calibiochem) 0.01g phenol red

Stock E was adjusted to pH 7.4 with 5M NaOH before making up to 100ml

100mls of stocks A, B and E and 10ml of C and D were made using sterile cell culture grade H_2O (BDH). All Stocks were sterilised using a (0.22mm) millipore filter and stored at 4^oC Stocks A,D & E were renewed every 3 months and stocks B and C every two weeks.

M2 Handling Medium (10mls)

A	1.0ml
B	0.16ml
C	0.1ml
D	0.1ml
E	0.84ml
H_2O (sterile culture grade BDH)	7.8ml
BSA	40mg

Solutions were sterilised using a millipore filter (0.22mm) before use.

M16 Culture Medium (10mls)

A	1.0ml
B	1.0ml
C	0.1ml
D	0.1ml
H_2O (sterile culture grade BDH)	7.8ml
BSA	40mg

Solutions were sterilised using a millipore filter (0.22mm) before use.

Appendix B:

KSOM Embryo Culture Media:

Stock Solutions:

Stock A (10x) (100ml)	95mM NaCl 2.5mM KCl 0.35mM KH_2PO_4 0.20mM $MgSO_4.7H_2O$ 10mM Na lactate (60%) 0.20mM Glucose 0.01 EDTA 0.06g (97.5 units/ml) Penicillin 0.05g (37.5units/ml) Streptomycin
Stock B (10x) (100ml)	25mM $NaHCO_3$ 0.01g phenol red
Stock C (100x) (10ml)	0.20mM Na Pyruvate
Stock D (100x) (10ml)	1.71mM $CaCl_2.2H_2O$
Stock E (100x) (10ml)	1mM L-glutamine
Stock F (10x) (100ml)	20mM HEPES (SIGMA)

Stock F was adjusted to pH 7.2 with 5M NaOH (use 30mls NaOH plus 40mls of water in first instance) before making up to 100ml

All stocks were filter sterilised using a millipore filter (0.22mm) and stored at 4°C. Stocks A,D,E & F were kept for 3 months then discarded. Stocks B and C were replaced every second week

KSOM Handling Medium (10ml)

A	1.0ml
B	0.2ml
C	0.1ml
D	0.1ml
E	0.1ml
F	1.0ml
H_2O (sterile culture grade BDH)	7.5ml
BSA	10mg

Solutions were sterilised using a millipore filter (0.22mm) before use.

KSOM Culture Medium (10ml)

A	1.0ml
B	1.0ml
C	0.1ml
D	0.1ml
E	0.1ml
H_2O (sterile culture grade BDH)	7.7ml
BSA	10mg

Solutions were sterilised using a millipore filter (0.22mm) before use.

Appendix C:

Acid Tyrode's solution:

0.14M NaCl
2.6mM KCl
1.4mM $CaCl_2$
0.5mM $MgCl_2.6H_2O$
0.2mM $NaH_2PO_4.H_2O$
5.5mM Glucose
0.12M $NaHCO_3$
0.4% polyvinyl pyrrolidone

Adjusted to pH 2.5 with 5M HCl. Filter sterilised using a millipore filter (0.22mm) and stored at 4°C

Bibliography:

Alonso, L., Melaragno, I., Bortolai, A., Takeno, S., and Brunoni, D. (2002). Tetraploid/diploid mosaicism: case report and review of the literature. *Annales de Genetique* **45,** 177-180.

Angell, R. R., Sumner, A. T., West, J. D., Thatcher, S. S., Glasier, A. F., and Baird, D. T. (1987). Post-fertilization polyploidy in human preimplantation embryos fertilized in vitro. *Human Reproduction* **2,** 721-727.

Bachvarova, R., and DeLeon, V. (1980). Polyadenylated RNA of mouse ova and loss of maternal RNA in early development. *Developmental Biology* **74,** 1-8.

Barlogie, B. (1984). Abnormal Cellular DNA Content As a Marker of Neoplasia. *European Journal of Cancer & Clinical Oncology* **20,** 1123-1125.

Barlow, P. W., and Sherman, M. I. (1972). The biochemistry of differentiation of mouse trophoblast: studies on polyploidy. *J. Embryol. Exp. Morphol.* **27,** 447-465.

Benkhalifa, M., Janny, L., Vye, P., Malet, P., Boucher, D., and Menezo, Y. (1993). Assessment of polyploidy in human morulae and blastocysts using co-culture and fluorescent in-situ hybridization. *Human Reproduction* **8,** 895-902.

Benn, P. (1998). Trisomy 16 and trisomy 16 mosaicism: A review. *American Journal of Medical Genetics* **79,** 121-133.

Bower, J. (1987). Chromosome organisation in polyploid mouse trophoblast nuclei. *Chromosoma* **95,** 76-80.

Brenner, C. A., Adler, R. R., Rappolee, D. A., Pedersen, R. A., and Werb, Z. (1989). Genes for extracellular matrix-degrading metalloproteinases and their inhibitor, TIMP, are expressed during early mammalian development. *Genes Devel.* **3,** 848-859.

Brodsky, V. Y., and Uryvaeva, I. V. (1985). "Genome Multiplication in Growth and Development. Biology of Polyploid and Polytene Cells." Cambridge University Press, Cambridge.

Brodsky, W. Y., and Uryvaeva, I. V. (1977). Cell polyploidy: its relation to tissue growth and function. *Int Rev Cytol* **50,** 275-332.

Carroll, S. G., Davies, T., Kyle, P. M., Abdel-Fattah, S., and Soothill, P. W. (1999). Fetal karyotyping by chorionic villus sampling after the first trimester. *Br. J. Obstet. Gynaecol.* **106,** 1035-1040.

Carson, D. D., Tang, J. P., and Julian, J. (1993). Heparan-Sulfate Proteoglycan (Perlecan) Expression By Mouse Embryos During Acquisition of Attachment Competence. *Developmental Biology* **155,** 97-106.

Chapman, V. M., Ansell, J. D., and McLaren, A. (1972). Trophoblast giant cell differentiation in the mouse: expression of glucose phosphate isomerase (GPI-1) electrophoretic variants in transferred and chimeric embryos. *Developmental Biology* **29,** 48-54.

Chapman, V. M., Whitten, W. R., and Ruddle, F. H. (1971). Expression of paternal glucose phosphate isomerase-1 (Gpi-1) in preimplantation stages of mouse embryos. *Devl. Biol.* **26,** 153 - 158.

Ciemerych, M. A., Mesnard, D., and Zernicka-Goetz, M. (2000). Animal and vegetal poles of the mouse egg predict the polarity of the embryonic axis, yet are nonessential for development. *Development* **127,** 3467-3474.

Clegg, K. B., and Piko, L. (1983). Quantitative Aspects of Rna-Synthesis and Polyadenylation in 1- Cell and 2-Cell Mouse Embryos. *Journal of Embryology and Experimental Morphology* **74,** 169-182.

Clouston, H. J., Fenwick, J., Webb, A. L., Herbert, M., Murdoch, A., and Wolstenholme, J. (1997). Detection of mosaic and non-mosaic chromosome abnormalities in 6- to 8-day-old human blastocysts. *Human Genetics* **101,** 30-36.

Cox, D. R., Smith, S. A., Epstein, L. B., and Epstein, C. J. (1984). Mouse trisomy 16 as an animal model for human trisomy 21 (Down syndrome): production of viable trisomy 16 <-> diploid mouse embryos. *Dev. Biol.* **101,** 416-424.
Culotta, E. (1991). How Many Genes Had to Change to Produce Corn. *Science* **252,** 1792-1793.

Davies, T. J., and Gardner, R. L. (2002). The plane of first cleavage is not related to the distribution of sperm components in the mouse. *Human Reproduction* **17,** 2368-2379.

Delhanty, J. D. A., Griffin, D. K., Handyside, A. H., Harper, J., Atkinson, G. H. G., Pieters, M., and Winston, R. M. L. (1993). Detection of Aneuploidy and Chromosomal Mosaicism in Human Embryos During Preimplantation Sex Determination By Fluorescent in-Situ Hybridization, (Fish). *Human Molecular Genetics* **2,** 1183-1185.

Delhanty, J. D. A., and Handyside, A. H. (1995). The Origin Of Genetic-Defects In the Human and Their Detection In the Preimplantation Embryo. *Oxford Reviews Of Reproductive Biology* **17,** 125-157.

Delhanty, J. D. A., Harper, J. C., Ao, A., Handyside, A. H., and Winston, R. M. L. (1997). Multicolour FISH detects frequent chromosomal mosaicism and chaotic division in normal preimplantation embryos from fertile patients. *Human Genetics* **99,** 755-760.

Duncan, S. A., Nagy, A., and Chan, W. (1997). Murine gastrulation requires HNF-4 regulated gene expression in the visceral endoderm: Tetraploid rescue of Hnf-4(-/-) embryos. *Development* **124,** 279-287.

Dvorak, P., Yoshiki, A., Dvorakova, D., Flechon, J. E., and Kusakabe, M. (1995). Cell mixing during the early development of mouse aggregation chimera. *Int. J. Dev. Biol.* **39,** 645-652.

Dyban, A. P., and Baranov, V. S. (1987). "Cytogenetics of Mammalian Embryonic Development." Clarendon, Oxford.

Eiben, B., Bartels, I., Bahrporsch, S., Borgmann, S., Gatz, G., Gellert, G., Goebel, R., Hammans, W., Hentemann, M., Osmers, R., Rauskolb, R., and Hansmann, I. (1990). Cytogenetic Analysis of 750 Spontaneous-Abortions With the Direct-Preparation Method of Chorionic Villi and Its Implications For Studying Genetic Causes of Pregnancy Wastage. *American Journal of Human Genetics* **47,** 656-663.

Eisenberg, B., and Wapner, R. J. (2002). Clinical proceduress in prenatal diagnosis. *Best Practice & Research in Clinical Obstetrics & Gynaecology* **16,** 611-627.

Epstein, C. J. (1985). Mouse monosomies and trisomies as experimental systems for studying mammalian aneuploidy. *Trends Genet.* **1,** 129-134.

Epstein, C. J. (1986). "The Consequences of Chromosome Imbalance." Cambridge University Press, New York.

Epstein, C. J., Smith, S. A., and Cox, D. R. (1984). Production and properties of mouse trisomy 15↔diploid chimeras. *Dev. Genet.* **4,** 159-165.

Epstein, C. J., and Travis, B. (1979). Preimplantation lethality of monosomy for mouse chromosome 19. *Nature* **280,** 144-145.

Everett, C. A., Stark, M. H., West, J. D., Davidson, D., and Baldock, R. A. (2000). Three-dimensional reconstruction of tetraploid<->diploid chimaeric mouse blastocysts. *J. Anatomy* **196,** 341-346.

Everett, C. A., and West, J. D. (1996). The influence of ploidy on the distribution of cells in chimaeric mouse blastocysts. *Zygote* **4,** 59-66.

Everett, C. A., and West, J. D. (1998). Evidence for selection against tetraploid cells in tetraploid↔diploid mouse chimaeras before the late blastocyst stage. *Genetical Research* **72,** 225-228.

Evsikov, S., and Verlinsky, Y. (1998). Mosaicism in the inner cell mass of human blastocysts. *Human Reproduction* **13,** 3151-3155.

Flaherty, L., Dibiase, K., Lynes, M. A., Siedman, J. D., Weinberger, O., and Rinchik, E. M. (1985). Characterisation of a Q subregion gene in the murine major histocompatability complex. *Proc.Natl.Acad.Sci. USA* **82,** 1503-1507.

Fleming, T. (1987). A quantitative analysis of cell allocation to trophectoderm and inner cell mass in the mouse blastocyst. *Dev. Biol.* **119,** 520-531.

Fleming, T. P., and Pickering, S. J. (1985). Maturation and Polarization of the Endocytotic System in Outside Blastomeres During Mouse Preimplantation Development. *Journal of Embryology and Experimental Morphology* **89,** 175-208.

Fleming, T. P., Warren, P. D., Chrisholm, J. C., and Johnson, M. H. (1984). Trophectoderm processes regulate the expression of totipotency within the inner cell mass of the mouse expanding blastocyst. *J. Embryol. Exp. Morph.* **84,** 63-90.

Friedrich, G., and Soriano, P. (1991). Promoter traps in embryonic stem cells: a genetic screen to identify and mutate developmental genes in mice. *Genes and Development* **5,** 1513-1523.

Fundele, R., Jägerbauer, E.-M., Kolbus, U., Winking, H., and Gropp, A. (1985). Viability of trisomy 12 cells in mouse chimaeras. *Roux's Arch Dev Biol* **194,** 178-180.

Gardner, L. I. (1982). The Lessons of Polyploidy - Relation to Congenital Asymmetry and the Russell-Silver Syndrome. *American Journal of Diseases of Children* **136,** 292-293.

Gardner, R. L. (1996). Can Developmentally Significant Spatial Patterning Of the Egg Be Discounted In Mammals. *Human Reproduction Update* **2,** 3-27.

Gardner, R. L., and Cockroft, D. L. (1998). Complete dissipation of coherent clonal growth occurs before gastrulation in mouse epiblast. *Development* **125,** 2397-2402.

Garner, W., and McLaren, A. (1974). Cell distribution in chimaeric mouse embryos before implantation. *J. Embryol. Exp. Morphol.* **32,** 495-503.

Giebelhaus, D. H., Heikkila, J. J., and Schultz, G. A. (1983). Changes in the Quantity of Histone and Actin Messenger-Rna During the Development of Pre-Implantation Mouse Embryos. *Developmental Biology* **98,** 148-154.

Giebelhaus, D. H., Weitlauf, H. M., and Schultz, G. A. (1985). Actin Messenger-Rna Content in Normal and Delayed Implanting Mouse Embryos. *Developmental Biology* **107,** 407-413.

Golbus, M. S., Bachmann, R., Wiltse, S., and Hall, B. D. (1976). Tetraploidy in a live-born infant. *J. Med. Genet.* **13,** 329-332.

Goldstein, S. R., Kerenyi, T., Scher, J., and Papp, C. (1996). Correlation between karyotype and ultrasound findings in patients with failed early pregnancy. *Ultrasound Obstet. Gynecol.* **8,** 314-317.

Goto, Y., Matsui, J., and Takagi, N. (2002). Developmental potential of mouse tetraploid cells in diploid <- > tetraploid chimeric embryos. *International Journal of Developmental Biology* **46,** 741-745.

Graham, C. F., and Deussen, Z. A. (1978). Features of cell lineage in preimplantation mouse development. *J. Embryol. Exp. Morphol.* **48,** 53-72.

Graham, C. F., and Lehtonen, E. (1979). Formation and consequences of cell-patterns in preimplantation mouse development. *J. Embryol. Exp. Morphol.* **49,** 277-294.

Gropp, A. (1976). Morphological consequences of trisomy in mammals. *In* "Embryogenesis in Mammals. Ciba Symposium 40", pp. 155-175. Elsevier, Amsterdam.

Gu, Z. Y., Nomura, M., Simpson, B. B., Lei, H., Feijen, A., van den Eijnden-van Raaij, J., Donahoe, P. K., and Li, E. (1998). The type I activin receptor ActRIB is required for egg cylinder organization and gastrulation in the mouse. *Genes & Development* **12,** 844-857.

Guillemot, F., Nagy, A., Auerbach, A., Rossant, J., and Joyner, A. L. (1994). Essential role of *Mash-2* in extraembryonic development. *Nature* **371,** 333-336.

Lu, J. Y., Chen, H. C., Chu, R. Y. Y., Lin, T. C. E., Hsu, P. I., Huang, M. S., Tseng, C. J., and Hsiao, M. (2003). Establishment of red fluorescent protein-tagged HeLa tumor metastasis models: Determination of DsRed2 insertion effects and comparison of metastatic patterns after subcutaneous, intraperitoneal, or intravenous injection. *Clinical & Experimental Metastasis* **20,** 121-133.

Hadjantonakis, A., Gertenstein, M., Ikawa, M., Okabe, M., and Nagy, A. (1998a). Non-invasive sexing of preimplantation stage mammalian embryos. *Nature genetics* **19,** 220-222.

Hadjantonakis, A. K., Gertsenstein, M., Ikawa, M., Okabe, M., and Nagy, A. (1998b). Generating green fluorescent mice by germline transmission of green fluorescent ES cells. *Mechanisms of Development* **76,** 79-90.

Hahnemann, J. M., and Vejerslev, L. O. (1997). European collaborative research on mosaicism in CVS (EUCROMIC) - Fetal and extrafetal cell lineages in 192 gestations with CVS mosaicism involving single autosomal trisomy. *American Journal of Medical Genetics* **70,** 179-187.

Harper, J. C., Dawson, K., Delhanty, J. D. A., and Winston, R. M. L. (1995). The use of fluorescent in-situ hybridization (FISH) for the analysis of in-vitro fertilization embryos: A diagnostic tool for the infertile couple. *Human Reproduction* **10,** 3255-3258.

Harper, J. C., and Delhanty, J. D. A. (1996). Detection of chromosomal abnormalities in human preimplantation embryos using FISH. *Journal of Assisted Reproduction and Genetics* **13,** 137-139.

Harrison, R. H., Kuo, H. C., Scriven, P. N., Handyside, A. H., and Ogilvie, C. M. (2000). Lack of cell cycle checkpoints in human cleavage stage embryos revealed by a clonal pattern of chromosomal mosaicism analysed by sequential multicolour FISH. *Zygote* **8,** 217-224.

Hassold, T. J. (1980). A cytogenetic study of repeated spontaneous abortions. *Am. J. Hum. Genet.* **44,** 151-78.

Henery, C., and Kaufman, M. H. (1991). Cleavage Rates of Diploid and Tetraploid Mouse Embryos During the Preimplantation Period. *Journal of Experimental Zoology* **259,** 371-378.

Henery, C. C., Bard, J. B. L., and Kaufman, M. H. (1992). Tetraploidy in Mice, Embryonic-Cell Number, and the Grain of the Developmental Map. *Developmental Biology* **152,** 233-241.

Hillman, N., Sherman, M. I., and Graham, C. F. (1972). The effect of spatial arrangement on cell determination during mouse development. *J. Embryol. Exp. Morphol.* **28,** 263-278.

Hogan, B., Beddington, R., Costantini, F., and Lacy, E. (1994). "Manipulating the mouse embryo. A laboratory manual." Cold spring Harbor Laboratory Press,

Hunter, S. M., and Evans, M. (1999). Non-surgical method for the induction of delayed implantation and recovery of viable blastocysts in rats and mice by the use of tamoxifen and Depo-Provera. *Molecular Reproduction and Development* **52,** 29-32.

James, R. M., Klerkx, A., Keighren, M., Flockhart, J. H., and West, J. D. (1995). Restricted distribution of tetraploid cells in mouse tetraploid↔diploid chimaeras. *Developmental Biology* **167,** 213-226.

Jenkins, T. M., and Wapner, R. J. (1999). First trimester prenatal diagnosis: Chorionic villus sampling. *Seminars in Perinatology* **23,** 403-413.

Johnson, M. H., and Ziomek, C. A. (1981a). The Foundation of 2 Distinct Cell Lineages Within the Mouse Morula. *Cell* **24,** 71-80.

Johnson, M. H., and Ziomek, C. A. (1981b). Induction of Polarity in Mouse 8-Cell Blastomeres - Specificity, Geometry, and Stability. *Journal of Cell Biology* **91,** 303-308.

Johnson, M. H., and Ziomek, C. A. (1983). Cell-Interactions Influence the Fate of Mouse Blastomeres Undergoing the Transition From the 16-Cell to the 32-Cell Stage. *Developmental Biology* **95,** 211-218.

Johnson, P., Duncan, K., Blunt, S., Bell, G., Ali, Z., Cox, P., and Moore, G. E. (2000). Apparent confined placental mosaicism of trisomy 16 and multiple fetal anomalies: case report. *Prenatal Diagnosis* **20,** 417-421.

Kalousek, D., Barrett, I. J., and McGillivray, B. C. (1989). Placental mosaicism and intrauterine survival of trisomies 13 and 18. *Am. J. Hum. Genet.* **44,** 338-343.

Kalousek, D. K. (1994). Current Topic: Confined placental mosaicism and intrauterine fetal development. *Placenta* **15,** 219-230.

Kalousek, D. K., and Dill, F. J. (1983). Chromosome mosaicism confined to the placenta in human conceptions. *Science* **221,** 665-667.

Kalousek, D. K., and Vekemans, M. (1996). Confined placental mosaicism. *Journal of Medical Genetics* **33,** 529-533.

Kaufman, M. H. (1992). "The Atlas of Mouse Development." Academic Press, London.

Kawarsky, S. J., Basrur, P. K., Stubbings, R. B., Hansen, P. J., and King, W. A. (1996). Chromosomal abnormalities in bovine embryos and their influence on development. *Biology of Reproduction* **54,** 53-59.

Keighren, M., and West, J. D. (1993). Analysis of cell ploidy in histological sections of mouse tissues by DNA-DNA *in situ* hybridization with digoxygenin labelled probes. *Histochem. J.* **25,** 30-44.

Kelly, A., and West, J. D. (1996). Genetic evidence that glycolysis is necessary for gastrulation in the mouse. *Developmental Dynamics* **207,** 300-308.

Kelley, T. E., and Rary, J. M. (1974). Mosaic tetraploidy in a two-year-old female. *Clin. Genet.* **6,** 221-224.

Kelly, S. J., Mulnard, J. G., and Graham, C. F. (1978). Cell division and cell allocation in early mouse development. *J. Embryol. Exp. Morphol.* **48,** 37-51.

Klisch, K., Schuler, G., Miglino, M. A., and Leiser, R. (2000). Genome multiplication in trophoblast giant cells of sheep, goat, water buffalo and deer: An image cytophotometric study. *Reproduction in Domestic Animals* **35,** 145-148.

Ko, M. S. H., Kitchen, J. R., Wang, X. H., Threat, T. A., Wang, X. Q., Hasegawa, A., Sun, T., Grahovac, M. J., Kargul, G. J., Lim, M. K., Cui, Y. S., Sano, Y., Tanaka, T., Liang, Y. L., Mason, S., Paonessa, P. D., Sauls, A. D., DePalma, G. E., Sharara, R., Rowe, L. B., Eppig, J., Morrell, C., and Doi, H. (2000). Large-scale cDNA analysis reveals phased gene expression patterns during preimplantation mouse development. *Development* **127,** 1737-1749.

Kohn, G., Mayall, B. H., Miller, M. E., and Mellman, W. J. (1967). Tetraploid-diploid mosaicism in a surviving infant. *Pediat. Res.* **1,** 461-469.

Koizumi, N., and Fukuta, K. (1995). Preimplantation Development of Tetraploid Mouse Embryo Produced By Cytochalasin-B. *Experimental Animals* **44,** 105-109.

Laverge, H., DeSutter, P., VerschraegenSpae, M. R., DePaepe, A., and Dhont, M. (1997). Triple colour fluorescent in-situ hybridization for chromosomes X, Y and 1 on spare human embryos. *Human Reproduction* **12,** 809-814.

Ledbetter, D. H., Zachary, J. M., Simpson, J. L., Golbus, M. S., Pergament, E., Jackson, L., Mahoney, M. J., Desnick, R. J., Schulman, J., Copeland, K. L., Verlinsky, Y., Yangfeng, T., Schonberg, S. A., Babu, A., Tharapel, A., Dorfmann, A., Lubs, H. A., Rhoads, G. G., Fowler, S. E., and Delacruz, F. (1992). Cytogenetic Results From the United-States Collaborative Study On Cvs. *Prenatal Diagnosis* **12,** 317-345.

Lestou, V. S., Desilets, V., Lomax, B. L., Barrett, I. J., Wilson, R. D., Langlois, S., and Kalousek, D. K. (2000). Comparative genomic hybridization: A new approach to screening for intrauterine complete or mosaic aneuploidy. *American Journal of Medical Genetics* 92, 281-284.

Lestou, V. S., and Kalousek, D. K. (1998). Confined placental mosaicism and intrauterine fetal growth. *Archives of Disease in Childhood* **79,** F223-F226.

Levak-Svajger, B., Levak-Svajger, A., and Skreb, N. (1969). Separation of germ layers in presomite rat embryos. *Experientia* **25,** 1311-1312.

Lo, C. (1983). Transformation by iontophoretic microinjection of DNA: multiple integrations without tandem insertions. *Mol. Cell. Biol.* **3,** 1803-1814.

Lo, C. (1986). Localization of low abundance DNA sequences in tissue sections by in situ hybridization. *J. Cell Sci.* **81,** 143-162.

Lu, T. Y., and Markert, C. L. (1980). Manufacture of diploid/tetraploid chimeric mice. *Proc. natn. Acad. Sci. U.S.A.* **77,** 6012-6016.

Lyon, M. F. (1970). X-ray induced dominant lethal mutations in male guinea-pigs, hamsters and rabbits. *Mutat. Res.* **10,** 133-140.

Ma, J., Svoboda, P., Schultz, R. M., and Stein, P. (2001). Regulation of zygotic gene activation in the preimplantation mouse embryo: Global activation and repression of gene expression. *Biology of Reproduction* **64,** 1713-1721.

Magnuson, T., Smith, S., and Epstein, C. J. (1982). The development of monosomy 19 mouse embryos. *J. Embryol. Exp. Morphol.* **69,** 223-236.

Maro, B., Johnson, M. H., Pickering, S. J., and Louvard, D. (1985). Changes in the distribution of membranous organelles during mouse early development. *J. Embryol. Exp. Morph.* **90,** 287-309.

McLaren, A. (1976). "Mammalian Chimaeras." Cambridge University Press, Cambridge.

McLaren, A., and Bowman, P. (1973). Genetic effects on the timing of early development in the mouse. *J. Embryol. Exp. Morphol.* **30,** 491-498.

Mintz, B., Gearhart, J. D., and Guymont, A. G. (1973). Phytohemagglutinin-mediated blastomere aggregation and development of allophenic mice. *Dev. Biol.* **31,** 195-199.

Mullen, R. J., and Whitten, W. K. (1971). Relationship of genotype and degree of chimerism in coat color to sex ratios and gametogenesis in chimeric mice. *J. Exp. Zool.* **178,** 165-176.

Munne, S., Magli, C., Adler, A., Wright, G., deBoer, K., Mortimer, D., Tucker, M., Cohen, J., and Gianaroli, L. (1997). Treatment-related chromosome abnormalities in human embryos. *Human Reproduction* **12,** 780-784.

Mystkowska, E. T., Ozdzenski, W., and Niemierko, A. (1979). Factors regulating the degree and extent of experimental chimaerism in the mouse. *J. Embryol. Exp. Morph.* **51,** 217-225.

Nagy, A., Gocza, E., Merentes Diaz, E., Prideaux, V., Ivanyi, E., Markkula, M., and Rossant, J. (1990). Embryonic stem cells alone are able to support fetal development in the mouse. *Development* **110,** 815-821.

Nagy, A., and Rossant, J. (1993). Production of completely ES cell-derived fetuses. *In* "Gene Targeting. A Practical Approach." (A. L. Joyner, Ed.), pp. 147-179. IRL Press; Oxford University Press, Oxford.

Nakamura, Y., Yamamoto, M., and Matsui, Y. (2002). Introduction and expression of foreign genes in cultured mouse embryonic gonads by electroporation. *Reproduction Fertility and Development* **14,** 259-265.

Neganova, I. E., Augustin, M., Sekirina, G. G., and Jockusch, H. (1998). LacZ transgene expression as a cell marker to analyse rescue from the 2-cell block in mouse aggregation chimeras. *Zygote* **6,** 223-226.

Niwa, K., Araki, M., and Iritani, A. (1980). Fertilization in vitro of Eggs and First Cleavage of Embryos in Different Strains of Mice. *Biology of Reproduction* **22,** 1155-1159.

Noomen, P., van den Berg, C., de Ruyter, J. L. M., Van Opstal, D., and Los, F. J. (2001). Prevalence of tetraploid metaphases in semidirect and cultured chorionic villi. *Fetal Diagnosis and Therapy* **16,** 129-132.

Pedersen, R. A. (1986). Potency, lineage and allocation in preimplantation mouse embryos. *In* "Experimental approaches to mammalian embryonic development" (J. Rossant and R. A. Pedersen, Eds.), pp. 3-33. Cambridge University Press, Cambridge.

Peyrieras, N., Hyafil, F., Louvard, D., Ploegh, H. L., and Jacob, F. (1983). Uvomorulin - a Non-Integral Membrane-Protein of Early Mouse Embryo. *Proceedings of the National Academy of Sciences of the United States of America-Biological Sciences* 80, 6274-6277.

Piko, L., and Clegg, K. B. (1982). Quantitative Changes in Total Rna, Total Poly(a), and Ribosomes in Early Mouse Embryos. *Developmental Biology* **89,** 362-378.

Piotrowska, K., Wianny, F., Pedersen, R. A., and Zernicka-Goetz, M. (2001). Blastomeres arising from the first cleavage division have distinguishable fates in normal mouse development. *Development* **128,** 3739-3748.

Piotrowska, K., and Zernicka-Goetz, M. (2001). Role for sperm in spatial patterning of the early mouse embryo. *Nature* **409,** 517-521.

Piotrowska, K., and Zernicka-Goetz, M. (2002). Early patterning of the mouse embryo - contributions of sperm and egg. *Development* **129,** 5803-5813.

Pratt, H. P. M., Ziomek, C. A., Reeve, W. J. D., and Johnson, M. H. (1982). Compaction of the Mouse Embryo - an Analysis of Its Components. *Journal of Embryology and Experimental Morphology* **70,** 113-132.

Pratt, H. P. M. (1987). Isolation, culture and manipulation of pre-implantation mouse embryos. *In* "Mammalian development: a practical approach" (M. Monk, Ed.), pp. 29-42. IRL Press, Oxford.

Pratt, T., Sharp, L., Nichols, T., Price, D. J., and Mason, J. O. (2000). Embryonic stem cells and transgenic mice ubiquitously expressing a tau-tagged green fluorescent protein. *Developmental Biology* **228,** 19-28.

Ram, P. T., and Schultz, R. M. (1993). Reporter Gene-Expression in G2 of the 1-Cell Mouse Embryo. *Developmental Biology* **156,** 552-556.

Randle, B. J. (1982). Cosegregation of Monoclonal-Antibody Reactivity and Cell Behavior in the Mouse Pre-Implantation Embryo. *Journal of Embryology and Experimental Morphology* **70,** 261-278.

Renard, J. P., Baldacci, P., Richouxduranthon, V., Pournin, S., and Babinet, C. (1994). A Maternal Factor Affecting Mouse Blastocyst Formation. *Development* **120,** 797-802.

Rinkenberger, J. L., Cross, J. C., and Werb, Z. (1997). Molecular genetics of implantation in the mouse. *Developmental Genetics* **21,** 6-20.

Robinson, W. P. (2000). Mechanisms leading to uniparental disomy and their clinical consequences. *Bioessays* **22,** 452-459.

Rossant, J., and Spence, A. (1998). Chimeras and mosaics in mouse mutant analysis. *Trends In Genetics* **14,** 358-363.

Rossant, J., and Vijh, K. M. (1980). Ability of outside cells from preimplantation mouse embryos to form inner cell mass derivatives *in vivo*. *Dev. Biol.* **76,** 475-482.

Rothstein, J. L., Johnson, D., Deloia, J. A., Skowronski, J., Solter, D., and Knowles, B. (1992). Gene-Expression During Preimplantation Mouse Development. *Genes & Development* **6,** 1190-1201.

Sharp, L. W. (2001). Using laser scanning confocal microscopy to characterise a transgenic mouse expressing tau tagged green fluorescent protein. *MSc Thesis, The University of Edinburgh.* .

Shimada, H., Kaname, T., Suzuki, M., Hitoshi, Y., Araki, K., Imaizumi, T., and Yamamura, K. I. (1999). Comparison of ES cell fate in sandwiched aggregates and co-cultured aggregates during blastocyst formation by monitored GFP expression. *Molecular Reproduction and Development* **52,** 376-382.

Sirard, C., de la Pompa, J. L., Elia, A., Itie, A., Mirtsos, C., Cheung, A., Hahn, S., Wakeham, A., Schwartz, L., Kern, S. E., Rossant, J., and Mak, T. W. (1998). The tumor suppressor gene Smad4/Dpc4 is required for gastrulation and later for anterior development of the mouse embryo. *Genes & Development* **12,** 107-119.

Smith, K., Lowther, G., Maher, E., Hourihan, T., Wilkinson, T., and Wolstenholme, J. (1999). The predictive value of findings of the common aneuploidies, trisomies 13, 18 and 21, and numerical sex chromosome abnormalities at CVS: Experience from the ACC UK Collaborative Study. *Prenatal Diagnosis* **19,** 817-826.

Snow, M., and Ansell, J. D. (1974). The chromosomes of giant trophoblast cells of the mouse. *Proc. R. Soc. Lond. Series B* **187,** 93-98.

Snow, M. H. L. (1975). Embryonic development of tetraploid mice during the second half of gestation. *J. Embryol Exp Morph* **34,** 707-721.

Spindle, A. (1982). Cell allocation in preimplantation mouse chimeras. *J. exp. Zool.* **219,** 361-367.

Squirrell, J. M., Wokosin, D. L., White, J. G., and Bavister, B. D. (1999). Long-term two-photon fluorescence imaging of mammalian embryos without compromising viability. *Nature Biotechnology* **17,** 763-767.

Steuerwald, N., Cohen, J., Herrera, R. J., and Brenner, C. A. (1999). Analysis of gene expression in single oocytes and embryos by real-time rapid cycle fluorescence monitored RT-PCR. *Molecular Human Reproduction* **5,** 1034-1039.

Stipoljev, F., Latin, V., Kos, M., Miskovic, B., and Kurjak, A. (2001). Correlation of confined placental mosaicism with fetal intrauterine growth retardation - A case control study of placentas at delivery. *Fetal Diagnosis and Therapy* **16,** 4-9.

Strickland, S., Reich, E., and Sherman, M. I. (1976). Plasminogen Activator in Early Embryogenesis: Enzyme Production by Trophoblast and Parietal Endoderm. *Cell* **9,** 231-240.

Stutz, A., Conne, B., Huarte, J., Gubler, P., Volkel, V., Flandin, P., and Vassalli, J. D. (1998). Masking, unmasking, and regulated polyadenylation cooperate in the translational control of a dormant mRNA in mouse oocytes. *Genes & Development* **12,** 2535-2548.

Surani, M. A., Barton, S. C., and Norris, M. L. (1984). Development of reconstituted mouse eggs suggests imprinting of the genome during gametogenesis. *Nature* 308, 548-550.

Sutherland, A. E., and Calarcogillam, P. G. (1983). Analysis of Compaction in the Pre-Implantation Mouse Embryo. *Developmental Biology* **100,** 328-338.

Sutherland, A. E., Speed, T. P., and Calarco, P. G. (1990). Inner Cell Allocation In the Mouse Morula - the Role Of Oriented Division During 4th Cleavage. *Developmental Biology* **137,** 13-25.

Svoboda, P., Stain, P., Hayashi, H., and Schultz, R. M. (2000). Selective reduction of dormant maternal mRNAs in mouse oocytes by RNA interference. *Development* **127,** 4147-4156.

Tanaka, M., Hadjantonakis, A. K., and Nagy, A. (2001). Aggregation chimeras. combining ES cells, diploid and tetraploid embryos. *Methods Mol. Biol.* **158,** 135-54.

Tang, P. C. (1999). Factors that influence the composition of mouse chimeras. *PhD Thesis, The University of Edinburgh.* .

Tang, P.-C., Ritchie, W. A., Wilmut, I., and West, J. D. (2000). The effects of cell size and ploidy on cell allocation in mouse chimaeric blastocysts. *Zygote* **8,** 33 - 43.

Tang, P.-C., and West, J. D. (2000). The effects of embryo stage and cell number on the composition of mouse aggregation chimaeras. *Zygote* **8,** 235-243.

Tang, P.-C., and West, J. D. (2001). Size regulation does not cause the composition of mouse chimaeras to become unbalanced. *Int. J. Dev. Biol.* **45,** 583-590.

Tarkowski, A., and Wroblewska, J. (1967). Development of blastomeres of mouse eggs isolated at the 4- and 8-cell stage. *J. Embryol. Exp. Morphol.* **18,** 155-180.

Tarkowski, A. K. (1961). Mouse chimaeras developed from fused eggs. *Nature* **190,** 857-860.

Tarkowski, A. K., Ozdzenski, W., and Czolowska, R. (2001). Mouse singletons and twins developed from isolated diploid blastomeres supported with tetraploid blastomeres. *International Journal of Developmental Biology* **45,** 591-596.

Tarkowski, A. K., Witkowska, A., and Opas, J. (1977). Development of cytochalasin B-induced tetraploid and diploid/tetraploid mosaic mouse embryos. *J. Embryol. Exp. Morphol.* **41,** 47-64.

Taylor, K. D., and Piko, L. (1987). Patterns of Messenger-Rna Prevalence and Expression of B1- Transcript and B2-Transcript in Early Mouse Embryos. *Development* **101,** 877-892.

Telford, N. A., Watson, A. J., and Schultz, G. A. (1990). Transition From Maternal to Embryonic Control in Early Mammalian Development - a Comparison of Several Species. *Molecular Reproduction and Development* **26,** 90-100.

Theiler, K. (1989). "The House Mouse Atlas of Embryonic Development." Springer-Verlag, New York.

Varmuza, S., Prideaux, V., Kothary, R., and Rossant, J. (1988). Polytene chromosomes in mouse trophoblast cells. *Development* **102,** 127-134.

Vaughan, J., Ali, Z., Bower, S., Bennett, P., Chard, T., and Moore, G. (1994). Human Maternal Uniparental Disomy For Chromosome-16 and Fetal Development. *Prenatal Diagnosis* **14,** 751-756.

Viuff, D., Greve, T., Avery, B., Hyttel, P., Brockhoff, P. B., and Thomsen, P. D. (2000). Chromosome aberrations in in vitro-produced bovine embryos at days 2-5 post-insemination. *Biology of Reproduction* **63,** 1143-1148.

Viuff, D., Hendriksen, P. J. M., Vos, P., Dieleman, S. J., Bibby, B. M., Greve, T., Hyttel, P., and Thomsen, P. D. (2001). Chromosomal abnormalities and developmental kinetics in in vivo-developed cattle embryos at days 2 to 5 after ovulation. *Biology of Reproduction* **65,** 204-208.

Viuff, D., Rickords, L., Offenberg, H., Hyttel, P., Avery, B., Olsaker, I., Williams, J. L., Callesen, H., and Thomsen, P. D. (1999). Mixoploidy is more frequent in bovine blastocysts produced in vitro than in blastocysts developed in vivo. *Theriogenology* **51,** 335-335.

Waldrip, W. R., Bikoff, E. K., Hoodless, P. A., Wrana, J. L., and Robertson, E. J. (1998). Smad2 signaling in extraembryonic tissues determines anterior- posterior polarity of the early mouse embryo. *Cell* **92,** 797-808.

Wang, Z. Q., Kiefer, F., Urbanek, P., and Wagner, E. F. (1997). Generation of completely embryonic stem cell-derived mutant mice using tetraploid blastocyst injection. *Mechanisms of Development* **62,** 137-145.

Warner, C. M., Exley, G. E., McElhinny, A. S., and Tang, C. Y. (1998). Genetic regulation of preimplantation mouse embryo survival. *Journal Of Experimental Zoology* **282,** 272-279.

Weber, R. J., Pedersen, R. A., Wianny, F., Evans, M. J., and Zernicka-Goetz, M. (1999). Polarity of the mouse embryo is anticipated before implantation. *Development* **126,** 5591-5598.

Wells, D., and Delhanty, J. D. A. (2000). Comprehensive chromosomal analysis of human preimplantation embryos using whole genome amplification and single cell comparative genomic hybridization. *Molecular Human Reproduction* **6,** 1055-1062.

Wells, D., Sherlock, J. K., Handyside, A. H., and Delhanty, J. D. A. (1999). Detailed chromosomal and molecular genetic analysis of single cells by whole genome amplification and comparative genomic hybridisation. *Nucleic Acids Research* **27,** 1214-1218.

West, J. D. (1984). Cell markers. *In* "Chimeras in Developmental Biology" (N. L. Douarin and A. McLaren, Eds.), pp. 39-63. Academic Press, London.

West, J. D. (1999). Insights into development and genetics from mouse chimeras. *Current Topics in Developmental Biology* **44,** 21-66.

West, J. D., Angell, R. R., Thatcher, S. S., Gosden, J. R., Hastie, N. D., Glasier, A. F., and Baird, D. T. (1987). Sexing the human pre-embryo by DNA-DNA in situ hybridization. *Lancet* **1,** 1345-1347.

West, J. D., and Flockhart, J. H. (1994). Genotypically Unbalanced Diploid↔Diploid Fetal Mouse Chimeras - Possible Relevance to Human Confined Mosaicism (Vol 63, Pg 87, 1994). *Genetical Research* **63,** 236-236.

West, J. D., Flockhart, J. H., and Kissenpfennig, A. (1995). A Maternal Genetic Effect On the Composition of Mouse Aggregation Chimeras. *Genetical Research* **65,** 29-40.

West, J. D., Gosden, J. R., Angell, R. R., West, K. M., Glasier, A. F., Thatcher, S. S., and Baird, D. T. (1988). Sexing whole human pre-embryos by in situ hybridization with a Y- chromosome specific DNA probe. *Human Reproduction* **3,** 1010-1019.

West, J. D., and Green, J. F. (1983). The transition from oocyte-coded to embryo-coded glucose phosphate isomerase in the early mouse embryo. *J. Embryol. Exp. Morphol.* **78,** 127-140.

Wianny, F., and Zernicka-Goetz, M. (2000). Specific interference with gene function by double-stranded RNA in early mouse development. *Nature Cell Biology* **2,** 70-75.

Wiley, L. M. (1984). Cavitation in the Mouse Preimplantation Embryo - Na/K-Atpase and the Origin of Nascent Blastocele Fluid. *Developmental Biology* **105,** 330-342.

Wilson, G. N., Vekemans, M. J. J., and Kaplan, P. (1988). Mca/Mr Syndrome in a Female Infant With Tetraploidy Mosaicism - Review of the Human Polyploid Phenotype. *American Journal of Medical Genetics* **30,** 953-961.

Winkel, G. K., Ferguson, J. E., Takeichi, M., and Nuccitelli, R. (1990). Activation of Protein Kinase-C Triggers Premature Compaction in the 4-Cell Stage Mouse Embryo. *Developmental Biology* 138, 1-15.

Wolstenholme, J. (1996). Confined placental mosaicism for trisomies 2, 3, 7, 8, 9, 16, and 22: Their incidence, likely origins, and mechanisms for cell lineage compartmentalization. *Prenatal Diagnosis* **16,** 511-524.

Wong, M. H., Hermiston, M. L., Syder, A. J., and Gordon, J. I. (1996). Forced Expression Of the Tumor-Suppressor Adenomatosis Polyposis-Coli Protein Induces Disordered Cell-Migration In the Intestinal Epithelium. *Proceedings Of the National Academy Of Sciences Of the United States Of America* **93,** 9588-9593.

Wu, L. Z., de Bruin, A., Saavedra, H. I., Starovic, M., Trimboli, A., Yang, Y., Opavska, J., Wilson, P., Thompson, J. C., Ostrowski, M. C., Rosol, T. J., Woollett, L. A., Weinstein, M., Cross, J. C., Robinson, M. L., and Leone, G. (2003). Extra-embryonic function of Rb is essential for embryonic development and viability. *Nature* **421,** 942-947.

Zambrowicz, B. P., Imamoto, A., Fiering, S., Herzenberg, L. A., Kerr, W. G., and Soriano, P. (1997). Disruption of overlapping transcripts in the ROSA beta geo 26 gene trap strain leads to widespread expression of beta- galactosidase in mouse embryos and hematopoietic cells. *Proceedings of the National Academy of Sciences of the United States of America* **94,** 3789-3794.

Zernicka-Goetz, M., Pines, J., Hunter, S. M., Dixon, J. P. C., Siemering, K. R., Haseloff, J., and Evans, M. J. (1997). Following cell fate in the living mouse embryo. *Development* **124,** 1133-1137.

Zimmet, J., and Ravid, K. (2000). Polyploidy: Occurrence in nature, mechanisms, and significance for the megakaryocyte-platelet system. *Experimental Hematology* **28,** 3-16.

Ziomek, C. A., Johnson, M. H., and Handyside, A. H. (1982). The developmental potential of mouse 16-cell blastomeres. *J. Exp. Zool.* **221,** 343-355.